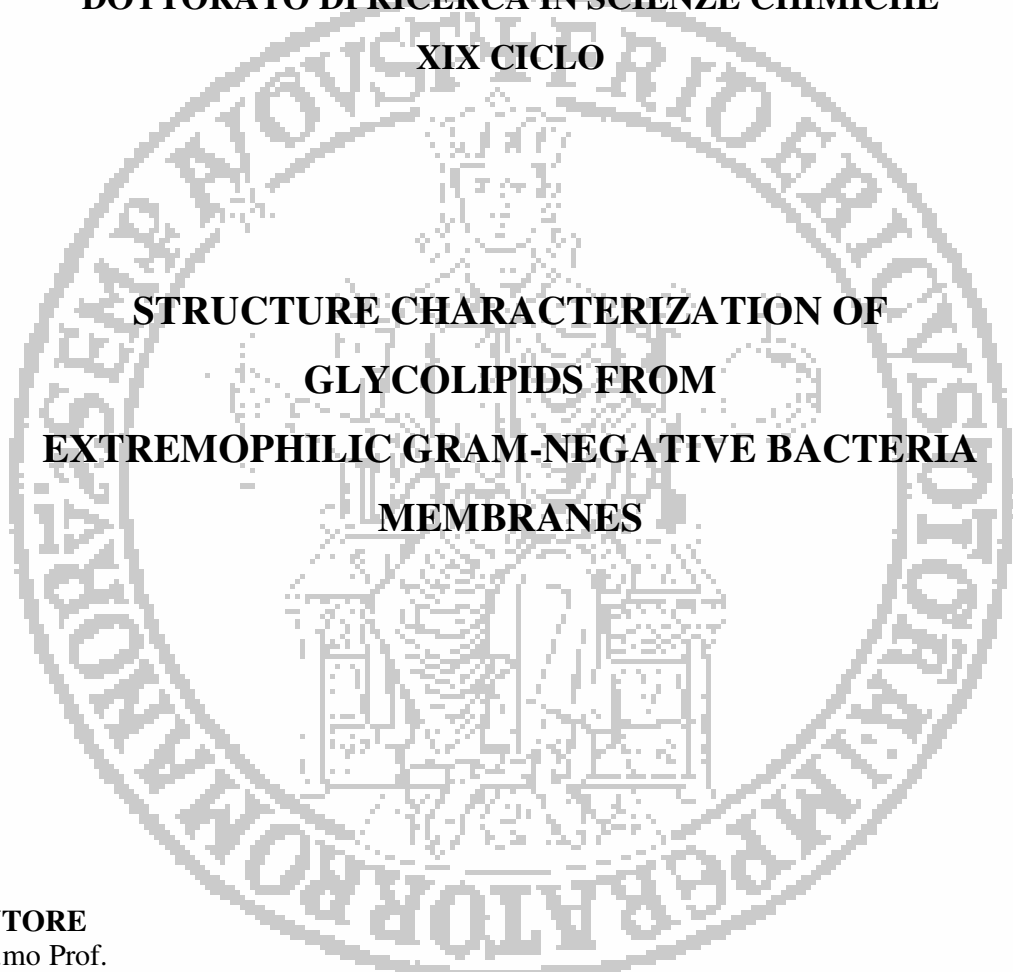UNIVERSITA' DEGLI STUDI DI NAPOLI

"FEDERICO II"

FACOLTA' DI SCIENZE MATEMATICHE, FISICHE E NATURALI

DOTTORATO DI RICERCA IN SCIENZE CHIMICHE
XIX CICLO

STRUCTURE CHARACTERIZATION OF
GLYCOLIPIDS FROM
EXTREMOPHILIC GRAM-NEGATIVE BACTERIA
MEMBRANES

TUTORE
Ch.mo Prof.
ANTONIO MOLINARO

RELATORE   **DOTTORESSA**
Ch.ma Prof.ssa   **SERENA LEONE**
ALESSANDRA NAPOLITANO

COORDINATORE
Ch.ma Prof.ssa
ROSA LANZETTA

Index

Preface

The present thesis work deals with the structure characterization of the glycolipids composing the outer cellular membrane of several extremophilic Gram-negative bacteria isolated from different environments. Extremophiles constitute a niche of organisms able to survive and thrive in environments inhospitable for the common mesophilic bacteria. The acclimatization process of these microbes is prompted by several modifications charging the structure of their biomolecules (proteins, nucleic acids and membrane lipids).

This study points out the development of peculiar structural features of the membrane glycolipids from the three classes of extremophiles investigated, namely marine bacteria, thermophiles and organic solvent tolerant bacteria. These particularities are dependent on the specific stress factors the microrganisms have to face.

Marine Bacteria must develop contemporaneous resistance to the several parameters typifying their isolation environment. In the present work, the microrganisms described are all barophilic and psychrofilic, with a variable halophilic character. Their outer membrane glycolipids are characterized by uncommon negative charge density, and can organize themselves in a rigid net of cross-linkages through the metallic ions, providing higher resistance to physical stressors.

Thermophile microorganisms need a reinforcement of the chemical structure of the glycolipids composing their membranes, in order to stem degradation prompted by elevated temperatures. Bacteria evolutionary adapted to heat have developed peculiar structure for their glycolipids, characterized, for instance, by the replacement of the typical ester linkages occurring between fatty acids and glycerol in glycerophospholipids with more thermostable alkyl chains.

Finally, organic solvents tolerant microrganisms have to balance the disrupting effect of organic molecules on membranes assembly. A tighter packing of the membrane can be a device for blocking this disrupting action and is achieved by introducing a high negative charge density in the outer layer of the membrane itself.

Portions of this work have been adapted from the following articles co-written by the author:

S. Leone, V. Izzo, A. Silipo, L. Sturiale, D. Garozzo, R. Lanzetta, M. Parrilli, A. Molinaro, A. Di Donato. A novel type of highly negatively charged lipooligosaccharide from

Pseudomonas stutzeri OX1 possessing two 4,6-O-(1-carboxy)-ethylidene residues in the outer core region. *Eur. J. Biochem* (2004)**, 271,** 2691-2704**.**

A. Silipo, S.Leone, R. Lanzetta, M. Parrilli, L. Sturiale, D. Garozzo, E. L.. Nazarenko, R. P. Gorshkova, E. P. Ivanova, N. M. Gorshkova , A. Molinaro. The complete structure of the lipooligosaccharide from the halophilic bacterium *Pseudoalteromonas issachenkonii* KMM 3549[T]. *Carbohyd. Res*. (2004) **339,** 1985-1993.

S. Leone, V. Izzo, L. Sturiale, D. Garozzo, R. Lanzetta, M. Parrilli,. A. Molinaro, A. Di Donato. Structure of minor oligosaccharides from the lipopolysaccharide fraction from *Pseudomonas stutzeri* OX1. *Carbohyd. Res*. (2004), **339,** 2657-2665.

A. Silipo, S. Leone, A. Molinaro, L. Sturiale, D. Garozzo, E. L. Nazarenko, E. P. Ivanova, R. Lanzetta and M. Parrilli. Complete structural elucidation of the novel lipooligosaccharide from the outer membrane of marine bacterium *Shewanella pacifica. Eur. J. Org. Chem.* (2005)*,* **11,** 2281-2291.

S. Leone, V. Izzo, R. Lanzetta, A. Molinaro, M. Parrilli, A. Di Donato. The structure of the O-polysaccharide from *Pseudomonas stutzeri* OX1 containing two different 4-acylamido-4,6-dideoxy-residues, tomosamine and perosamine.
Carbohyd. Res. (2005), **340,** 651-656.

S. Leone, A. Molinaro, E. Pessione, R. Mazzoli, C. Giunta, L. Sturiale, D. Garozzo, R. Lanzetta, M. Parrilli. Structural elucidation of the core-lipid A backbone from the lipopolysaccharide of *Acinetobacter radioresistens* S13, an organic solvent tolerant Gram-negative bacterium. *Carbohyd. Res*. (2006), **341,** 582-590.

S.Leone, A.Molinaro, B. Lindner, I. Romano, B. Nicolaus, M. Parrilli, R. Lanzetta, O. Holst. The structures of glycolipids isolated from the highly thermophilic bacterium *Thermus thermophilus* Samu-SA1. *Glycobiology* (2006) **16***,* 766-775.

S. Leone, A. Molinaro, F. Alfieri, V. Cafaro, R. Lanzetta, A. Di Donato, M. Parrilli. The biofilm matrix of *Pseudomonas* sp. OX1 grown on phenol is mainly constituted by alginate oligosaccharides. *Carbohyd. Res*. (2006), **341**, 2456-2461.

S.Leone, A.Molinaro, I. Romano, B. Nicolaus, R. Lanzetta, M. Parrilli, O. Holst. The structures of the cell wall teichoic acids from the thermophilic microrganism *Geobacillus thermoleovorans* strain Fango. *Carbohyd. Res*. (2006) **341***,* 2613-2618.

1

Introduction

1.1 Extremophiles

Extremophiles are prokaryotic microrganisms belonging to the two Dominia Archaea and Bacteria, either of Gram-positive and Gram-negative family, endowed with the capacity to stand unhospital habitats and conditions usually lethal for mesophilic microrganisms. Many different physical and chemical parameters can determine the optimal habitat for such microrganisms, i.e. high or low temperatures, high pressures, high ionic strenght, acidic or alkaline pH, strict anaerobiosis, desiccation or radiations, that are only some of the typical conditions in which extremophiles can survive and thrive. Interestingly, many obliged extremophiles are not only characterized by the skill of surviving in harsh habitats, but they require such conditions to survive (Danson *et al.,* 1992; Morell, 1997). On the basis of the physical or chemical parameters these microrganisms can stand, further divisions have been recognized among the wide class of extremophiles. In particular, **thermophiles** are able to stand extremely high temperatures, ranging from 40°C up to 100°C; **psycrophiles** are able to survive in frozen habitats, i.e. glaciers or polar seas; **acidophiles** and **alkalophiles** can cope with extreme pH values; **halophiles** stand extreme salinity and **barophiles** require elevated pressure for proliferation (**Table 1.1**).

Table 1.1 - Principal classes of extremophiles and typical stressors characterizing their environments.

Thermophiles	Temperature from 40°C to 100°C.
Psycrophiles	Temperature from 10°C to -20°C.
Barophiles (Piezophiles)	Pressure up to 40 MPa
Halophiles	Salt concentrations from 3 M to saturation of NaCl.
Organic Tolerant Bacteria	Toxic organic substances up to supersaturating conditions.
Acidophiles	Low pH values (2 ÷ 6)
Alkalophiles	High pH values (10 ÷ 13)

Often, extremophiles are isolated in environments, i.e. deep-sea habitats, where two or more of such conditions (high ion concentration, high pressure, low temperature) can be encountered. Thus, they are referred to as polyextremophiles, formally belonging to two or more of the above categories at the same time.

Besides the classical definition above given for extremophiles, it is actually possible to define another class of microrganisms able to thrive in harsh conditions. The industrial development and the uncontrolled pollution have, in fact, generated a variety of contaminated sites, where elevated concentration of highly toxic substances accumulate, preventing mesophile microrganisms blooming. Bacteria have been isolated from these environments, which can not strictly be considered extremophiles, although exhibiting a pronounced tolerance towards organic substances. Nevertheless, it is generally believed that the mechanisms developed for the survival in such polluted sites must resemble the ones allowing proliferation in more classical extreme conditions (Sardessai and Bohsle, 2002; Ramos *et al.,* 2002). Moreover, these bacteria are often endowed with the ability of methabolize a wide range of highly toxic compounds, thus they are central in the developement of what is up to date widely known as the environmental biotechnology.

The general interest around extremophiles arose in the 60's, after the first works on thermophile Archaea (Brock, 1969), that constitute the majority of extremophiles isolated up to now. Hyperthermophile Archaea are thought to be among the most ancient forms of life known up to now, therefore, studies on extremophiles are also aimed to a deepest understanding of the origin and development of life.

Together with the development of enzymatic systems, extremophiles often show structural modifications of their biomolecules in order to warrantee the correct cell physiology in unhospital environments. The extraordinary stability shown by extremophiles cells is associated either to the singular structure of lipids and glycolipids composing the cellular membranes and to the production of exopolysaccharides allowing the formation of biofilms, multicellular aggregates hold together by a matrix of exocellular substances. The present thesis is focused on the structure elucidation of the membrane constituents of several extremophile bacteria belonging to the family of Gram-negative bacteria. All of the presented microrganisms were isolated in extreme environments characterised by diverse stressors. The aim is to establish a parallel between the membrane constituents of diverse classes of extremophiles, in order to understand whether the exposure to different environmental conditions can lead to similar adaptative structure changes in the classical cell membrane architecture.

1.2 Responses of bacterial cells to environmental stressors

The effects of the physical and chemical stresses on cellular balance depend on the peculiar isolation environment. Nevertheless, it is generally accepted that, to overcome the inhospitable conditions, adaptations of physiology, enzymology and genetics have been accomplished, in order to protect biological molecules from denaturation and to allow bacterial survival. Thus, specific biological systems have been developed, able to counteract external stresses, including enzymatic systems provided with extraordinary stability towards denaturating agents, often noticeable for their potential applications in industrial or biotechnological processes (Antranikian *et al.*, 2006). The first example of the usage of an enzyme from an extremophile is represented by the thermozime from *Thermus aquaticus*, widely used in the Polymerase Chain Reaction (PCR). Indeed, several enzymes from psycrophiles or acidophiles are actually employed in diverse industrial fields, for example polymer degrading enzymes like amylases, pullulanases, xylanases and proteases that play an important role in food, detergent and paper industries (see section 1.3).

Extremophiles have to deal with unfriendly conditions that can effect the functionality and the correct arrangement of the cell. The effects on cell physiology depend on the type of extreme the bacterium has to face, and several responses in bacterial and archaeal cells have been already described, involving physiology and structure changes in the biomolecules. Exposure to environmental stressors may, in fact, alter the conformation, and therefore the functionality, of lipids, nucleic acids and proteins composing the cell.

In the following sections an overview is presented of the responses encountered in relation to specific stressor ingenerating them. The studies performed so far have been aimed to the detection of metabolic and transcriptional alteration, as well as structural changes charging the cytoplasmic membrane. Nevertheless, for what concerns Gram-negative bacteria, the role of the Outer Membrane molecules, and especially of the constituent glycolipids, has not been significantly investigated yet.

1.2.1 Exposure to high temperature - Thermophiles

High (up to more then 100°C) or low (to -20°C) temperatures define the habitat for thermophiles and psycrophiles respectively. Hot environments are encountered in correspondence of volcanic areas above and below the sea level, where mineralized water comes to the surface, and in the deep rock formations heated by the earth's interior. This

conditions impose a burden on the organisms to the functioning of cellular metabolism (van de Vossenberg *et al.,* 1998; Adams, 1993), and high stability is required for enzymes and other macromolecules.

In case of mesophilic organisms, exposure to heat shock conditions transiently induces the synthesis of the so-called Heat Shock Proteins (HSPs), following the increase of the intracellular σ^{32} factor, the prokaryotic initiation enzyme factor for heat shock. Although first characterised in correspondence of heat shock events, HSPs rate of synthesis can be altered under several stress conditions, and a sensible production is observed also in response to drastical changes in pH, osmolarity, UV irradiation, and the presence of variously toxic substances such as ethanol, antibiotics, aromatic compounds or heavy metals (Ramos *et al.,* 2001). The synthesis of HSPs is triggered by the accumulation, within the cell, of misfolded proteins, as a consequence of the stress condition. HSPs act like chaperones for the other biomolecules, assuring their correct folding and translocating them into the right cell compartments, even in case of altered functionality of the cell itself.

Heat shock may also effect the cytoplasmic membrane structure. Changes in temperature result in alterations of the lipid composition, in order to retain the liquid-crystalline state of the membrane. In Bacteria, this can be done by increasing the length of the acyl chains, the ratio of *iso to anteiso* branching and/or the degree of saturation (Reizer *et al.*, 1985; Prado *et al.*, 1988). These changes are performed to balance the heat-increased reaction rate of basal ion permeation across the membrane, with immediate consequences on the bioenergetic equilibrium of the cell. In fact, when the coupling ions, i.e. protons or sodium ions, permeate too fast, the organism is unable to establish the physiological gradient across the membrane. The growth temperature-dependent alterations in fatty acids composition seem to be aimed to maintaining the proton permeability of the citoplasmic membrane at a rather constant level (van de Vossenberg *et al.*, 1998). In some thermophilic organisms, i.e. *Bacillus stearothermophilus*, this "homeo-proton permeability adaptation" cannot be maintained, and the bacterium uses other mechanisms to maintain the energy balance, like the increase in respiratory rate or the shift to less permeable sodium ions as coupling ions (De Vrij *et al.,*1988).

In Archaea, the acyl chains undergo cyclization or transition from the diether to tetraether (**Figure 1.1**). These tetraether lipids in Archea show lowered proton permeability due to the hindrance brought to the lipid layer of the membrane (Yamauchi *et al.*, 1993). Moreover, ether linkages are far more resistant to oxidation and to high temperature than ester linkages,

as well as to enzymatic degradation by phospholipases (Choquet *et al.* 1994). Consequently, membranes composed by tetraether lipids result more termostable (Chang, 1994).
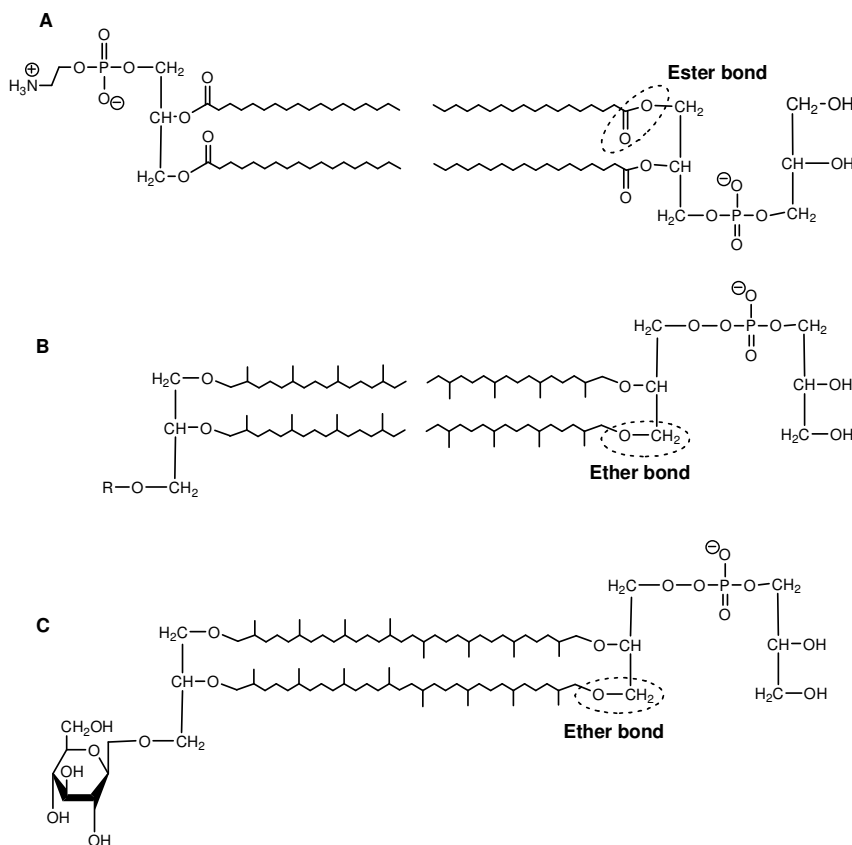
Figure 1. 1- General structure of (**A**) bacterial ester-linked phospholipids; (**B**) archaeal diether lipids and phospholipids and (**C**) tetraether lipids from thermophile Archaea.

1.2.2 Exposure to low temperature - Psycrophiles

The effect of cold shock on bacterial and archeal cells is opposite to that attained by heat shock. Psycrophiles are naturally encountered in water environments in polar regions. Compared to the habitual growth temperatures, cold effects on the cell physiology can derive from the decrease in the rate of biochemical reactions and from the high viscosity of the aqueous environment, which increases by a factor higher than two between 37°C and 0°C (D'Amico *et al.*, 2006). In such a circumstance, cells experience modifications that may reflect the need to maintain optimal membrane fluidity, against the rigidification associated with temperature lowering. Low temperature, in fact, strongly affects the assembly of the cell

membranes, by strengthening the weak interactions holding together the lipid layer. As a consequence, the permeability to ions and nutrient substances is strongly decreased. In *Escherichia coli,* it has been observed an increase in the unsaturation degree within the Lipid A structure (Carty *et al.*, 1999, see section 1.5.3) whereas a change in the fatty acids branching profile in the Gram-positive microrganism *Bacillus subtilis* has been detected (Klein *et al.*, 1999). Moreover, a shortening in the fatty acids chain length can be observed (Chintalapati *et al.*, 2004). All of these strategies have the ultimate effect of introducing steric constrains, changing the packaging order or reducing the number of interactions in the membrane. Further adaptations that have been suggested to increase the membrane fluidity include an increased content of large lipids head groups, proteins and non-polar carotenoid pigments within the membrane organization.

Another effect of low temperature is the alteration of some enzymes or supramolecular structures, which show modified conformations negatively effecting the metabolic flux. Key biological activities involving nucleic acids, such as DNA replication, transcription and translation, can also suffer from exposure to low temperatures through the formation of secondary or super-coiled structures.

A down temperature shift induces in Gram-negative mesophiles the synthesis of the so-called Cold Shock Proteins (CSPs) (Leeson *et al.*, 2000). Similarly to HSPs, CSPs function as chaperones to assure the correct functioning of several processes such as transcription, translation, protein folding and the regulation of membrane fluidity itself. In obliged pyscrophilic microrganisms, analogous of the CSPs exist, the so-called Cold-Acclimation Proteins (CAPs). Although structurally and functionally related to CSPs, the CAPs are constitutively rather than transiently expressed by the psycrophiles. Obliged psycrophiles also express Antifreeze Proteins (AFPs) (D'Amico *et al.*, 2006), that bind to ice crystals through a large complementary surface creating thermal hysteresis and lowering the temperature at which the microrganism can grow. These proteins have been recently isolated and described in Antartic lake bacteria (Gilbert *et al.*, 2004).

Cryoprotection in cold adapted bacteria is often achieved through the synthesis of the disaccharide trehalose or other exopolysaccharides (EPSs). Trehalose is thought to have a colligative effect, and it probably helps also in preventing cold-induce protein denaturation and aggregation (Phadtare, 2004). Indeed, the occurrence of high concentrations of EPSs modify the physico-chemical environment of bacterial cells, participating in cell adhesion to surfaces and in water retention. Moreover, EPS matrices can favour the sequestration and

local concentration of nutrients, retain and protect extracellular enzymes against cold denaturation and act as cryoprotectans as well. (Mancuso Nichols *et al.*, 2005).

In order to stem the rate lowering for biochemical processes due to low temperature, psycrophiles have also evolved cold-adapted enzymes, endowed with specific activities at low temperature, comparable, and sometimes even higher, than mesophilic enzymes. The contradistinctive feature of such enzymes is the activity-stability-flexibility relationship: enhanced flexibility, in fact, compensates the freezing effect got by cold habitats (Johns and Somero, 2004). Even if the conformation of these cold-adapted proteins is similar to that encountered in mesophilic microrganisms, they undergo structural modifications in order to attenuate the strength and the number of conformation stabilizing factors. Common trends in such direction include the reduction of the number of ion pairs, hydrogen bonds and hydrophobic interactions, the weakening of inter-subunits interactions, higher interaction with the solvent and higher accessibility to the active site.

1.2.3 Exposure to high pressures - Barophiles

Microrganisms adapted to high pressures are termed barophiles or piezophiles. Barophile bacteria are commonly isolated from marine environments, either in sea depths or in proximity of hydrothermal vents. Therefore, they often show a simultaneous thermophilic or psycrophilic character (ZoBell and Morita, 1957). Conventionally, a distinction is made between barophilic and barotolerant bacteria: the first are able to stand pressure higher than 40 MPa. Piezophile Archaea and Bacteria are closely related to shallow-water microbes, thus indicating that high pressure selection has not required the evolution of dramatically different lineages of life. Among the Gram-negative barophile bacteria, several belong to the genus *Shewanella* (Horikoshi, 1998). The effects associated to high pressure exposure can be globally related to the change in system volume accompanying either physiological and biochemical processes (Bartlett, 2002). Model studies performed on *E.coli* pressure stressed cells evidenced the possibility to variously adapt to the hyperbaric condition in dependence to other growth conditions. For example, cultures performed at low temperature or acidic pHs showed a marked pressure-dependent growth. The nutrients provided also influence the resistance to high pressures (Marquis, 1994).

The most relevant effect observed in microrganisms exposed to elevated pressures is the concomitant expression of both HSPs and CSPs (Bartlett *et al.,* 1995). The synthesis of such proteins is triggered as well in strict barophiles undergoing decompression. An explanation of

this apparent paradox can be found in the similar effect that high pressure and high or low temperature effect on living organisms. In fact, high pressure and heat can destabilize protein quaternary, and, in minor amount, tertiary structure, whereas, as in case of cold shock, pressure can effect the membrane arrangement, as well as protein synthesis, by forcing more rigid conformations. HSPs and CSPs, with their chaperon function, limit the damages induced by elevated pressure, assisting membrane integrity, translocation processes and the stability of the macromolecules in the same way as during heat or cold shock events.

The effect of pressure shock can be also observed in a change in cytoplasmic membrane structure, mostly for what concerns the nature of constituent fatty acids. Physically, the rigidifying effect of pressure on membrane physiology is due to the increase in hydrocarbon chains order, that raises the temperature of the membrane transition from the gel to the liquid-crystalline state (Driscoll *et al.,* 1991). Pressure increases bilayer thickness by reducing the kinking effect of acyl chains and results primarily in a tighter packing of fatty acyl chains. This results in membranes assuming an ordered array, where molecular motion is restricted. Many deep-sea organisms modulate their membrane fluidity and composition in response to pressure. An increasing depth of isolation, and therefore physiological pressure, is correlated to increasing proportion of membrane fluidizing unsaturated fatty acids. This effect was demonstrated on the deep-sea bacterium *Photobacterium profundum*, progressively increasing culture pressure. The effect of such a solicitation is the increase of the proportion of both mono- and omega-3 poly-unsaturated fatty acids (PUFAs). Mutants unable to produce such fatty acids appear considerably pressure sensitive (Allen *et al.,* 1999). The production of PUFAs is uncommon in most bacteria, but observed in a high proportion of isolates from low temperature deep sea environments. Conversely to mono-unsaturated fatty acids, they do not appear as a product to piezoadaptation, even if they are involved in such process, but most likely as the result of symbiotic interactions with deep-sea fauna, where they are needed as essential fatty acids. The finding has also a considerable biomedical interest, since they are now largely used as dietary supplements for prevention of human cardiovascular diseases.

One possible explanation for all these structural rearrangements is the maintenance of the membrane within a narrow range of viscosity, according to a process termed "homeoviscous adaptation" (Macdonald and Cossins, 1985). Simultaneously, this would allow the retention of a liquid-crystalline state, in the primary seek for permeability optimization to protons and sodium cations, to optimize bioenergetic processes such as proton translocation and ATP synthesis (van de Vossenberg *et al.,* 1995). Interestingly, comparable effect are observed either in mesophiles when pressure stressed and in barophiles following decompression.

1.2.4 Exposure to high salt concentrations - Halophiles

Mesophile bacteria can survive osmolarities up to 0.85 M NaCl. The class of extremophiles referred to as halophiles is able to thrive salt concentrations ranging from 3 M to saturation of NaCl. Considering the salt content of the sea water, in average equivalent to about 0.5 M NaCl, halophilic Bacteria and Archaea can be isolated in dry areas where evaporation rate is high. The osmotic shock condition generated induces comparable effect as desiccation, and consequences of such a condition are DNA damage, denaturing effect on proteins and an increase in the melt temperature of membranes, resulting in a transition of lipids to the gel phase at a temperature at which they should be in the liquid-crystalline phase. Often, salt requirement and/or tolerance for these microrganisms is strongly affected by growth temperature and, for instance, in certain halophilic archea as *Haloferax volcanii* the minimum and optimum salt concentrations shift to higher values with increasing temperature (Mullakhanbhai and Larsen, 1975). To cope with the high and often oscillating salinity of their environments, the aerobic halophilic bacteria, similarly to all other organisms, need to balance their cytoplasm with the osmotic pressure exerted by the external medium, that prompts dehydration phenomena. These microbes adapt to such a condition usually by reducing water loss and enabling a rapid recovery upon rehydration. The widest salt tolerance up to now referred is described in a Gram-negative bacterium, *Halomonas elongata*, that shows as well the widest range of salt tolerance, ranging between 0.05 M to saturation (Vreeland, 1987). All of the mechanisms employed to achieve a low intracellular ion concentration are based on energy-dependent processes. Despite the external sodium concentration, halophiles keep the cytoplasm relatively free of sodium, that is expelled by active efflux mechanisms. Instead, they use less toxic potassium ions and a wide range of compatible solutes, often zwitterionic organic molecules like glycine betaine, to achieve osmotic equilibration. The internal potassium ion concentration for extreme halophiles can be up to 3 M and is needed to maintain the osmotic pressure in a salty environment (Lai and Gunsalus, 1992). *Halobacterium halobium* can generate an electrochemical proton gradient across the membrane by respiration or by the light driven proton pump bacteriorhodopsin (Murakami and Konishi, 1998). This bacterium is provided with a H^+/Na^+ antiporter that expels sodium ions. On the other hand, specific transport systems are needed to accumulate potassium ions to high intracellular concentrations (Lanyi *et al*., 1976). Nevertheless, a

minimum concentration of Na$^+$ is essential for growth, maybe because of the requirement for Na$^+$ gradients to drive transport processes in the cell membrane.

Osmotic shock induces in cells of mesophilic bacteria the synthesis and intracellular accumulation of the disaccharides sucrose and trehalose, that acts as osmoprotectants in bacteria and yeasts (cfr. 1.2.2 and **Figure 1.2**) (Welsh and Herbert, 1999).

Another effect observed in case of sudden exposure to high salt concentrations is the transient cessation of cell replication. In fact, during the initial phase of the adaptation, protein synthesis and amino acids uptake is inhibited (Ventosa *et al.*, 1998). In *Halomonas elongata,* the production of High-Salt-Related proteins has been reported (Mojica *et al.,* 1997), probably with assistance function towards biochemical process. Membrane-bound enzymes are
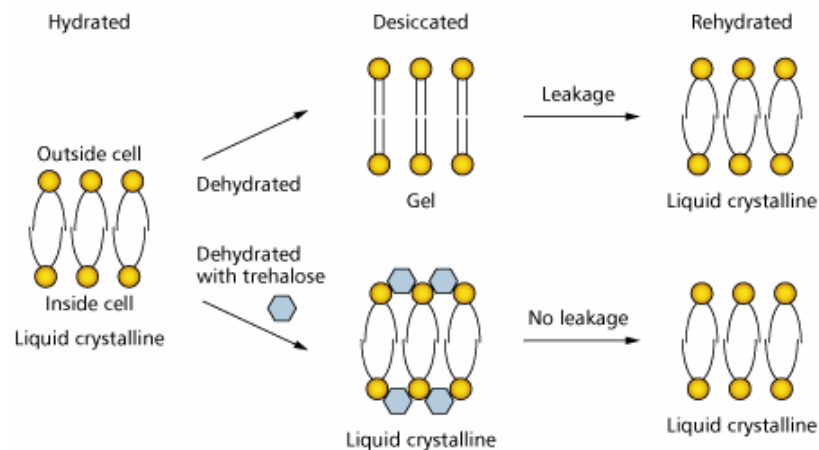
Figure 1.2 - Effect of the disaccharide trehalose on the membrane arrangement in dehydration conditions

strongly effected by salt concentration and its fluctuations, which can lead to misfolding and consequent loss of activity. Strictly halophilic microrganisms produce membrane enzymes requiring high salt concentrations for functioning, *e.i.* the lactate-dehydrogenase from *H. halodenitrificans* (Baxter and Gibbons, 1954) or the alkaline phosphatase of *Pseudomonas halosaccharolytica* (Yamada *et al.,* 1954). In the case of both the alkaline and acid phosphatases from *H. elongata*, it has been detected a sort of adaptation to NaCl concentration, and the enzymes are fully active only at the same growth concentration of the bacterium.

As already said, salinity affects also membranes and, more in general, cell envelope behaviour. The cytoplasmic membrane acts in fact as a barrier between the cytoplasm, low in salt, and the external environment with its high and fluctuating salinity. Then, the properties of this membrane are regulated by the outside salt concentration to adjust such functions as

ion permeability and the activity of the integral membrane proteins. This regulation is performed by adjustments both in the kind of phospholipids, that mainly compose the membranes, and in the nature of their fatty acids. It has been demonstrated that the higher the salinity, the higher is the content of negatively charged phospholipids at the expense of neutral phospholipids. At higher salt concentrations, in fact, the amount the uncharged phospholipids phosphatidylethanolamine (PE) is decreased and there is a concomitant rising in the quantity of charged phospholipids as phosphatidylglycerol (PhG) and diphosphatidylglycerol (cardiolipin, CL) (**Figure 1.3**). The first hypothesis postulated to explain such a phenomenon was that negatively charged phospholipids assured the charge balance at the membrane surface exposed at the high Na^+ concentration. It has been later demonstrated that a significantly lower concentration of ionic groups on the membrane than the one expressed by stressed cells is enough to induce a negative-charge shielding of the membrane (Russel and Kogut, 1985).
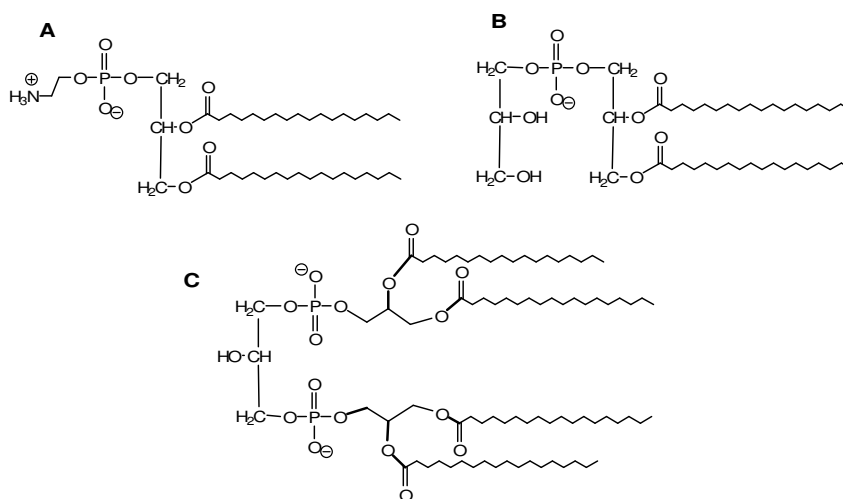
Figure 1.3 - Structure of the membrane phospholipids: **(A)** phosphatidyletanolamine (PE), **(B)** phospatidylglycerol (PhG) and **(C)** cardiolipin (CL).

The second hypothesis postulated a role for these charged phospholipids in the regulation of the selective permeability of membrane to cations. At the moment, the most widely accepted theory is that changes in polar lipids provide a mechanism to preserve the membrane lipid bilayer structure. Studies on membrane templates exploiting liposomes demonstrated that PE, containing unsaturated fatty acids, exhibits the tendency to form nonbilayer phases in saline environments; conversely, PhG forms bilayer. The correct balance in the PE/PhG ratio

is necessary to preserve the integrity of the membrane bilayer in the face of an increased predisposition of PE rich regions of the membrane to form non-bilayer structures when the external salinity raises. The tendency to form such structures could activate specific phospholipids-synthesizing enzymes located in the membrane, resulting in a rise in the proportion of PhG, that prefer the lamellar phase. Moreover, the hydrophilic cell surface makes the cell more attractive to water molecules in a water poor environment, and hydrated cell surfaces may help to obtain cytoplasmic water, thereby preventing desiccation (Hart and Vreeland, 1988). Phospholipid structure in halotolerant bacteria vary also in fatty acid chain structure. In Gram-negative halophiles the content of cyclopropane and unsaturated fatty acids generally increases with salt concentration, with a corresponding decrease in branched fatty acids. Cyclopropane fatty acids are synthesized by addiction of a methyl group donated by *S*-adenosylmethionine across the double bond of a monounsaturated fatty acid by a cyclopropane fatty acid synthetase (Monteoliva-Sanchez *et al.,* 1993). Physical properties of such molecules are intermediate between those of the corresponding saturated isomer and the unsaturated fatty acid from which it was derived. While the monounsaturated fatty acids increase membranes fluidity, an opposite effect is achieved by cyclopropane fatty acids. Therefore, the correct involvement of such fatty acids in the membrane organization is still to be understood.

Comprehension of the mechanisms regulating halotolerance and responses to desiccation stress is an important issue also under a medical point of view. In fact, infectious outbreaks in hospitals of pathologies caused by virulent strains such as *Acinetobacter baumannii* or *Burkholderia cepacia* have been attributed to their ability to survive prolonged periods of desiccation, and thus to counteract osmotic and dehydration shocks (Jawad *et al.,* 1998).

1.2.5 Exposure to organic solvents – Organic Tolerant Bacteria

Many microorganisms, belonging in particular to the Gram-negative family, have been isolated, that are able to cope with toxic organic solvents up to the supersaturating condition, that is in presence of a second phase of the solvent. Organic solvents are naturally present at low concentrations in the environment, and they are normally mineralized by microbial activities. Nowadays, human pollution has generated a number of water and soil sites where these substances can be present at high, sometimes lethal, concentrations. Organic solvents have been used in the past as antimicrobial compounds, but many bacterial strains have developed, thriving with this kind of molecules through a wide set of adaptive responses,

involving changes in the cell morphology and physiology (Ramos *et al.*, 2002; Isken and de Bont, 1998). Because most of these strains require an adaptation period to thrive with this external stressor, they can not be considered strictly extremophiles, and they are referred to as solvent tolerant bacteria. The toxicity of organic solvents towards bacteria relates to their hydrophobicity, that is quantified by the logarithm of the partition coefficient of the compound between *n*-octanol and water (log P_{ow}). Solvents with a log P_{ow} below 4 are considered extremely toxic for the microrganisms, since they are soluble in the bilayers composing the cytoplasmic membrane, where they can accumulate destroying their ordered structure. Damages charging the cell membrane can impair vital functions through the loss of ions, metabolites, lipids and proteins, the dissipation of the physiological pH gradient and electric potential. Typical organic solvents exerting damaging effects on bacterial cells are the aromatics, namely benzene, toluene, styrene, the xylenes and the phenols, as well as long chain alcohols and relatively polar solvents like acetone or ethanol. Solvent tolerance mechanisms have been extensively studied for bacteria belonging to the genus *Pseudomonas*, among which the majority of the resistant strains has been encountered. To stem organic molecules penetration into the cell, changes are observed in the lipid composition of both the cytoplasmic and outer membrane of Gram-negative bacteria. This second possibility does not occur for Gram-positives, and this could be one of the causes at the basis of their minor resistance to organic molecules.

Two major mechanisms for changing fatty acids composition, and thus the fluidity of the lipid bilayer, have been detected: the *cis* to *trans* isomerization of unsaturated fatty acids and the increased synthesis of saturated respect to unsaturated fatty acids. These are sometimes accompanied by a change of FA chain length, aimed to the maintenance of the membrane fluidity. The first mechanism occurs as a short term adaptation, in the first stage of the exposure to organic solvents. Saturated fatty acids are produced in a higher amount in presence of non polar organic substances, whereas polar solvents induce an increase in unsaturation degree (Ingram, 1976; 1977). This device changes the membrane fluidity through the "homeoviscous adaptation" observed also under other types of environmental pressures (cfr. 1.2.3). Small organic molecules have in fact the effect of rising the membrane fluidity, and the isomerization to *trans* of the double bonds counteracts this phenomenon. Chronologically, this is the first response ingenerated in the bacterial cell and, for example, it has been shown that resistant strains of *P. putida* adopt this device within a minute from the initial exposure to solvents (Loffeld and Keweloh, 1996; Ramos *et al.,* 2001). This mechanism allows the cell to first adapt to the new environmental condition, under which the

denser membrane packaging is a selective advantage. The long term response of an increase of the saturated fatty acids content has been observed only in some organic resistant strain, for example after at least 15 min exposure of *P. putida* to *o*-xylene (Pinkart and White, 1997), but there is no evidence of such a process in other *Psudomonas* strains (Ramos *et al.,* 1997). The effect of the increased saturated fatty acid content produces on the membrane status a similar effect of the *trans* isomerisation.

Effects on phospholipids polar heads also modify membrane fluidity, and, as in case of osmotic shock, an increase in the level of PhG and CL is observed at the expenses of PE (Weber, 1996). In this case, this response is related to the higher PhG and CL transition temperature than PE, that decrease the membrane fluidity. In some strains, it is also possible to detect a raise in the turnover rate of the phospholipids, to repair the damage exploited by organic substances. In fact, the limited turnover of the fatty acids metabolism in mutant strains inhibited for this function leads to the formation of blebs on the membrane surface, with consequent loss of integrity of the cell. This has been observed, for example, in *P. putida* strain Idaho, but not in other resistant strains, suggesting that different strains must have developed different mechanisms to adapt to solvent exposure.

Effects correlated to organic solvents exposure can be also detected in the outer membrane constituents. Lipopolysaccharides (LPSs) are the main constituent of Gram-negative Outer Membrane, but their involvement in the adaptation process is only partially investigated (see chapter 5). Nevertheless, it has been noticed that a supplement of Ca^{2+} and Mg^{2+} cations to the culture medium improves bacterial survival. LPSs are likely cross linking these ions thus reducing their electrostatic repulsion and realizing a denser packing of the membrane.

The entrance of toxic molecules into cellular compartments is limited, in many microorganisms, through the development of extrusion mechanisms, based on active transport, to detoxify the cytoplasm. The major group of extrusion mechanisms comprehends the so-called multidrug resistance efflux system (MDR), exploited by several bacteria in order to expel from the cytoplasm many structurally and functionally unrelated toxic compounds (Lomovskaya *et al.*, 1999; 2001). These systems show no substrate specificity and are employed in antibiotic resistance mechanisms as well, since the physical characteristic of the substrate, the Van der Waals interactions they can establish with the active site and the flexibility of these sites determine the substrate selection. MDR transporter have been encountered in several organisms and not only in Gram-negative bacteria. In this latter case, they all belong to the family of the resistance-nodulation-cell division (RND), and expel toxic substances across the cell envelope in a single energy-coupled step (Koronakis *et al.,* 2000).

Structure insights on these proteins are only at an early stage. The most extensive works have dealt with the RND pump from resistant *E. coli* strains, but analogous systems have been found in *P. putida* as well (Kieboom *et al.,* 1998; Kim *et al.,* 1998). The RND pumps are normally made of three components: a cytoplasmic membrane export system that acts as an energy dependent extrusion pump, using the proton motive force as the energy source to export the substrates; a membrane fusion protein, a lipoprotein anchored to the cytoplasmic membrane, and an outer membrane factor, that forms a solvent accessible tunnel spanning both the periplasmic space and the outer membrane.

It was recently demonstrated (Kobayashi *et al.*, 2000) that the solvent tolerant *Pseudomonas* sp. IH-20000 produced membrane vescicles after the addition of toluene to the colture medium. These vescicles are made of phospholipids, lipopolysaccharides and small amount of proteins, and are used to remove the aromatics from the cytoplasmic space, but there is still no evidence that they are formed to remove the toxic substances from the cell.

Finally, a common feature of some organic solvent tolerant bacterium is represented by the metabolic activity developed for some substrates, that can be degraded to non-toxic substances and introduced in other metabolic cycles (cfr. Chapter 5). Although this mechanism can help reducing the toxicity of chemicals, it seems that this is of secondary importance in cells protection. Several organic resistant strains, in fact, show no metabolic activity towards these substances, whereas mutants of the solvent degrading strains knocked out for this mineralizing activity express the same resistance to aromatics than non-degrading strains. Nevertheless, the metabolic pathways developed by organic tolerant microrganisms provide many future perspectives for a possible industrial employment, as well as for their use in bioremediation processes (see 1.3).

1.3 Biotechnological potential of extremophiles

The great pulse received to the study of extremophiles derives in part from their biotechnological and industrial potential. The demand for biocatalysts compatible with the conditions used in industrial processes arises from their higher chemical precision compared to conventional techniques, which could lead to more efficient productions of single stereoisomers, fewer side reactions and a lower environmental impact. Extremophiles proteins and enzymes (also termed "extremozymes"), that can cope with extraordinary reaction

systems, could find application in industry and in the field of bioconversions (see below) (van den Burg, 2003).

Two examples of the huge applicability of extremozymes in widely spread processes are the Taq polymerase from *Thermus aquaticus* and cellulase 103 from alkalophiles isolated from soda lakes. Taq polymerase is the key enzyme of the Polymerase Chain Reaction (PCR), a methodology widely applied in molecular biology, while the cellulase 103 is used as a detergent agent from many industries. Carbohydrate degrading enzymes, such as glucoamylases, xylanases, pullulanases from thermophile microrganisms can be employed in industrial processes working at high temperature, where better solubility of many substrates can be achieved, as well as in food industry. In the same way, analogous enzymes from psychrophiles, acidophiles, alkalophiles, can be adapted to the specific industry requirement. Psychrophile proteases and lipases have a great potential in detergent industry, specially because of the recent efforts to minimize energy consumption associated to cleaning processes. Halophile enzymes have been found of special interest in the development of processes working in aqueous/organic or non-aqueous media. Their use in low-salinity media has been greatly prompted by the exploitation of reverse micelles, where these enzymes are trapped and working.

A special position among the potentially useful extremophiles is occupied by the organic tolerant and degrading microrganisms. These microbes could play a key role in the development of biotechnological processes within the new branch known as "green chemistry". This is the development and application of chemical processes and products to reduce or eliminate the use and generation of substances hazardous to human health and environment. When this aim is pursued through the usage of microrganisms or their enzymatic systems, these techniques define the field of environmental biotechnology, conventionally divided into the three branches of biomonitoring of environmental pollutants, bioconversions and bioremediation of contaminated soils. The biomonitoring accomplishes a preventive function, exploiting specific transcriptional responses of some microorganisms, immobilized in biosensors, to toxic pollutants, *i.e.* heavy metals or polychlorobiphenyls (PCB), in order to evaluate their presence, abundance and availability within the environment.

Bioconversions represent the usage of peculiar metabolic pathways of specific microbes in order to convert toxic substances into products useful for chemical industry, as for example ethanol, acetone and some organic acids. Pharmaceutical industry can as well take advantage from microbial production of some amino-acids, vitamins and antibiotics. The reactions leading to the production of these substances are performed by enzymes, thus assuring

extreme purity, regioselectivity and stereoselectivity of the products in mild reaction conditions.

Finally, bioremediations employ microrganisms, or their enzymatic systems after immobilization in bioreactors, to recover water and soils contaminated by oils or industrial wastes. Many toxic substances of common usage in industry can be recognised as a substrate for the metabolism of microrganisms, particularly belonging to the genus *Pseudomonas*. A great interest is paid to the degradation of the so called "recalcitrant" pollutants, substances exhibiting a strong resistance either to physico-chemical and biological degradation. Among these substances, halogenated or hydroxylated aromatic hydrocarbons, potentially carcinogenic in humans. In *Pseudomonas* sp. OX1, formerly known as *Pseudomonas stutzeri* OX1, particularly toxic phenols and xylenes are digested through a catabolic pathway distinct in two moments, an upper pathway, in which they are transformed in catechols through the action of hydroxylases, and a lower pathway, that produces intermediates directly introduced in the citric acid cycle (see section 5.3).

1.4 Bacterial Cell Envelope: architecture and functions

The architecture of the cell envelope is a peculiar characteristic of the microrganism, and is strictly related to the resistance and survival of the extremophiles in unhospital environments. What is known as the conventional arrangement of the cell membrane can be modified by the occurrence of diverse stressors, depending on the disrupting potential of these. In general, biological membranes are constituted by lipid mono- or bi-layers with polar headgroups oriented towards the water phase and the hydrophobic hydrocarbons chains repelled by water to the interior of the membrane. At the optimal growth temperature of the microrganism, these lipids are in a liquid-cristalline state (Melchior, 1982), which forms a sort of two-dimensional solvent matrix for membranes proteins, as described in the "fluid mosaic" model (Singer and Nicolson, 1972), and at the same time generates and maintains specific solutes concentration gradients across the membrane, indispensable for the correct physiology of the cell. Thus, the maintenance of a correct assembly of the membrane structure appears of vital importance in every microrganism.

In Archaea, the cell membrane is composed, either in mesophilic and in extremophilic strains, by peculiar isoprenoid and isoprenyl glycerol ether-linked lipids (cfr. **Figure 1.1**),

with fully saturated acyl chains (de Rosa *et al.* 1991; Koga *et al.,* 1995; Yamauchi *et al.*; 1995, Kates, 1996, Gulik *et al.,* 1985). The remarkable resistance offered by these lipids to hydrolysis at high temperature and at acidic and alkaline pHs, as well as the production of sort of cell walls, the S-layers (Kandler and König, 1985), have been just proposed as the feature allowing the development of archaeal extremophile strains.

In Bacteria, the cytoplasm is separated from the surrounding environment by a complex series of layers composing the cell envelope. The organisation of such assembly allows the distinction of two different families among the Bacterial domain: Gram-positives and Gram-negatives. In Gram-positive bacteria (**Figure 1.4**), the cytoplasm is separated by the surrounding environment by a cytoplasmic membrane, composed by a lipid bilayer hosting proteins. The cytoplasmic membrane is in turn surrounded by a thick cell wall (20 ÷ 80 nm), the peptidoglycan or murein. From this cell wall, that confers mechanical resistance to the cell, the characteristic Teichoic Acids (TAs) and Lipoteichoic Acids (LTAs) protrude (Fisher, 1990; Archibald *et al.*, 1968), polyanionic molecules endowed with antigenic function. Of these, teichoic acids comprise between 20-50% of the Gram-positive cell wall. While lipoteichoic acids are embedded in the cytoplasmic membrane through a lipid anchor (acylated glycerol), TA are linked directly to muramic acid of the peptidoglycan through a phosphodiester bond (Neuhaus and Baddiley, 2003).
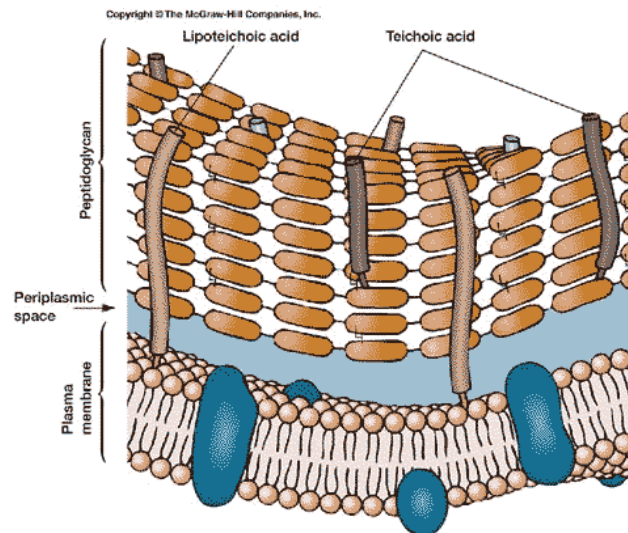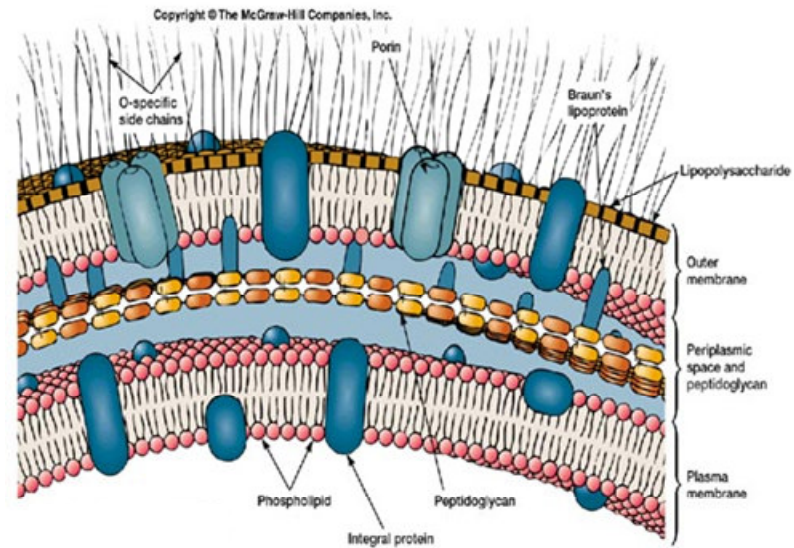

Figure 1.4 – Cell Envelope organization in Gram-positive bacteria

The Cell Wall also constitutes the site of covalent linkages for other polysaccharides, distincted, basing on their structure, in Teichuronic Acids (Hancock and Baddiley, 1985) and other neutral or acidic polysaccharides that cannot be assigned to any of the former groups (Araki and Ito, 1989). Together with the TAs, these polymers are often referred to as "Secondary Cell Wall Polymers" (SCWPs), since they play a secondary role in the assembly of the cell wall. Actually, teichoic acids and teichuronic acids play a pivotal role in the cell physiology. More recent investigations have pointed out the existence of non-classical SCWPs, in correspondence with the bacterial cell surface-layer (S-layers). These are typically composed of protein and glyco-protein species arranging in a regular two-dimensional lattice on the Gram-positive cell surface (Schaffer and Messner, 2005). The S-layers, together with the SCWPs, contribute to the creation of a microenvironment, in which the microrganisms can survive under unfavourable conditions, and are expecially expressed in the extremophile Gram-positive strains.

Differently, in Gram-negative bacteria, the Cell Envelope is composed by a cytoplasmic membrane, composed by glycerophospholipids and organised as in Gram-positive bacteria, surrounded by the peptydoglycan layer. In this case, the thickness of the murein layer is considerably lower (5 ÷ 10 nm) than in Gram-positive bacteria and a second membrane, the Outer Membrane (OM) encloses the cell wall. The OM constitutes a distinctive feature of Gram-negative bacteria, and is connected to the PG layer through peculiar lipoproteins, the Braun Lipoproteins (BLP). The OM has a peculiar asymmetrical organization, and it is made of glycerophospholipids and lipoproteins in the inner leaflet and by Lipopolysaccharides (LPSs) in the outer leaflet. The OM hosts several proteins (Outer Membrane Proteins, OMPs), among which the Porins, responsible for the formation of pores with transport function through the semipermeable membrane (**Figure 1.5**).

The Cell Envelope role in both Archaea and Bacteria is not merely structural. The correct assembly and physiology of the Cell Envelope is primarily associated to the regulation of its permeability by nutrients, ions and toxic substances. Although it behaves like a barrier, in fact, at the same time the permeation of molecules across the membrane is of vital importance to allow changes in the cell composition in response to the external environment and for the physiology of the cell itself. The permeation can occur basically with either active and passive processes. Small hydrophobic molecules, for instance, can move across the lipid bilayers into the cytoplasmic space without any specific transport mechanisms, by what is called the basal permeation process or passive diffusion.

Figure 1.5 - Cell Envelope organization in Gram-negative bacteria

Larger or hydrophobic substances can penetrate the membrane through the pores generated by the Porines, exploiting the facilitated diffusion, whereas ionic substances can employ hydrophilic pores through the membrane (ion channels) that allow the entrance of certain inorganic ions. In general, these channels are quite specific for the type of solute they will transport. Finally, carrier molecules are embedded into the membrane that permeate themselves at a significant rate taking other molecules along in what is referred to as the active transport mechanism.

In case of virulent Gram-positive and Gram-negative bacterial strains, the molecules composing the Cell Envelope are also strictly involved either in the colonisation and infection of the host organisms. In particular, carbohydrate containing molecules can mediate the adhesion and penetration of the microrganism into the host cells and the thrive of microbial colonies through the generation of a matrix (biofilm), where the optimal habitat for the microrganism is preserved. Peptidoglycan, Teichoic acids and Lipoteichoic acids for Gram-positives and Lipopolysaccharides for Gram-negative bacteria are also endowed with antigenic function and are recognised by a pattern of specific receptors of the host immune systems cells.

In order to achieve these functions of transport, protection and virulence, the delicate equilibrium of the cell envelope has to be maintained. To cope with unfriendly external factors, the physical properties of extremophiles membranes have to be preserved against the stressors they have to deal with. To counterbalance the effect of the physical and chemical

stressors, the bacterial cells trigger specific mechanisms, that involve structural changes in the molecules composing the membranes (cfr. 1.2). In the present thesis, the effect of the extreme environments on Gram-negative cell envelope will be investigated, and we will look for the structural peculiarities developed by the Outer Membrane constituents. Thus, particular attention will be paid to the glycolipid fraction composing the most external part of the cell, in the majority of cases the LPSs, given their direct involvement in the interaction with the external environment.

1.5 Lipopolysaccharides: structure and activity

The biological activity of the LPS is strictly connected to its structure. Its typical architecture is organised into three chemically and biogenetically distinct regions. Moving from the inside of the cell, the first portion is represented by the glycolipid moiety termed Lipid A, to which the Core oligosaccharide is covalently linked. In the so called "Smooth-type" LPSs, the Core is in turn glycosylated by a polysaccharide, the O-specific-chain (O-chain), that represents the most variable part of the molecule. These three portion have well distinct structures, activity and biosynthesis, and they can be considered separately (**Figure 1.6**).
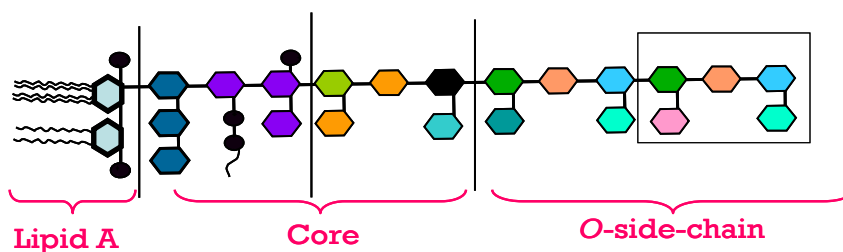
Figure 1.6 - General structure of Smooth type LPS (S-LPS)

1.5.1 The Lipid A

The Lipid A constitutes the most conservative portion of the molecule and it is maintained, with few variations, among the genus (Zähringer *et al.*, 1999). Its typical architecture is made by a disaccharide backbone of 2-amino-2-deoxy-D-glucose (glucosamine, GlcN) connected by a β-(1-6) glycosidic linkage. The reducing GlcN unit, α-configured, (GlcN I) is always phosphorylated at *O*-1, while the non-reducing GlcN (GlcN II) is phosphorylated at *O*-4. Both monosaccharides are variously acylated at *N*-2 and *O*-3 by long chain 3-hydroxy-fatty acids, so-called "primary fatty acids". This terminology allows a distinction from the "secondary"

fatty acids, esters-linked, when present, to the β-hydroxyl groups. The hydrophobic portion of the Lipid A provides the anchorage of LPSs to the Outer Membrane. In general, the Lipid A fraction isolated by single bacterial strains reveals intrinsic heterogeneity, due either to changes in acylation pattern and in the number of phosphate groups, eventually substituted by non acylated glycosyl or non-glycosyl groups, often in non-stoichiometric amounts. As a general feature, the polar substituents of the Lipid A backbone carry negative groups (as phosphate, pyrophosphate, galacturonic acid), positive charges [2-aminoethanol (Etn), 4-deoxy-4-amino-L-arabinopyranose (Ara4N)], or zwitterionic groups, (2-aminoethanolphosphate). Their presence can be considered as a regulating element, affecting the electrostatic interaction of negatively charged residues with divalent cations, such as Ca^{2+} or Mg^{2+} in the medium, as well as a tool for resistance to certain antibiotics.

The number, nature and distribution of the fatty acid chains varies according to the genus, and is responsible of the Lipid A endotoxic activity. LPSs, also known as endotoxins, are in fact recognised by the immune system of the host organism during the infectious events. The Lipid A is the real endotoxic principle of the molecule, and triggers the innate immune response of the infected organism. The innate immune system is the first line of host defence against pathogens, acting in the first stages of the infection (Akira *et al.,* 2006). Different microrganisms are recognised via a limited number of germline-encoded pattern-recognition receptors (PRRs) that identify microbial components, known as Pathogen Associated Molecular Patterns (PAMPs). The PAMPs are specific and vital for the microrganisms, and they can not be altered through a mimic mechanism by the colonising cell. The Lipid A can be considered a PAMP for Gram-negative bacteria. Most of the pathogenic phenomena associated with the infection are induced by the interaction of the Lipid A with a specific receptor, termed Toll-like Receptor 4 (TLR-4), acting as a PRR. This interaction is mediated by several proteins (**Figure 1.7**). Different Gram-negative bacteria produce structurally different Lipid A, varying in their phosphate and acyl pattern. This structural variability is responsible for three-dimensional changes in the overall Lipid A assembly, leading to changes in the induced response of the innate immune system and consequently in the toxicity of the Lipid A itself. It has been observed that the higher acylation degree in the Lipid A family, the higher pathogenic effect is ingenerated in the host immune system, and that asymmetrical fatty acid distribution on the glucosamine backbone considerably increase the toxicity of Lipid A. In the same way, the absence of one phosphate groups on the disaccharide reduces the pathogenicity associated with the microrganism (Seydel *et al.*, 2000).
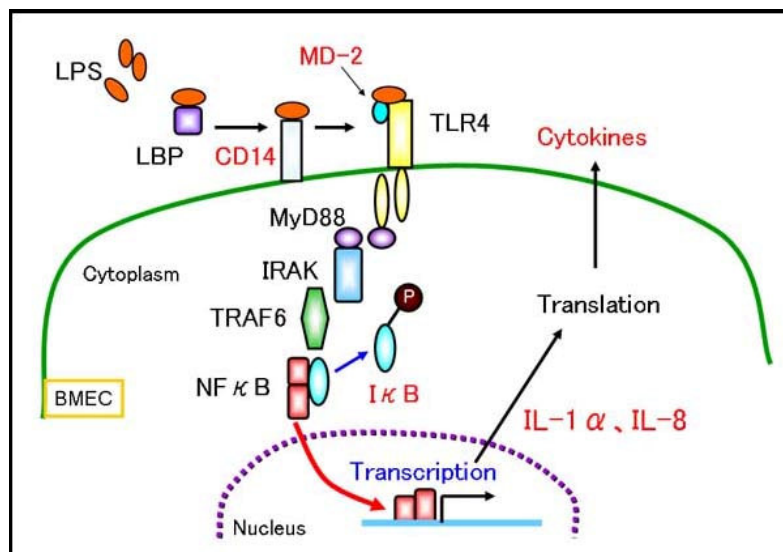
Figure 1.7 - The recognition of LPS by mammal innate immune system

As integrating part of the Outer Membrane, structural changes can occur in Lipid A in response to environmental stressing conditions, mostly for what concerns the fatty acids composition to counterbalance the alterations effected by physical and chemical agents.

1.5.2 The Core oligosaccharide

Covalently linked to the *O*-6 of the GlcN II of the Lipid A disaccharide backbone, the LPS molecule carries the Core oligosaccharide (Holst, 1999). This is an oligosaccharide built of up to 15 monosaccharides, and is characterised by major *intra*-genus variability compared to the Lipid A portion. The classical depiction of the Core realizes a distinction into two zones, the Inner and the Outer Core. The Inner Core is more conservative and characterised by the occurrence of peculiar monosaccharides, whereas the latter hosts a higher structural variability even among the same genus. The structural element common to all bacterial Core oligosaccharides is the occurrence of a distinctive acid monosaccharide, the 3-deoxy-D-*manno*-oct-2-ulopyranosonic acid (Kdo), performing the linkage of the Core to the Lipid A. Up to date, the only case in which the Kdo is quantitatively replaced by its 8-amino derivative, is represented by the Core oligosaccharide from some *Shewanella* strain, as for example in *S. pacifica* (Silipo *et al.,* 2005, cfr. 3.2). In the majority of the cases, indeed, the Core hosts additional Kdo units, as well as other peculiar monosaccharides, the Heptoses, typically in L-*glycero*-D-*manno* configuration (L,D-Hep). Nevertheless, some LPS contain D-*glycero*-D-*manno*-heptopyranoses (D,D-Hep), biosynthetic precursors of the L,D-Hep (Coleman, 1983; Kocsis and Kontrohr, 1984; Ding *et al.*, 1994). Sometimes, these

monosaccharides can even lack within the Core region of LPSs (Vinogradov *et al.*, 1998, 2002; Leone *et al*, 2006, cfr. 5.2.1). Additional Kdo units can sometimes be replaced by the stereochemically similar D-*glycero*-D-*talo*-oct-2-ulopyranosonic acid (Ko), as observed in some *Acinetobacter* (Kawahara *et al.,* 1987) or *Burkholderia* (Kawahara *et al.*, 1994, Silipo *et al.,* 2006) strains.

The Outer Core region usually contains common neutral and acidic monosaccharides, as well as aminosugars. Within the overall Core structure it is possible to find phosphate or pyrophosphate groups, and occasionally non-glycidic substituents like aminoacidic residues. The type and amount of such substituents can vary depending on the strain and on the cultural condition of the bacterium. The occurrence of such groups can, in fact, modulate the global charge density of the molecule, therefore influencing the permeability of the membrane and the complexation capacity respect to ions present in the medium. For this reason, these charged groups are among the first subjects for structure modification of the cell surface during the exposure of the cell to harsh cultural conditions.

The Core of some rough strain, is recognised by the aquired immune system, that develops specific antibodies against epitopes localized within the oligosaccharide, leading to the rise of the immune memory.

1.5.3 The O-specific side chain

Bacterial lipopolysaccharides can be classified into two main categories, the "Rough-type LPSs" (R-LPSs) and the "Smooth-type LPSs" (S-LPSs). The distinction among these two classes arises from the appearance conferred to the surface of the colonies on Agar plates, and is originated by a fundamental structural divergence: in fact, while R-LPSs are composed only by the Lipid A and Core regions, in the S-LPSs it is also possible to detect a distal polysaccharide, protruding from the cell surface towards the external environment. This polysaccharide moiety usually has a regular structure, and is conventionally named O-specific side chain (O-chain, O-polysaccharide). The O-chain constitutes the antigenic determinant of the LPS. Different strains among the same species and genus can, in fact, produce highly different O-polysaccharides, specifically recognised by the host acquired immune system, that produces specific antibodies against them. Structurally, the O-chain can be an omo- or hetero-polysaccharide. The regularity within the structure is provided by the biosynthesis mode, in which oligosaccharide blocks are transferred to a growing polysaccharide chain, and the overall length of the chain can vary considerably among the strains. Bacterial O-

polysaccharides can often contain rare monosaccharides. This has been observed, for instance, in the LPS from *Legionella pneumophila* (Knirel *et al.*, 1997), in which there was the first finding of the acidic monosaccharide termed Legionamminic acid (Leg) or in *Shewanella putrefaciens*, where the Shewanellose (She) was first isolated. (Shashkov *et al.*, 2002) (**Figure 1.8**).
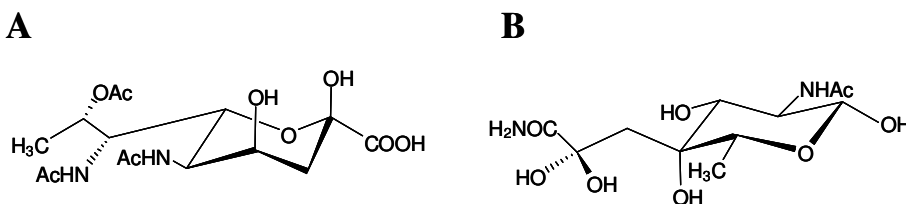
Figure 1.8 - Unusual monosaccharides from bacterial *O*-polysaccharides: (**A**) Legionamminic acid from *Legionella pneumophila* and (**B**) Shewanellose from *Shewanella putrefaciens*

Apart from peculiar sugar residues, bacterial O-polysaccharides can harbour a large number of non-glycidic substituents, including aminoacids and small acyl groups, like acetyl, formyl or pyruvyl groups.

When present, these substituents are strictly correlated to the virulence of the strain. In fact, the introduction of such groups, present in variable percentages within the structure, is a device used by the bacterial cell to elude the host immune systems. For instance, in the pathogen strain *Pseudomonas aeruginosa*, the occurrence of variable amounts of acetyl substituents within the polysaccharide, strongly enhances the infectious power of the bacterium.

Like for the Core and Lipid A, the O-chain is strongly effected by external factors which it directly interacts with. Acidic monosaccharides, as well as non glycidic residues, can be used to regulate the mechanical and reological traits of the Outer Membrane, thus modulating the overall response of the bacterium to the external influences.

1.6 Aims of the work

The biological role of several biomolecules in the adaptation process to several physical and chemical stressors has been extensively studied. Peculiar structural features and/or the triggering of several transcriptional responses have been at the origin of bacterial acclimatization to unfriendly environment, as well as of archaeal flourishing in inhospitable conditions (see 1.2). In particular, Ramos *et al.* reviewed the biochemical responses encountered in Gram-negative cells to face different stressors, focusing on the alterations in

membranes structure and composition and on protein synthesis. Changes occurring in lipids composing the cytoplasmic membrane have been explored, but little is known about the role of Lipopolisaccharides in such processes, although they compose the outermost layer of the cell envelope, thus representing the ultimate barrier of the cell against the external environment. The direct involvement of membrane glycolipids, and in particular LPSs, in the interaction with the surroundings, suggests the existence of a strict correlation between their primary and secondary structure and the survival skills of extremophilic Gram-negatives. In this work, the structure elucidation was performed on LPS and glycolipid fractions extracted from several extremophiles, in order to understand the molecular mechanisms leading to the adaptation to various physical and chemical stressors.

2

Structure Characterization of Glycolipids

2.1 Lipopolisaccharides and Glycolipids extraction

The first step in the understanding of the primary structure of LPSs is represented by their extraction from the intact bacterial cells. This is conventionally achieved through two complementary procedures, that lead to the selective isolation of R-LPS and S-LPS respectively. After the culture, the cells are first treated for the extraction of the Lipooligosaccharide fraction, that, when present, can be isolated through the Petroleum Ether/ Chloroform/ 90 % Phenol (PCP) procedure (Galanos *et al.*, 1969). With this procedure, the lipophilic LOS is extracted within the solvent mixture after cell homogenization. Subsequent to light solvents removal by evaporation, the LOS is precipitated from the residual phenol with water. This procedure allows to obtain the LOS free from other cellular contaminants. After this first extraction, cells undergo a second treatment with 90% Phenol/ Water 1:1, by vol. (Westpahl and Jann, 1965). The two phases recovered from this treatment are extensively dialysed against water and subjected to preliminary purification by enzymatic digestion with nucleases (DNase and RNase) and proteases. The presence of the long O-chain within S-LPSs should induce their solubilization within the water extract, but several factor, as for example the real polysaccharide chain length, the occurrence within the repeating unit of hydrophobic groups as well as charged monosaccharides, can modulate LPS solubility. Thus, it can be detected either in the water or in the phenol extract. The screening for detection of LPS is realized by SDS polyacrylamide electrophoresis gel (PAGE) followed by silver nitrate staining (Kittelberger and Hilbink, 1993). The presence of LPS is testified by the observation of the typical "ladder-like" migration pattern, due to the presence of molecules differing in their structure for the number of repeating units composing the polysaccharide moiety. This natural poly-dispersion of the LPS is related to the biosynthetic origin of such molecules (cfr. 1.5.3), in which the growing polysaccharide is built by insertion of pre-assembled repeating units. Conversely, LOS appear as fast migrating bands at the bottom of the gel, given its low molecular weight. Residual contaminations after the enzymatic treatment can be removed by low pressure chromatography or HPLC, either gel-permeation or ionic exchange based.

The phenol/ water procedure allows the recovering of other kinds of glycolipids as well. For instance, in case of Gram-positive bacteria, this procedure, or its modification employing butanol instead of phenol, is used for recovering Teichoic and Lipoteichoic Acids (see section 4.1). It is demonstrated, in the present thesis, that this method offers a good alternative also for the isolation of glycolipids composing the membranes of LPS deficient Gram-negative bacteria, as observed in the case of *Thermus thermophilus* Samu-Sa1 (see section 4.2).

2.2 Structure determination of Glycolipids

After extraction and purification, the complete structure determination of glycolipids is achieved through a sequence of steps aimed to the definition of the molecular features of both the lipid and saccharidic moiety composing the molecule. During these analyses, the first problem is represented by the poor solubility conferred by the typical amphiphilic nature of glycolipids, that determines the tendency to form micelles and prevents the analyses both in water and in apolar organic solvents. Several strategies have been developed to overcome this obstacle, including the usage of solvent mixtures and chemical modifications or degradation of the molecules to improve dissolution in simple solvent systems. After splitting, the glycidic and lipidic moieties can be studied separately. In case of LPS characterization, the typical approach exploits two complementary procedures, aimed to the determination of Lipid A and oligo- or polysaccharide structures in different moments.

The first technique provides the delipidation of the Lipid A by means of alkaline treatment in two steps. During the first treatment with anhydrous hydrazine, ester-linked primary and secondary fatty acids are removed. Subsequently, stronger hydrolysis with 4M KOH allows removal of amide-linked fatty acids. This approached is generally used for LOSs, since it yields an homogeneous phosphorylated oligosaccharide, comprehensive of the Lipid A saccharidic backbone, that can be easily subjected to chemical and spectroscopical analyses. Obviously, base-labile substituents of glycidic or non-glycidic nature are lost during the work up.

The matching approach for the structure determination is based on mild acid hydrolysis of the LPS. The conditions used have to be chosen carefully, not to completely hydrolyze the acid-labile glycosydic linkages, and the standardized procedure exploits the usage of aqueous 1% acetic acid or 100 mM acetate buffer. This condition is sufficient to cleave the extremely acid-labile glycosidic linkage between the Kdo and the Lipid A, thus releasing the oligo-/poly-saccharide moiety in the water solution. The insoluble Lipid A can then be collected

simply by centrifugation, and this is the standard way to obtain Lipid A samples for further characterisation. A disadvantage of such methodology is that the reducing Kdo unit freed by the hydrolysis establishes an equilibrium among its various conformations (α and β anomers of pyranose and furanose rings, condensed or anhydro forms). This lead to inhomogeneous samples with particularly disadvantageous effects in NMR experiments on short oligosaccharides. Therefore, this procedure is preferred for the structure determination of S-LPSs, since the effects of the reducing end are lost on the overall polysaccharide. Nevertheless, for oligosaccharides structure investigation, the acidic approach can serve as a complement to the alkaline degradation, in order to evaluate the occurrence of base-labile groups lost during the alkaline treatment (i.e. pyrophosphate groups). An alternative approach is based on the usage of milder alkaline conditions, in order to selectively *O*-deacylate the LOS with Hydrazine. Base-labile substituents can mostly survive these conditions, and analyses of the partially degraded molecule can be performed as well, in order to complete the structure depiction of the molecule.

2.3 Structure determination of the glycidic portion

The structure determination of the saccharidic portions so far obtained can be sketched in the following steps:

- Qualitative and quantitative determination of the monosaccharides
- Determination of the absolute configuration
- Determination of the ring sizes
- Determination of the glycosylation sites for each monosaccharide
- Determination of the anomeric configurations
- Analysis of the monosaccharides sequence

Carbohydrates containing molecules, in fact, are characterised by a great structural variability, arising from the large number of possible building blocks composing them, and by the great variety of possible dispositions and conformations they can assume. The first four points in the above scheme are achieved through a large use of analytical techniques based on specific chemical derivatizations and Gas Chromatography (GC). The remaining information is obtained by NMR and MS experiments.

2.3.1 Chemical analyses on oligo-/ poly-saccharides

Chemical analyses by GC and GC-MS on carbohydrates can only be realized after conversion of the monosaccharides into volatiles derivatives. The appropriate choice of the derivatization technique to be employed can highlight specific features of the monosaccharides within the native structure of the molecule.

The quali/quantitative determination of the monosaccharides is achieved by means of two procedures. Treating the polysaccharides with hydrochloric anhydrous methanol leads to solvolysis of the molecule and to the formation of the *O*-methyl glycoside from each monosaccharide. Subsequent acetylation with acetic anhydride in pyridine leads to the production of the peracetylated *O*-methyl glycosides, that can be analysed by GC-MS. This methodology is particularly suitable for labile residues (i.e. Kdo). Comparison of the retention times from the GC analysis and of the fragmentations from the MS spectra with opportune standards leads to the identification of the monosaccharides. Quantification can then be achieved using an internal standard, usually peracetylated inositol.

Due to the acidic nature of the reaction system during the solvolysis, several isomers can form for each monosaccharide (i.e. pyranose and furanose either α and β anomers), and as many peaks are observed in the corresponding chromatogram. Although not severely influencing the identification of the monosaccharides, this can lead to their misquantification.

This puzzling situation does not appear when the monosaccharides are derivatized, after stronger acid hydrolysis with Trifluoroacetic Acid (TFA), as acetylated alditols. In this case, the carbonyl moiety of the free monosaccharides is reduced with $NaBH_4$, thus providing a single molecule for each monosaccharide. Acetylated alditols are then analysed by GC-MS.

The standard GC-MS columns employed in monosaccharide analysis do not allow a distinction between enantiomers. To determine the absolute configuration for each monosaccharide, the sample is solvolysed with an optically pure chiral alcohol, i.e. (+)-2-octanol or (+)-2-buthanol. In this way, enantiomers originate diasteroisomeric molecules that, after acetylation, can be identified by GC-MS.

The last information obtainable through GC-MS concerns the ring size and the glycosylation sites of the monosaccharides. To obtain these data, the oligo/polysaccharide is extensively methylated with CH_3I in DMSO in strongly alkaline conditions. Then, the permethylated oligo-polysaccharide is hydrolysed in acidic conditions and reduced with a marked hydride ($NaBD_4$). The alditols so obtained have free hydroxyl groups at the positions previously involved in glycosydic linkages and cyclization, that can be acetylated. These

derivatives can be analysed by GC-MS and the fragments observed in the MS spectra are diagnostic for specific substitution patterns of acetyl and methoxyl groups, since molecule cleavages preferably occur in correspondence of a methoxyl group, better sustaining the positive charge because of resonance effects. The information obtained from these chemical analyses will help and confirm the interpretation of subsequent NMR and MS experiments.

2.3.2 NMR spectroscopy in oligo-/poly-saccharides structure elucidation

Nuclear Magnetic Resonance has provided the most useful tool in the field of structure determination of carbohydrates. The power of such technique resides in the possibility of analysing the molecules in solution in a native situation, due the good solubility observed for oligo- and poly-saccharides in aqueous systems. In case of the analysis of *O*-deacylated samples, the tendency to form micelles is still observed. The solubility can then be improved by recording the spectra in denaturating conditions, for instance in perdeuterated SDS solutions. During the structure study on a glycolipids, the nuclei usually observed are ^{1}H and ^{13}C, as well as ^{31}P, to detect phosphate groups and unusual phosphorous containing substituents.

A typical ^{1}H-NMR spectrum for an oligo-/polysaccharide can be analysed dividing it into three main zones:

- The region between 5.5 and 4.6 ppm of the anomeric protons signals
- The region between 4.6 and 2.6 ppm of the ring proton signals
- The region between 2.5 and 1.0 ppm of the deoxy positions signals

The region of ring protons signals is considerably narrow, and usually the identification of all chemical shifts is not made possible on the basis of the sole one dimensional analysis. Structure characterization of carbohydrates received a great pulse from the development of two dimensional NMR techniques. In particular, TOCSY and DQF-COSY spectra allow the correct identification and assignment of all ring protons signals and, on the basis of these data, the assignment of all ^{13}C resonances usually follows from the analysis of an ^{1}H,^{13}C-HSQC spectrum. The information provided by the 2D NMR analysis concerns first of all the relative configurations of the monosaccharides. In general, protons orientations on the rings can be deduced by comparison with standard chemical shifts and from the $^3J_{H,H}$ coupling constant values, that follow the Karplus law and assume high values (8 ÷ 10 Hz) in case of *trans*-diaxial orientation of vicinal protons and considerably lower values (< 4Hz) in case of equatorial/axial and *trans*-diequatorial orientation. The values for all ring couplings can be

obtained from the DQF-COSY spectrum, and these may help to recognise the monosaccharides previously identified by means of chemical analyses within the overall structure of the macromolecule. Anomeric proton and carbon chemical shifts are the first hint for the anomeric configuration determination of each monomer, since usually α-configured proton signals appear at lower fields respect to corresponding β-anomers, whereas the opposite situation occurs for carbon chemical shifts. Anomeric configurations are then confirmed by the $^3J_{1,2}$ and by $^1J_{C,H}$ values. This last value is obtained from the HSQC spectrum recorded without decoupling during acquisition. Finally, the *intra*-residue pattern of dipolar correlations gives the last proof for specific configurations: for example, in the 2D NOESY or ROESY spectra, NOE effects between H-1/H-3 and H-5 are univocally diagnostic for a β-*gluco*-configuration. The analysis of the $^1H,^{13}C$-HSQC spectrum allows the full assignment for monosaccharides carbon chemical shifts. The anomeric region, in this case, ranges between 95 and 110 ppm, and α-configured residues are usually characterised by lower carbon chemical shifts. Ring carbons signals appear in the zone of the spectrum between 65 and 85 ppm. A downfield displacement of the resonance of a carbon, in comparison with the standard values, may be originated by an effect known as "glycosiylation shift", namely the shift at higher (2 ÷ 10 ppm) chemical shift values of the carbon signals in correspondence of the glycosylation sites. The extent of such an effect depends on the relative configuration of the glycosylating monosaccharide, and is usually lower for *manno*-configured residues. The detection of these effects is a confirmation of the results obtained from the methylation analysis of the oligo-/polysaccharide. The region among 65 and 60 ppm contains the signals of the CH_2 signals of the primary alcoholic positions of the monosaccharides. DEPT editing of the $^1H,^{13}C$-HSQC spectrum can help individuating such groups, since they appear in antiphase respect to the ring carbinolic protons. The region between 50 and 60 ppm is characteristic for nitrogen-bearing carbons resonances. Thus, the observation of signals in such a zone of the spectrum is a proof of the occurrence of amino-sugars. Finally, at high field, it is possible to observe signals for deoxy groups like the Kdo methylene group or methyl groups of deoxy-sugars or non glycidic substituents.

The confirmation of the cyclization ring dimension is inferred by the observation of *intra*-residual long range correlations in the $^1H,^{13}C$-HMBC spectrum, *i.e.* H-1/C-5 and C-1/H-5 for pyranosidic rings or H-1/C-4 and C-1/H-4 for furanosidic rings. Furanosidic rings are also indicated by a low field displacement of all the ring resonances of the monosaccharide.

Information concerning the sequence of the monosaccharides within the oligosaccharide (or the repeating unit of the polysaccharide) is then deduced from the observation of the *inter*-

residual dipolar correlations in 2D NOESY and ROESY spectra and from the existence of scalar long range correlations, in the ^{1}H,^{13}C-HMBC spectrum, among the ^{1}H and ^{13}C nuclei involved in glycosidic linkages. The arising of Nuclear Overhauser Effect can in fact occur between protons not farer than 5 Å, a requirement satisfied by the protons geminal to a glycosidic linkage. These effects are then diagnostic of the proximity of two monosaccharides, and give the final definition of the structure of the oligosaccharide.

Finally, NMR spectroscopy can help in the understanding of the nature of non-glycosidic substituents within the oligosaccharide, to clarify their structure and their attachment position. Substituent groups containing phosphorous atoms are detected by means of either mono and two-dimensional ^{31}P-NMR spectroscopy. In particular, with the help of a ^{1}H,^{31}P-HSQC spectrum, it is possible to immediately locate phosphorous containing groups within the oligosaccharide structure.

2.3.3 Mass spectrometry in glycolipids structure elucidation

NMR spectroscopy is not the only tool in structure determination of oligo- and polysaccharides. Mass spectrometry constitutes an essential and complementary technique in the understanding of glycolipids, and particularly R-LPSs, primary structure. Apart from the Electronic Impact MS used in GC-MS analyses, techniques allowing the definition of the molecular weight of the intact molecule are particularly useful, since they can provide additional information to the NMR analyses. Oligosaccharides deriving from acid or alkaline degradation of LPS contain a great number of potentially ionising groups (hydroxyl or phosphate functions), thus they are particularly suitable for negative mode ion detection. MALDI-TOF analysis, in particular, gives an ideal profile of the sample by sketching all the molecules composing it, thus providing a picture of the eventual presence of glycoforms differing for the presence of one or more glycidic or non-glycidic residue, removing the need for purification of the single molecular species.

Recently, the possibility of recording MS spectra, and specially MALDI MS spectra, on intact LOS samples has developed. These spectra allow the depiction of the molecular weight comprehensive of the heterogeneity inferred by the Lipid A. The usage of high energy Laser source allows to cleave the labile linkage between the Kdo and the Lipid A, in a similar way to the 1% acetic acid treatment. Combining these data with the MS analysis of the Lipid A portion (see below) it is possible to obtain information on the overall molecule structure without the need of any chemical derivatization.

2.4 Structure determination of the lipidic portion

Like for the structure determination of the glycidic portion, the analysis of the Lipid A and, in general, of the lipidic portion of Glycolipids is achieved through a series of chemical analyses aimed to carbohydrates and fatty acids determination and quantification. Subsequently, these analyses are integrated with NMR and MS data.

2.4.1 Chemical analyses for lipids determination

Monosaccharides, absolute configuration, cyclization and glycosylation sites determination are obtained as previously described for oligo- and polysaccharides. Fatty acids (FAs) determination is usually achieved through GC-MS analysis of their Methyl Ester derivatives (FAMEs). FAs are freed from the molecule either trough solvolysis with hydrochloric methanol, that directly yields the FAMEs, or through acid or alkaline hydrolysis. In this second case, they are converted into their FAME with diazomethane. The choice of hydrolysis conditions allow the selective detection of the linkage type of the fatty acids. For example, ester-linked fatty acids are analysed after selective cleavage of their linkages through an alkaline approach, for instance with CH_3ONa, whereas amide-linked fatty acids are detected by difference on the total fatty acid content, inferred after strong acidic hydrolysis.

2.4.2 NMR analysis of glycolipids

The problem of the poor solubility of Glycolipids introduces some difficulty in the execution of NMR spectra. Lipid A usually shows a discrete solubility in DMSO at relatively high temperatures (~ 40°C). Other glycolipids, for instance the ones isolated from *Thermus thermophilus* SAMU Sa-1 (see 4.2), are better soluble in solvent mixtures, as for example $CHCl_3$/MeOH 1:2, by vol. When the definition of optimal solubility is not possible, chemical derivatization can be used. The analysis of the spectra in solution is then performed as in the case of oligo- and polysaccharides.

2.4.3 MS analyses of Lipid A and Glycolipids

Mass Spectroscopy is the most useful tool in Lipid A and Glycolipids structure determination. After the definition of the saccharidic backbone, in fact, MALDI-TOF or ESI

analyses allow the description of the acylation pattern of the molecule. Also in this case, the chemical nature of these species makes them suitable for negative ionization. Intact Lipid A MS analyses describes the overall molecular weight, but several degradative approaches have been realised to fully describe the acylation profile of the molecule. First of all, Lipid A and Glycolipids can be selectively *O*-deacylated, for example with Hydrazine. MS analysis of the *O*-deacylated products allows the determination of the amide linked fatty acids. More useful in case of Lipid A analysis is the treatment with NH_4OH (Silipo *et al.,* 2002). This procedure selectively cleaves the ester linked acyloxyacyl groups, leaving untouched the amide-linked acyloxyacil groups. MS analysis of the ammonium treated Lipid A allows the detection of the primary and secondary fatty acids present on the amide functions of the GlcN disaccharide. In case of asymmetrical distribution of fatty acids on the backbone, particularly useful is the execution of positive ion MS spectra. The positive ionization can be promoted by removing negatively charged groups, i.e. the phosphate polar heads, by selective treatment with 48% HF. During the execution of positive ion MS spectra, selective ionization after fragmentation of the GlcN backbone occurs, and the oxonium ion is visible only for the non-reducing GlcN (Domon and Costello, 1988). The execution of positive mode spectra on both the intact and ammonium treated Lipid A samples allows the final determination of the structure and of the complete FA acylation pattern.

Other techniques than MALDI-TOF can be very useful in the structure determination of Glycolipids. For instance, high resolution techniques, like the ESI-FT ICR-MS, allow the determination of the exact molecular mass for unknown molecules, and the matching of these data with experimental values provides an uncontrovertable proof of the determined structure.

3

Marine Bacteria

3.1 Introduction

Bacteria are ubiquitous in watery environment. The majority of microrganisms living in marine environment can be considered extremophilic, since they are usually forced to face at least one physical extreme, namely salinity, pressure or high/low temperature. Depending on the specific isolation sites, marine bacteria can thus be classified under the categories previously defined (see. 1.2). Deep-sea microrganisms are usually barophiles and psycrophiles, whereas bacteria living in hydrothermal-vents are obliged barophiles and thermophiles. All of marine bacteria have adapted over millions of years in order to thrive these unusual environments and find a niche for survival. These adaptation provide special significance for biotechnology and evolutionary phylogeny studies and allows us an overlook on evolution, because these bacteria are not only tolerant to many stresses, but many of these deep-sea environment have remained substantially unchanged for eons. Nowadays, great part of the interest about marine bacteria is due to their ability of producing several biologically active molecules, including antibiotics, toxins and antitoxins, antitumor and antimicrobial agents, as well as enzymes with a wide spectrum of action. These bacteria are a rich source of natural products which could be valuable in the drug discovery process within disease areas such as cancer, cardiovascular disease, ageing, obesity, and diabetes. For example, they are the major source of omega-3 and omega-6 fatty acids, which then make their way through the food chain to humans. Moreover, marine bacteria have shown a great biotechnological potential, since many strains exhibit degrading ability towards hydrocarbons (Head *et al.*, 2006).

Gram-negative marine bacteria are heterotrophic aerobic or facultatively anaerobic microrganisms affiliated to the genera *Alteromonas, Pseudoalteromonas, Glaciecola, Idiomarina, Colwellia* and *Shewanella*.

In the present thesis, in particular, we will focus on three members of the genera *Pseudoalteromonas, Shewanella* and *Alteromonas* respectively, all belonging to the Alteromonadaceae family of the γ-subclass of proteobacteria. These bacteria are essential components of marine environments and can be encountered in diverse habitats, including

coastal and open water areas, deep-sea and hydrothermal vents, bottom sediments as well as marine plants and animals, with which they can establish symbiotic interactions. Several polysaccharides, both exopolysaccharides and O-polysaccharides, have been described from *Pseudoalteromonas* bacteria (Nazarenko *et al.*, 2003), and they share the common feature of an acidic character and the presence of unusual sugar and non-sugar substituents, with the absence of any structural similarity of the repeating units. In particular, several unusual uronic and amino-uronic acids have been detected, among which 2,4-diamino-2,4,6-trideoxy-D-glucose (bacillosamine, Hanniffy *et al.,* 1998; 1999) or 2-amino-2,6-dideoxy-D-glucose (quinovosamine, Muldoon *et al.,* 2001), as well as higher monosaccharides like legionamminic acid or its epimers, and their derivatives (5-acetamido-3,5,7,9-tetradeoxy-7-formamido-L-*glycero*-L-*manno*-non-ulosonic acid, Pse5Ac7Fo in *P. distincta* KMM 638) (Muldoon *et al.,* 2001), and non-glycidic decorations like (*R*)-lactic acid, sulphate and glycerophosphate (Gorshkova *et al.,* 1993; 1998; Rougeaux, *et al.,* 1999). Other typical components include various *N*-acyl derivatives of 6-doxyaminosugars.

The genus *Pseudoalteromonas* originates from a revision of the genus *Alteromonas,* first established by Baumann and co-workers (Baumann *et al.,* 1972), that produced the partition of the genus *Alteromonas* in two genera: *Pseudoalteromonas* and *Alteromonas*, (Gauthier *et al.,* 1995). The newly defined *Alteromonas* genus comprises few validly described species, namely *A. macleodii*, *A. marina, A. stellipolaris, A. litorea* and *A. addita*. All of these strains were isolated from extreme environments, e.g. deep-sea hydrothermal vents characterised by high pressures, high-temperature gradient and high concentrations of toxic elements. The newest species added to the genus, *A. addita*, was first isolated from sea water samples collected at various depth in the Pacific Ocean region of Chazma Bay (Sea of Japan), during a study on free-living microbial colonies in radionuclides contaminated environments (Ivanova *et al.*, 2005), and constitutes one of the objects of the present study.

The genus *Shewanella* comprises more than 20 validly described species, including both free-living and symbiotic forms, and members of this family have been isolated from various marine sources, including water, sediments, fish, algae, marine animals and other. They are responsible of the spoilage of the protein-rich foods and two strains, *S. putrefaciens* and *S. algae* (Myers and Nealson, 1990; Semple and Westlake, 1987) are known as opportunistic pathogens of humans and marine animals and recognised as the causative agents of soft tissues bacteremia and sepsis. Their ability to mediate the co-metabolic bioremediation of halogenated organic pollutants and destructive oxidation oxidation of crude petroleum adds to their interest. Members of this genus have also been studied for their involvement in a variety

of anaerobic processes including the dissimilar reduction of manganese and iron oxides, uranium, thiosulphate and elemental sulphur among others. Because of their metabolic versatility and wide distribution in a variety of aquatic habitats, *Shewanella* and related microrganisms play a crucial role in the cycling of organic carbon and other nutrients. O-polysaccharides from *Shewanella* have been isolated and characterised. Also in this case, as for *Pseudoalteromonas*, acidic polysaccharides have been identified, often containing peculiar monosaccharides or acidic non carbohydrate substituents, i.e. the malic acid in the O-polysaccharide from *S. algae* BrY (Vinogradov *et al.,* 2003) or the peculiar monosaccharide Shewanellose, a novel *C*-branched sugar [(2-acetamido-2,6-dideoxy-4-*C*-(3'carboxamide-2',2'-dihydroxypropyl)-D-galactose] first found in the O-polysaccharide from *S. putrefaciens* A6 together with a derivative of the 8-epilegionamminic acid (cfr. 1.5.3) (Shashkov *et al.,* 2002).

In the present section, the structure of the complete R-LPSs from *Shewanella pacifica* strains KMM 3601, KMM 3605 and KMM 3772, from *Alteromonas addita* KMM 3600[T] and of the LOS and LPS from *Pseudoalteromonas issachenkonii* KMM 3549[T] are extensively described.

3.2 *Shewanella pacifica* KMM 3601, KMM 3605 and KMM 3772

The three strains KMM 3601, KMM 3605 and KMM 3772 of the genus *Shewanella* were first isolated from seawater samples collected in Chazma Bay in the Sea of Japan, North-West Pacific Ocean, during the taxonomic survey of free-living microbial populations of the bay, contaminated by radionuclides. During the course of this work, seventy *Shewanella* strains of different phenotypes were isolated, (Ivanova *et al.,* 2003), the majority of which showed high level of 16S rRNA gene sequence identity (99%) to *S. japonica* (Ivanova *et al.,* 2001), skilled with particular metabolic features, e.g. agar-digesting and haemolytic activities, production of PUFA. The analysis of the strains KMM 3601, KMM 3605 and KMM 3772 allowed the assignment of this group of *Shewanella*-like strains to a new species, *Shewanella pacifica* (Ivanova *et al.,* 2004). The LOS fractions from the three strains under examination were extracted from dried cells with the PCP procedure (see 2.1) and purified by means of gel permeation chromatography. The compositional monosaccharide analysis of the LOSs showed the presence of L-*glycero*-D-*manno*-heptose (L,D-Hep) and D-*glycero*-D-*manno*-heptose (D,D-Hep), 2-amino-2-deoxy-D-glucose (D-GlcN), D-glucose (D-Glc) and 8-amino-8-deoxy-*manno*-oct-2-ul-osonic acid (Kdo8N). The presence of this last residue was established

by GC-MS of its acetylated *O*-methyl glycoside derivative which showed the two characteristic fragments (*m/z* 374 and 402, oxonium cations). Moreover, it was detected the presence of D-glyceric acid. Methylation analysis of the de-phosphorylated product showed the presence of terminal-Glc, terminal-Hep, 6-substituted-GlcN, 2-substituted-Hep and 2,6-di-substituted-Hep.

Fatty acids were analysed as their FAME derivatives and identified as (*R*)-3-hydroxytridecanoic acid [C13:0(3-OH)], as major component, both in amide and in ester linkage, and tridecanoic acid (C13:0) present exclusively in ester linkage. In minor amount, C14:0(3-OH), C12:0(3-OH), C14:0, C12:0 and C11:0 fatty acid residues and in addition, *iso*- and *anteiso*-type carbon skeleton C13:0(3-OH) fatty acids were found. Compositional analyses yielded identical results for the LOS fractions isolated from the three bacteria, as well as the NMR spectra on the partially degraded product. Therefore, the structure described belongs indistinctly to the three strains.

3.2.1 Core Oligosaccharide structure elucidation

The Core oligosaccharide was isolated after alkaline degradation of the LOS and was submitted to full 2D NMR and MS analyses. The primary structure of the oligosaccharide was established by ^{1}H, ^{31}P and ^{13}C NMR spectroscopy, as described in chapter 2, and chemical shifts are reported in **Table 3.1**. Anomeric configurations were assigned as described in section 2.3.2, on the basis of the chemical shifts, of $^3J_{1,2}$ values determined from the DQF-COSY experiment and of $^1J_{C,H}$ values deriving from a coupled ^{1}H,^{13}C-HSQC. All sugars were identified as pyranose rings, based on ^{1}H and ^{13}C NMR chemical shifts and on the HMBC spectrum that showed intra-residual scalar connectivity between H-1/C-1 and C-5/H-5 of residues (for Kdo8N from C-2/H-6). In **Figure 3.1** is reported the ^{1}H-NMR spectrum of the oligosaccharide. Six major anomeric signals are identifiable within the anomeric region, relative to six different spin systems referred to as **A-F**. Their identification was possible by the complete assignment of all proton signals and the determination of the $^3J_{H,H}$ vicinal coupling constant values. Residues **A-E** possessed the α-configuration, ($^1J_{C,H}$ = 173 Hz).

In particular, residue **A** was plainly identified as the phosphorylated GlcN I of Lipid A skeleton, because of its chemical shifts and the multiplicity of the anomeric signal (double doublet, $^3J_{1,2}$ = 3.1 Hz and $^3J_{H,P}$ = 7.8 Hz). Spin systems **B-D** possessed low $^3J_{1,2}$ and $^3J_{2,3}$ values, diagnostic of H-2 equatorial orientation, and, starting from H-2 signals, it was possible, by TOCSY spectrum, to assign all the other resonances within the spin systems

leading to identify these three residues as heptoses. Spin system **E** was identified as α-glucose since it had all typical $^3J_{H,H}$ vicinal coupling constant values.
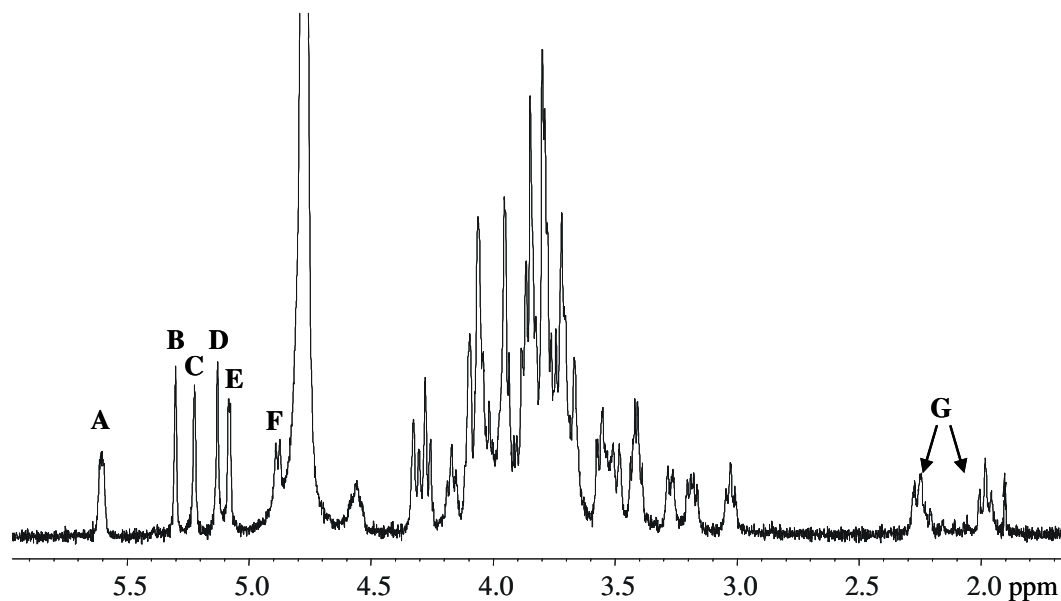
Figure 3.1 - ^{1}H-NMR spectrum of the alkaline degradation product from *Shewanella Pacifica*. Capital letters refer to the identified spin systems described in **Table 3.1.**

Table 3.1 – ^{1}H, ^{13}C (*italic)* and ^{31}P (**bold**) chemical shifts of the oligosaccharide deriving from strong alkaline treatment of the LOS from *Shewanella pacifica*.

Residue	1	2	3	4	5	6	7	8
A	5.531	3.070	3.780	3.434	4.152	3.872/4.290		
6-GlcN	*92.8*	*52.5*	*70.2*	*70.8*	*73.4*	*70.4*		
	2.410							
B	5.308	3.965	3.799	3.860	3.862	4.055	3.720	
2-Hep	*100.1*	*81.2*	*73.1*	*67.6*	*73.1*	*70.3*	*64.2*	
C	5.234	4.104	4.283	3.856	4.066	4.110	3.804/3.822	
2,6-Hep	*100.7*	*82.2*	*73.7*	*68.2*	*70.5*	*79.2*	*63.1*	
D	5.146	4.067	3.854	3.849	3.665	4.018	3.789	
t-Hep	*103.3*	*71.4*	*71.9*	*68.2*	*73.4*	*70.4*	*64.2*	
E	5.097	3.570	3.748	3.420	3.870	3.753/3.800		
t-Glc	*101.8*	*72.8*	*74.9*	*70.9*	*72.9*	*61.7*		
F	4.692	2.880	3.721	3.898	3.531	3.577/3.694		
6-GlcN	*100.9*	*56.8*	*75.1*	*73.5*	*75.3*	*62.7*		
				3.210				
G	-	-	1.980/2.282	4.544	4.342	3.926	3.977	3.196/3.504
5-Kdo8N	*175.0*	*101.7*	*36.1*	*69.9*	*75.2*	*74.6*	*67.1*	*43.9*
				2.000				

To the residue **F** was assigned β-anomeric configuration, on the basis of $^3J_{1,2}$, $^1J_{C,H}$ values (7.8 and 162 Hz, respectively) and, furthermore, ROESY experiment that showed for these sugar residues intra-residual NOE connectivity between H-1 and H-3/H-5 signals. It was identified to be the β-GlcN of Lipid A backbone, since its H-2 was correlated to a nitrogen-bearing carbon signal in the HSQC spectrum (56.8 ppm).

In addition, in the high field region of the spectrum, the characteristic diasterotopic H-3 methylene signals of a Kdo-like residue (residue **G**) were visible at 1.98 ppm (H-3$_{ax}$) and 2.28 ppm (H-3$_{eq}$). The α-configuration was established on the basis of the chemical shifts of the H-3 protons and by the $^3J_{7,8a}$ and $^3J_{7,8b}$ coupling constant values of 7.1 and 3.0 Hz, respectively (Birnbaum *et al.,* 1987; Holst *et al.,* 1994). For residue **G**, in particular, ROESY experiment was useful for the identification of H-6 resonance, given the very low $^3J_{5,6}$ value (less than 1 Hz). A nitrogen-bearing antiphase methylene signal present in the DEPT-HSQC spectrum, correlated with H-8$_a$ and H-8$_b$ of Kdo8N.

By comparison with the ^{13}C chemical shifts of unsubstituted residues, several low-field shifted signals suggested glycosylation, namely, at *O*-6 of residue **A** and **F**, *O*-5 of **G**, *O*-2 of **B** and *O*-2 and O-6 of **C**.

Phosphate substitution was established on the basis of ^{31}P NMR spectroscopy. The ^{31}P-NMR spectrum showed the presence of three monophosphate monoester signals (**Table 3.1**). The site of substitution was inferred by ^{1}H,^{31}P-HSQC spectrum that showed correlations of ^{31}P signals with H-1**A**, H-4**F** and H-4**G**.

The sequence of the monosaccharide residues was determined on the basis of the NOE contacts detected in the ROESY spectrum (**Figure 3.2**), and by ^{1}H,^{13}C-HMBC correlations. The typical Lipid A carbohydrate backbone was eventually assigned on the basis of the NOE signal between H-1**F** and H-6$_{a,b}$**A**. Kdo8N **G** was substituted by heptose **C**, as indicated by the NOE cross peak found between H-1**C** and H-5**G**, and, in addition, between H-1**C** and H-7**G**. Heptose **C** was linked to heptose **D** by *O*-2 since NOE effects between H-1**D** and H-1/H-2**C** were present. **B** residue was linked at *O*-6 of **C**, since its H-1 signal gave a strong NOE cross peak with H-6**C**. Finally, **B** residue was substituted at *O*-2 by glucose **E**, actually, H-1**B** and H-2**B** gave NOE effect with H-1**E**. The ^{1}H,^{13}C-HMBC spectrum contained all the basic scalar correlations to describe the primary structure of the oligosaccharide, namely, H-1/C-1**F** with C-6/H-6**A**, H-1/C-1**C** with C-5/H-5**G**, H-1/C-1**D** with C-2/H-2**C**, H-1/C-1**B** with C-6/H-6**C** and H-1/C-1**E** with C-2/H-2**B**.

The absolute configuration of C-6 carbon of heptoses was established taking into account the diagnostic C-6 chemical shift values of unsubstituted L,D-Hep and D,D-Hep occurring

around 69.0 and 72.0 ppm, respectively (Susskind *et al.,* 1998). Accordingly, the *C*-6 resonances at 70.3 and 70.4 ppm for **B** and **D** residues are in agreement with their L,D configuration. Thus, since in the methylation data a D,D-Hep was detected, it must be identified as **C** residue, the only left heptose spin system. The significant low field displacement of its C-6 signal, 79.2 ppm, is just in agreement with an *O*-6 glycosylated D-*glycero*-D-*manno*-heptose residue. Furthermore, the above NOE contacts found in the ROESY spectrum between **C** and **G** residues are only possible in case of an identical absolute configuration of both residues (Bock *et al.,* 1994). Thus, Kdo8N must possess D-configuration.
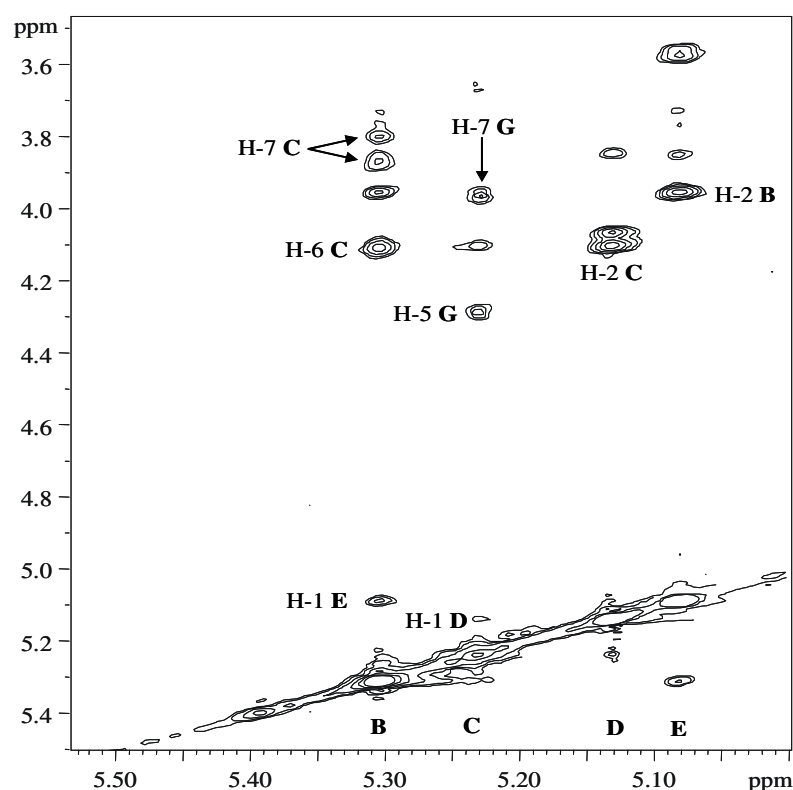
Figure 3.2 - Zoom of the anomeric region of the ROESY spectrum of the oligosaccharide from alkaline degradation of the LOS from *Shewanella pacifica.* Letters refer to the diagnostic *inter*-residual correlations between the spin systems described in **Table 3.1**

In order to confirm these spectroscopical data, the Mosher methodology for the determination of the absolute configuration of chiral alcohols was used. An aliquot of LOS was de-phosphorylated with 48% HF and subsequently treated with 2 M MeOH/HCl, in order to obtain the *O*-methyl glycosides derivatives of the monosaccharides composing the oligosaccharide. The sample was then *N*-acetylated and *O*-deacetylated with NH₄OH, and the *N*-acetyl, *O*-methyl glycosides obtained were separated by reverse phase chromatography. Kdo8N was exclusively recovered as its bicyclo 1,5-lactone derivative, in accordance with

what previously observed for Kdo in the case of acid degradation of Kdo-containing oligosaccharides (Auzanneau, *et al.,* 1988). The characterization of this compound was achieved by means of spectroscopical analyses. In particular, the occurrence of the bicyclic derivative was suggested by the presence in the ^{1}H-NMR spectrum, at 3.178 ppm, of a single signal for the methoxyl group at the anomeric position. Conversely, no signal was detected for the carboxy-methyl group, expected in the case of the monocyclic derivatives. In the ^{1}H-NMR spectrum of this compound (**Figure 3.3)**, the signals for the spin system were clearly recognisable. In order to define the resonances pattern, a COSY spectrum was recorded. The relative configuration of the chiral centres of the bicyclic system was assigned through the detection of the $^{3}J_{H,H}$ coupling constants, deduced from the high resolution ^{1}H-NMR spectrum. To enhance the resolution of the signals and allow the careful determination of these values, the spectrum was recorded in CD_3OD at 281 K.
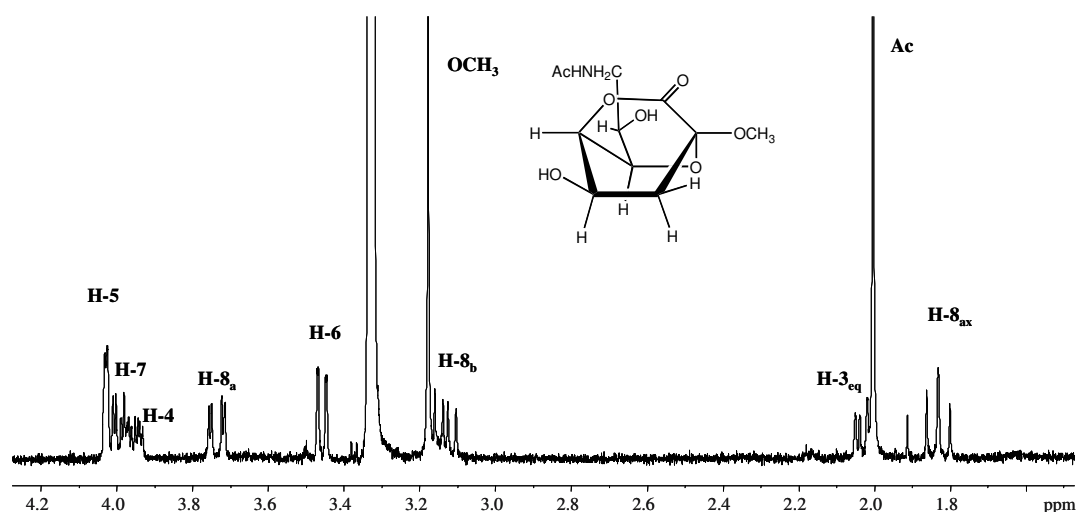
Figure 3.3 – High resolution ^{1}H-NMR spectrum of the 1,5-lactone derived from methanolysis of the LOS from *S.pacifica.* The structure of the molecule is sketched in the figure.

The chemical shifts for this molecule, together with corresponding signal multiplicity and the coupling constant values, are reported in **Table 3.2**, and pointed out the occurrence of the lactone sketched in **Figure 3.3**. In particular, H-4 and H-6 possessed a *pseudo*-axial orientation, whereas H-5 was located in one of the bridging position of the bicyclic system. Thus, the molecule described possessed only two free hydroxyl positions, at C-4 and C-7. The relative configurations pattern, remained then univocally defined. In order to obtain the information about the absolute configuration of this monosaccharide, the Mosher's procedure was applied (Dale and Mosher, 1973).

50

Table 3.2 - ^1H and ^{13}C chemical shifts of the 1,5-lactone derivative of the Kdo8N after methanolysis of the LOS from *Shewanella pacifica*.

| Proton	δ_H (mult)	δ_C
1	-	173.8
2	-	99.8
3_{ax}	1.832 t (12.0)	34.0
3_{eq}	2.029 dd (12.0, 5.0)	34.0
4	3.957 m	67.7
5	4.029 dd (2.4, 1.1)	65.9
6	3.458 dd (1.1, 8.8)	73.9
7	3.993 m	67.1
8_a	3.458 dd (3.5, 13)	43.3
8_b	3.132 dd (7.1, 13)	43.3
OCH_3	3.179 s	50.9
NHAc	2.029 s	22.2 (174.7)[b]

According to this methodology, the absolute configuration of chiral secondary alcohols can be established *via* NMR, after the introduction of a chiral adjuvant ester group. In particular, according to this procedure, the sample was divided into two aliquots and converted into the bis-(*S*)- and bis-(*R*)-α-methoxy-α-trifluoromethyl-phenylacetate (MPTA) esters at *O*-4 and *O*-7 with the corresponding enantiomerically pure chlorides. The absolute configuration at C-4 and C-7 was then independently determined, due the relative location of the two chiral groups and assuming that no relative influence was exerted by the two ester groups upon the intermediate positions. The Mosher methodology has to be applied with special attention if the molecule under analysis contains additional chiral centres or steric constrains, as in the case of carbohydrates. Nevertheless, this procedure had already been applied in the absolute configuration determination of alcoholic groups in monosaccharides (Adinolfi, *et al.,*1998), and its reliability had already been verified. After formation of the MPTA ester derivatives, each aliquot of the sample underwent complete NMR analysis. The chemical shifts for each proton of the bis-(*S*)- and the bis-(*R*)-MPTA ester derivative were assigned and compared. On the basis of these data, the parameter $\Delta\delta_{R-S}$, defined as the chemical shift difference between homologous positions in the two diasteroisomers, could be calculated. These data are reported in **Table 3.3**. Mosher's methodology is based on the assumption that, given the hindrance of the ester group, only one of the possible conformations is in average preferred over the other. From its position in the favoured conformation, the phenyl substituent of the MPTA ester group exerts a shielding or deshielding effect on the vicinal protons. The amount of such effect is different depending on the absolute configuration of the ester substituent, and is quantified by the parameter $\Delta\delta_{R-S}$.

Table 3.3 - [1]H chemical shifts (ppm)[a] and $\Delta\delta_{R\text{-}S}$ for the bis-(*R*)- and bis-(*S*)-MPTA ester derivatives of the 1,5-lactone from Kdo8N.

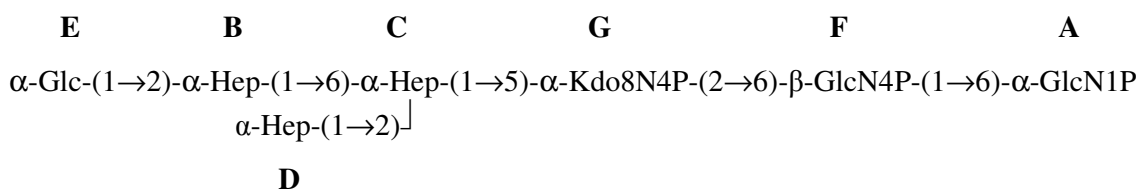| Proton	bis-(*R*)-MPTA	bis-(*S*)-MPTA	$\Delta\delta_{R\text{-}S}$
3_{ax}	2.074	2.172	-0.098
3_{eq}	2.347	2.257	0.090
4	5.418	5.252	0.166
5	4.493	4.044	0.449
6	3.531	3.113	0.418
7	4.363	4.423	-0.060
8_a	3.649	3.714	-0.065
8_b	2.650	2.778	-0.128

The pattern of upfield/downfield displacement of the resonances for each position is then diagnostic of the absolute configuration of the chiral centre. The effects observed on the molecule in the present case are schematized in **Figure 3.4**. As reported in **Table 3.3**, $\Delta\delta_{R\text{-}S} <$ 0 were detected for H-3_{ax} and H-8, whereas H-5 and H-6 exhibited $\Delta\delta_{R\text{-}S} > 0$. As already observed during the analysis of the absolute configuration of the monosaccharide caryophyllose (Adinolfi *et al.,* 1998), the apparent ambiguity regarding the $\Delta\delta_{R\text{-}S}$ value for H-3_{eq} must not surprise, since restrains of the application of the Mosher methodology have to be taken into account when using it for molecules with several chiral centers and in particular for monosaccharides. Previous observations, in fact, already led to conclude that the relative, instead of the absolute, shifts of the NMR signals have to be considered for this class of molecules. Indeed, comparing the $\Delta\delta_{R\text{-}S}$ for H-3_{eq} and for H-5, it is clear that the a more sensitive downfield shift occurs for this latter signal, preventing from misinterpretation of spectral data. Then, on the basis of these values, it is possible to establish the occurrence of *R* configuration at both C-4 and C-7. From this information, the configuration at C-4 and C-7 was established to be *R*. The relative configurations pattern for the remaining ring positions was indeed known on the basis of the spectroscopical analysis performed on the 1,5-lactone of Kdo8N, and the occurrence of *R* configuration was then confirmed also for C-5 and C-6. These values are compatible with a D-*manno*-configuration of the monosaccharide, thus confirming the configuration proposed on the basis of NMR investigation on the oligosaccharide.
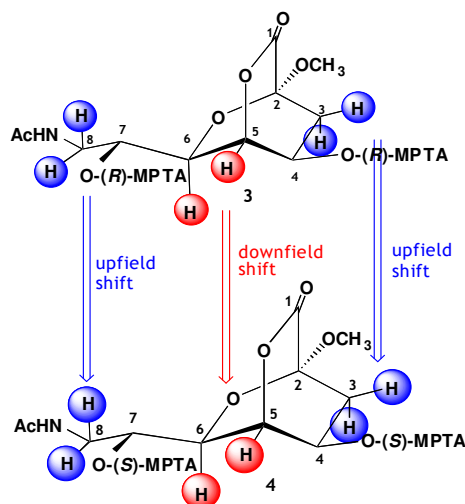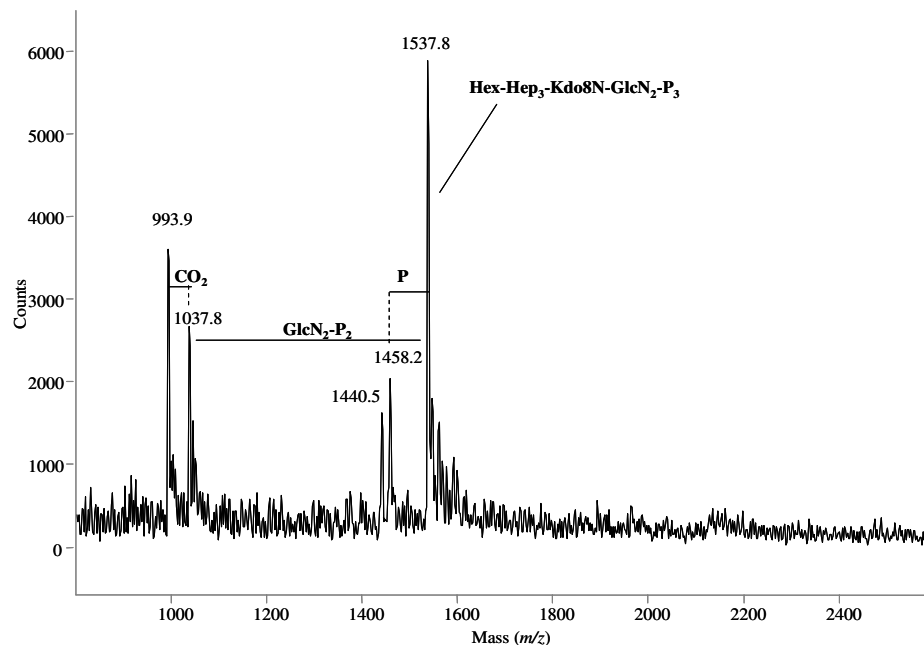
Figure 3.4 - Comparison of the shielding/deshielding effect exerted by (*R*)- and (*S*)-MPTA ester groups on corresponding position of the 1,5-lactone of Kdo8N

The MALDI MS spectrum (**Figure 3**.5) of the fully de-acylated oligosaccharide was in full agreement with the above structural hypothesis since it contained an ion peak at *m/z* 1537.8 matching with the Hex Hep$_3$ Kdo8N Glc$_2$N P_3 structure. Moreover, it showed an additional informative ion peak at *m/z* 1037.8 arising by an in-source β-elimination of Kdo containing oligosaccharide ions (Gibson *et al.,* 1997) (B-type ions, Domon and Costello, 1988), hence, the bis-phosphorylated Lipid A disaccharide is missing in this fragment (Δ*m/z* 500). In the MALDI MS spectrum, a minor ion lacking phosphate, at *m/z* 1458.2, was also visible and, in agreement, in the NMR analysis spin system **G** was also found with an alternative H-4 resonance, at 4.010 ppm, indicative of no phosphate substitution at *O*-4 position.

The finding of this non-phosphorylated Kdo8N residue in the alkaline treated product may be attributed to the occurrence in the intact LOS of a phosphodiester bond at its *O*-4 position that is cleaved under the harsh alkaline conditions (see below). Thus, the primary structure of the oligosaccharide backbone derived by alkaline degradation of the LOS from *S. pacifica* has the following structure:

    E   **B**   **C**   **G**   **F**   **A**

α-Glc-(1→2)-α-Hep-(1→6)-α-Hep-(1→5)-α-Kdo8N4P-(2→6)-β-GlcN4P-(1→6)-α-GlcN1P
               α-Hep-(1→2)⌐

                   D

Figure 3.5 - Negative MALDI MS spectrum of the fully deacylated oligosaccharide from *Shewanella pacifica.*

The detection of the labile substituents lost during the strong alkaline treatment was achieved by submitting a second aliquot of LOS to mild *O*-deacylation with anhydrous hydrazine. The obtained product (de-*O*-LOS) was analysed by chemical analysis, NMR spectroscopy and MS spectrometry. For the execution of NMR spectra, denaturing conditions were applied in order to improve the product solubility and the sample was solved in 1% perdeuterated SDS solution (700 μl), to which 5 μl 32% NH_4OH (pD 9.5) were added. The carbohydrate skeleton of de-*O*-LOS was in full agreement with the oligosaccharide from alkaline treatment, actually seven spin systems were identified, **A'-G'** (**Table 3.4, Figure 3.6**). In analogy with the previous oligosaccharide, all the proton resonances were determined and, by these, all the carbon signals present in the HSQC spectrum were assigned.

Spin system **C'**, identified as 2,6-disubstituted heptose, showed some slight divergence with respect to **C,** concerning chemical shifts of its H/C-6 and H/C-7. The sequence of the oligosaccharide chain was inferred by NOE contacts present in the ROESY spectrum (not shown) where all the diagnostic *inter*-residue cross peaks allowed the assignment of the above Core-Lipid A oligosaccharide structure. Furthermore, few additional spin systems attributable to non carbohydrate substituents were present in the 2D homonuclear NMR spectra.
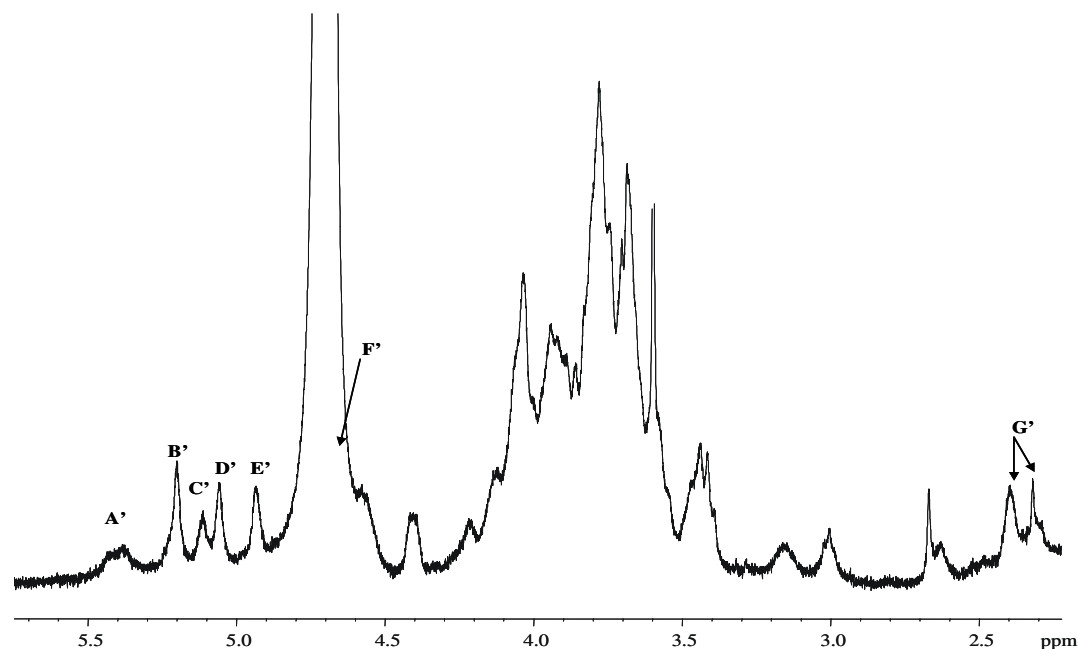
Figure 3.6 - ^{1}H-NMR spectrum in denaturating conditions on the *O*-deacylated LOS from *Shewanella pacifica*

One of these consisted of a hydroxy-methylene signal at 3.89, 3.85/63.9, correlating, in the COSY spectrum, to a carbinolic methine signal at 4.50/77.6 ppm, and since both methylene and methine signals correlated to a carboxyl group in the HMBC spectrum, the presence of glyceric acid was deduced.

Five signals were found in the ^{31}P NMR spectrum which correlated in the ^{1}H,^{31}P-HSQC spectrum with different proton signals (**Figure 3.7**). Three of these were directly assigned to *O*-1**A'**, *O*-4**F'** and *O*-4**G'**, whereas the fourth phosphate group was present as phosphodiester group, since it correlated either with H-7 signal of heptose **C'** and H-2 signal of glyceric acid. Thus, a phosphoglyceric moiety was present and was attached to *O*-7 position of heptose **C'**. The fifth ^{31}P signal, a typical pyrophosphate signal at –11.0 ppm, correlated to a H-4**G'** proton signal and to an ethanolamine spin system, which was also detectable in 2D homonuclear NMR spectra. On this basis, it was possible to conclude that Kdo8N possessed two alternative phosphate substituents at position *O*-4, either a simple phosphate group, or, in minor amount, a pyrophosphoethanolamine group.

In addition to the above discussed NMR signals, the spectra also showed the spin systems attributable to the two acyl chains amide linked to GlcN disaccharide (**Table 3.4**). These fatty acids were analysed by GC-MS of their FAMEs, revealing, as major component, the presence of (*R*)-3-hydroxytridecanoic acid [C13:0(3-OH)] and, in minor amounts, (*R*)-3-hydroxydodecanoic acid [C12:0(3-OH)] and (*R*)-3-hydroxytetradecanoic acid [C14:0(3-OH)].
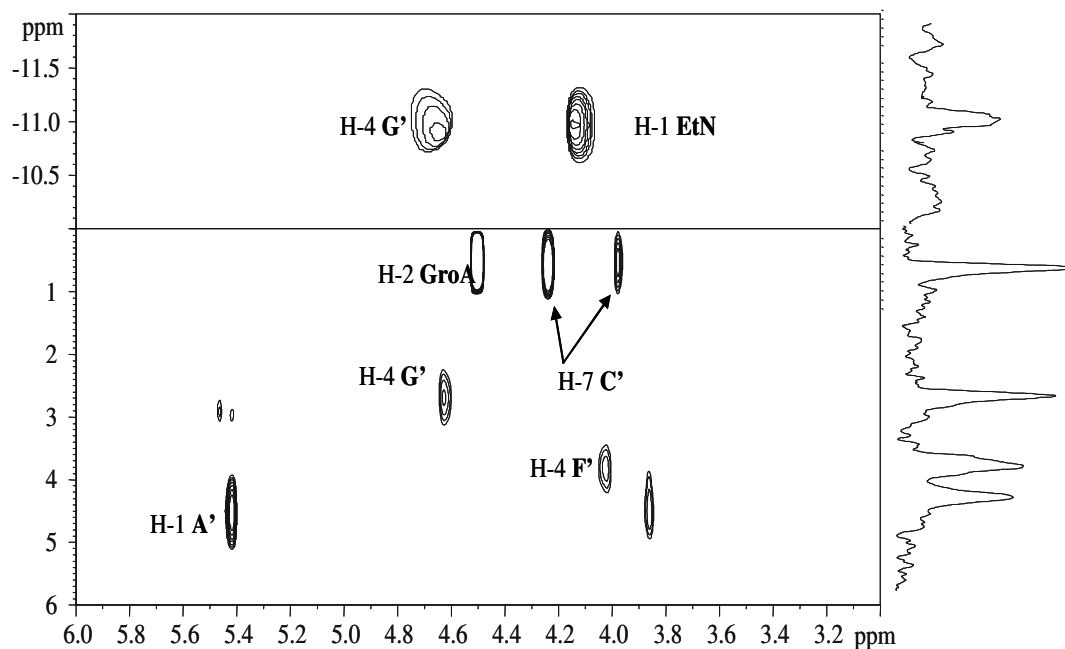
Figure 3.7 - Section of the ¹H,³¹P-HSQC and projection of ³¹P-NMR spectra of the *O*-deacylated oligosaccharide. Cross peaks relevant for the localization of the phosphate groups are indicated with labels referred to **Table 3.2**. EtN is the Ethanolamine residue.

The MALDI MS spectrum (**Figure 3.8a**) of de-*O*-LOS showed various diagnostic ion peaks, in agreement with the above structural hypotheses. The ion at *m/z* 2129.1 was in agreement with the structure bearing two *N*-linked C13:0(3-OH) residues, whereas the ion at *m/z* 1961.0 could be attributed to the same structure lacking the phosphoglyceric moiety. Interestingly, there were no ion peaks attributable to the lack of glyceric acid, suggesting that the phosphate group on the heptose unit, when present, always carries a glyceric acid moiety.
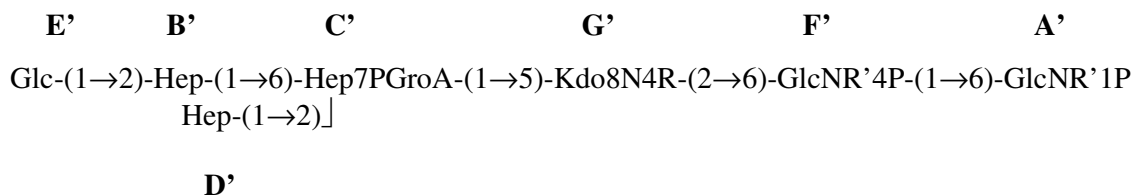
Moreover, as for the first oligosaccharide MS spectrum, ion peaks arising from an in-source β-elimination, as well as the Core and Lipid A fragments signals, were present. The ion at *m/z* 1204.5 and its de-carboxylated derivative were identifiable as the complete core oligosaccharide structure inclusive of phosphorylated Kdo8N, while the structure with the Kdo8N carrying the additional pyrophosphoethanolamine group was in account for the ion at *m/z* 1327.5. As for Lipid A ion peaks, in accord with fatty acid analysis, the one at *m/z* 923.6 was responsible of di-acyl Lipid A possessing the two *N*-acyl C13:0(3-OH) residues. The two other ion peaks, at *m/z* 909.6 and 937.4, could be attributed to minor Lipid A ion species possessing either a C14:0(3-OH) or a C12:0(3-OH) fatty acid residue (Δ*m/z* 14). Accordingly, the two homologue additional ion peaks were also visible as molecular ion peaks of the *O*-deacylated LOS (**Figure 3.8b**).
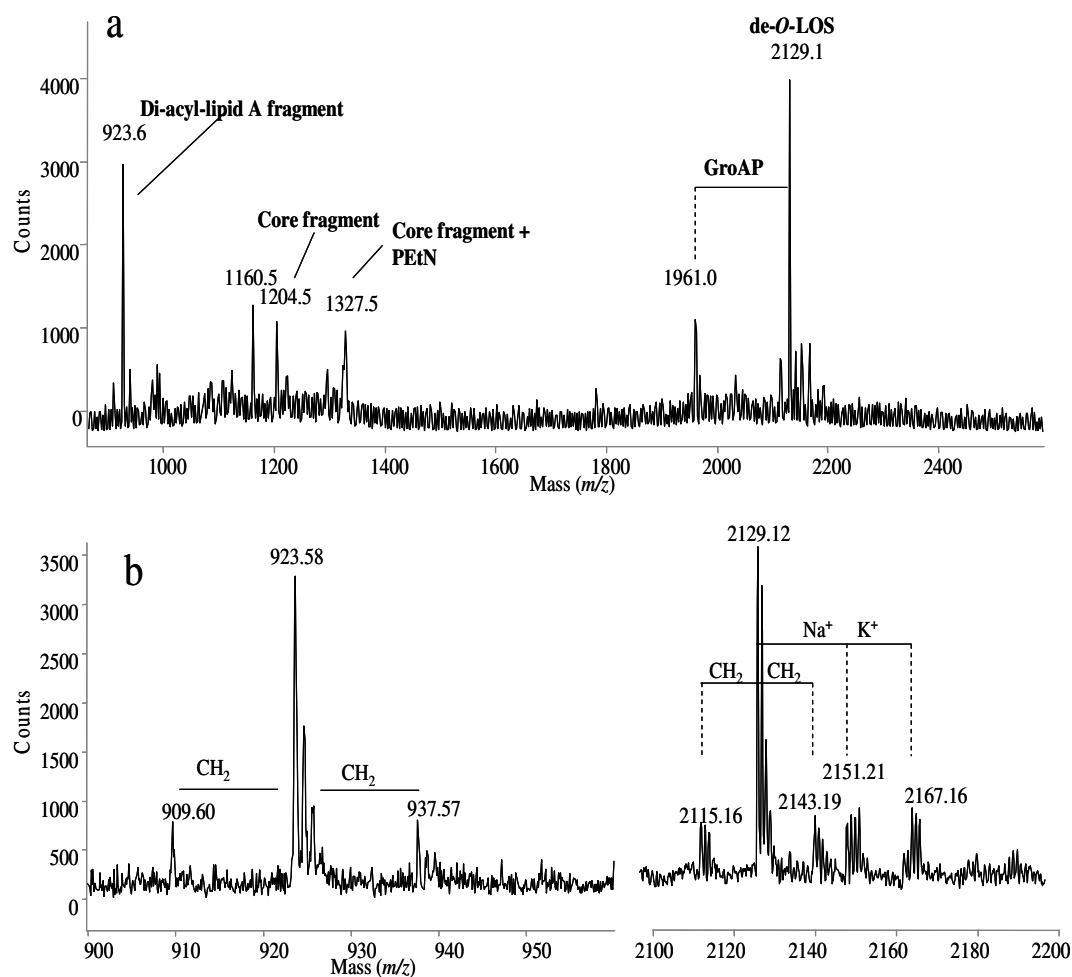
Figure 3.8 - Negative ion MALDI-TOF mass spectrum of **a**) de-O-acylated lipooligosaccharide recorded in linear mode and **b**) sections of the spectrum recorded in reflector mode in which are visible the molecular ions (right) and lipid A fragments (left).

Thus, the LOS obtained after mild alkaline degradation possesses the chemical structure below:

E'   **B'**   **C'**   **G'**   **F'**   **A'**

Glc-(1→2)-Hep-(1→6)-Hep7PGroA-(1→5)-Kdo8N4R-(2→6)-GlcNR'4P-(1→6)-GlcNR'1P
         Hep-(1→2)⌋

         D'

Where R = P or PPEtN and R' = C13:0(3-OH) or one C13:0(3-OH) and one C12:0(3-OH)/ C14:0(3-OH).

57

Table 3.4 - ^{1}H, ^{13}C (*italic*) and ^{31}P (**bold**) chemical shifts of the oligosaccharide deriving from strong alkaline treatment of the LOS from *Shewanella pacifica*.

Residue	1	2	3	4	5	6	7	8
A'	5.498	3.870	3.841	3.522	4.017	3.770/4.172		
6-GlcN	*93.0*	*54.7*	*70.2*	*69.7*	*71.0*	*68.0*		
	4.49							
B'	5.298	3.909	4.155	3.877	3.871	4.043	3.791	
2-Hep	*96.7*	*80.8*	*70.1*	*66.7*	*72.1*	*68.9*	*63.7*	
C'	5.249	4.149	4.039	3.871	3.996	4.152	3.990/4.220	
2,6-Hep	*100.7*	*78.3*	*69.8*	*66.7*	*73.3*	*76.0*	*64.2*	
							0.58	
D'	5.155	4.129	3.965	3.813	3.705	4.051	3.853	
t-Hep	*102.4*	*70.4*	*70.7*	*66.5*	*73.2*	*68.6*	*63.9*	
E'	5.034	3.662	3.771	3.500	3.898	3.810/3.747		
t-Glc	*100.8*	*71.8*	*73.0*	*69.8*	*72.2*	*60.9*		
F'	4.639	3.923	3.914	4.031	3.691	3.560/3.680		
6-GlcN	*100.8*	*55.2*	*73.3*	*73.7*	*74.2*	*62.5*		
				3.85				
G'	-	-	2.340/2.400	4.613	4.275	3.872	3.947	3.057/3.293
5-Kdo8N	*175.0*	*101.7*	*34.4*	*69.3*	*75.2*	*72.1*	*70.4*	*43.5*
				2.30				
	-	4.502	3.850/3.890					
GroA	*173.8*	*77.6*	*63.9*					
			0.58					
	4.093	3.008						
EtNPP	*64.0*	*43.0*						
	-11.0							
C13:0(3-OH)	-	2.481	4.010	1.510				
	174.6	*44.2*	*67.9*	*36.9*				

## 3.2.2 Characterization of the Lipid A

At this stage, the most of the structural elucidation of the LOS from *S. pacifica* was completed, but the full fatty acid distribution on the intact LOS molecule remained to be established. The MALDI MS spectrum (**Figure 3.9a**) of the intact LOS showed, at high molecular masses three patterns of ion peaks assignable to three different molecular species, one being in very major amount. Each pattern of ions contained peaks with difference of 14 Da, in accordance with the presence of different *O*-acyl fatty acids, as already established by compositional analysis. At low molecular masses, the expected fragments arising from bond cleavage between Kdo and the Lipid A moiety were found. The core ion peaks were in complete accordance with the above discussed data, actually the ion at *m/z* 1204.7 and its

decarboxylated derivative were present, and, in minor amount, the peak containing phosphoethanolamine was also visible. Beside the core oligosaccharide ion peaks, the hexa-acyl Lipid A pattern of ion peaks was visible around *m/z* 1741.0. This latter ion, for instance, was identifiable as a bis-phosphorylated glucosamine disaccharide containing as primary fatty acids, two C13:0(3-OH) residues in amide linkage and two C13:0(3-OH) in ester linkage and as secondary fatty acids two C13:0. All the other peaks differed for 14 Da and were attributable to the high heterogeneity of primary and secondary fatty acids which was also reflected in the heterogeneity of molecular ions.

Thus, the major molecular ion peak was endorsed as a hexa-acyl Lipid A while the minor molecular ion species were attributable at a penta-acyl Lipid A lacking an *O*-linked primary fatty acid (ions around *m/z* 2720.5) and a tetra-acyl Lipid A species lacking either an *O*-linked primary fatty acid and a secondary fatty acid (ions around *m/z* 2523.9). The determination of the complete acylation pattern of Lipid A was achieved after isolation of the glycolipid moiety by means of acetate buffer hydrolysis. An aliquot of the obtained Lipid A was then treated by 12% NH_4OH and then analysed via MALDI MS (see 2.4.3). The negative ion mode MALDI mass spectrum (**Figure 3.9b**) showed a pattern of ion peaks, which was straightforwardly attributed. The ion at *m/z* 1107.4 was ascribed to a tri-acylated bis-phosphoryl Lipid A species with two amide-linked 13:0(3-OH) residues, one of which was substituted at *O*-3 position by a secondary 12:0 acyl chain. The other peaks again differed for 14 Da, owing to the presence of fatty acids with different length. The ions at *m/z* 1027.3 and 1041.3 were attributable to the same Lipid A species but lacked a phosphate residue lost during the acid hydrolysis carried out to get the Lipid A. Thus, one of the two secondary fatty acids present in the hexa-acyl species was linked as acyloxyacyl-amide moiety. The other secondary fatty acid must be obviously linked at position *O*-3 of the ester linked primary fatty acids.

The location of these two acyloxyacyl moieties on the disaccharide backbone was established by analysis of the positive ion MALDI-TOF of the de-phosphorylated Lipid A. The spectrum (not shown) contained several pseudomolecular ions [M+Na]$^+$ with the same acylation pattern of the intact Lipid A. At low molecular masses, ion peaks attributable to oxonium ions were present and deriving by the in source cleavage of the glycoside linkage under high power laser settings. The ion at *m/z* 963.9 was consistent with a tetra-acylated oxonium fragment, carrying one residue of GlcN II, two 13:0(3-OH), one 12:0 and one 13:0, thus indicating both the acyloxyacyl amide and acyloxyacyl moieties were located on GlcN II. Oxonium fragments related to the presence of fatty acids with different length (± 14 Da) were

also visible. These data, together with the information previously obtained on the Core oligosaccharide structure, define the complete LOS structure from *Shewanella pacifica*, that can be represented as it follows (Silipo *et al.,* 2005) (**Figure 3.10**).
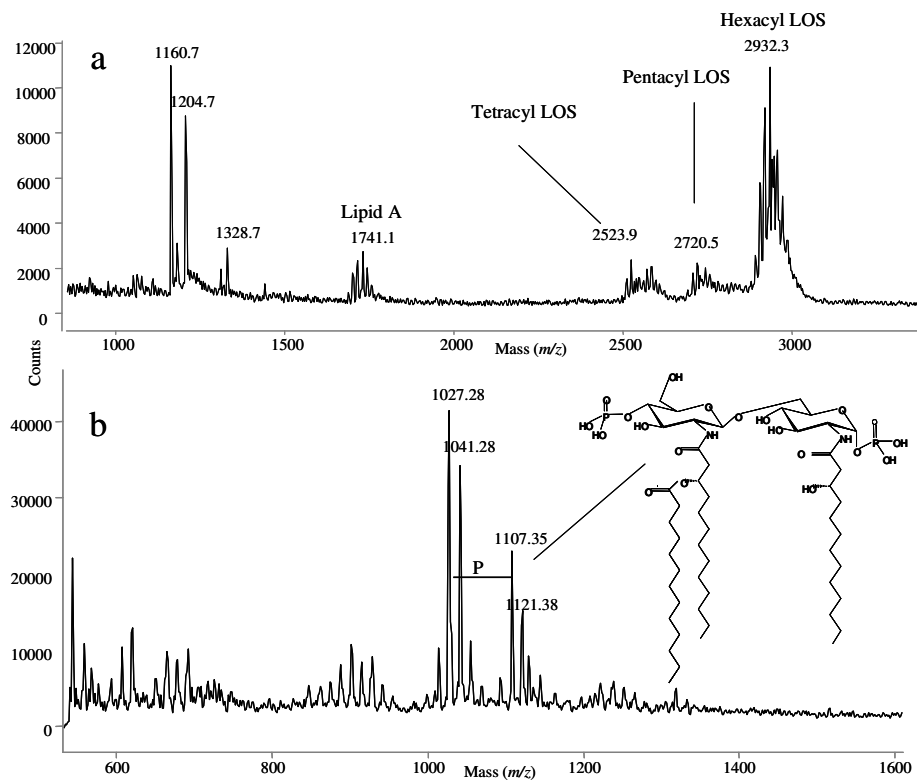
Figure 3.9- Negative ion MALDI-TOF mass spectrum of **a**) intact lipooligosaccharide, and **b**) Ammonium Hydroxide treated Lipid A fraction of *Shewanella pacifica*. The main ion peak at m/z 1107.4 is illustrated.
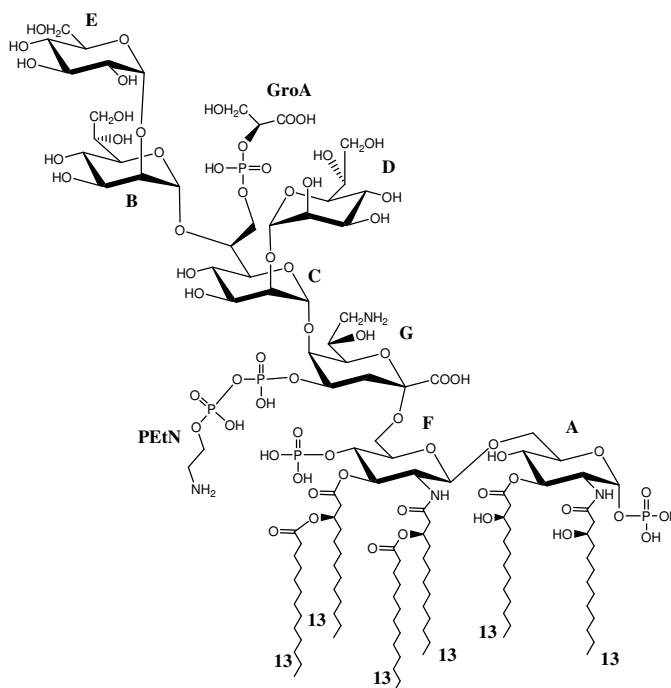
Figure 3.10 - Complete structure of the LOS from *Shewanella pacifica.* Lipid A fatty acids are represented as in the main molecular species. Letters refer to the spin systems described in **Table 3.4**.

3.3 *Alteromonas addita* KMM 3600[T]

Alteromonas addita KMM 3600[T] represents the type strain of the newest species added to the genus *Alteromonas* (Ivanova *et al.*, 2005). Like *Shewanella pacifica,* this Gram-negative bacterium was isolated from sea water samples collected at various depths in the Pacific Ocean region of Chazma Bay (Sea of Japan), during a study on free-living microbial colonies in radionuclides contaminated environments. Although genetically related to the other defined *Alteromonas* species, *A. addita* can be distinguished by a combination of phenotypic, genotypic and phylogenetic characteristics, as for example the range of salinity and temperature growth, the presence of haemolytic activity and the ability to hydrolyse agar. In fact, this microrganism is slightly psycrophilic, showing an optimal growth temperature between 4 and 37°C, is neutrophilic and halophilic. In the present section, the complete structure is described of the LPS fraction isolated from *Alteromonas addita* KMM 3600[T]. As already observed for the only other species belonging to the same genus, *A. macleodii* ATCC 27126[T], this fraction is composed solely by a deep-rough LOS (Liparoti *et al.*, 2006). The occurrence of the short chain LOS is likely in relation to the ability, developed by the genus

Alteromonas, to adapt to harsh marine environments, as the high saline, radionuclides contaminated ones from which this bacterium was isolated.

3.3.1 Core Oligosaccaride structure elucidation

The LOS fraction was extracted from dried cells of *Alteromonas addita* KMM 3600[T] by means of both PCP and phenol/ water extraction. SDS PAGE showed in both cases the occurrence of an identically, fast migrating molecular species, whose chemical composition was determined as previously described, resulting in 6-D-GlcN, t-L,D-Hep, t-D-Glc and 5-Kdo, all in pyranose rings, in the relative ratio 2:1:1:1.

Fatty acids were analysed by GLC-MS of their methyl ester derivatives and were identified as ester linked (*R*)-3-hydroxy-decanoic acid [10:0(3-OH)], (*R*)-3-hydroxy-dodecanoic acid [12:0(3-OH)], (*R*)-3-hydroxy-tridecanoic acid [13:0(3-OH)], dodecanoic acid [12:0] and tetradecanoic acid [14:0] and amide linked (*R*)-3-hydroxy-tetradecanoic acid [14:0(3-OH)]. Minor percentages of [13:0(3-OH)] were also found to be present in amide linkage.

In order to isolate and characterize the oligosaccharide fraction, alkaline treatment with hydrazine followed by strong hydrolysis with KOH was realised in order to *O,N*-deacylate the Lipid A. The ^{1}H-NMR spectrum (**Figure 3.11**) recorded on the oligosaccharide fraction obtained showed a quite simple appearance.
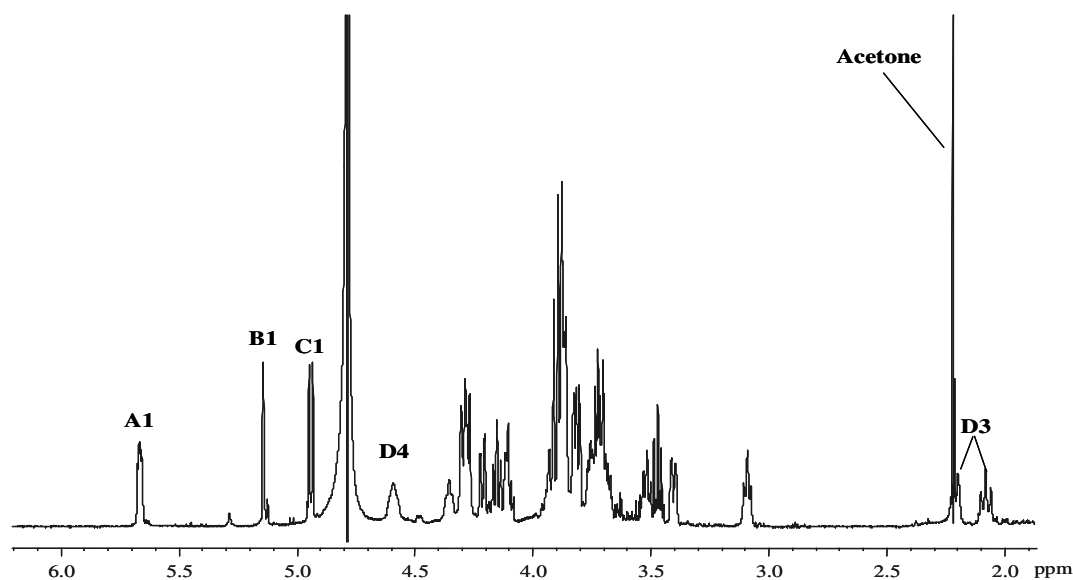
Figure 3.11 - ^{1}H-NMR spectrum of *Alteromonas addita* oligosaccharide obtained after strong alkaline treatment of LOS. Capital letters refer to relevant signals of the spin systems described in **Table 3.5**

Three signals could be easily recognised within the anomeric region of the spectrum (**A-C**, in order of decreasing chemical shift), and allowed the identification of three distinct spin systems. Moreover, at high fields, the typical signals for the diasterotopic methylene group of a Kdo residue (**D**) could be identified, at 2.092 and 2.200 ppm. The full assignment of the proton, carbon and phosphorous resonances for the identified monosaccharides was realised on the basis of a complete set of 2D NMR experiments as described in chapter 2 and in the previous section. All of these data are collected in **Table 3.5**.

The anomeric signal at 5.660 ppm (H-1**A**) appeared, in the ^{1}H-NMR spectrum, as a double doublet, with a $^3J_{1,2}$ = 3.0 Hz, diagnostic of an α-configured residue, and a $^3J_{H,P}$ = 7.9 Hz, suggesting phosphorilation at *O*-1. The *O*-phosphorilation was also confirmed by the observation, in the ^{1}H,^{31}P-HSQC spectrum, of a cross peak with a phosphate signal at 1.46 ppm. Residue **A** was identified as the α-GlcN belonging to the Lipid A disaccharide backbone.
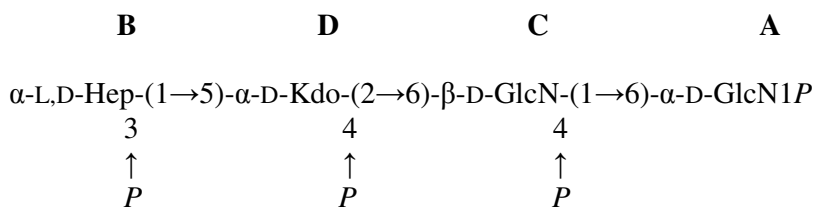
The glycosylation at *O*-6 was proven by the observation of the typical down-field displacement of C-6 resonance (70.2 ppm), in agreement with the methylation data. Anomeric signal H-1**B** appeared as a singlet, due to the small $^3J_{H1,H2}$ value (< 2 Hz). This residue was identified, on the basis of the typical chemical shift values, as the expected L,D-Hep. Moreover, the down-field displacement of H-3 (4.362 ppm), and the existing correlation, in the ^{1}H,^{31}P-HSQC spectrum, with a phosphate group at 1.33 ppm, pointed out the occurrence of phosphorylation at *O*-3. Residue **C** was identified as the non-reducing β-GlcN belonging to the Lipid A backbone on the basis of anomeric and ring proton and carbon chemical shifts and of the high $^3J_{H,H}$ coupling constant values.

Table 3.5 - ^{1}H- ^{13}C- (*italic*) and ^{31}P- (**bold**) NMR chemical shifts of the oligosaccharide obtained by alkaline degradation of the LOS from *Alteromonas addita* KMM 3600^T. Numbers in brackets refer to the Kdo residue.

Residue	1(3$_{ax}$)	2(3$_{eq}$)	3(4)	4(5)	5(6)	6(7)	7(8)
A	5.660	3.404	3.899	3.488	4.160	3.860/4.270	
6-α-GlcN	*91.69*	*55.4*	*69.7*	*71.0*	*73.7*	*70.2*	
	1.46						
B	5.147	4.309	4.362	3.902	4.218	4.117	3.733/3.818
t-α –Hep	*101.5*	*70.3*	*76.8*	*67.1*	*74.4*	*73.5*	*63.3*
			1.33				
C	4.951	3.094	3.877	3.869	3.762	3.523/3.729	
6-β-GlcN	*100.23*	*56.5*	*73.2*	*75.3*	*75.2*	*63.7*	
				1.85			
D	2.092	2.200	4.595	4.283	3.829	3.915	3.693/3.927
5-α-Kdo	*35.1*		*71.5*	*74.4*	*72.8*	*70.7*	*64.7*
			2.03				

The typical *intra*-residual correlations for a residue in β-*gluco* configuration, namely H-1/H-3, H-1/H-5, were observable in the 2D ROESY spectrum. Also in this case, phosphorilation was detected at *O*-4 (δ_P = 1.85 ppm), in accordance with the typical Lipid A backbone architecture. Finally, the resonances for the Kdo residue **D** were fully assigned starting from the high field signals for the methylene group at C-3. On the basis of the chemical shift values found for H-3$_{ax}$ (2.092 ppm) and H-3$_{eq}$ (2.200 ppm), it was possible to establish the α-configuration of this residue.

The signal for H-4 appeared down-field shifted and showed, in the ^{1}H-NMR, a broad appearance, due to the couplings with the protons H-3$_{ax}$, H-3$_{eq}$, H-5 and with a phosphate group. In fact, phosphorylation at *O*-4 was confirmed by the presence of a correlation with a phosphate signal at 2.03 ppm in the ^{1}H,^{31}P-HSQC spectrum. No signal was detected for the Glc residue, expected on the basis of chemical analyses. The monosaccharides sequence within this oligosaccharide was established on the basis of the NOE contacts detected in the 2D ROESY spectrum. The typical Lipid A glucosamine backbone was proven by *inter*-residual NOE correlation between H-1**C** and H-6**A**. The linkage between the heptose residue **B** and *O*-5 of the Kdo **D** was confirmed by the dipolar correlation between H-1**B** and H-5**D** and H-7**D** and, in addition, between H-5 of **B** and H-3$_{ax}$**E**. These NOE contacts are also diagnostic of the D-configuration of the Kdo residue, since they are only possible if the two monosaccharide rings possess the same absolute configuration. On the basis of GC-MS analyses, the absolute configuration of the heptose had already been stated, namely L-*glycero*-D-*manno*-heptose, thus, Kdo **E** must possess D-configuration. Therefore, the structure found so far for the oligosaccharide from *A. addita* KMM 3600^T was the following:

<div align="center">

B   **D**   **C**   **A**

α-L,D-Hep-(1→5)-α-D-Kdo-(2→6)-β-D-GlcN-(1→6)-α-D-GlcN1*P*

3   4   4

↑   ↑   ↑

P   *P*   *P*

</div>

This tetrasaccharide structure found further confirmation in the MALDI spectrum recorded (not shown), in which a peak is visible, at 1072.0 *m/z*, representing the exact molecular mass of the oligosaccharide. Neither NMR or MS data showed signals for the expected glucose residue.

In order to find and locate this monosaccharide, an aliquot of intact LOS was analysed by MALDI MS. The negative ion spectrum (**Figure 3.12**) presented three main ion clusters, all characterised by the typical heterogeneity of the Lipid A, regarding the type and number of fatty acids contained. The most abundant series of signals, around 2236.0 *m/z*, was originated by the intact penta-acyl LOS species. The ion cluster around 2065.5 *m/z* was generated by minor amounts of tetra-acyl LOS.
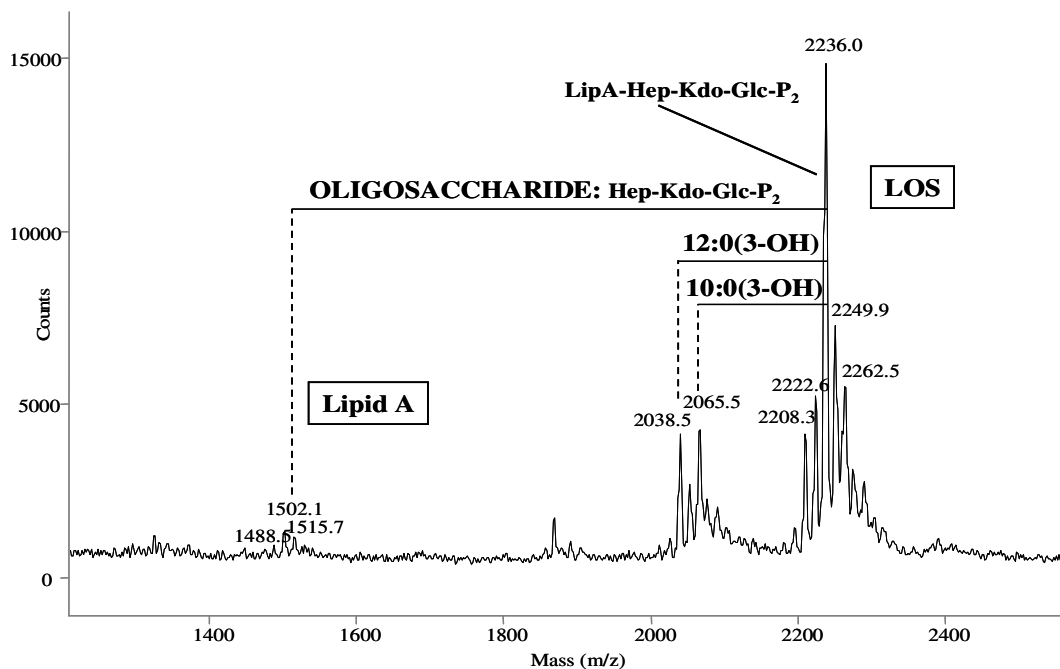
Figure 3.12 - Negative-ion MALDI-TOF mass spectrum of the native lipooligosaccharide fraction from *Alteromonas addita* KMM 3600[T].

Moreover, it was possible to detect the peaks generated by the Lipid A, at 1502.1 *m/z*, due to the in source cleavage of the labile linkage with the Kdo unit (see 2.4.3). This allows the observation of a difference with the peaks of the intact LOS corresponding to the oligosaccharide molecular mass, namely 733.9 *m/z*, corresponding to the structure Kdo-Hep-Glc-P_2. On the basis of these data, it was possible to deduce that the Glc unit, actually present in the intact molecule, was quantitatively lost during the alkaline treatment, and thus connected to the molecule through a more labile linkage. To understand the nature of such a linkage, milder treatment with hydrazine was performed, to selectively *O*-deacylate the sample (de-*O*-LOS). The negative MALDI spectrum recorded on this sample (**Figure 3.13**) showed the peak for the de-*O*-LOS, at 1686.6 *m/z*, together with its Na^+ and K^+ adducts. This molecular weight corresponds to the exact mass of the species composed by $GlcN_2$-Kdo-Hep-

Glc-P_4-[14:0(3-OH)]$_2$. Again, it was possible to detect the peak originated by the *O*-deacylated Lipid A, at 952.1 *m/z*, namely GlcN$_2$-P_2-[14:0(3-OH)]$_2$. One important considerations arising from this data is that the Glc unit, detected in the intact LOS spectrum, is still present in the hydrazine treated sample, and belonged to the Core oligosaccharide. In order to locate it, a full NMR analysis was realised also on this sample. To overcome the poor solubility of the partially acylated sample, these spectra were recorded in denaturating conditions, using a solution of 1 mg/ml perdeuterated SDS in D$_2$O in presence of 5μl 33% NH$_4$OH. In this way, a full series of 2D spectra, namely TOCSY, DQF-COSY, ROESY, ^{1}H,^{13}C-HSQC and ^{1}H,^{31}P-HSQC, could be recorded.
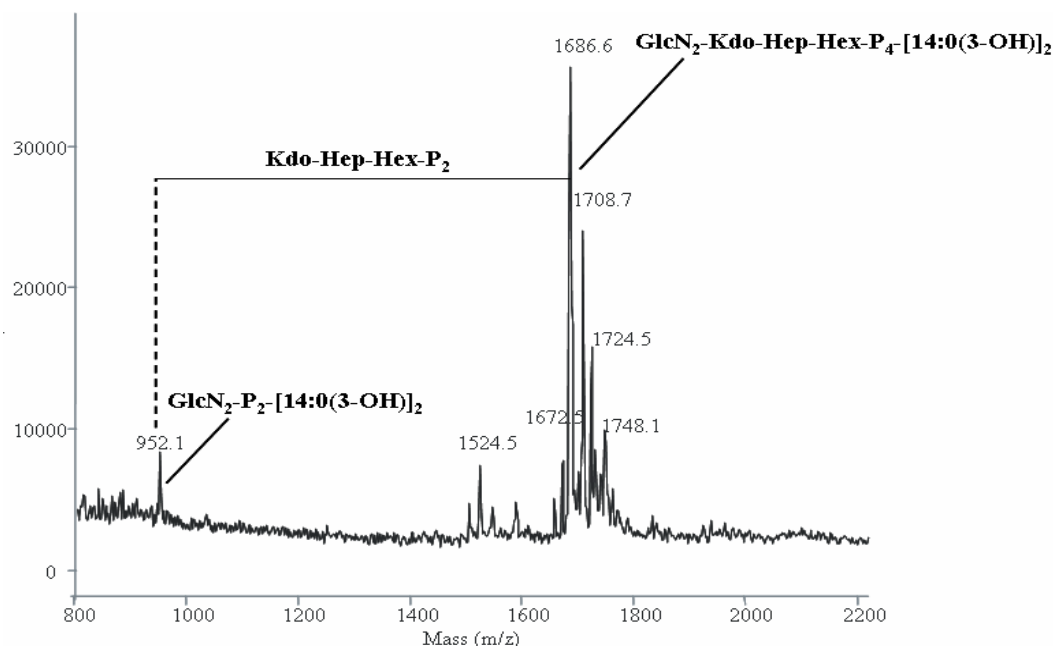
Figure 3.13 - Negative-ion MALDI-TOF mass spectrum of the hydrazine treated lipooligosaccharide fraction from *Alteromonas addita* KMM 3600^T**.**

The ^{1}H-NMR spectrum of the de-*O*-LOS (**Figure 3.14**) showed, within the anomeric region, four signals. The high field signal of the methylene group of the Kdo residue partially merged, in this spectrum, with the signals generated by fatty acid residues. Nevertheless, all chemical shifts could be clearly distinguishable from the 2D spectra. On the basis of the same considerations made for the completely deacylated oligosaccharide, it was possible to fully assign the proton and carbon resonances for the identified spin systems (**Table 3.6**). The residues **A**, **B**, **C** and **D** were respectively identified as the corresponding spin systems in the previously analysed oligosaccharide. The anomeric signal at 5.511 ppm (H-1**E**) appeared as a

double doublet with $^3J_{1,2} = 3.0$ Hz, diagnostic of an α-configured residue, and a $^3J_{H,P} = 7.9$ Hz. On the basis of the chemical shift values, the residue was recognised as the expected α-Glc, and the *O*-phosphorylation at the anomeric position suggested the occurrence of a phosphodiester bridge connecting this residue to the oligosaccharide.
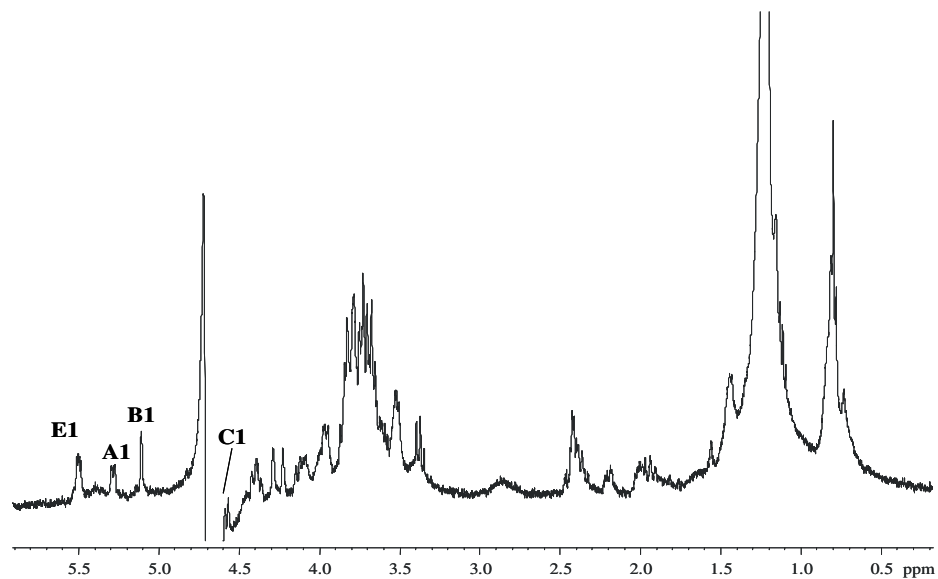
Figure 3.14 - ^{1}H-NMR spectrum recorded in denaturating conditions on the hydrazine treated Lipooligosaccharide fraction from *Alteromonas addita* KMM 3600^T. Capital letters refer to the identified spin systems described in **Table 3.6**
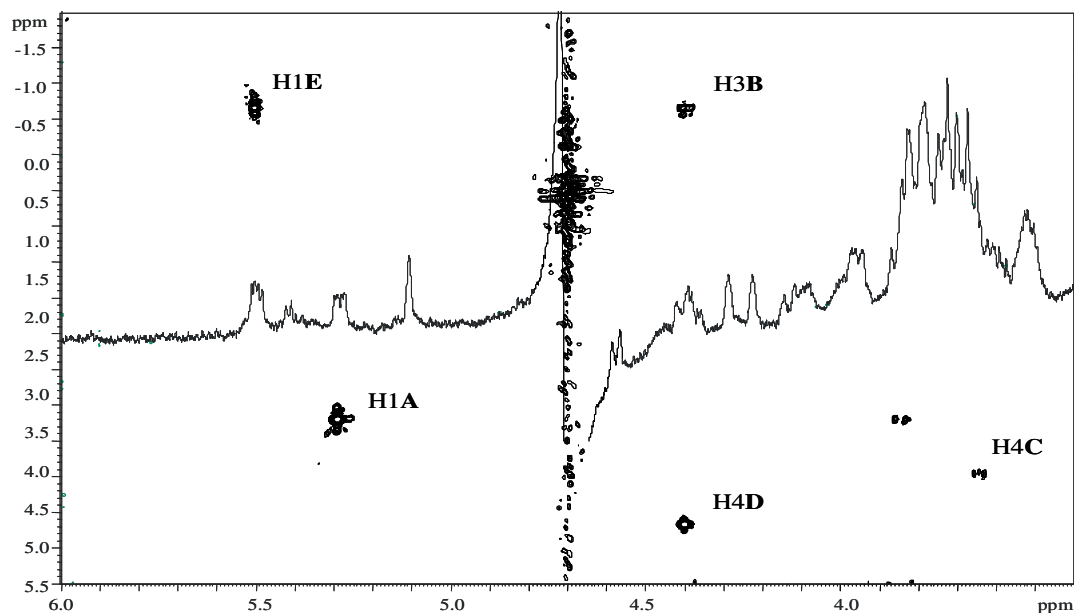
Figure 3.15 - Zoom of the ^{1}H,^{31}P-HSQC spectrum and, overlaied, of the 1H-NMR spectrum of the *O*-deacylated LOS fraction from *Alteromonas addita* KMM 3600^T. The spectrum shows cross peaks relevant for the localization of the phosphate groups on the residues described in **Table 3.4.**

This hypothesis was confirmed by the observation, in the ^{1}H,^{31}P-HSQC spectrum (**Figure 3.15**), of a cross peak with the phosphate group signal at -1.18 ppm, in turn correlating with the proton at 4.403 ppm, namely H-3 of the Hep residue **B**. This phosphodiester linkage was cleaved by the strong alkaline treatment leaving the phosphate group attached to the Hep residue, and originating the previously observed oligosaccharide.

Thus, the complete structure of the oligosaccharide from *Alteromonas addita* R10SW13^T can be represented as it follows:

```
        B               D               C               A

α-L,D-Hep-(1→5)-α-D-Kdo-(2→6)-β-D-GlcN-(1→6)-α-D-GlcN1P
        3               4               4
        ↑               ↑               ↑
α-D-Glc-(1→P            P               P

    E
```
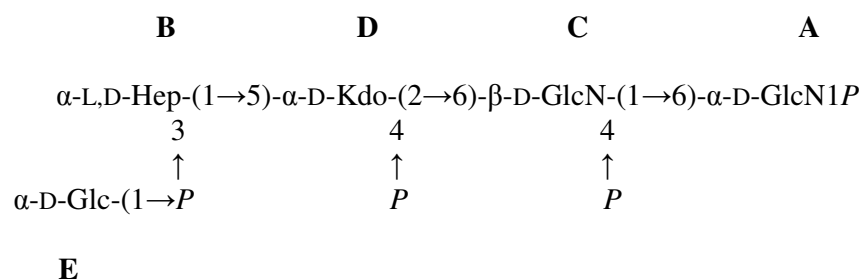
The occurrence of a phosphodiester bridge connecting two monosaccharide residues is a rare but not unique feature of the Core region of bacterial LPSs. It was, in fact, already detected in the oligosaccharides from the LPSs of *Shewanella oneidensis* (Vinogradov *et al.,*

Table 3.6 - ^{1}H- ^{13}C- (**bold**) and ^{31}P- (*italic*) NMR chemical shifts of the *O*-deacilated LOS from *Alteromonas addita* KMM 3600^T obtained by mild alkaline degradation. Numbers in brakets refer to the Kdo residue.

Residue	1(3$_{ax}$)	2(3$_{eq}$)	3(4)	4(5)	5(6)	6(7)	7(8)
A	5.297	3.841	3.710	3.515	3.956	4.141/3.825	
6-α-GlcN	*92.4*	*54.1*	*71.4*	*69.7*	*71.1*	*68.2*	
	3.18						
B	5.111	4.292	4.401	3.759	4.095	3.641	3.764/3.648
t-α-Hep	*99.9*	*69.2*	*76.1*	*66.4*	*71.4*	*73.2*	*61.9*
			-1.18				
C	4.576	3.755	3.636	3.718	3.758	3.692/3.533	
6-β-GlcN	*100.4*	*54.9*	*74.4*	*74.7*	*73.0*	*62.9*	
				3.94			
D	1.930	2.200	4.476	4.231	3.842	3.793	3.645
5-α-Kdo	*34.5*		*68.6*	*72.6*	*71.9*	*70.4*	*63.8*
			4.74				
E	5.511	3.522	3.677	3.383	3.826	3.660/3.772	
t-α-Glc	*95.7*	*71.4*	*73.2*	*69.5*	*73.2*	*61.8*	
	-1.18						

2003) and of *Arenibacter certesii* (Silipo *et al.,* 2005), both isolated from marine environments. Thus, it seems likely that the introduction of such a structure peculiarity may occur as an adaptative response to the inhospitable marine habitat.

3.3.2 Characterization of the Lipid A

In order to isolate the Lipid A moiety from the LOS of *Alteromonas addita* KMM 3600[T], an aliquot of the sample was hydrolysed in mild acid conditions with acetate buffer. The Lipid A fraction was then collected as precipitate by centrifugation and analysed by mass spectrometry. The negative-ion MALDI-TOF spectrum (**Figure 3.16**) showed two distinct ion clusters (**1-2**). The most abundant species (**1**) was represented by the main ion peak at *m/z* 1501.9, that was in account for two glucosamines, two phosphate groups (P), two 14:0(3-OH) one 12:0(3-OH), one 10:0(3-OH) and one 12:0 residue. This penta-acylated species represents the most abundant form of the Lipid A family from *A. addita* KMM 3600[T]. Ion peaks, differing by 14 and 28 Da, were detectable, caused by diverse fatty acids chain lengths and explained on the basis of the previous chemical analysis. A minor amount of mono-phosphoryl penta-acyl Lipid A was present as well, in which the peaks differed from the related species in the main cluster by $\Delta m/z = 80$, a phosphate group. This species was an artefact produced during the hydrolysis to obtained the Lipid A, since mass differences of 80 Da were not detected either in MS analysis of the intact LOS and of the de-*O*-LOS. The proposed molecular formulas corresponding to the ion peaks are collected in **Table 3.7**.
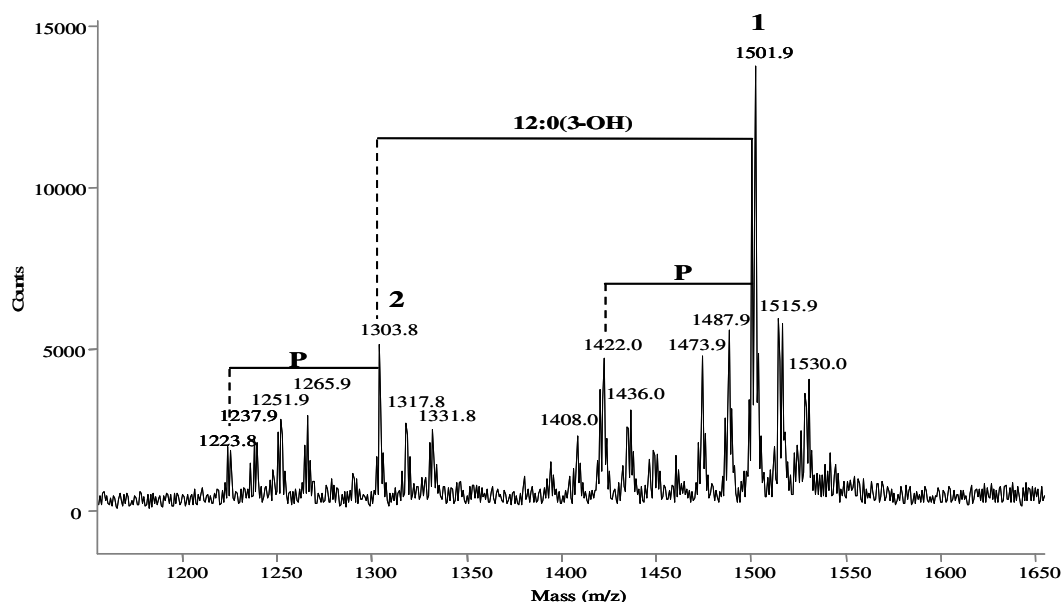
Figure 3.16 - Negative-ion MALDI mass spectrum of the intact Lipid A fraction from *Alteromonas addita* KMM 3600[T]. Numbers refer to the relevant ion peak clusters described in **Table 1** and in the text.

Species **2** was identified as the tetra-acyl Lipid A, and the main peak at *m/z* 1303.8 differed from the peak at *m/z* 1501.9 for the absence of the 12:0(3-OH) residue.

Table 3.7 - Proposed acyl and phosphate content of the molecular species composing the Lipid A fraction from *Alteromonas addita* KMM 3600^T.

Observed ion (*m/z*)	Species	Fatty acids and phosphate substitution
1501.9	**1**	GlcN$_2$-P$_2$-[14:0(3-OH)]$_2$-12:0(3-OH)-10:0(3-OH)-12:0
1515.9	**1**	GlcN$_2$-P$_2$-[14:0(3-OH)]$_2$-13:0(3-OH)-10:0(3-OH)-12:0
1530.0	**1**	GlcN$_2$-P$_2$-[14:0(3-OH)]$_2$-12:0(3-OH)-10:0(3-OH)-14:0
1487.9	**1**	GlcN$_2$-P$_2$-14:0(3-OH)-13:0(3-OH)-12:0(3-OH)- 10:0(3-OH)-12:0
1473.9	**1**	GlcN$_2$-P$_2$-[13:0(3-OH)]$_2$-12:0(3-OH)-10:0(3-OH)-12:0
1422.0	**1**	GlcN$_2$-P-[14:0(3-OH)]$_2$-12:0(3-OH)-10:0(3-OH)-12:0
1436.0	**1**	GlcN$_2$-P-[14:0(3-OH)]$_2$-13:0(3-OH)-10:0(3-OH)-12:0
1408.0	**1**	GlcN$_2$-P-14:0(3-OH)-13:0(3-OH)-12:0(3-OH)- 10:0(3-OH)-12:0
1303.8	**2**	GlcN$_2$-P$_2$-[14:0(3-OH)]$_2$-10:0(3-OH)-12:0
1317.8	**2**	GlcN$_2$-P$_2$-14:0(3-OH)-13:0(3-OH)-12:0(3-OH)-12:0
1331.8	**2**	GlcN$_2$-P$_2$-[14:0(3-OH)]$_2$-10:0(3-OH)-14:0
1223.8	**2**	GlcN$_2$-P-[14:0(3-OH)]$_2$-10:0(3-OH)-12:0
1237.9	**2**	GlcN$_2$-P-14:0(3-OH)-13:0(3-OH)-12:0(3-OH)-12:0
1251.9	**2**	GlcN$_2$-P-[14:0(3-OH)]$_2$-10:0(3-OH)-14:0
1265.9	**2**	GlcN$_2$-P-14:0(3-OH)-13:0(3-OH)-12:0(3-OH)-14:0

Mono-phosphoryl tetra-acyl Lipid A was indicated by the presence of ion peaks differing by 80 Da, as reported in **Table 3.7**. In order to locate the fatty acids on the disaccharide backbone, an aliquot of Lipid A was treated with NH$_4$OH (see 2.4.3). The negative-ion MALDI-TOF spectrum of the ammonium treated sample (**Figure 3.17**) showed a single main peak at *m/z* 1134.0, originated by the species containing two GlcN, two phosphate groups and two 14:0(3-OH) as amide substituents and one secondary 12:0. The minor peak at *m/z* 1120.0 indicated the species containing a 13:0(3-OH) instead of one 14:0(3-OH), as expected on the basis of the chemical analysis for the *N*-linked fatty acids. The peak at *m/z* 1054.0 was originated by the tri-acyl mono-phosphoryl Lipid A, while the peak at *m/z* 951.7 indicated the species lacking of the 12:0 residue. The ion peak at *m/z* 1332.2 derived from minor amount of only partially hydrolyzed Lipid A. In order to understand the position of the secondary 12:0 on the GlcN disaccharide, a positive-ion MALDI spectrum was recorded (not shown). Beside the pseudomolecular ion peaks for the above described species, it was possible to observe, at lower molecular weights, the oxonium ion originating after cleavage of the disaccharide by the laser source, and corresponding to the non-reducing GlcN of the Lipid A carrying a

phosphate group, one 14:0(3-OH) and the 12:0 substituent at *m/z* 650.8, that allowed the location of the 12:0 on the acylamide group on GlcN II.
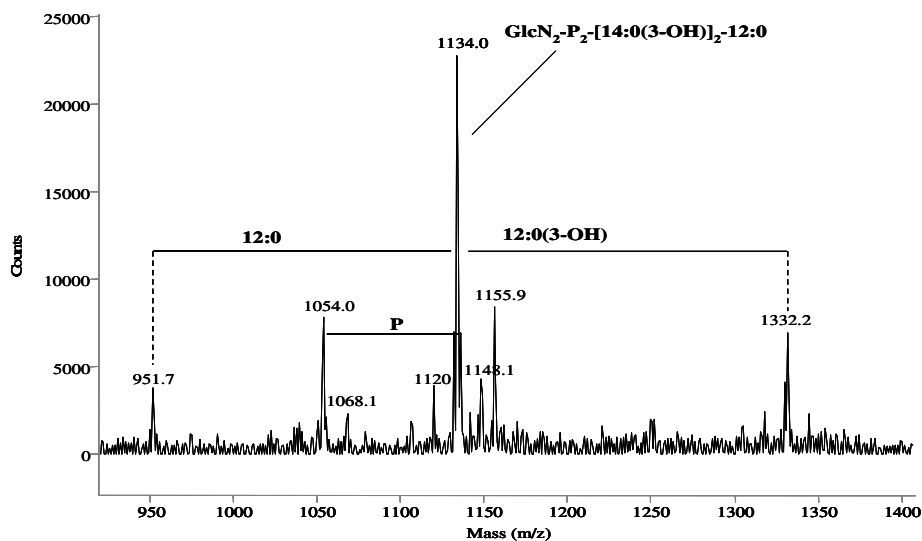
Figure 3.17 - Negative-ion MALDI mass spectrum of the ammonium treated Lipid A fraction from *Alteromonas addita* KMM 3600[T].

To position the ester-linked primary fatty acids, the same analysis was carried on the intact Lipid A sample (**Figure 3.18**), and pointed out the presence of a 12:0(3-OH) as primary substituent at *O*-3 of the non reducing GlcN unit. Still, the molecular weight of the intact Lipid A was in account for one more primary 10:0(3-OH) residue, that could be placed at *O*-3 of the reducing GlcN residue. The typical glucosamine backbone, the anomeric configuration of the glycosidic linkage and the position of the phosphate groups were typical for the Lipid A structure, as already inferred by the spectroscopic analysis of the deacylated oligosaccharide portion, as described above (3.3.1). On the basis of these observations, we can depict the main LOS species from *Alteromonas addita* KMM 3600[T] as described in **Figure 3.19**.
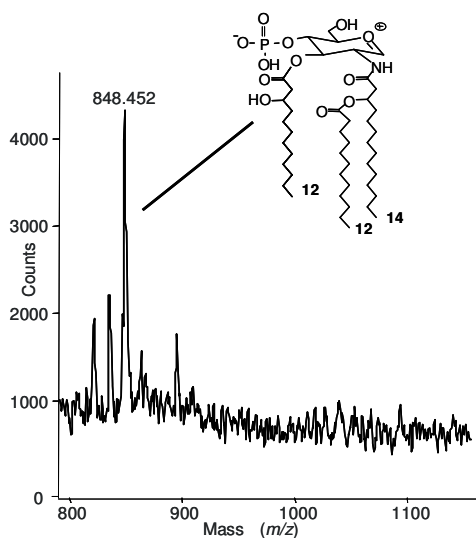
Figura 3.18 - Section of the positive-ion MALDI mass spectrum of the intact Lipid A fraction from *Alteromonas addita* KMM 3600[T]. The structure sketches fatty acids substitution.
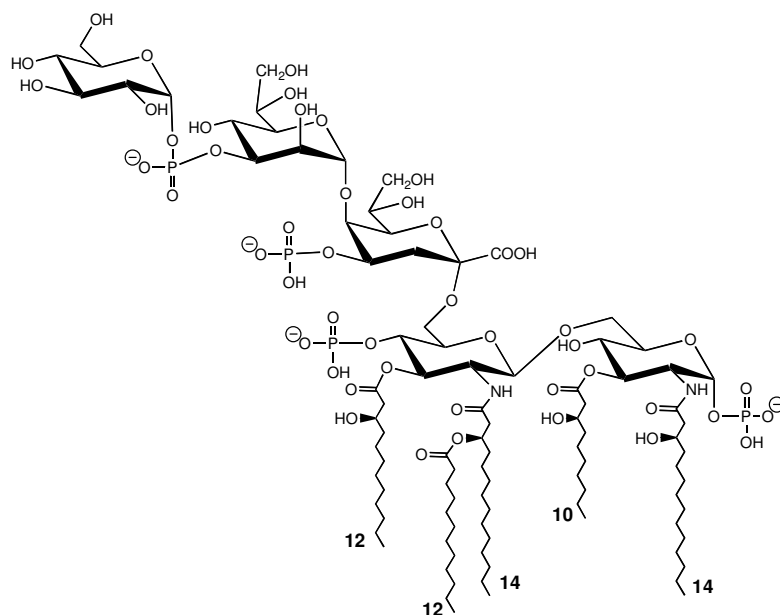
Figura 3. 19 - Complete structure of the main LOS from *Alteromonas addita* KMM 3600[T].

3.4 *Pseudoalteromonas issachenkonii* KMM 3549[T]

Pseudoalteromonas issachenkonii KMM 3549[T] is a Gram-negative, aerobic, marine bacterium with polar flagella isolated from the thallus of the brown alga *Fucus evanescens*, collected in the Kraternaya Bight of the Kurile Islands in the Pacific Ocean (Ivanova *et al.,* 2001; 2002). The bacterium was shown to belong to the genus *Pseudoalteromonas* according

to 16S rDNA gene sequence analysis and DNA-DNA hybridisation showed 27–54% relatedness between strain KMM 3549[T] and other type strains of this genus.

This halophilic organism has bacteriolytic, proteolytic and haemolytic activity and degrades algal polysaccharides, producing a number of glycosyl hydrolases (fucoidanases, laminaranases, alginases, agarases, pullulanases, β-glucosidases, β-galactosidases, β-N-acetylglucosaminidases and β-xylosidases).

In the following sections, structural elucidation of the R-LPS and S-LPS components from *P. issachenkonii* KMM 3549[T] is reported.

3.4.1 Characterization of the Core Oligosaccharide

The LOS fraction from *P. issachenkonii* was extracted from dried cells with PCP and purified by gel permeation chromatography. The SDS-PAGE showed, after silver nitrate staining, a band migrating to the bottom of the gel, in accordance with the LOS nature of this fraction. The compositional monosaccharide analysis of LOS identified L,D-Hep, D-Gal, D-GlcN, D-Glc and Kdo. Methylation analysis showed the presence of t-Gal, 5-Kdo, 6-GlcN, 7-Hep, and, in minor amount 4,7-Hep, 4-Gal and t-Glc. Fatty acids analysis revealed, as major components, the presence of (*R*)-3-hydroxydodecanoic acid [C12:0(3-OH)] and (*R*)-3-hydroxyundecanoic acid [C11:0(3-OH)] both in amide and in ester linkages and of dodecanoic acid (C12:0) and undecanoic acid (C11:0) exclusively in ester linkage. In minor amount C10:0(3-OH), C13:0(3-OH), C10:0 were found.

Alkaline degradation of LOS yielded an oligosaccharide mixture differing in the length of oligosaccharide chain and the degree of phosphorylation, whose primary structure was defined by ^{1}H, ^{31}P and ^{13}C NMR spectroscopy.

Anomeric configurations were assigned on the basis of the chemical shifts, of $^3J_{1,2}$ values which were determined from the DQF-COSY experiment and of $^1J_{C,H}$ deriving from ^{1}H,^{13}C-HSQC registered without decoupling during acquisition. All these data are presented in **Table 3.8**.

All sugars were identified as pyranose rings, based on ^{1}H and ^{13}C NMR chemical shifts and on the HMBC spectrum that showed *intra*-residual scalar connectivity between H-1/C-1 and C-5/H-5 of residues (for Kdo from H-2/C-2 and C-6/H-6).

The anomeric region of the ^{1}H-NMR spectrum (**Figure 3.20**) contained six major anomeric signals, in non stoichiometric ratio, relative to six different spin systems (**A-F**). Their

identification was possible by the complete assignment of all proton signals and the determination of the $^3J_{H,H}$ vicinal coupling constant values.

Three residues (**A**, **B** and **D**) possessed the α-configuration, as showed by a coupled HSQC ($^1J_{C,H}$ = 173 Hz). In particular, they were identified as the GlcN I of the Lipid A skeleton, 7-Hep and t-Glc, respectively. For spin system **B**, further set of signals present in minor amount were visible in the TOCSY spectrum, and they were all ascribed at heptose residue (**B1**) in different chemical/magnetic environment. Three residues (**C**, **E** and **F**) had anomeric β-configuration, based on their $^3J_{H1, H2}$ values and a HSQC registered without decoupling during acquisition ($^1J_{C,H}$ = 162 Hz).

This assumption was also supported by a NOESY experiment that showed for these sugar residues intra-residual NOE connectivity from H-1 to H-3 and to H-5. Residue **C** was identified as the β-GlcN of Lipid A backbone. Spin systems **E** and **F** were both identified as galactose residues owing to the small $J_{H,H}$ values for H-3/H-4 and H-4/H-5. Another set of signals was present for spin system **F** that was characterised by different ring proton resonances (**F1**).
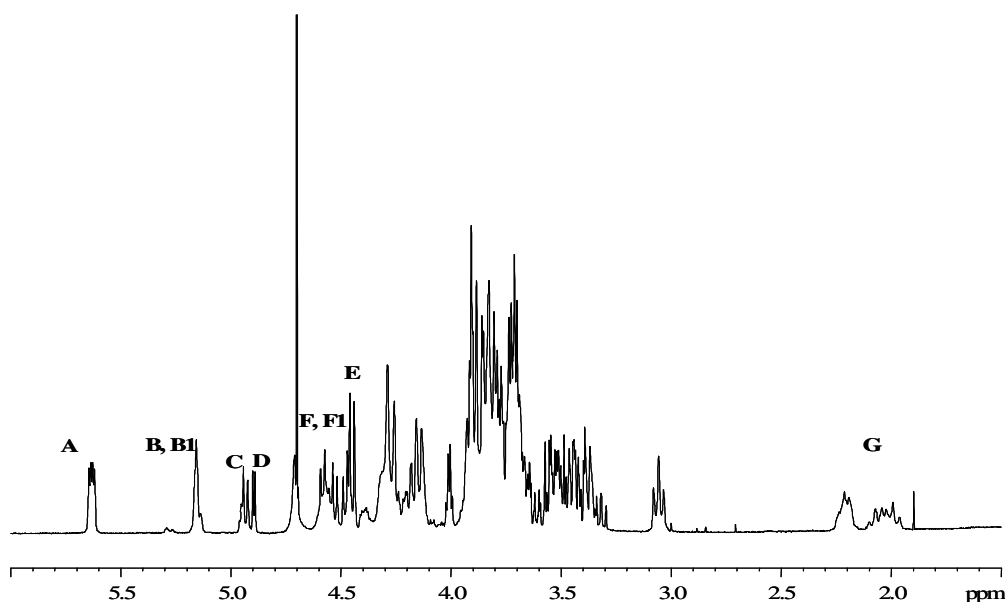
Figure 3.20 - ^{1}H-NMR spectrum of oligosaccharide mixture **1-3** deriving from alkaline degradation of the LOS from *Pseudoalteromonas issachenkonii*. Anomeric signals are designated by capital letters and refer to **Table 3.8**.

The characteristic diasterotopic H-3 methylene signals of a Kdo (residue **G**) were present at 1.97 ppm (H-3$_{ax}$) and 2.22 ppm (H-3$_{eq}$). The α-configuration was established on the basis

of the chemical shifts of the H-3$_{eq}$ and H-5 protons and by the values of the $^3J_{7,8a}$ and $^3J_{7,8b}$ coupling constants of 7.1 and 3 Hz, respectively (Birnbaum *et al.,*1987; Holst *et al.,* 1994).

Table 3.8 - ^{1}H- ^{13}C- (*italic*) and ^{31}P- (**bold**) NMR chemical shifts of oligosaccharides **1-3** in their tetraphosphorylated form. In parenthesis chemical shift values are given for the triphosphorylated form. Numbers in brakets refer to the Kdo residue.

Residue	1(3$_{ax}$)	2(3$_{eq}$)	3(4)	4(5)	5(6)	6(7)	7(8)
A	5.63	3.36	3.88	3.43	4.15	4.27/3.85	
6-α-GlcN	*90.9*	*54.7*	*70.1*	*70.3*	*72.8*	*69.8*	
	2.57						
B	5.15	4.08	4.46	3.82	4.18	4.10	4.20/3.81
			(4.08)				
7-α-Hep	*100.1*	*70.9*	*73.0*	*72.2*	*75.8*	*70.0*	*71.0*
			2.10				
B1	5.15	4.12	4.41	3.99	4.44	4.12	4.20/3.81
			(4.10)				
4,7-α-Hep	*100.1*	*69.8*	*69.7*	*78.7*	*73.0*	*69.5*	*71.0*
			1.98				
C	4.94	3.05	3.84	3.83	3.71	3.50/3.70	
6-β-GlcN	*99.8*	*55.8*	*72.2*	*72.8*	*75.2*	*63.7*	
			2.83				
D	4.89	3.49	3.77	*3.41*	4.13	3.75/3.91	
t-α-Glc	*100.4*	*72.2*	*73.4*	*70.2*	*69.7*	*61.0*	
E	4.46	3.54	3.65	3.90	3.69	3.90/3.78	
t-β-Gal	*103.8*	*71.2*	*73.6*	*68.8*	*76.5*	*61.1*	
F	4.58	3.48	3.67	*3.92*	3.65	3.70	
t-β-Gal	*103.9*	*72.6*	*74.9*	*70.1*	*76.9*	*60.9*	
F1	4.52	3.59	3.73	4.00	3.80	3.80	
4-β-Gal	*103.8*	*71.0*	*72.9*	*77.4*	*75.9*	*60.9*	
G	1.97	2.22	4.56	4.29	3.83	3.88	3.89/3.70
5-α-Kdo	*34.6*		*70.1*	*72.8*	*72.9*	*63.7*	
			1.96				

The ^{13}C-NMR chemical shifts were assigned by the HSQC experiment, using the assigned proton resonances. Six main anomeric signals were apparent (**Table 3.8**), beside a large number of carbon signals relative to ring carbon, two nitrogen bearing carbon signals evidently belonging Lipid A skeleton and, in addition, at high fields, a methylene carbon signal of Kdo unit was found.

Lowfield shifted signals indicated substitutions at *O*-6 of residues **A** and **C** (see below), *O*-5 of **G**, *O*-7 (**B**), *O*-4 and *O*-7 (**B1**), *O*-4 (**F1**), while **E**, **F** and **D** were terminal residues.

Phosphate substitution was inferred on the basis of ^{31}P-NMR spectroscopy. The ^{31}P-NMR spectrum showed the presence of four monophosphate monoester peaks (**Table 3.8**). The ^{1}H,^{31}P-HSQC spectrum showed correlations for P1/H-1**A** (GlcN I), P2/H-4**C** (GlcN II) and

P3/H-4**G** (Kdo), P4/H-3**B** (Hep). The sequence of the monosaccharide residues was determined using NOE effects of the ROESY and NOESY spectra (**Figure 3.21**) and by means of ^{1}H, ^{13}C-HMBC.

The typical Lipid A carbohydrate backbone was assigned on the basis of the NOE signal between H-1**C** and H-6$_{a,b}$**A**. In the case of Kdo unit **G**, it was substituted by heptose **B** as indicated by the NOE effect found between H-1**B** and H-5 and H-7**G**, and, in addition, between H-5**B** and H-3$_{ax}$**G**. Moreover, these NOE effects implied the same absolute configuration for both residues involved in the NOE contact and thus, indicative of the sequence α-L-D-heptose-(1→5)-α-D-Kdo.

Heptose **B** was, in turn, substituted at *O*-7 by galactose **E** as demonstrated by the NOE cross peak between H-1**E** and H-7$_{a,b}$**B**. As for **G** Kdo location, its linkage to unit **C** was deduced by exclusion. In particular, the linkage to *O*-6 of **C** was inferred by taking into account the slight downfield displacement of the carbon signal C-6 (63.7 ppm, **Table 3.8**) indicating its involvement in a glycosydic linkage with a ketose residue.

The ^{1}H,^{13}C-HMBC spectrum confirmed either attachment points of the residues, deduced by glycosylation shifts, and the sequence proposed for the oligosaccharide, determined by NOE data, as it contained all the significant long range scalar correlations. In fact, together with *intra*-residual long range cross peaks, *inter*-residual long range connectivity were found, among others, between H-1/C-1**C** and C-6/H-6**A**, H-5/C-5**G** and C-1/H-1**B**, H-7/C-7**B** and C-1/H-1**E**.
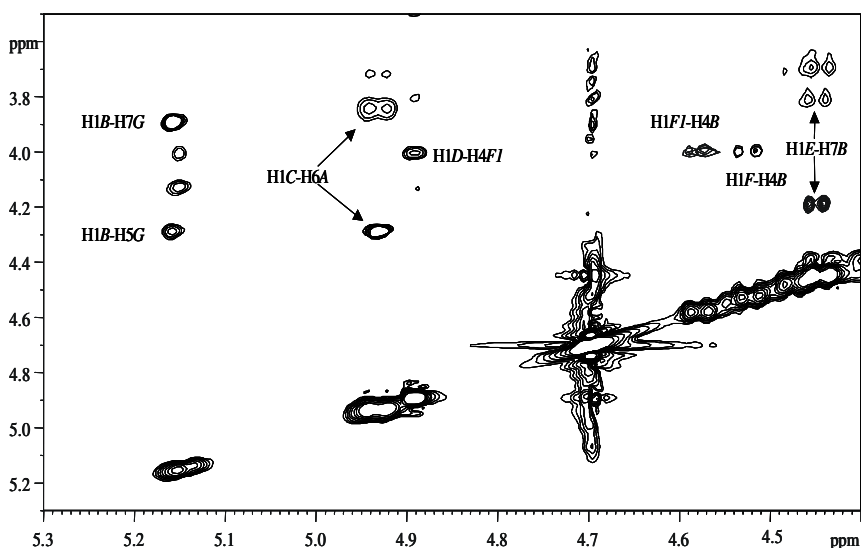
Figure 3.21 – Zoom of the anomeric region of a NOESY spectrum of the oligosaccharide mixture **1-3.** Annotations refer to interresidual dipolar correlations. Capital letters refer to residues as denoted in **Table 1.**

Thus, the major core glycoform of the lipooligosaccharide from *P. issachenkonii* could be identified as the following:

E	**B**	**G**	**C**	**A**

β-Gal-(1→7)-α-Hep3*R*-(1→5)-α-Kdo4*P*-(2→6)-β-GlcN4*P*-(1→6)-α-GlcN1*P*

a R = P
b R = H

1
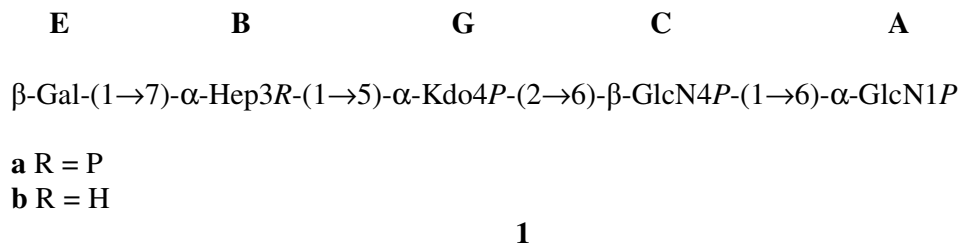
On the basis of this first oligosaccharide sequence, other minor Core glycoforms, slightly differing from this one could be identified.

One of these (**1b**) was only lacking phosphate group to *O*-3 of heptose while all the rest of the chain was unaltered. A different and longer core glycoform (**2a**) was characterised by the presence a further terminal residue (β-Gal **F**) linked to *O*-4 of heptose (**B1**). This was testified by the NOE cross peak between H-1 of **F** and H-4 of **B1** in the NOESY spectrum and furthermore, by the long range correlation between H-1/C-1**F** and C-4/H-4**B1**.

Hence, a further different Core glycoform was found for the LOS from *P. issachenkonii* as follows:

E	**B1**	**G**	**C**	**A**

β-Gal-(1→7)-α-Hep3*R*-(1→5)-α-Kdo4*P*-(2→6)-β-GlcN4*P*-(1→6)-α-GlcN1*P*
    β-Gal-(1→4)⌐

     F
a R = P
b R = H

2
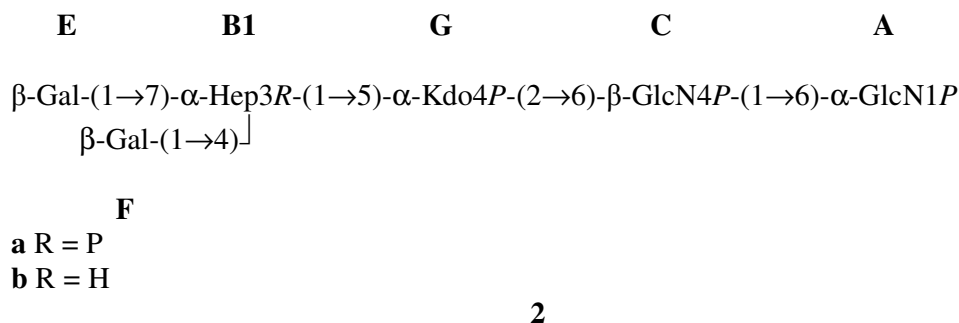
Even for this oligosaccharide, an alternative form, devoid of the phosphate at *O*-3 of heptose, was found (compound **2b**).

Another oligosaccharide variant was also found. This oligosaccharide chain was characterised by the presence of a further glucose unit (**D**) linked to *O*-4 of galactose (**F1**). Actually, in the NOESY spectrum, a cross peak between H-1**D** and H-4**F1** was detectable, corroborated by the long range correlation between H-1/C-1**D** and C-4/H-4**F1**. Thus the third

and last core glycoform (compound **3**) for the LOS from *P. issachenkonii* was identified as the following:

<div align="center">

E   **B1**   **G**   **C**   **A**

β-Gal-(1→7)-α-Hep-(1→5)-α-Kdo4*P*-(2→6)-β-GlcN4*P*-(1→6)-α-GlcN1P

    α-Glc-(1→4)-β-Gal-(1→4)⌐

D   **F1**

</div>
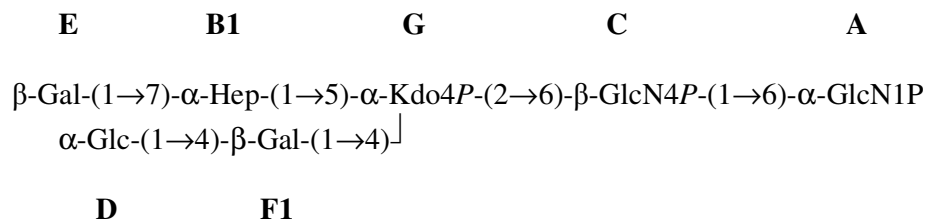
Interestingly, this oligosaccharide chain was present only in its tri-phosphorylated form, where the three phosphate residues on Lipid A and Kdo were plainly evident, thus, with no phosphate residue at *O*-3 of the heptose unit.

A MALDI mass spectrum (**Figure 3.22**) of the oligosaccharide mixture obtained by alkaline treatment confirmed the above structural hypotheses, as all ion peaks corresponding to the above compounds **1-3** were present.
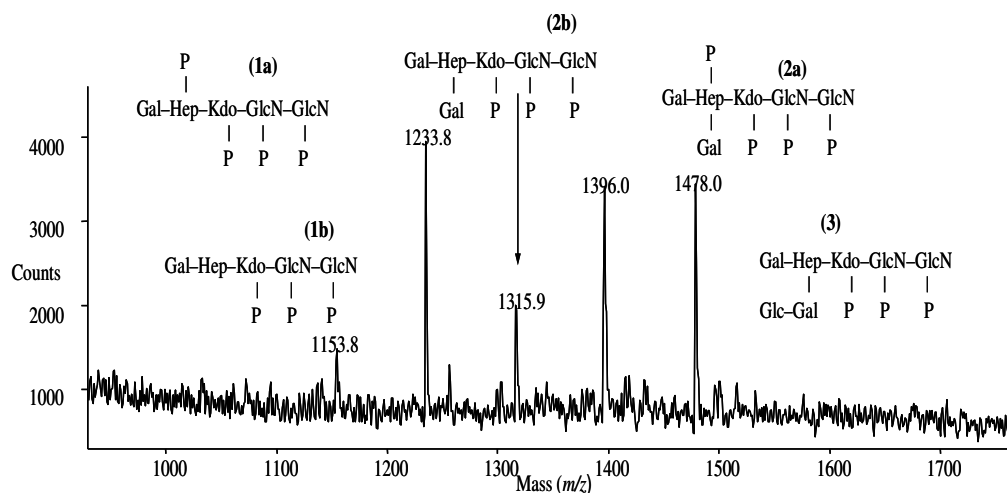
Figure 3.22 - Negative ion MALDI-TOF- mass spectra of oligosaccharides **1-3** from *Pseudoalteromonas issachenkonii* obtained in linear mode. The main ion peaks are assigned as sketched in the figures.

3.4.2 Characterization of the Lipid A

In order to reveal the correct structure of Lipid A, an aliquot of intact LOS was analysed by MALDI MS spectrometry. The MALDI mass spectrum contained peaks for the intact LOS

molecule, as well as ions originated by the described β-elimination (Domon and Costello, 1988 and previous sections). Therefore the mass spectrum could be divided into three subspectra (**Figures 3.23a, 3.23b** and **3.23c**) and following interpretation was straightforward. At high molecular masses (**Figure 3.23b**), in the range 1800-2300 Da, various series of ion peaks were present consequently to the LOS heterogeneity. Within each series, ions differing for 14 Da, due to fatty acids heterogeneity, were distinguishable.

The peak at *m/z* 2253.9 was consistent with a tetra-acyl Lipid A with compound **3** core oligosaccharide skeleton. The peak at *m/z* 2172.0 was ascribed as a tetra-acylated Lipid A with compound **2a** oligosaccharide skeleton, whereas at *m/z* 2009.5 a peak attributed to a tetra-acylated Lipid A with compound **1a** oligosaccharide skeleton was found. The other peaks differed for a phosphate moiety and/or fatty acid residue.

A careful look to lower molecular masses region allowed also an accurate Lipid A identification. The spectrum (**Figure 3.23c**) showed ion peaks attributable to both Lipid A and core oligosaccharide forms. In particular, the ion series at *m/z* 1445.9, 1275.8 and 1077.7 were all identifiable with Lipid A species. The ion at *m/z* 1275.8, was attributable to a tetra-acyl Lipid A carrying three C12:0(3-OH) and a C12:0 residues, the ion at *m/z* 1445.9 was consistent with a penta-acylated Lipid A bearing an additional C10:0(3-OH), while the peak at *m/z* 1077.7 was consistent with a tri-acylated Lipid A carrying two C12:0(3-OH) and a C12:0 residues. Given the fatty acid heterogeneity, several other peaks, differing for ±14 Da with respect to the above ions, were present. At lower mass range of the spectrum, ions from Core oligosaccharide were also present, in full accordance with the above structural description. As already described (Gibson *et al.,* 1997), these ions underwent additional neutral losses of a CO_2 group.

In order to assign the secondary fatty acid location, the LOS was selectively hydrolysed with ammonium hydroxide and the obtained product was analysed by MALDI MS spectrometry. The spectrum registered in negative mode contained a main ion peak centred at *m/z* 1077.7 and attributable to tri-acyl Lipid A species carrying two C12:0(3-OH), one of which bearing an additional C12:0 residue. The positive mode MALDI spectrum (not shown) showed the presence of oxonium ions arising from the cleavage of the glycoside linkage of GlcN II at *m/z* 621.5 and minor peaks at *m/z* 635.3 and 607.1. The fragment at *m/z* 621.5 could be ascribed to a di-acyl species carrying a C12:0(3-OH) and a C12:0 and testified the presence of the secondary fatty acid exclusively linked to the primary amide bound fatty acid on GlcN II.
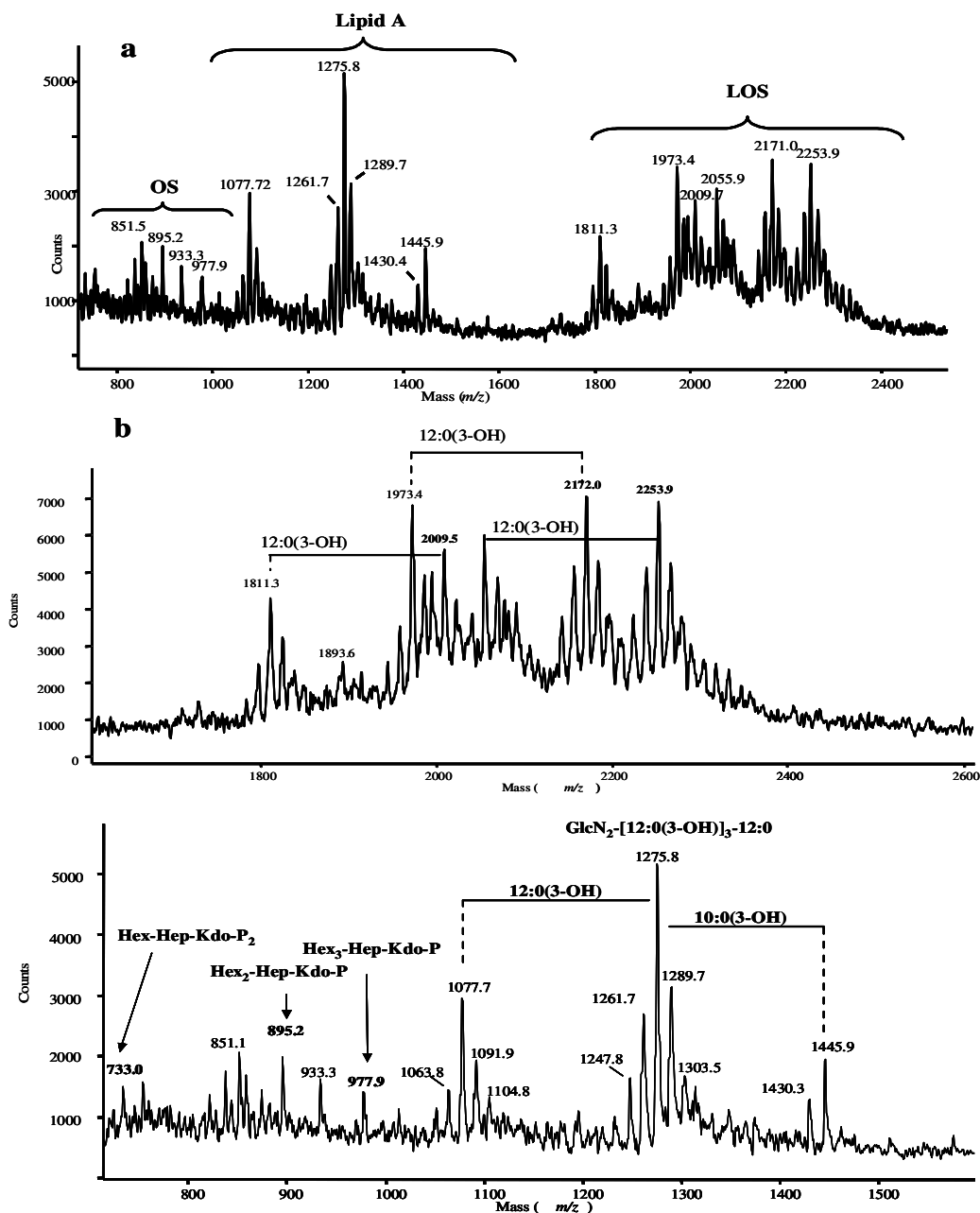
Figure 3.23 - (**a**) Negative ion MALDI-TOF- mass spectrum of intact LOS of *Pseudoalteromonas issachenkonii* obtained in linear mode at high laser intensity. Sections of the same spectrum at high (**b**) and low (**c**) molecular masses. The other ion peaks are explained by fatty acids ($\Delta m/z$ 14) and phosphate ($\Delta m/z$ 80) heterogeneity

Thus, the complete structure of the Lipid A from *P. issachenkonii* was also established, and is depicted in **Figure 3.24** .
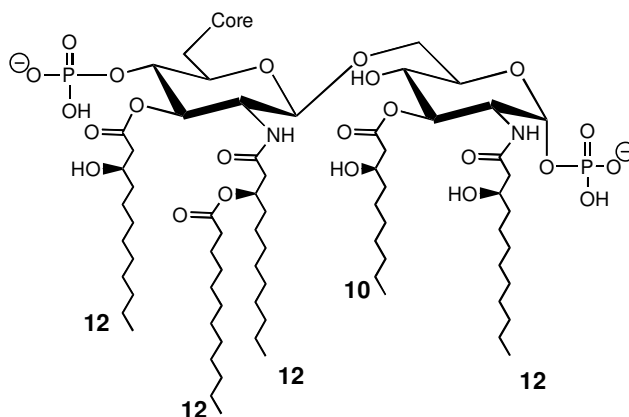
Figura 3.24 – Complete structure of the main Lipid A species from the LOS of *Pseudoalteromonas issachenkonii* KMM 3549[T]

3.4.3 Characterization of the O-chain

The S-LPS from *Pseudoalteromonas issachenkonii* was recovered in the water phase deriving from the hot phenol/water extraction (see 2.1), purified by means of enzymatic digestion with DNase, RNase and Proteinase K. The O-polysaccharide was obtained after mild acetic acid hydrolysis of the LPS and purified by Gel Permeation Chromatography on a Sephacryl S-100 column. Chemical analyses for monosaccharide determination were performed as described in section 2.2 and pointed out the occurrence of GlcN, 2-amino-2-deoxy-mannuronic acid (ManNA) and of a peculiar 3,5,7,9-tetradeoxy-5,7-diamino-non-ulosonic acid (NonA, i.e. Legionamminic Acid, cfr. 1.5.3 and **Figure 3.25**). ^{1}H-NMR spectrum (**Figure 3.26**) of the polysaccharide showed two signals within the anomeric region (**A-B**), while a third spin system (**C**) could be identified starting from the signals at 2.96/1.74 ppm, relative to the diasterotopic methylene group at C-3 of the non-ulosonic acid residue previously identified. In the region around 2.00 ppm the signals for five magnetically distinct acetyl methyl groups could be recognised, whereas at higher field two doublets where identified as the C-3 methyl of an Alanine residue (**Ala**, 1.36 ppm), present in a stoichiometric ratio, and the methyl at C-9 of residue **C**.
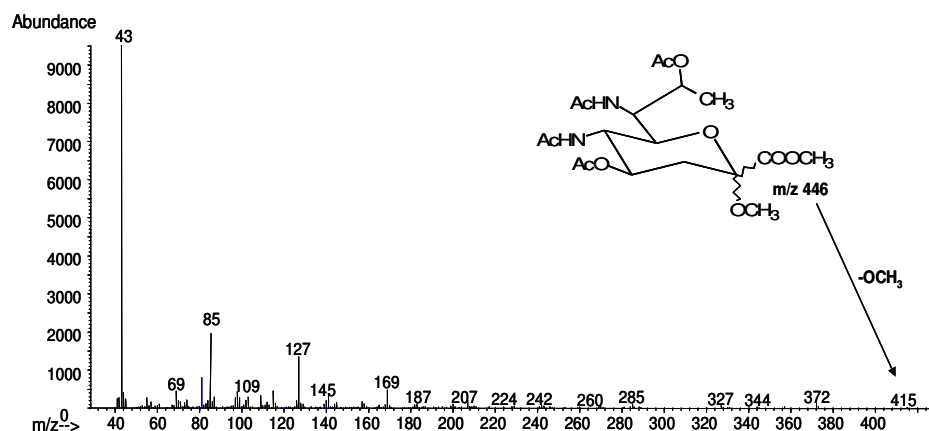
Figure 3.25 - Identification by MS fragmentation of the peracetylated *O*-methyl glycoside derivative from 3,5,7,9-tetradeoxy-5,7-diamino-non-ulosonic acid
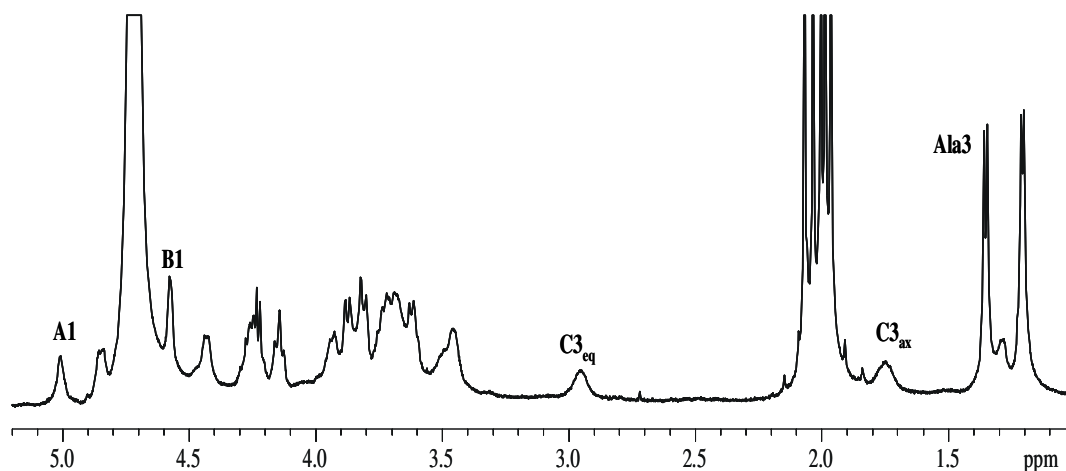
Figure 3.26 – ^{1}H-NMR spectrum of the *O*-polysaccharide from *Pseudoalteromonas issachenkonii.* Capital letters refer to the identified spin systems described in **Table 3.7.**

Complete chemical shift assignment for the three residues was achieved by means of two-dimensional NMR analysis and, in particular, DQF-COSY, TOCSY and NOESY spectra allowed the complete description of proton resonances patterns, from which, with the help of the ^{1}H,^{13}C-HSQC and HMBC spectra, all ^{13}C resonances were assigned (**Figure 3.27, Table 3.9**). In particular, the complete definition of proton resonances for spin system **C** was made possible through the detection, in the TOCSY spectrum, of two distinct series of signals relative to C-9 methyl group (down to H-6) and from the C-3 methylene group signals (up to C-5), as evidenced in **Figure 3.28**. Residues **A** and **B** were identified, on the basis of chemical shifts and of the diagnostic *intra*-residual dipolar correlation in the NOESY spectrum H-1**A/**

H-2**A**, H-1**A/** H-3**A** and H-1**A/** H-5**A** of H-1**B/** H-3**B** and H-1**B**/H-5 as β-ManNA and β-GlcN, respectively.

Moreover, in the same spectrum, *inter*-residual correlations H-1**A**/H-4**B** and H-1**B/**H-4**C** suggested the attachment of residue **A** to *O*-4 of the β-GlcN residue, in turn linked at *O*-4 of residue **C**. This residue, lacking of an anomeric proton, was correctly located within the polysaccharide repeating unit through the observation, in the HMBC spectrum, of a strong long range correlation between H-4**A** and C-2**C**, testifying the attachment of residue **C** *O*-4 of residue **A**.
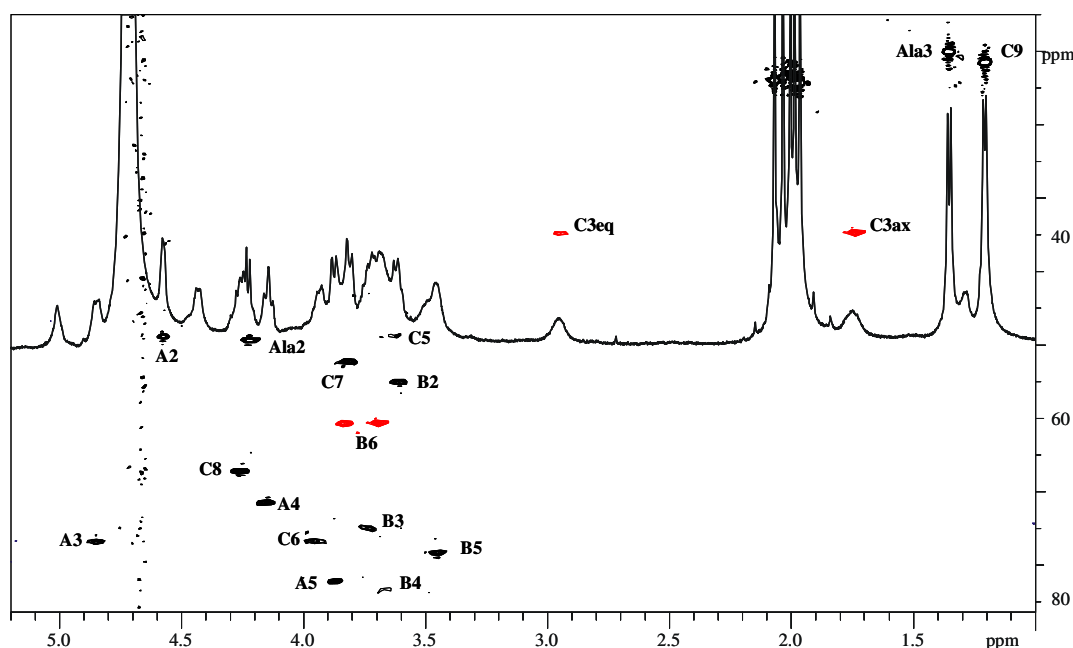
Figure 3.27 – ¹H, ¹³C-HSQC spectrum on the polysaccharide from *Pseudoalteromonas issachenkonii*. The spectrum is multiplicity edited, grey cross peaks indicate CH₂ signals. Letters refer to the spin systems described in **Table 3.9**.
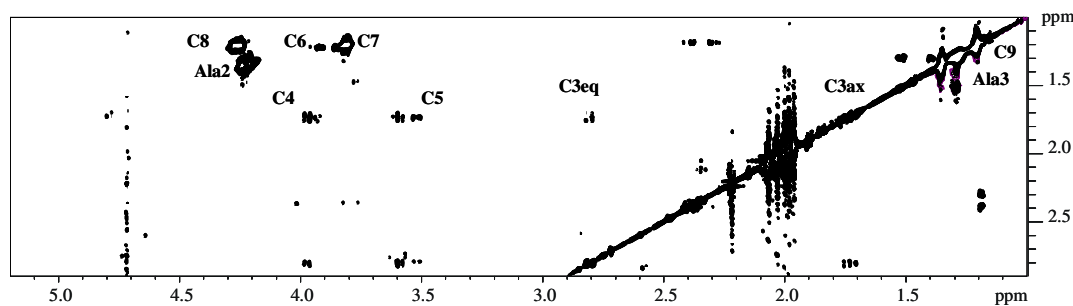
Figure 3.28 – Zoom of the TOCSY spectrum of the *O*-chain from *P. issachenkonii* KMM 3549. Letters refer to the spin systems described in **Table 3.9** and show the occurrence of two distinct patterns of resonances for the branching chain (H-6/H-9)and the ring portion (H-3/H-5) of the non-ulosonic acid residue.

Table 3.9 – [1]H and [13]C (*italic*) for the identified spin systems in the *O*-polysaccharide from *Pseudoalteromonas issachenkonii* KMM 3549

| Residue	1	2(3$_{ax}$)	3(3$_{eq}$)	4	5	6	7	8	9
4-β-ManNA	5.01	4.59	4.86	4.16	3.88	-			
A	*98.7*	*51.5*	*74.2*	*69.7*	*78.7*	*175.7*			
4-β-GlcN	4.44	3.61	3.74	3.67	3.44	3.70			
B	*103.1*	*56.5*	*73.1*	*79.8*	*75.1*	*61.0*			
NonA	-	1.74	2.96	3.49	3.65	3.93	3.82	4.29	1.20
	177.9	*100.9*	*40.31*	*76.8*	*51.5*	*73.2*	*53.4*	*66.3*	*21.2*
Ala	-	4.23	1.36						
	178.6	*51.6*	*19.7*						

Previous studies on the configuration of non-ulosonic acids isolated from bacterial O-antigens, showed that these monosaccharides can be studied as to two distinct systems, namely the ring substituents and the branching chain. In order to determine the relative configurations of the chiral centres in residue **C**, *intra*-residual dipolar correlations were observed between H-3$_{ax}$**C** and H-5**C** and between H-4**C** and H-6**C**, from which it was possible to deduce that all the ring substituent assumed an axial orientation. The relative configuration of the branching chain composed by C-7, C-8 and C-9 was determined on the basis of the ^{13}C chemical shift value for C-9 methyl group and by comparison with literature data. In fact, this subunit can be assimilated to a threonine or allothreonine residue. A marked chemical difference between carbon chemical shift of the methyl signal depending on the relative orientation of substituents exists between these two isomers. In particular, in threonine, the methyl chemical shift is 20.2 ppm, while the *erythro* orientation of substituent in allothreonine produces considerably lower values, around 17.0 ppm (Staaf *et al.,* 1999).

Considering the chemical shift for C-9 of 21.2 ppm, it is possible to infer that the substituent at C-7 and C-8 must own a *threo* relative configuration. These data, combined with those regarding the ring protons orientation, allow the description of four possible isomer structures, represented in **Figure 3.29**. The definitive configuration of monosaccharide **C** remains up to now unsolved.

Location of acetyl groups was made possible on the basis of the scalar long range correlations detected in the HMBC spectrum in which all the methyl signals around 2.00 ppm showed correlation with carbons around 175.0 ppm, in turn correlating with signals for H-2**A,** H-3**A**, H-2**B**, H-5**C** and H-7**C** (see **Table 3.10**).
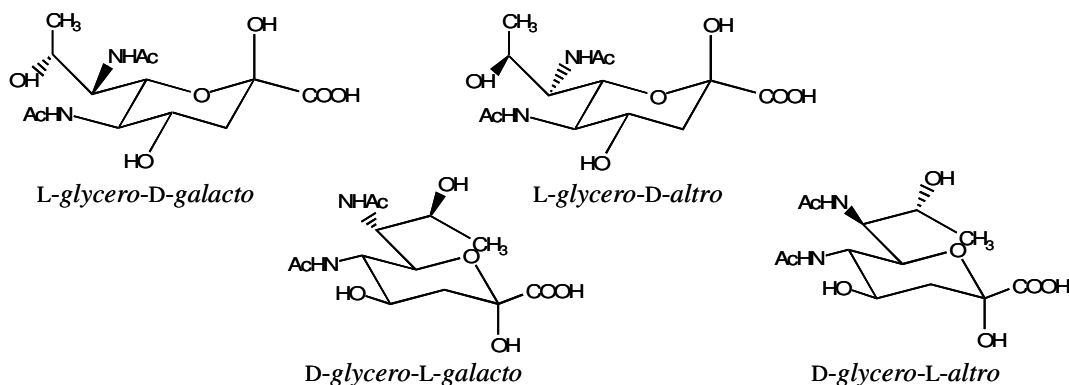
Figure 3.29 – The four possibile diasteroisomers satisfying NMR constrains for relative configuration of 3,5,7,9-tetradeoxy-5,7-diamino-non-ulosonic acid from the *O*-polysaccharide from *Pseudoalteromonas issachenkonii* KMM 3549.

The usage of such a solvent system allows the observation of the amidic proton resonances, that can not be detected when using D_2O as solvent due to proton exchange. In the region around 8.0 ppm, five signals were now visible. The NOE effects observed within a wgt-NOESY spectrum allowed the identification of the four acetamido groups previously defined and led to confirmation of their location (**Figure 3.30**). The amide signal at 8.22 ppm was produced by the amide moiety of the Ala residue. The observation of a NOE with H-5**A** pointed out the occurrence of an amide linkage between the aminoacid and the carboxyl group at C-6 of β-ManNAcA. Conversely, the position of the Alanine residue was not made immediately clear. In order to locate this residue, a complete series of 2D NMR experiments was recorded on the sample solubilizing the sample in H_2O/D_2O 9:1.

Table 3.10 – [1]H and [13]C (*italic*) chemical shifts for the amide linked substituent groups within the *O*-polysaccharide from *Pseudoalteromonas issachenkonii* KMM 3459[T].

Linkage site	NH	C=O	CH₃(CHₐ)	CH₃
N-2 A	8.58	-	2.01	
	-	*176.7*	*22.4*	
C-5 A	8.22	-	4.23	1.36
	-	*179.4*	*51.6*	*19.7*
N-2 B	8.03	-	1.97	
	-	*175.9*	*22.9*	
N-5 C	7.81	-	1.99	
	-	*176.2*	*23.2*	
N-7 C	8.41	-	1.98	
	-	*175.3*	*22.0*	
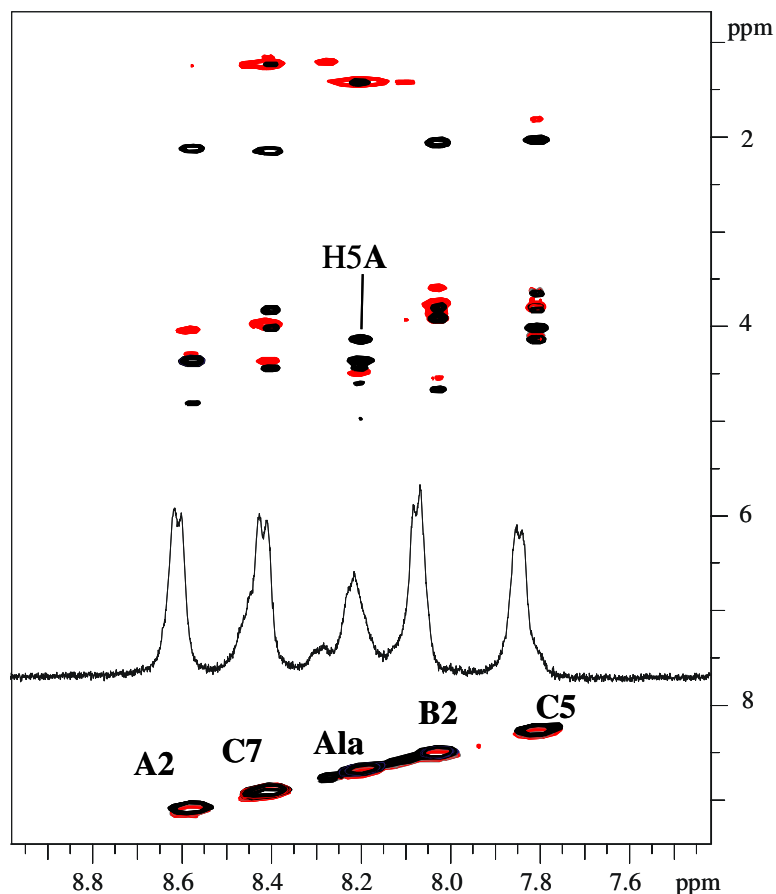
Figure 3.30 – Zoom of the amide protons region of the TOCSY (grey) and NOESY (black) spectra recorded in H_2O/D_2O 9:1 on the *O*-polysaccharide from *Pseudoalteromonas issachenkonii* KMM 3549. Labels along the diagonal refer to the identified amide moieties as reported in **Table 3.8.** The diagnostic cross-peak for location of the Alanine residue is indicated.

From all the above data, is thus possible to deduce the structure of the repeating unit of the *O*-chain from *Pseudalteromonas issachenkonii*, illustrated in **Figure 3.31**. In the figure sketched, the configuration for the non-ulosonic acid is arbitrarily chosen among the four above proposed structure.
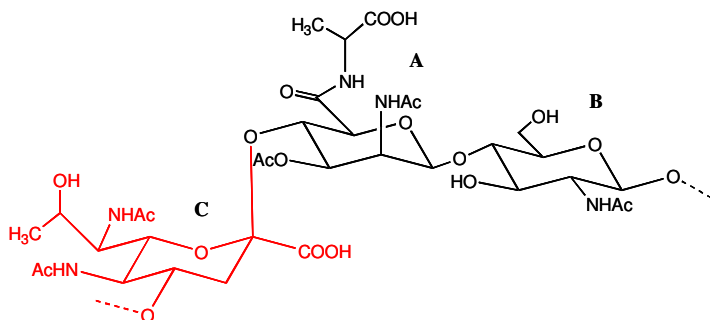
Figure 3.31 – The complete structure of the *O*-chain repeating unit from *Pseudoalteromonas issachenkonii* KMM 3549. The non-ulosonic acid residue is presented in one of the four possible diasteroisomers proposed in **Figure 3.26.**

3.5 Conclusions

The LOSs structures characterised for the three marine bacteria presented show interesting common features, offering important points for discussion.

In the case of *Shewanella pacifica* LOS, interesting chemical features are represented by the occurrence of the 8-amino-derivative of Kdo, as well as by the D,D-Hep residue, bearing at *O*-6 the phosphoglyceric acid unit. As highlighted in section 1.5.2, this motif has been already encountered, apart from the occurrence of glyceric acid, in previous studies on other *Shewanella* oligosaccharides (Vinogradov *et al.,* 2003; 2004). Usually, Gram-negative bacteria share a pretty conservative architecture of the Lipid A-Inner Core region, and the Kdo always represents the attachment point of the Oligosaccharide to the glycolipid moiety. The replacement of such monosaccharide with its derivatives has been reported, up to date, only in few cases, namely the cited *Shewanella* examples, and in one *Acinetobacter* strain (Vinogradov *et al.,* 1997, cfr. Section 5.2.1) Kdo coexists with its 3-hydroxy-derivative of (Ko).

Another unusual and novel feature of the LPS from *S. pacifica* is the presence of glyceric acid, attached *via* phosphodiester linkage to the D,D-Hep. Although this is a key molecule of primary metabolism of Gram-negative bacteria, it was never detected in the core of LPSs. This molecule contributes to the total enhancement of negative charge density, a property closely related to the resistance expressed by barophiles and psychrophiles to their natural habitats. Under the same point of view, it is possible to relate the uncommonly short-chained LOS structure constituting the LPS fraction from *Alteromonas addita* KMM 3600^T to a specific environmental demand. Moreover, the occurrence of the deep-rough LOS decorated with five negative charges (inferred by the phosphate groups and by the Kdo residue) appears also as a distinctive genus feature, since a similar arrangement has been previously set on light for *A. macleodii,* where, in a similar fashion, the LPS fraction was constituted exclusively by a deep-rough LOS (Liparoti, *et al.,* 2006). Moreover, as in *Shewanella pacifica* LOS, the unusual phosphodiester bridge was detected. This rare structural feature is likely to become a sort of distinctive trait for extreme adapted marine bacteria. Apart from the two cases presented, it was encountered also in the LOS structure from *Arenibacter certesii* (Silipo *et al.,* 2005), where it connects, as in *A. addita* example, two monosaccharide residues.

The LOS structure from *Pseudoalteromonas issachenkonii*, on the other hand, owns a Core structure with a less striking negative charge density, inferred by the variable phosphate

content detected. Although this molecule is endowed with a negative charge density, the most valuable contribution is inferred by the O-polysaccharide moiety composing the S-LPS. In fact, as illustrated in section 3.4.3, the repeating unit of the polysaccharide is made of a trisaccharide of 2-amino-mannuronic acid, glucosamine and a non-ulosonic acid. Two over three of these monosaccharides are acidic residues, that provide the polysaccharide and consequently the whole outer membrane, with a net anionic character.

The occurrence of such a high amount of negative charges has been proposed to play a crucial role in the supramolecular arrangement of LPS in the external membrane. In fact, a dense cross-linkages net is established *via* the electrostatic interactions with bivalent cations present in the environment (Ca^{2+}, Mg^{2+}) between the LPSs molecules, contributing to the rigidity and stability of the cell envelope (Alexander and Rietschel, 2001; Raetz and Whitfield, 2002). This feature may act in the direction of enhancing mechanical resistance of Gram-negatives cell toward such stressors like pressure and/or osmotic pressure characterizing sea environments.

4

Thermophilic Bacteria

4.1 Introduction

Water containing terrestrial, subterranean and submarine areas harbour a variety of thermophilic and hyperthermophilic bacteria and archaea, which are able to grow optimally in a wide temperature range. Microrganisms thriving between 40 and 80°C are referred to as thermophiles, whereas hyperthermophiles are adapted to temperatures above 80°C. Thus, their enzymes, nucleic acids and proteins have to be stable and work at temperatures often above 100°C, where usually small biomolecules rapidly decompose. The majority of hyperthermophiles and thermophiles has been recognised among the archaeal domain. Nevertheless, many Gram-positive and Gram-negative bacteria can often express thermophily. Thermophiles are a source for a great number of molecules with a great biotechnological potential. The so-called "thermozymes" may be employed in many industrial processes, where the usage of high temperature is mandatory. At the same time, a thermozyme, the Taq polymerase from *Thermus aquaticus*, is the key enzyme in the Polymerase Chain Reaction (PCR), up to date one of the most widespread techniques used in molecular biology. The strategies played by thermophiles in their adaptation process have been described in section 1.2.1. In this chapter, we will focus on the structure characterization of the membrane component of two Gram-negative bacteria, *Thermus thermophilus* Samu-Sa1 and *Geobacillus thermolevorans* strain Fango. Both microrganisms have been isolated in Italy, in the volcanic flegrean area.

Microrganisms belonging to the genus *Thermus* have been extensively studied either for their enzymatic systems, in the perspective of a possible biotechnological utilization, and for their membrane composition. For what concerns the cell surface, this genus exhibits several borderline behaviour. *Thermus* cell wall architecture is characterised by a complex and multilayered organization, in which a thick peptidoglycan is sandwiched between the cytoplasmic membrane and an outer membrane as in case of Gram-negative bacteria. The last layer of such a structure is made of a protein S-layer masked by amorphous material.

It is generally believed that a crucial role in the thermal stability these bacteria are endowed with is provided by the particular structure of all cell envelope components. The

molecular arrangement of both the murein and the outer membrane appears to be central in the adaptation process to high temperatures (Brock, 1978).

The peculiar structure of *Thermus* peptidoglycan was analysed for *T. thermophilus* HB8 (Quintela *et al.*, 1995) and it showed an intermediate structure between standard Gram-positive, for what concerns mostly the chemical composition and peptide bridges, and Gram-negative bacteria, mostly for what concerns the degree of cross linking and the glycan chain mean length. Moreover, it was found for the first time that about the 25% of the total muropeptides were amidated at the δ NH$_2$ of the Ornithine residue by Aspartic Acid. Even though this peculiarity appeared as one of the causes of the extreme thermal stability showed by *Thermus* genus, further studies proved that other species, namely *T. aquaticus* YT-1 and *Thermus* ATCC27737 did not show such a feature, although they still exhibit strong resistance to heat.

According to the extraordinary membrane architecture, several kinds of polar glycolipids have been isolated from the membranes of *Thermus* (Pask-Hughes and Shaw, 1982; Wait *et al.*, 1997, Lu *et al.,* 2004) and *Meiothermus* (Yang, 2004) bacteria, that share some common structural features, mainly concerning the kind and sequence of monosaccharides present and the nature of the lipid component, and that are strongly thought to be at the basis of the resistance to the high temperature.

The genus *Geobacillus* is a relatively new genus defined after a reclassification of thermophilic bacilli. The genus *Bacillus* is a large collection of aerobic and facultatively anaerobic rod-shaped bacteria, usually belonging to the Gram-positive family. *Geobacillus* is a genus first isolated into geothermally heated oil reservoirs (with a temperature of 50-60°C or more), where the liquid hydrocarbons are the prevailing organic matter. This generates a unique ecological niche for the thriving of thermophilic, hydrocarbons oxidizing bacteria and, in fact, many species belonging to this genus exhibit metabolic activity toward long chain hydrocarbons (Nazina *et al.*, 2001). Although generally classified as Gram-positives, some *Geobacillus* species exhibits negative staining to the Gram assay. The occurrence of such a behaviour was for instance observed in the slightly thermophilic bacterium *G. thermoleovorans* strain Fango. This prompted us to investigate the membrane composition of this microrganism, looking for unusual compounds that could explain this phenomenon.

4.2 *Thermus thermophilus* **Samu-Sa1**

Thermus thermophilus Samu-SA1, is a thermohalophilic bacterium first isolated in the shallow marine hot springs on Mount Grillo, in Italy (Romano *et al.*, 2004). After culture, dried cells were washed with 1% aqueous phenol to remove exocellular polysaccharides and subsequently extracted utilizing the hot phenol/ water procedure, thus applying the protocol conventionally adopted for isolation of LPSs from the outer membrane of Gram-negative bacteria. By chemical analyses, a lipid containing fraction was detected in the phenol extract, that was first purified by enzymatic digestion with RNase, DNase and Proteinase K. Analysis by thin layer chromatography evidenced the presence of two fractions, isolated by silica-gel chromatography, and the major one underwent complete chemical analysis.

Fatty acids analysis revealed the presence of *iso-* and *anteiso*-branched pentadecanoic (15:0) and heptadecanoic (17:0) acid and minor amounts of *iso-* and *anteiso*-branched tetradecanoic (14:0), hexadecanoic (16:0) and octadecanoic (18:0) acid. GC-MS analyses of the acetylated *O*-methyl glycosides showed the presence of glucose (Glc), galactose (Gal) and 2-amino-2-deoxy-glucose (GlcN), present in non-stoichiometric amounts. Despite the Gram-negative staining observed, no trace of 3-hydroxy fatty acids or Kdo was detected, indicating the definitive absence of LPS. Indeed, three additional constituents, degraded by strong hydrochloric methanol treatment, could be detected after milder methanolysis and acetylation. These were identified, on the basis of the ion fragmentation in the MS spectra, as glycerol (Gro), glycerol-phosphate (GroP) and GlcNAcyl, in which the acyl moiety was 17:0.

Three late eluting components were also found, that were identified, by EI-MS and CI-MS analyses after either acetylation or trimethylsililation, as octadecane-1,2-diol (OD), heptadecaneyl-amine (HA), and its *N*-glyceroyl derivative. The mass spectra for the acetyl derivatives of these two species are presented in **Figure 4.1.**

Long-chain alkyldiols were previously found as components of polar glycolipids from other *Thermus* species (Wait *et al.*, 1997), where they are thought to replace acyl-glycerol in the glycolipid structure, whereas the occurrence of glyceric acid and long-chain alkylamine was a new finding.

Glycosylation sites and ring size of the monosaccharides were determined by methylation analysis, leading to the identification of 2-Glc, 2-Gal, 6-GlcN, t-GlcN, all in pyranose form, and terminal galactofuranose (t-Gal*f*).
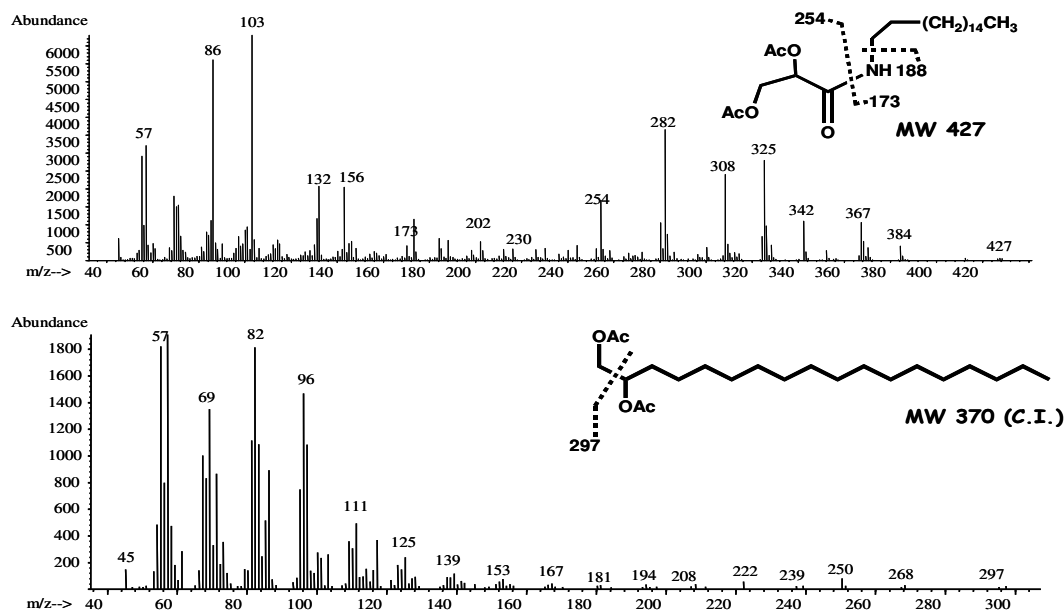
Figure 4.1 - EI mass spectra of the acetyl derivatives of *N*-glyceroyl-heptadecane-amine and octadecane-1,2-diol. Molecular weights referred to the sketched structures are obtained from chemical ionization spectra.

4.2.1 NMR and ESI FT-MS analysis of the crude glycolipid extract

The poor solubility of glycolipids in many common solvent systems is one of the major obstacles in their structure determination. This problem is typically overcome introducing chemical modifications, usually peracetylation, in order to improve the solubility and allow the execution of experiments in solution, in particular the recording of NMR spectra (see section 2.4.2). In the present case, optimal solubility for the sample was found in $CHCl_3$:CH_3OH (1:2, by vol.), and this allowed the recording of a full set of 1D and 2D NMR experiments on the native glycolipids. ESI FT-MS, as well as NMR analyses, demonstrated the existence of a mixture. In particular, the charge deconvoluted ESI FT-MS mass spectrum obtained in the positive ion mode (**Figure 4.2**) revealed at least three different species with monoisotopic masses of 1176.857 u, 1409.979 u and 1467.977 u , each one accompanied by a panel of correlated ions originating from different acyl chain length (Δm = 14 u) and from sodium attachment (Δm = 22 u). In 1D and 2D NMR spectra, partially overlapping signals of diverse glycolipid species were visible. In particular, in the region between 5.200 and 4.600 ppm of the ^{1}H-NMR spectrum, signals for at least six anomeric protons (**A-F** in order of decreasing chemical shift) were visible (**Figure 4.3**). Moreover, in the same region of the spectrum, signals were present for at least four acylated carbinolic protons (**G-L**). In the aliphatic region, between 2.500 and 0.500 ppm signals were identified deriving from protons
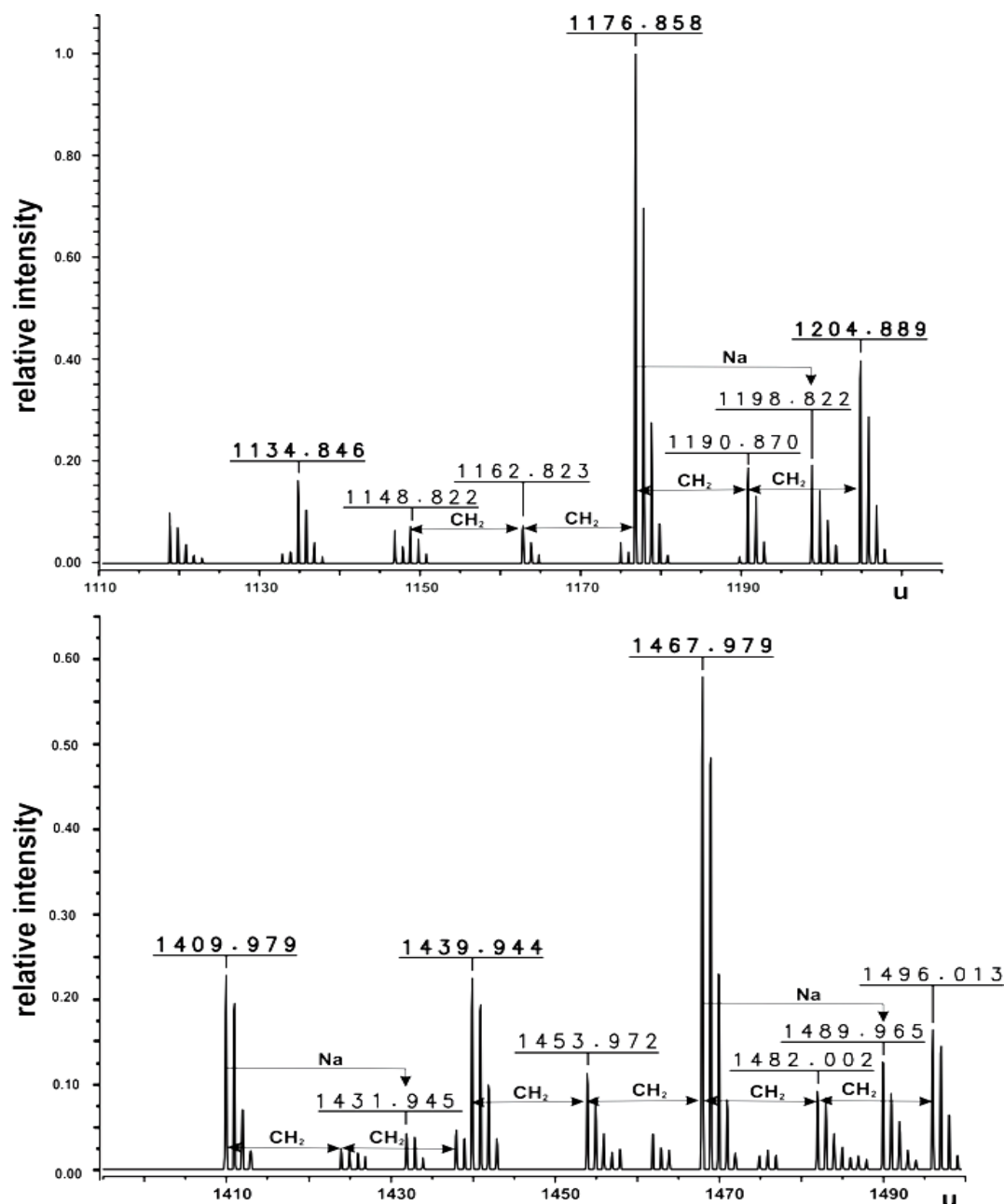
Figure 4. 2 - Details of the charge deconvoluted ESI FT mass spectra obtained in the positive ion mode from the mixture of glycolipids from *Thermus thermophilus* Samu-SA1.

belonging to the amino-methylene group and to particularly deshielded aliphatic methylene groups (**Tables 4.1 and 4.2**). By DQF-COSY and TOCSY spectra, the full assignment of proton resonances of the components of the mixture was possible. Subsequently, ^{13}C chemical shifts were assigned from observed correlations in the ^{1}H,^{13}C-HSQC spectrum (**Figure 4.3, Table 4.1**). For the monosaccharides, the $^3J_{H,H}$ coupling constant values derived from the DQF-COSY spectrum established for each residue anomeric and relative configurations. All

residues, except residue **A** (see below)**,** were pyranoses, as proven by the observed carbon chemical shifts values and by the *intra*-residual long range correlations between C-1/H-5 and H-1/C-5, that appeared for each residue in the ^{1}H,^{13}C-HMBC spectrum. The ^{1}H signal at 5.028 ppm (H-1**A**) correlated, in the TOCSY spectrum, to proton signals at 4.079, 4.015, 3.943, and 3.725 ppm.

All of these signals showed, in the ^{1}H,^{13}C-HSQC spectrum, correlations with down-field shifted carbon signals, up to 84.4 ppm, suggesting the occurrence of a furanose ring, as confirmed by the *intra*-residual H-1/C-4 and C-1/H-4 correlations in the ^{1}H,^{13}C-HMBC spectrum. In the same spectrum, the $^1J_{C,H}$ anomeric coupling constant values were also observable, since the pulse sequence used to carry out this experiment contained a low pass filter, set to a value of 145 Hz. In this way, the rising of $^1J_{C,H}$ couplings for ring C-H could be selectively avoided, while it was still possible to recover the $^1J_{C,H}$ for anomeric protons and carbons (Bubb, 2003). The $^1J_{C,H}$ coupling constant value of 174.0 Hz for spin system **A**, together with the ^{13}C chemical shift of the anomeric carbon signal and the *intra*-residual NOE correlations observed, was diagnostic for the α-anomeric configuration of this residue, thus identified as t-α-Gal*f*.
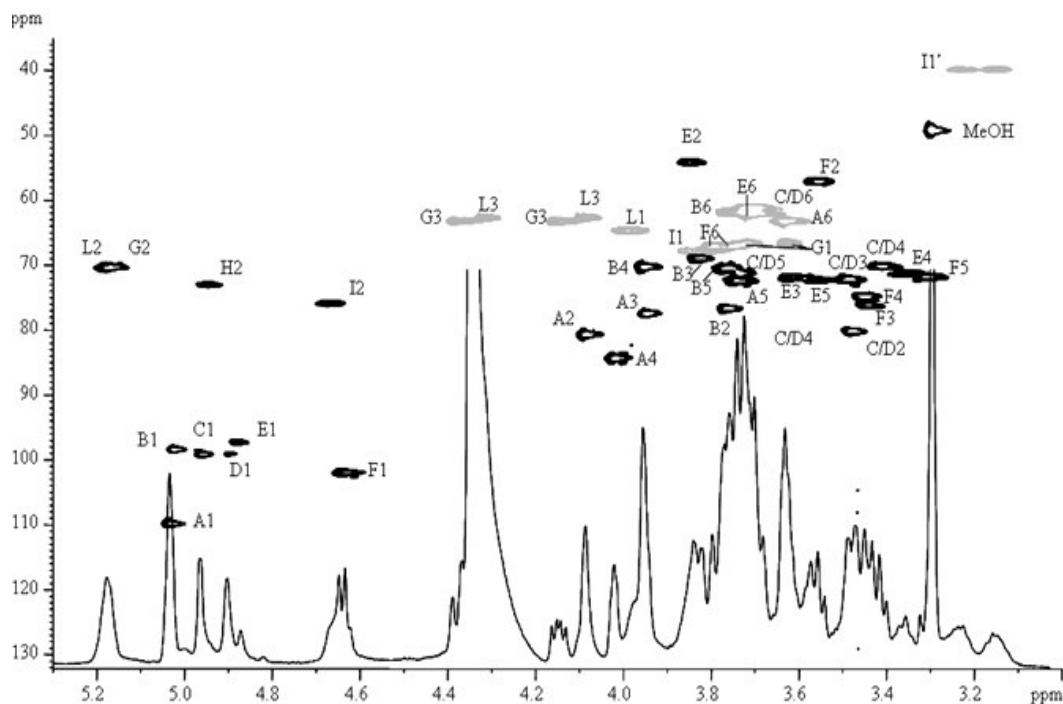
Figure 4.3 - Zoom of the ^{1}H, ^{13}C-HSQC and, overlaid, ^{1}H NMR spectrum of the mixture comprising **GL1, GL2** and **PGL** in their native form. The spectrum is edited for detection of signals multiplicity. Methylene groups are designed in grey. Letters refers to the identified spin systems in **Table 4.1.**

The $^1J_{C,H}$ anomeric coupling constant values for the other spin systems were similarly obtained. For spin system **B** (5.019 ppm), α-*galacto* configuration was identified, on the basis of the low $^3J_{H,H}$ values for H-1/H-2, H-3/H-4 and H-4/H-5 (3.4, 3.6 and <1 Hz, respectively). Typical down-field shift due to glycosylation was observed for the C-2 resonance, proving the substitution at *O*-2 of this residue. Thus, this residue was a 2-α-Gal.

On the basis of similar considerations, residue **B** was identified as 2-α-Gal, while residues **C** and **D** were recognised as 2-α-Glc units. The finding that these two residues shared the same pattern of resonances, except for their H-1, supported the idea that they represented the same monosaccharide, in slightly different chemical and magnetical environments.

Table 4.1 - ^{1}H and ^{13}C (*italic*) chemical shifts for **GL1, GL2** and **PGL.** Values refer to internal methanol (δ_H 3.300, δ_C 49.5). Numbers in brackets refers to the N-glyceroyl-heptadecane-amine residue (**I**), n.a.: not assigned.

Residue	1	2	3	4 (1')	5 (2')	6 (3')
t-α-Gal*f*	5.028	4.079	3.943	4.015	3.725	3.630
A	*109.7*	*80.6*	*77.5*	*84.4*	*72.4*	*63.0*
2-α-Gal	5.019	3.775	3.821	3.948	3.760	3.741/3.393
B	*98.2*	*76.7*	*68.8*	*70.1*	*70.4*	*61.2*
2-α-Glc	4.956	3.472	3.484	3.406	3.726	3.723
C	*99.0*	*80.2*	*72.0*	*70.1*	*71.2*	*61.3*
2-α-Glc	4.900	3.473	3.484	3.406	3.726	3.723
D	*99.1*	*80.2*	*72.0*	*70.1*	*71.2*	*61.3*
t-α-GlcNAc	4.985	3.843	3.484	3.406	3.726	3.723
E	*97.1*	*54.1*	*71.7*	*71.3*	*72.2*	*61.9*
6-β-GlcNAcyl	4.629	3.553	3.448	3.445	3.304	3.770/3.804
F	*102.8*	*57.1*	*74.7*	*74.2*	*71.9*	*67.1*
Gro	3.631/3.710	5.169	4.140/4.381			
G	*66.6*	*70.4*	*63.2*			
OD	3.523/3.580	4.950	1.532	1.240	n.a.	
H	*69.8*	*73.2*	*25.1*	*29.2*	*n.a.*	
GroAN(CH₂)₁₆CH₃	-	4.661	3.830	3.152/3.273	1.488	n.a.
I	*170.1*	*76.4*	*68.0*	*39.7*	*64.5*	*n.a.*
Gro	3.983	5.176	4.084/4.312			
L	*64.5*	*70.2*	*65.6*			

For residue **E**, $^3J_{H,H}$ values and *intra*-residual NOE connectivity revealed the α-*gluco* configuration. Moreover, the C-2 chemical shift value at 54.1 ppm, in the typical region of nitrogen-bearing carbons, implied the occurrence of 2-amino-2-deoxy-glucose. A typical proton resonance down-field shift due to acetylation was observable for H-2 (3.843 ppm).

Actually, this signal correlated in the ^{1}H,^{13}C-HMBC spectrum to a carbon at 173.4 ppm, which correlated to the methyl signal of the acetyl group at 1.998 ppm. Thus, this residue was identified as terminal 2-acetamido-2-deoxy-α-glucopyranose (t-α-GlcNAc).

Residue **F** (H-1 at 4.629 ppm) was identified as 2-deoxy-2-amino-glucose on the basis of the C-2 resonance at 57.1 ppm and of the high $^{3}J_{H,H}$ values, while the diagnostic NOE correlations observed between H-1, H-3 and H-5, and the $^{1}J_{C,H}$ anomeric coupling constant value (165 Hz) unambiguously proved the β-*gluco* configuration. Substitution occurred at *O*-6, as testified by the glycosylation shift for C-6 (67.1 ppm). Also, an acylation shift was observed for H-2 (3.553 ppm). In the HMBC spectrum, H-2 correlated to a carboxyl signal at 176.9 ppm which correlated to a proton at 2.218 ppm, identified as H_α to the carboxyl group of a fatty acid alkyl chain. This information proved the existence of the amide linkage with a fatty acid, namely, on the basis of previous chemical analysis, with 17:0. Thus, residue **F** was identified as 6-substituted-2-acylamido-β-glucopyranose (6-β-GlcNAcyl).

Table 4.2 - ^{1}H and ^{13}C (*italic*) chemical shifts for the identified acyl residues in the glycolipids mixture.

Linkage site	C=O	CH$_{2\alpha}$ (CH$_3$)	CH$_{2\beta}$	(CH$_2$)$_n$
N-2 E	-	1.998	-	-
	173.4	*22.1*	-	-
N-2 F	-	2.218	1.578	1.242
	176.9	*35.8*	*26.1*	*29.7*
O-2 G	-	2.240	1.543	1.242
	174.4	*34.6*	*29.8*	*29.7*
O-3 G	-	2.252	1.544	1.242
	174.5	*34.5*	*25.2*	*29.7*
O-2 L	-	2.227	n.a.	1.242
	172.5	*34.5*	*n.a.*	*29.7*
O-3 L	-	2.249	n.a.	1.242
	173.1	*34.5*	*n.a.*	*29.7*
O-2 H	-	2.252	n.a.	1.242
	177.1	*32.5*	*n.a.*	*29.7*

Of the anomeric region of the ^{1}H-NMR spectrum, signals at 5.169, 5.176, 4.950 and 4.661 ppm correlated in the ^{1}H,^{13}C-HSQC spectrum with carbon resonances at 70.4, 70.2, 73.2 and 76.4 ppm. These signals allowed the identification of four spin systems, designed **G**, **L**, **H**, and **I** respectively. In particular, the signal at 5.169 ppm (H-2**G**) showed correlations in the DQF-COSY with two diasterotopic methylene groups, at 4.140/4.381 (H-3$_a$/H-3$_b$**G**) and 3.631/3.710 (H-1$_a$/H-1$_b$**G**) ppm. On the basis of the chemical shifts for protons and carbon

signals (**Table 4.1**) and of the observed long-range correlations with carboxyl group resonances at 174.4 and 174.5 ppm, it was possible to identify residue **G** as a glycerol moiety acylated at *O*-2 and *O*-3. The identified resonances for the acyl moieties are collected in Table II**.** Full attribution was impossible because of the merging of methylene signals of the long fatty acid chains into one broad signal at 1.242 ppm.

Residue **H** was identified as the expected octadecane-1,2-diol, on the basis of the observed scalar correlations (DQF-COSY) of the signal at 4.950 ppm (H-2**H**) with one hydroxymethylene group (3.523/3.580 ppm, H-1$_a$/H-1$_b$**H**) and a methylene group in the aliphatic region (1.532 ppm). Chemical shifts for the other protons and carbons of the alkyl chain were only partially distinguishable (**Table 4.1**). In this case, acylation occurred at *O*-2, as proven by the long range correlation with the carboxyl at 177.1 ppm.

Residue **I** was identified as the *N*-glyceroyl-heptadecaneyl-amine unit. The signal at 4.661 ppm (H-2**I**) showed a correlation with a methylene signal at 3.830 ppm, that gave a scalar correlation with a carboxyl carbon at 170.1 ppm (C-1**I**, ^{1}H,^{13}C-HMBC). The same carbon signal also showed a correlation to the methylene signal at 3.152/3.237 ppm, which was identified as H-1'**I** and, thus, as the aminomethylene position, on the basis of the carbon chemical shift value (39.7 ppm).

A second glycerol unit was identified (**L**), starting from the resonances of H-2 at 5.176 ppm, from which two correlations with hydroxymethylene groups, resonating at 4.084/4.312 (H-3$_a$/H-3$_b$**L**) and 3.983 ppm (H-1$_{a/b}$**L**), could be identified. Correlations were observed for H-2 and H-3 with carbonyl groups (172.5 and 173.1 ppm), suggesting acylation at *O*-2 and *O*-3, while the observed down-field displacement of the H-1 resonance, compared to the analogous position of residue **G**, implied phosphorylation at this site, in consistency with chemical analyses.

Connectivity between the identified spin systems were established on the basis of the *inter*-residual dipolar correlations detected in the 2D ROESY spectrum and scalar long-range correlations observed in the ^{1}H,^{13}C HMBC spectrum. In particular, proton H-1**A** gave a strong NOE connectivity with H-2**B** and a scalar correlation with the carbon resonance at 76.7 ppm, suggesting the attachment at *O*-2 of the α-Gal*p* residue. This was linked at *O*-6 of residue **F**, namely the β-GlcNAcyl residue, as confirmed by the occurrence of the dipolar correlation H-1**B**/H-6**F** and of the long-range correlation between H-1**B** and C-6**B**. A cross peak appeared in the ROESY spectrum between H-1**F** and a proton at 3.472 ppm, identified as H-2 of residues **C** and **D**. The information deriving from both ROESY and ^{1}H, ^{13}C-HMBC spectra showed that residue **C** was linked to *O*-1 of residue **G**. In fact, a long-range correlation existed

between H-1**C** and the carbon at 66.6 ppm (C-1**G**). Residue **D** appeared to be linked at *O*-1 of residue **H,** namely the octadecane-1,2-diol.

These data can be summarized in the following structure:

$$\alpha\text{-Gal}f\text{-(1-2)-}\alpha\text{-Gal-(1-6)-}\beta\text{-GlcNAcyl-(1-2)-}\alpha\text{-Glc-(1-1)-R}$$

<div align="center">

A   **B**   **F**   **C/D**

</div>
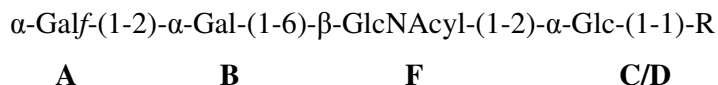
R=Gro (**G**) or OD (**H**)

Thus, the tetrasaccharide backbone is either linked to the glycerol unit **G** or to the octadecane-1,2-diol **H**.

Residue **E** (t-α-GlcNAc) showed a NOE correlation with H-2**I**, and an additional long-range correlation with C-2**I** that indicated the presence of the fragment α-GlcNAc-(1-2)-*N*-glyceroyl-heptadecane-amine. These two spin systems, as well as the glycerol-phosphate **L**, did not show any dipolar or long-range correlation in NMR spectra with the structures so far identified, thus appearing as isolated fragments, likely belonging to a different molecular species within the blend (see below).

4.2.2 Purification and complete characterisation of GL1, GL2 and PGL from *T. thermophilus* Samu-SA1

In order to find out further structural details, mild *O*-deacylation with anhydrous hydrazine was performed, and the product was purified on silica-gel. Two fractions were obtained, composed by *O*-deacylated glycolipids (**de-*O*-GL1** and **de-*O*-GL2**), and ESI FT-MS and 1D and 2D-NMR analyses were performed on both products. The approximate molar ratios of monosaccharides in both fractions were Gal:Glc:GlcN 2:1:1.

NMR spectra recorded on the more abundant fraction (**de-*O*-GL1**) appeared rather simplified comparing to that of the initial mixture (**Figure 4.4**). Nevertheless, the tetrasaccharide linked to the octadecane-1,2-diol already identified was clearly recognisable. This affirmation was proven by the NOE correlation in the ROESY spectrum between H-1 of the 2-α-Glc residue with H-1**H** and by the observation of the scalar long-range *inter*-residual correlation in the ^{1}H,^{13}C-HMBC with C-1**H**.
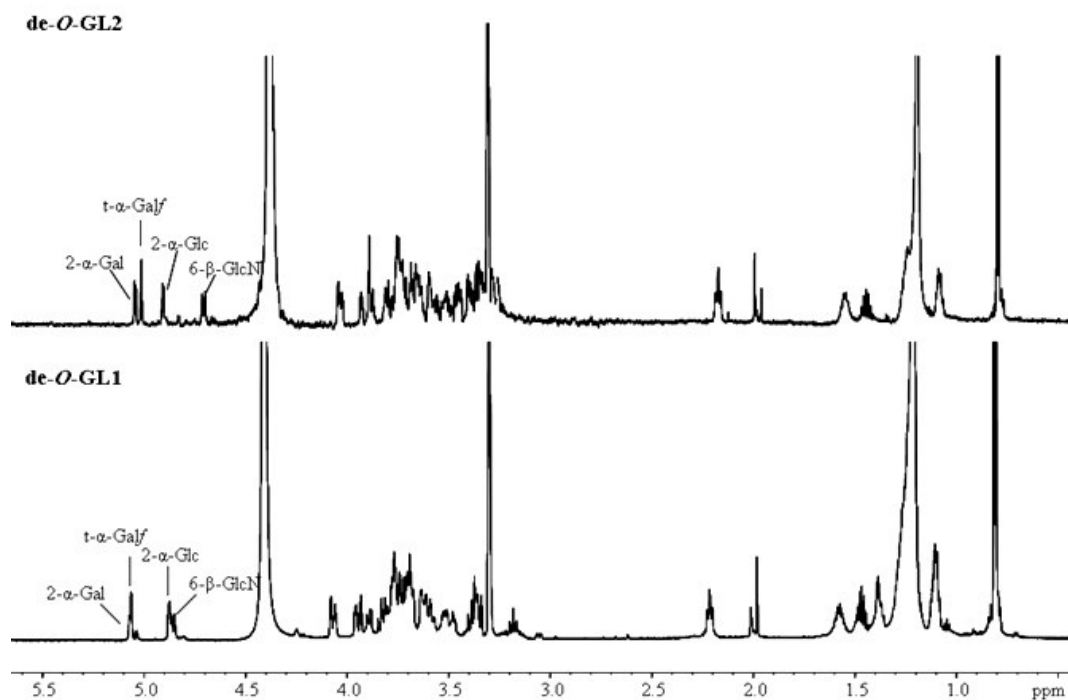
Figure 4.4 - Comparison of ^{1}H-NMR spectra of the products obtained after purification of *O*-deacylation of the glycolipid extract from *Thermus thermophilus* Samu-SA1. The identified spin systems are representative of the conserved structure of the tetrasaccharide moiety.

Final confirmation of the proposed structure was provided by ESI FT-MS of the **de-*O*-GL1** (**Figure 4.5**), The charge deconvoluted mass spectrum revealed an abundant peak with an monoisotopic mass of 1185.760 u which is in an excellent agreement with the calculated mass (1185.7597 u) of a molecule composed of OD-Hex$_3$-HexN-17:0. Comparison with the ESI-MS spectra of the mixture, led to the identification of the first molecular species in the native form (**GL1**, **Figure 4.6**), where the molecule appeared to be *O*-acylated at *O*-2 of the OD residue by a 15:0, as testified by the molecular mass of 1409.979 u, differing from 1185.760 u by one 15:0 unit.

The NMR data (**Figure 4.4**) of the second isolated fraction (**de-*O*-GL2**) showed high analogy with **de-*O*-GL1**, the only structural difference being the occurrence of a glycerol moiety instead of the long-chain diol. Also in this case, the tetrasaccharide structure was recognised after complete 2D NMR analysis, and resulted identical to the structure already found in **de-*O*-GL1.**

ESI-MS spectrum on **de-*O*-GL2** (**Figure 4.5**) showed an intensive molecular peak with 991.519 u, in agreement to the proposed species Gro-Hex$_3$-HexN-17:0, with a minor peak at 829.465 u (Δm = 162 u), suggesting the presence of a minor compound lacking of a hexose
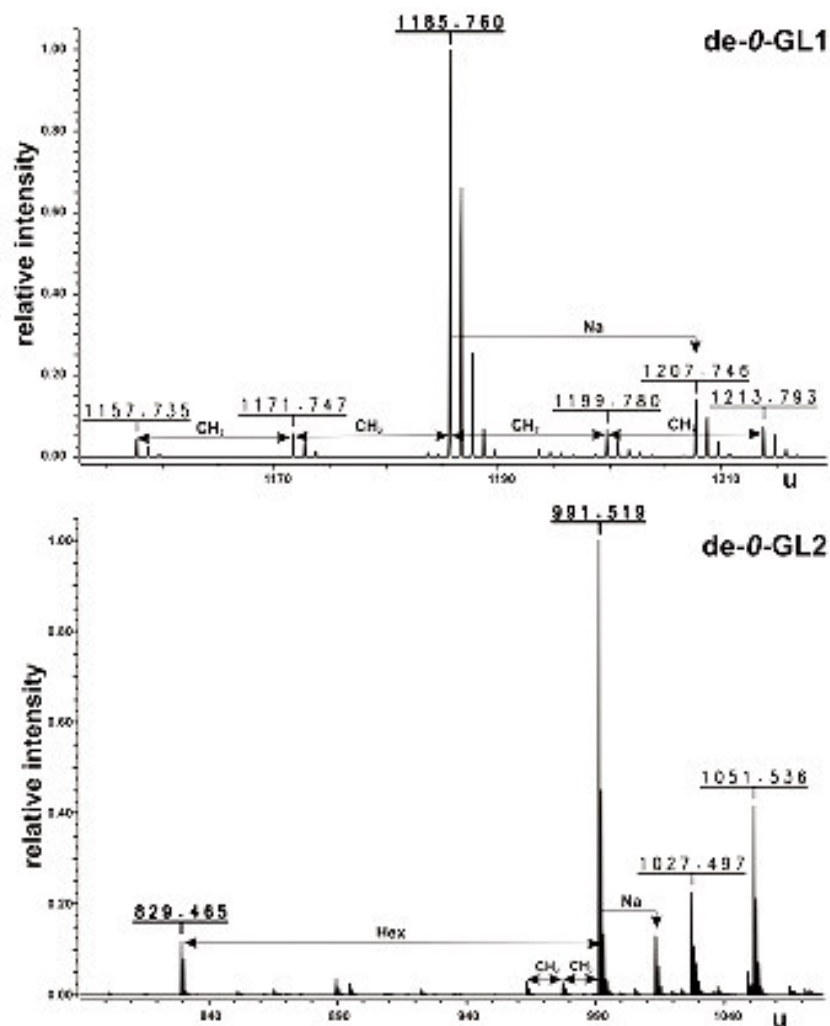
Figure 4.5 - Charge deconvoluted ESI FT mass spectra of the separated fractions obtained from the glycolipid extract of *Thermus thermophilus* Samu-SA1 after *O*-deacylation. The major peaks correspond to the exact mass of characterised **de-O-GL1** and **de-O-GL2** (see **Table 4.4**)

residue. This minor form was not distinguishable in the NMR spectra. The two ion peaks visible in this spectrum at 1027.497 u (Δm = 36 u) and 1051.536 u (Δm = 60 u) were likely due to artefacts deriving from the purification procedure applied, since neither chemical analysis and NMR investigation showed any species that could generate these molecular ions. Moreover, analogous mass differences are undetected in the intact mixture spectrum. The comparison with the ESI-MS spectrum of the blend, allowed to relate **de-*O*-GL2** to the species represented by the peak with a mass of 1467.977 u, identified as the molecular ion peak for the second glycolipid (**GL2**, **Figure 4.6**). In fact, the mass difference of 476 u between the two peaks was consistent with the presence of one 15:0 and one 17:0 residues, suggesting that *O*-2 and *O*-3 of the glycerol unit must be esterified by these two residues. In

the same way, the species with a molecular mass of 1439.949 u was in account for a minor compound acylated by two 15:0 units.

It was not possible to find any product related to the phospholipid present in the native mixture, likely due to total degradation during *O*-deacylation. Nevertheless, it was possible to compare the composition of the two glycolipids so far identified with the results of the chemical and spectroscopical analyses performed on the native mixture (**Table 4.3**), deducing the identity of the third expected molecule.

Table 4.3 - Comparison between chemical compositions, obtained by GC-MS and NMR, of the native glycolipid extract and the constituent species, **GL1, GL2** and **PGL.**

Native mixture	GL1	GL2	PGL
t-α-Galf	X	X	-
2-α-Gal	X	X	-
2-α-Glc	X	X	-
t-α-GlcNAc	-	-	X
6-β-GlcNAcyl	X	X	-
Gro	-	X	-
GroP	-	-	X
octadecane-1,2-diol	X	-	-
GroAN(CH$_2$)$_{16}$CH$_3$	-	-	X

This was identified as a phospholipid (**PGL**), containing in its structure the fragment α-GlcNAc-(1-2)-*N*-glyceroyl-heptadecane-amine, previously identified, and acyl-glycerolphosphate. This hypothesis was supported by the detection, in the ESI spectrum executed on the mixture, of a peak with mass of 1176.857 u (**Table 4.4**), which was consistent with Gro-HexNAc-GroAN(CH$_2$)$_{16}$CH$_3$-P-C$_{17:0}$-C$_{15:0}$ (**PGL, figure 4.6**). From this mass spectrum it was also possible to deduce that the glycerol unit was esterified, in the most abundant species, by one 15:0 and one 17:0. It was also possible to detect a highly heterogeneous acylation pattern, indicated by the occurrence of ions with $\Delta m = 14$ u, a methylene group, suggesting variability in the chain length of fatty acid residues. Moreover, the family of ions centred at 1134.846 u ($\Delta m = 42$ u, acetyl group)*,* indicated the presence of a small amount of a compound where the GlcN residue was not acetylated. The absence of dipolar correlations between the glyceramide and the acyl-glycerol units, observed in the previous NMR data, was explained with the existence of a phospho-diester bridge connecting the two fragments, as confirmed by the detection of glycerol phosphate in chemical analysis. Such a structure was earlier found in bacteria belonging to the genus *Deinococcus*, a genus

phylogenetically related to *Thermus* (Huang and Anderson, 1989, 1992). **Figure 4.6** summarizes the structures of **GL1, GL2** and **PGL**.

Table 4.4 - Measured and calculated exact molecular masses of the identified glycolipids from *Thermus thermophilus* Samu-SA1. The measured masses were taken from the charge deconvoluted mass spectra given in **Figg. 4.1** and **4.4.**

|	Measured mass (u)	Calculated mass (u)	Molecular Formula
GL1	1409.979	1409.9739	OD-Hex$_3$-HexN-17:0-15:0
GL2	1467.979	1467.9793	Gro-Hex$_3$-HexN-(17:0)$_2$-15:0
	1439.944	1439.948	Gro-Hex$_3$-HexN-17:0-(15:0)$_2$
PGL	1176.858	1176.8502	Gro-HexNAc-GroAN(CH$_2$)$_{16}$CH$_3$-P-17:0-15:0
	1204.889	1204.8817	Gro-HexNAc-GroAN(CH$_2$)$_{16}$CH$_3$-P-(17:0)$_2$
	1134.846	1134.8399	Gro-HexN-GroAN(CH$_2$)$_{16}$CH$_3$-P-17:0-15:0
de-*O*-GL1	1185.760	1185.7597	OD-Hex$_3$-HexN-17 :0
de-*O*-GL2	991.519	991.5199	Gro-Hex$_3$-HexN-17:0
	829.465	829.4671	Gro-Hex$_2$-HexN-17:0
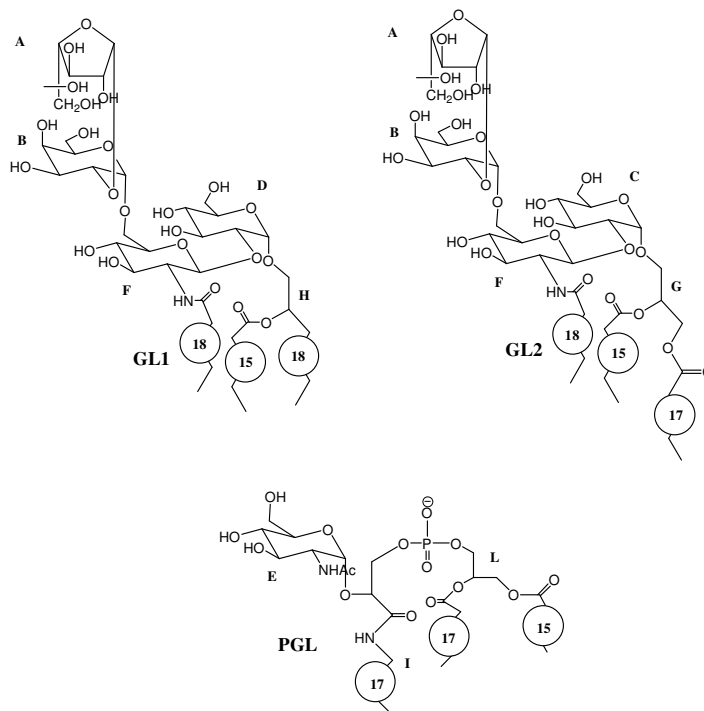
Figure 4.6 - Structure of the **GL1, GL2** and **PGL** composing the glycolipid component isolated by *Thermus thermophilus* Samu-SA1.In the circle, in bold, the total number of carbon atoms of the most abundant alkyl chain is indicated. Letters refer to NMR analysis (**Table 4.1**)

4.3 *Geobacillus thermoleovorans* **strain Fango**

Geobacillus thermoleovorans strain Fango (ATCC BAA-872) is an aerobic, endospore forming and thermophilic microrganism, first isolated from a geothermal soil sample in Italy (Stufe di Nerone, Lucrino, Na). *Geobacillus thermoleovorans* is characterized by phenotypic heterogeneity and genotypic homogeneity. As already observed in section 4.1, the typical cell wall structure of *Geobacillus* genus is Gram-positive, but the Gram-stain reaction may vary between negative and positive depending on the strain (Nazina *et al.,* 2004). This unusual behaviour prompted us to study the chemical composition of the cell wall. Also in this case, the conventional hot phenol/ water extraction was performed. The water phase collected after the extraction was enzymatically digested to remove nucleic acids and proteins and subsequently purified by size exclusion chromatography. A first purification on a Sephacryl S-400 column yielded two fractions, and both underwent chemical analyses for detection of the monosaccharide content. GC-MS analysis of acetylated *O*-methyl glycosides derivatives identified in both fractions a high amount of glycerol (Gro) and glycerolphosphate (GroP), suggesting the occurrence of teichoic acids (TAs), essential cell-wall constituents of Gram-positive bacteria (Archibald *et al.,* 1968). These are polyanionic molecules, of which, based on the composition of the main chain, four structural types can be distinguished, i.e. poly(polyol phosphates), poly(glycosylpolyol phosphates), poly(polyol phosphate-glycosyl phosphates), and poly(polyol phosphate-glycosylpolyol phosphates) (Neuhaus and Baddiley, 2003). Of these, the first two are most often occurring. Poly(polyol phosphates) contain as polyol moieties glycerol, erythrol, ribitol, arabinitol or mannitol. Teichoic acids comprise between 20-50% of the Gram-positive cell wall. While lipoteichoic acids are embedded in the cytoplasmic membrane through a lipid anchor (acylated glycerol), TA are linked directly to muramic acid of the peptidoglycan through a phosphodiester bond (Archibald *et al.,* 1968; Fisher, 1990; Neuhaus and Baddiley, 2003).

Of the two fractions collected from the gel permeation chromatography, the most retained one was entirely constituted by TAs (**TA1**). The not retained, high molecular mass fraction was mainly composed by lipid components that eluted as micelle aggregates. From this fraction, a second and different teichoic acid fraction (**TA2**) was purified by size exclusion HPLC on a TSK G-5000 column. GC-MS analyses of **TA1** showed additional presence of t-D-Gal*p* while **TA2** possessed, beside this monosaccharide, minor amounts of t-D-Glc*p*N, 2-D-Glc*p* and 3-D-Glc*p*. After treatment with 48% aqueous HF and methylation, additional Hex-*O*-Gro fragments could be detected.
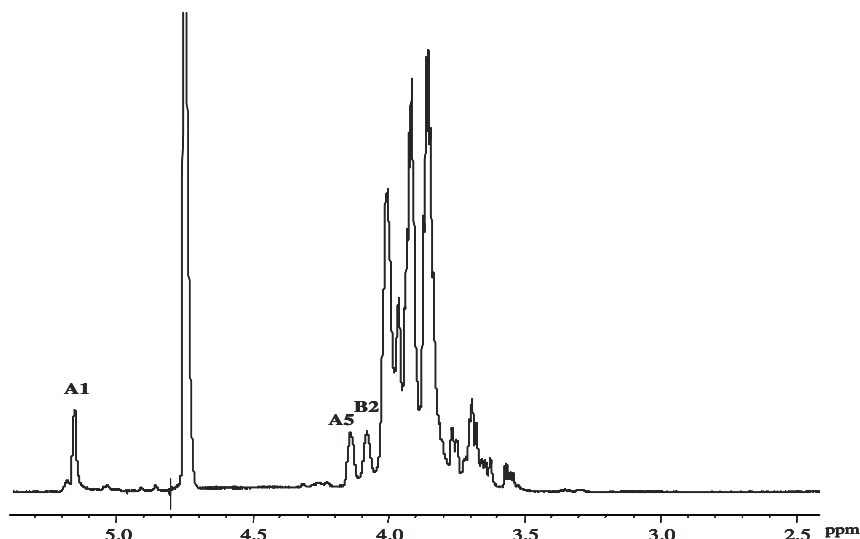
Figure 4.7 - ^{1}H-NMR spectrum of **TA1** from *Geobacillus thermoleovorans* strain Fango. Capital letters refer to the spin systems described in **Table 4.5.**

On the isolated fractions, a complete 1D and 2D NMR spectroscopical analysis was performed. ^{1}H-NMR on **TA1** (**Figure 4.7**) showed a highly homogeneous product. A single signal (H-1**A**) appeared in the anomeric region of the spectrum at 5.150 ppm. On the basis of TOCSY and of DQF-COSY spectra, all resonances were assigned for t-Gal*p* (**Table 4.5**), on the basis of chemical shift and the small $^3J_{3,4}$ and $^3J_{4,5}$ values. A coupling constant of 3.4 Hz for $^3J_{1,2}$ identified, together with the typical chemical shifts for anomeric proton and carbon, the α-configuration. ^{13}C NMR resonances were deduced from a ^{1}H,^{13}C-HSQC spectrum (not shown). In this spectrum, signals for at least two magnetically different glycerol units (**B** and **C**) were identified. In particular, residue **B** presented down-field displacement of the C-2 resonance (75.1 ppm), compared to residue **C**, likely due to glycosylation. This hypothesis was confirmed by a 2D ROESY spectrum, in which a strong dipolar correlation between H-1**A** and H-2**B** were found. These data were coherent with the occurrence of two different repeating units, one composed by glycerol-phosphate and the other one by glycerol-phosphate substituted by t-α-D-Gal*p*:

→1)-Gro-(3P→   and   **→1)-Gro-(3P→**
                                                                                        2
                                                                                        ↑
                                                                                        1
                                                                                α-D-Gal*p*
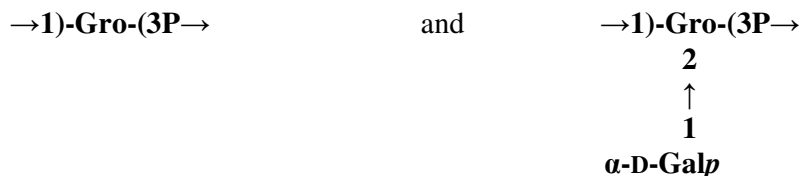
It was not possible to evaluate the exact ratio between the two units due to the overlapping of the signals of the glycerol units between 4.200 and 3.500 ppm.

The second teichoic acid fraction (**TA2**), isolated after HPLC purification, gave a rather complex NMR spectrum. At least four different anomeric signals, designed **D**, **E**, **F** and **F'**, were visible in the region between 5.200 and 4.700 ppm (**Figure 4.8**). These signals were present in non-stoichiometric amounts, suggesting the occurrence of more than one type of repeating unit within the TA structure. A complete assignment of proton resonances was possible for the major spin systems, on the basis of DQF-COSY and TOCSY spectra, while ^{13}C resonances were obtained from a ^{1}H,^{13}C-HSQC spectrum (**Table 4.5, Figure 4.8**). Spin system **D** was identified as t-α-D-Gal*p*, on the basis of the same considerations applied for residue **A** in **TA1**. The signal at 5.031 ppm accounted for the presence of at least two major magnetically different glucose units (H-1**E/E'**), identified on the basis of the small $^3J_{1,2}$ as α-D-Glc*p* units. In particular, residue **E** was identified as t-α-D-Glc*p*, while the down-field displacement of the C-2 resonance of residue **E'** (78.6 ppm) identified it as 2-substituted-α-D-Glc*p*. In the TOCSY spectrum, an alternative and very minor spin system (3-substituted α-D-Glc*p* **E''**) was identified on the basis of the H-3 signal at 3.776 ppm that correlated in the ^{1}H,^{13}C-HSQC spectrum with a carbon signal at 81.3 ppm. The two minor anomeric signals at 4.894 and 4.845 ppm (H-1**F/F'**) were identified as the anomeric signals of two t-α-D-Glc*p*NAc units, in accordance with chemical analysis and on the basis of the C-2 chemical shift values. The *N*-acetylation was proven by the down-field shift of H-2 and by the occurrence of acetyl methyl group resonances around 2.000 ppm. The full assignment of proton and carbon ring signals could not be achieved owing to the complete overlap with the more abundant spin systems.

With the help of a ^{1}H,^{13}C-HSQC spectrum (**Figure 4.9**), three magnetically different glycerol phosphate units could be identified (**G, H** and **I**). In particular, residue **G** was recognised as glycosylated glycerol phosphate, on the basis of the C-2 chemical shift value (75.1 ppm), while residues **H** and **I** did not show substitution at *O*-2. Minor signals were also observed for a glycerol residue substituted at *O*-2 by an alanine residue (**L**), previously undetected. The presence of an alanine residue in non-stoichiometric amounts was suggested by a methyl doublet signal at 1.25 ppm the ^{1}H-NMR spectrum. In the COSY spectrum, this signal correlated with a proton at 4.245 ppm which in turn correlated in a ^{1}H,^{13}C-HSQC spectrum with a carbon resonance at 53.3 ppm.
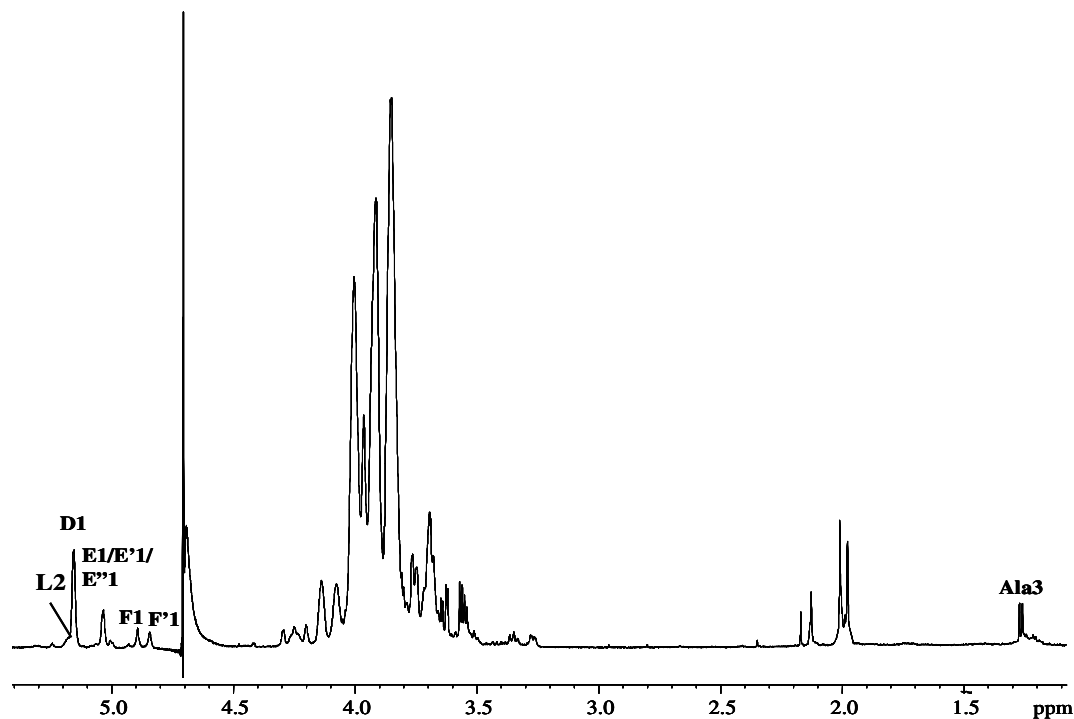
Figure 4.8 - ^{1}H-NMR spectrum of **TA2** from *Geobacillus thermoleovorans* strain Fango. Capital letters refer to the spin systems described in **Table 4.5**, and chemical shifts refer to internal acetone (2.225 ppm).

On the basis of dipolar correlations observed in the 2D ROESY spectrum (**Figure 4.10**), residues **D**, **E**, **E'** and **E''** appeared to be directly linked to glycerol-phosphate units, since their anomeric signals all gave NOE connectivity with H-2**G**. Residues **F** gave a strong NOE contact with H-2**E'**, thus providing evidence for the occurrence of a disaccharide unit bound to a glycosylated glycerol-phosphate unit. An *inter*-residual dipolar correlation was also visible between H-1**F'**/H-3**E''**, showing that minor amounts of the terminal D-Glc*p*NAc residue could be attached to *O*-3 of the glucose residue. On the other hand the occurrence of substitution by Ala to the glycerol residue **L** was proposed by the comparison with data previously reported for other TA structures (Sadovskaya *et al.,* 2004; Vinogradov *et al.,* 2006).

Table 4.5 – ¹H and ¹³C (*italic*) chemical shifts for the cell wall teichoic acids **TA1** and **TA2** from *Geobacillus thermoleovorans* strain Fango.

	Residue	H1/C1	H2/C2	H3/C3	H4/C4	H5/C5	H6/C6
TA1	**t-α-Gal**	5.150	3.762	3.859	3.956	4.137	3.684
	A	*97.9*	*67.9*	*69.5*	*69.2*	*70.7*	*61.3*
	GroP	4.006	4.074	3.973			
	B	*65.2*	*75.1*	*65.0*			
	GroP	3.930	4.013	3.851			
	C	*66.2*	*69.1*	*66.3*			
TA2	**t-α-Gal**	5.155	3.751	3.859	3.964	4.135	3.675
	D	*97.8*	*68.1*	*70.5*	*69.1*	*70.8*	*61.0*
	t-α-Glc	5.031	3.263	3.545	3.347	3.679	3.631
	E	*98.0*	*71.0*	*72.3*	*68.4*	*71.0*	*62.0*
	2-α-Glc	5.028	3.827	3.757	3.511	3.679	3.631
	E'	*97.1*	*78.6*	*69.4*	*68.5*	*71.0*	*62.0*
	3-α-Glc	5.031	3.263	3.776	3.511	3.679	3.631
	E''	*98.0*	*71.0*	*81.3*	*68.5*	*71.0*	*62.0*
	t-αGlcNAc	4.894	4.202	3.832	3.950	3.728	*n.a.*
	F	*99.6*	*51.5*	*70.6*	*n.a.*	*n.a.*	*n.a.*
	t-α-GlcN	4.845	4.292	3.838	*n.a.*	*n.a.*	*n.a.*
	F'	*99.2*	*50.8*	*n.a.*	*n.a.*	*n.a.*	*n.a.*
	GroP	3.393	4.077	3.977			
	G	*65.3*	*75.1*	*66.0*			
	GroP	3.918/3.848	4.001	3.635/3.560			
	H	*66.1*	*69.4*	*61.9*			
	GroP	3.808	3.853	3.635			
	I	*66.4*	*69.4*	*61.9*			
	GroP		5.182	4.012			
	L		*71.8*	*64.7*			
	Ala	-	4.245	1.250			
		n.a.	*53.3.*	*16.5*			
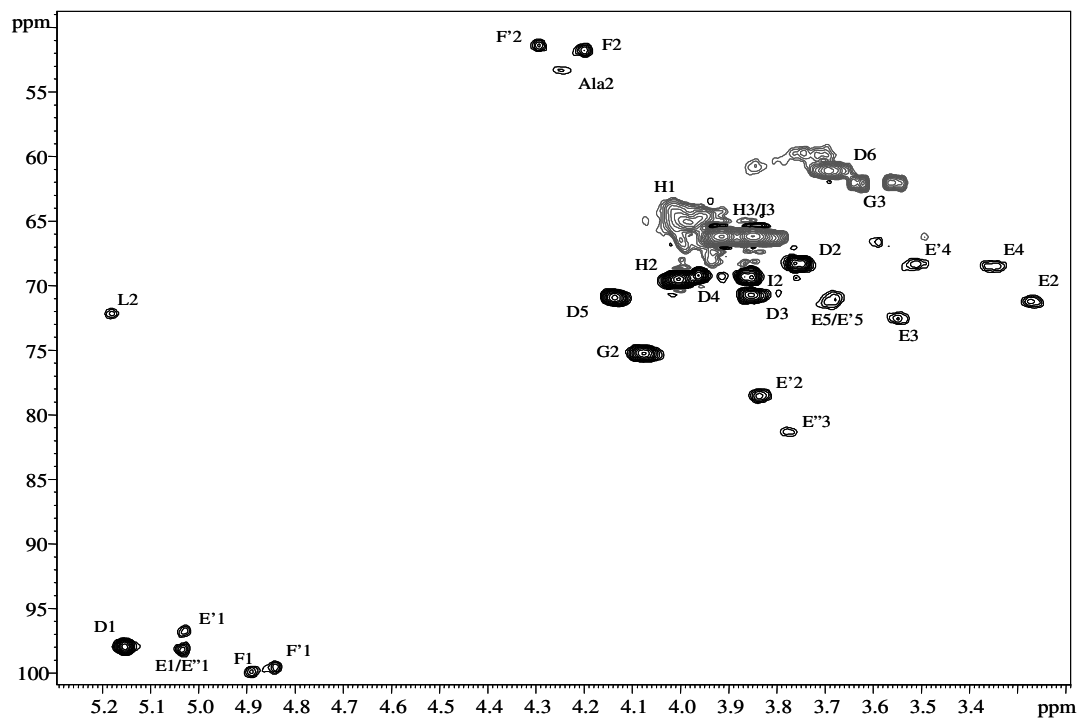
Figure 4.9 - Section of the ^{1}H,^{13}C-HSQC spectrum of **TA2** from *Geobacillus thermoleovorans* strain Fango. The spectrum was edited for the detection of signal multiplicity. Methylene groups are shown in grey. Letters refer to the identified major spin systems in **Table 4.5.**
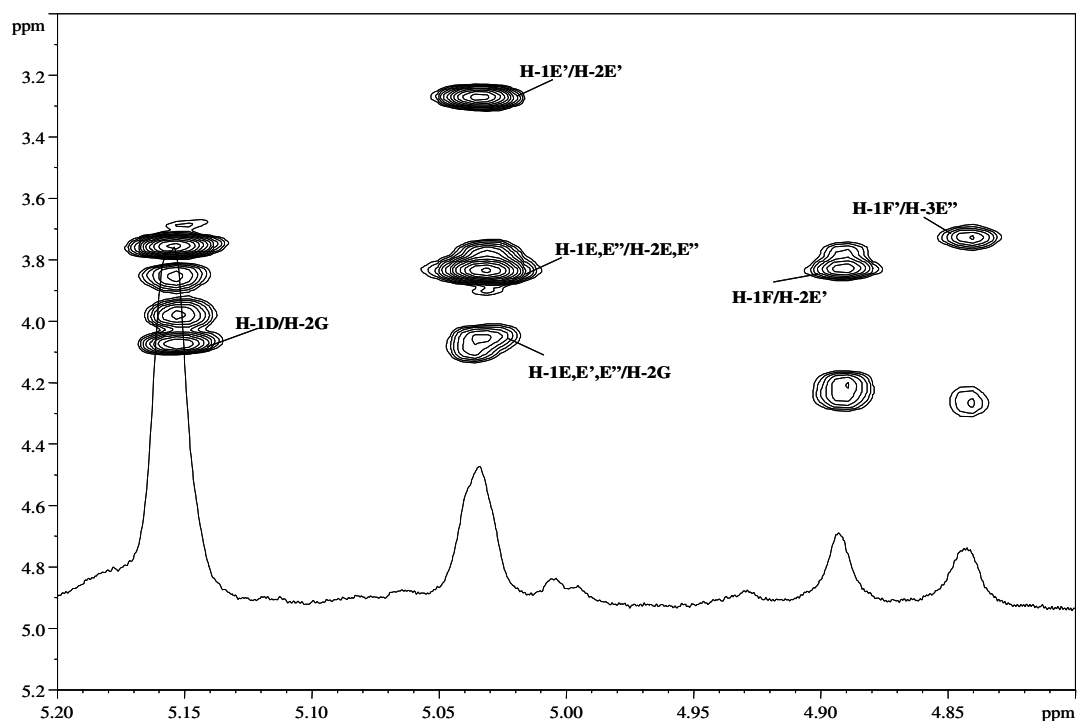
Figure 4.10 - Zoom of the anomeric region of the 2D ROESY spectrum of **TA2** from *Geobacillus thermolevorans* Fango. Letters refer to the diagnostic *intra-* and *inter-*residual dipolar correlations.

In summary, **TA2** contained a blend of structures, where several different repeating units were simultaneously present. In particular, the most abundant repeating units were identical to the ones previously defined for **TA1**, namely glycerol phosphate and glycerol phosphate substituted by t-α-D-Gal*p*. Also, minor units could be found, in which substitution at *O*-2 of glycerol phosphate was effected, in order of decreasing abundance, by t-α-D-Glc*p*, by the disaccharides t-α-D-Glc*p*NAc-(1→2)-α-D-Glc*p* or t-α-D-Glc*p*NAc-(1→3)-α-D-Glc*p*, or by an alanine residue.

These additional minor structures are the following:

→1)-Gro-(3P→	→1)-Gro-(3P→	→1)-Gro-(3P→	→1)Gro(3P→
2	2	2	2
↑	↑	↑	↑
1	1	1	**D-Ala**
α-D-Glc*p*	**α-D-Glc*p*NAc-(1→2)-α-D-Glc*p***	**α-D-Glc*p*NAc-(1→3)-α-D-Glc*p***	
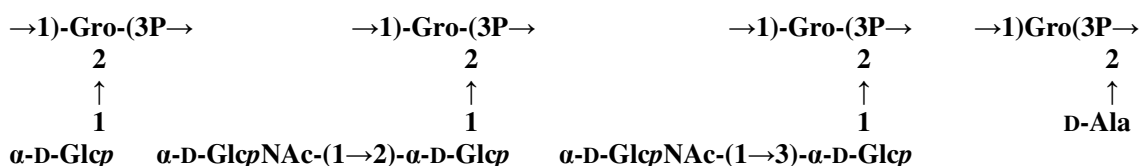
Nevertheless, on the basis of our analysis, it was not possible to state whether the structures defined are present in a single, extremely variable glycerol polymer with non stoichiometric appendages, or if they constitute different building blocks of chains with the same chromatographic behaviour. It is noteworthy that **TA2** constitutes only the minor percentage of the total teichoic fraction isolated from *Geobacillus thermoleovorans* strain Fango, whereas the most abundant species is represented by **TA1**.

The D configuration of the Ala residue in **TA2** is proposed on the basis of the literature data where the totality of Ala substitution in TAs is accomplished by D enantiomer (Neuhaus and Baddiley, 2003). In fact, substitution by D-Ala is one of the characteristic features of TA structure, and its presence and abundance play a crucial role concerning the structure of the cell envelope and the toxicity of TA (Neuhaus and Baddiley, 2003; Ward, 1981; de Vos, 2005; Steen *et al.,* 2005). It is known that during the biosynthesis of TA the isomerization of L-Ala into D-Ala is realised by an isomerase that acts prior to the formation of the ester linkage with the glycerol unit (Perego *et al.,* 1995; Linzer and Neuhaus, 1973).

4.4 Conclusions

Both thermophile microrganisms characterised in the present section, despite the negative response expressed to the Gram assay, did not produce LPSs as components of their membrane. In the case of *Geobacillus thermoleovorans* Fango, the finding of typical Theicoic

Acids represented the evidence for the occurrence of a classical Gram-positive membrane architecture. Comparison of the structure characterised with literature data does not offer a clue for the existence of a relation among them and the unconventional environment where this microrganism was first isolated. Its extraordinary heat resistance must be provided by other Cell Envelope constituents, likely S-layer proteins (see section 1.4), or by a peculiar peptidoglycan architecture, that were not investigated in the present work.

   Thermus thermophilus Samu-Sa1 is instead a proper Gram-negative bacterium, and the absence in its Outer Membrane organization of LPSs had already been proven by previous studies on *Thermus thermophilus* HB8 (Silipo *et al.,* 2004), concomitantly with the detection and characterization of a membrane associated polysaccharide with a non-repeating unit. The finding in *T. thermophilus* Samu-Sa1 of atypical glycolipids (see section 4.2) can suggest the hypothesis that the chemico-physical role, conventionally played by LPSs, may be accomplished by these molecules, provided as well with a lipid portion, forming the main part of the outer leaflet of the membrane itself, and with a saccharide part directed towards the surrounding environment. Polar glycolipids and phosphoglycolipids have been found to be the major components of the cell wall of *Thermus* bacteria (Pask-Hughes and Shaw, 1982). The two glycolipids reported in section 4.2 share a tetrasaccharide structure, in which a long-chain alkyl diol may replace glycerol. This feature was already found in *Thermomicrobium roseum* (Jackson *et al.*, 1973; Perry, 1992), as well as in the membrane composition of *Thermus scotoductus* and *Thermus filiformis* (Wait *et al.*, 1997).

   In our opinion, the occurrence of long chain alkyl diols within membrane glycolipids structure can be seen as one of *Thermus* adaptive responses to environmental stressors, due the greater chemical strength of the alkyl chain compared to the more labile ester bonds of acyl-glycerol. This adaptative response somehow resembles that observed in Archaea, where tetraether-linked glycolipids are synthesized in case of heat exposure (cfr. section 1.2.1).

    Other thermophilic species also express uncommon structural features, as for example long-chain ethers in *Aquifex pyrophilus* (Huber *et al.,* 1992) or α,ω-dicarboxylic fatty acids in *Thermotoga maritima* (De Rosa *et al.,* 1989), that may result in an increased resistance to heat, regarding either chemical stability or the preservation of physical properties of the whole membrane. Nevertheless, it is presently not possible to state whether these chemical peculiarities represent a type of evolutionistic answer to environmental pressures. The same consideration can be done concerning the presence of the unusual phospholipid structure, that, interestingly, is closely related to compounds previously found in *Deinococcus* (Huang and Anderson, 1989; 1992). *Deinococcus* genus (Murray, 1986) and *Thermus* genus (da Costa and

Rainey, 2001), belong to the same Phylum BIV, but in different Families (*Deinococcaceae* and *Thermaceae*, respectively). *Deinococcus* is, like *Thermus*, an extremophilic genus (Murray, 1986), endowed with high resistance to heat, desiccation and radiation. From a biological point of view, it was proposed that the phospholipids isolated from *Deinococcus* could be chosen as taxonomic genus markers. The detection of the same kind of molecules in bacteria belonging to the genus *Thermus* contradicts this idea. Indeed, we can consider that *Thermus* and *Deinococcus* are philogenetically related, and the finding in both of similar membrane components can open a debate on existing analogies in the metabolic patterns of the two genera. Moreover, the consideration that both species can survive in extreme environments once again suggests a crucial involvement of these membrane compounds in the increased resistance to stress factors respect to common mesophilic Gram-positive and Gram-negative bacteria.

5

Organic Solvent Tolerant Bacteria

5.1 Introduction

Organic solvents, introduced into the ecosystem as pollutants by human activities, create extreme environments where an unusual kind of extremophiles can thrive. Bacteria able to tolerate high amounts of organic and toxic substances have been recently isolated, and they all developed changes in their cytoplasm and membrane composition to suppress lethal effects triggered by pollutants. These effects are particularly tough in the case of organics with a log P_{ow} below 4 (see section 1.2.5), since they preferably locate in the cell membranes, disrupting their organization and altering the cell physiology. In particular, bacteria able to blossom in presence of organic compounds as concentrated as a second phase have been reported, and they are now crucial in the development of new biotechnological strategies for decontamination of polluted sites, mostly in the case of such substances of difficult physical and chemical degradation, which can be converted, through specific enzymatic systems, into non-toxic substances. The effects of exposure to organic solvents on Gram-negative bacterial cells have been already described in section 1.2.5. In the present section, the structure study of the LPS fraction from two organic solvent tolerant bacteria, *Pseudomonas* sp. OX1 and *Acinetobacter radioresistens* S13, will be presented. Differently from the other bacteria presented in this work, organic solvent tolerant bacteria are not obliged extremophiles, meaning that they can grow optimally on both organic matter or conventional cultural media. This is not true for the other extremophiles, who require the maintenance of the extreme parameters characteristic of their native habitats to raise, and allows a comparative study of the OM components in the presence and in the absence of the pollutants, in order to find out whether they have or not a direct influence on the cell surface architecture. This study led to noticeable results, mostly in the case of *Pseudomonas* sp. OX1. Moreover, it has been found that colonies of this bacterium grown under stress conditions are able to produce a biofilms, dense bacterial communities, characterised by close associations of bacterial cells, generally attached to a solid surface and surrounded by a saccharide matrix. Exopolysaccharides (EPSs) are the major components of bacterial biofilm matrices and they mediate the transport of chemicals to and from the microrganisms, showing also ion exchange properties, due to

negatively charged surface functional groups, which bind to cationic species. EPS matrix also provides an effective barrier that restricts penetration of chemically reactive biocides, antibiotics and antimicrobial agents. It has been shown that bacteria living in biofilm matrices can be up to 1000 times more resistant to antibacterial compounds than planktonic bacteria. Given the chemical nature of antibiotics, similar biofilm-mediated mechanisms can also be involved in resistence to chemicals. In the present chapter, the structure of the EPS substance produced by *Pseudomonas* sp. OX1 was isolated and characterised.

5.2 *Acinetobacter radioresistens* S13

Bacteria of the genus *Acinetobacter* are ubiquitous, generally non-pathogen microrganisms belonging to the family of *Moraxellaceae* (Towner *et al.,* 1991). These bacteria have gained interest, in the last thirty years, because of the identification of some *Acinetobacter* species causing severe nosocomial infections, particularly in compromised patients. Among the 19 genomic species identified within the genus until now, the ones detected in human clinical isolates usually belong to the so-called *A. calcoaceticus – A. baumannii* complex (Gerner-Smidt, 1992; Joly-Guillou, 2005), comprehensive of four distinct genomic species of ascertained virulence. Other *Acinetobacter* genomovars are only occasionally associated to human infections, i.e. *Acinetobacter lwoffii*, a common coloniser of food, able to trigger gastritis in debilitated patients with no history of *Helicobacter pylori* colonisation (Rathinavelu *et al.,* 2003). *Acinetobacter radioresistens* S13 is a non-pathogenic, solvent tolerant Gram-negative bacterium, isolated from the soil surrounding an activated sludge pilot plant in Torino, in Italy, and selected for its catabolic activity towards phenol and benzoate (Pessione and Giunta, 1997). For this reason, this microbe is the object of studies aimed to find out possible applications in the field of bioremediation. In the following sections, the structure study of the LOS isolated from *A. radioresistens* S13, after cultures performed in various media, is presented. The structures found show always the same appearance, independently from the culture conditions, and exhibit a strong homology, especially in the Inner Core-Lipid A portion, with oligosaccharides from other *Acinetobacter* strains, and particularly with the core region of the virulent *A. baumannii* strain ATCC 19606 (Vinogradov *et al.,* 2002). Therefore, apart from the interest connected to solvent adaptation, they can be proposed as templates for model studies on pathogenic *Acinetobacter* strains. It is in fact known that the factors prompting pathogenesis by *Acinetobacter* virulent strains

include capsular polysaccharides (CPSs) and LPSs, that act in synergy by blocking the access of the human complement to the bacterial cell wall, thus preventing its lytic activity on bacterial membranes (Goel and Kapil, 2001). Moreover, the endotoxic centre of the molecule is represented by the Lipid A (Zähringer *et al.,*1994; 1999; Medzhitov, 2001), usually conservative among the genus. The molecular details triggering the powerful immune response can thus be analysed exploiting this non-pathogenic model strain, since in the present work, the first depiction of a Lipid A from *Acinetobacter* strain is given.

5.2.1 Core Oligosaccharide structure elucidation

The LOS was extracted by PCP procedure (see section 2.1) from the dried cells of *Acinetobacter radioresistens* S13 grown supplying acetate, phenol or benzoate as only carbon source, and in all cases it was identified by SDS-PAGE, where, after silver staining, the typical migration to the bottom of the gel was visible. Chemical analyses for detection of monosaccharides were performed as described (section 2.1) and led to the identification of 6-GlcN, 6-Glc, 4-Glc, t-Glc, t-GlcN, t-GalN, 4,5-Kdo, 4,7-Kdo, t-Kdo and, in minor amount, 4,6-Glc. Ester linked and amide linked fatty acids were identified after GC-MS analyses of their FAME (see section 2.4.1) as it follows: amide linked 14:0(3-OH); 12:0(3-OH), both in ester and amide linkage, secondary 12:0 and, in minor amount, (*S*)-2-hydroxy-dodecanoic acid [12:0(2-OH)].

The Core oligosaccharide was analysed by means of NMR and MS analyses following alkaline (oligosaccharide 1, **OS1**) or mild acid degradation (oligosaccharide 2, **OS2**) of the LOS. **OS1** was isolated by gel permeation chromatography after complete de-acylation of the LOS by anhydrous hydrazine and hot KOH. In the ^{1}H-NMR spectrum (**Figure 5.1**), eight major anomeric protons could be identified, belonging to eight distinct spin systems (**A–H**), beside the presence of a minor anomeric signal **N** at 4.505 ppm. In the high field region, between 1.741 and 2.791 ppm, signals were visible for three diastereotopic methylene groups of three distinct Kdo residues (**I–M**). For each spin system, the full assignment of the ^{1}H and ^{13}C resonances was attained from DQF-COSY, TOCSY, ^{1}H,^{13}C-HSQC (**Figure 5.2**) and ^{1}H,^{13}C-HMBC spectra (**Table 5.1**). All the monosaccharides were present as pyranose rings, according to the methylation data and to the correlations observed in the HMBC spectrum. In the low-field region of the proton spectrum, the signal at 5.932 ppm was assigned to H-4 signal of **B** spin system, that was identified as 2-amino-2,4-dideoxy-α-hex-4-enopyranosyluronic acid (ΔHexNA), in fact in the TOCSY spectrum correlations within **B**

spin system ended at H-4 at low fields (5.932 ppm), that was at its turn correlated, in the ^{1}H,^{13}C-HSQC spectrum, to an olefin carbon signal at 104.7 ppm. This residue clearly derived from a HexNA residue that lost the substituent at *O*-4 by a β-elimination, due to the alkaline treatment leading to **OS1**.
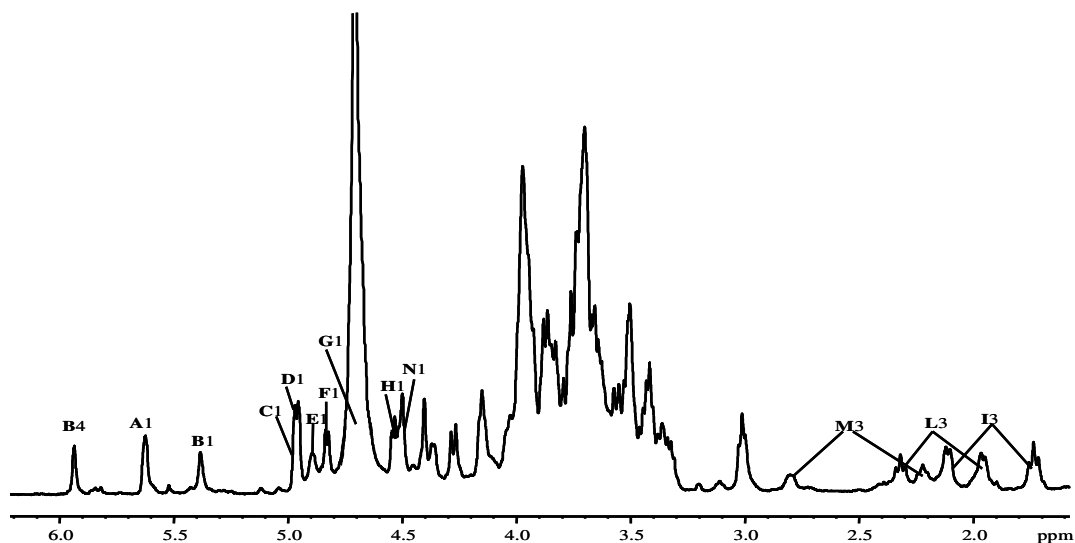
Figure 5.1 - ^{1}H-NMR of **OS1** obtained after alkaline degradation of the LPS from *A. radioresistens* S13. Anomeric signals and Kdo methylene groups are designed with capital letters and refer to **Table 5.1.**
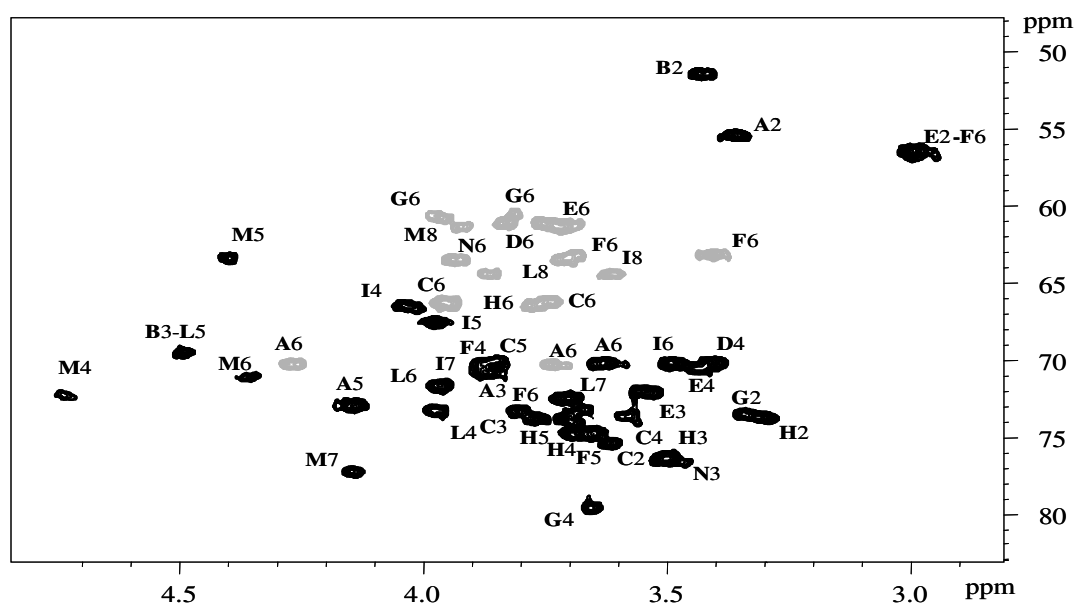
Figure 5.2 - Zoom of the ^{1}H,^{13}C-HSQC spectrum of the *O,N*-deacylated LOS from *Acinetobacter radioresistens* S13. All the heteronuclear correlation are assigned according to the letters in **Table 5.1**. The experiment was recorded with carbon multiplicity editing and grey signals refer to methylene groups.

116

On the basis of the same considerations applied to the NMR analyses of the other oligosaccharides, residues **A, E** and **F** were identified as GlcNs. Typical down-field displacement for the carbon resonances indicated glycosylation at *O*-6 of residues **A**, **C, F** and **H**, *O*-4 of residues **G, M** and **L**, *O*-5 of residue **L**, and *O*-7 of the residue **M,** whereas **D**, **E** and **I** were terminal residues (**Figure 5.2**).

Table 5.1 - [1]H and ^{13}C chemical shifts of **OS1** from *Acinetobacter radioresistens* S13. Numbers in brackets refer to Kdo residues, n.d. is not determined.

	1 (3_{ax-eq})	2 (4)	3 (5)	4 (6)	5 (7)	6 (8)
6-α-GlcN	5.632	3.364	3.871	3.643	4.140	4.272/3.736
A	90.8	54.9	70.3	69.9	72.5	69.8
ΔHexNA	5.371	3.428	4.490	5.932		
B	91.3	50.9	69.0	104.7	n.d.	n.d.
6-α-Glc	4.960	3.566	3.761	3.490	3.871	3.741/3.959
C	98.0	71.5	73.4	71.9	70.3	66.2
t-α-Glc	4.942	3.531	3.708	3.403	3.693	3.824
D	98.1	71.6	73.7	70.0	72.4	60.6
t-β-GlcN	4.880	3.000	3.586	3.441	3.512	3.736
E	99.3	55.9	73.2	70.1	75.9	60.6
6-β-GlcN	4.821	3.008	3.815	3.960	3.692	3.401/3.691
F	100.3	55.9	72.8	71.2	73.9	62.7
4-β-Glc	4.712	3.350	3.647	3.650	3.695	3.980/3.827
G	102.0	73.0	74.3	79.1	74.1	60.3
6-β-Glc	4.532	3.320	3.504	3.691	3.753	3.952/3.782
H	103.3	73.1	75.9	74.6	73.6	66.4
t-β-Glc	4.505	3.281	3.460	3418	3.462	3.891
N	103.3.	73.6	76.5	70.3	76.6	61.1
t-Kdo	1.741/2.100	4.032	3.975	3.496	3.869	3.615/3.870
I	35.0	66.1	67.1	70.1	70.2	64.3
4,5-Kdo	2.312/1.960	3.980	4.496	3.970	3.701	3.941/3.714
L	35.0	73.3	69.0	71.6	72.4	63.4
4,7-Kdo	2.226/2.791	4.730	4.402	4.351	4.147	3.968
M	n.d.	72.2	63.4	71.2	77.0	60.3

One minor signal was visible in correspondence of an alternative C-4 signal of **H** (**H'**), at 79.1 ppm, suggesting non-stoichiometric substitution at *O*-4. The sequence of the monosaccharides within the oligosaccharide chain was deduced from the 2D-ROESY spectrum, where diagnostic cross-peaks were present for each anomeric signal with the proton on the glycosylation site of the next residue (**Figure 5.3**).

The following NOE contacts were revealed in the spectrum: H-1**F/**H-6**A**; H-1**E/** H-7**M**; H-1**B/**H-4**M**; H-1**G/**H-3**B**; H-1**H/**H-4**G**; H-1**C/**H-6**H**; H-1**D/**H-6**C**. The proximity of the residues was further confirmed by the scalar long range correlations of the ^{1}H,^{13}C-HMBC

spectrum, where the cross peaks H-1**G**/C-3**B**; H-1**E**/C-7**M**; H-1**B**/C-4**M**; H-1**H**/C-4**G** and C-1**H**/H-4**G**; H-1**C**/C-6**H** and H-1**D**/C-6**C** were visible. The non-stoichiometric β-Glc residue (**N**) was linked, when present, to *O*-4 of residue **H'**, as shown by NOE contact H-1**N**/H-4**H'**, and as expected on the basis of methylation analysis, which indicated the presence of a 4,6-Glc.

The sequence of Kdo trisaccharide was inferred from the dipolar couplings detected in the ROESY experiment. The presence of a cross-peak in the ROESY spectrum, in correspondence of H-3$_{eq}$**I** and H-6**L** resonances, is only possible in case of 2-4 glycosidic linkage between these two residues, both possessing α-configuration (Holst *et al.*, 1995).
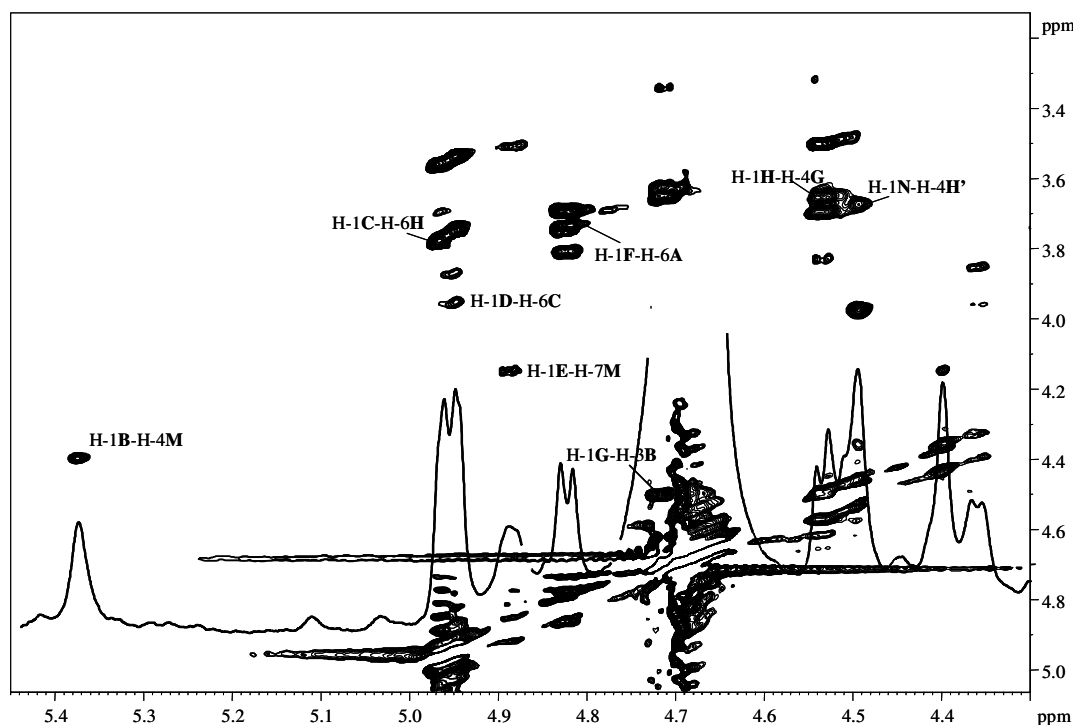
Figure 5.3 - Zoom of the anomeric region of negative levels of the ROESY spectrum on **OS1** obtained after alkaline degradation on the LPS from *A. radioresistens* S13. ^{1}H-NMR is overlapped. Interresidual correlations diagnostic of glycosylation are indicated and refer to **Table 5.1**.

The 2-5 linkage between Kdo **L** and **M** was proven by the NOE contacts of H-5 **L** with H-5 **M**, H-3$_{ax}$ **M**, H-3$_{eq}$ **M** and H-4 **M**. By comparison with the oligosaccharide from *A. baumannii* ATCC 19606 (Vinogradov *et al.*, 2002), where a similar inner core skeleton is present, α-configuration was attributed to residue **M**. In fact, also in this case, the 4,5-Kdo, residue **L**, showed an inversion in the usual chemical shift values for H-3$_{ax}$ and H-3$_{eq}$ (2.312 and 1.960 ppm, respectively) and unusual low-field chemical shift values for Kdo **M**,

118

substituted by ΔHexNA residue. Only two ^{31}P-NMR signals were present (3.40 and 2.87 ppm), that were plainly assigned to *O*-1 and *O*-4' of the lipid A disaccharide backbone by ^{1}H,^{31}P-HSQC.

All of these informations suggested the following structure:

| D | C | H | G | B | M | L | F | A |

α-Glc-(1→6)-α-Glc-(1→6)-β-Glc-(1→4)-β-Glc-(1→3)-α-ΔHexNA-(1→4)-α-Kdo-(2 →5)-α-Kdo-(2→6)-β-GlcN4P-(1→6)-α-GlcN1P

4   7   4

R ⌋   β-GlcN-(1⌋   α-Kdo-(2⌋

E   **I**

R = H o β-Glc (**N**)
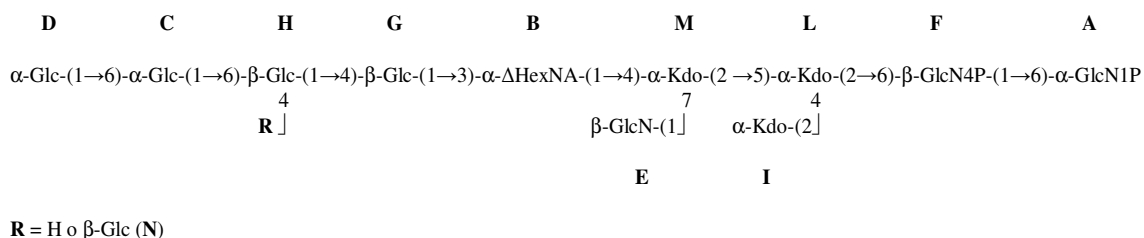
This structure was further confirmed by the MALDI-MS spectrum (**Figure 5.4**). The main ion at *m/z* 2125.7 (Kdo_3-Glc_4-$GlcN_3$-ΔHexNA-P_2) was in full agreement with the molecular mass of the major oligosaccharide structure and the ion at *m/z* 2287.7 (Δ*m/z* 162) bears an additional Glc residue. Ions of shorter oligosaccharide chains, differing from the full oligosaccharide by one to four Glc units were visible. Furthermore, for each of these oligosaccharides, a related ion peak was also present lacking *m/z* 220, that is, without one Kdo residue. These peaks are diagnostic of partially assembled oligosaccharides where the terminal Kdo residue (**I**) was missing.

The full structure of core region of the LOS was achieved performing NMR and MS analyses on the oligosaccharide obtained by 1% acetic acid hydrolysis of the acid labile glycoside bond of Kdo and following purification by GPC (**OS2**). The ^{1}H-NMR spectrum (**Figure 5.5**) of this product showed the presence of a heterogeneous mixture, likely due to the different arrangements of the Kdo as reducing end of the oligosaccharide. Nevertheless, it was possible to recognise the same spin systems of the core moiety already found in **OS1** with exception of residue **B**, that in this case was identified, on the basis of the $^3J_{H,H}$ values from the DQF-COSY spectrum, as 3,4-disubstituted 2-deoxy-2-amino-glucuronic acid (GlcNA) and of an additional anomeric signal (**O**) at 5.702 ppm. The full attribution of the ^{1}H and ^{13}C resonances oligosaccharide **2** was carried out on the basis of the DQF-COSY, TOCSY, ROESY and ^{1}H, ^{13}C-HSQC spectra (**Table 5.2**). For spin system **O**, the ^{13}C chemical shift of C-2 (51.2 ppm), the small $^3J_{1,2}$, $^3J_{3,4}$ and $^3J_{4,5}$ values, the chemical shift values of anomeric proton and carbon signals led to the identification of α-GalN. In agreement, H-5 of **O** spin

system was only detectable by ROESY experiment since in the TOCSY spectrum the very low $^3J_{4,5}$ impaired any magnetisation transfer over H-4.
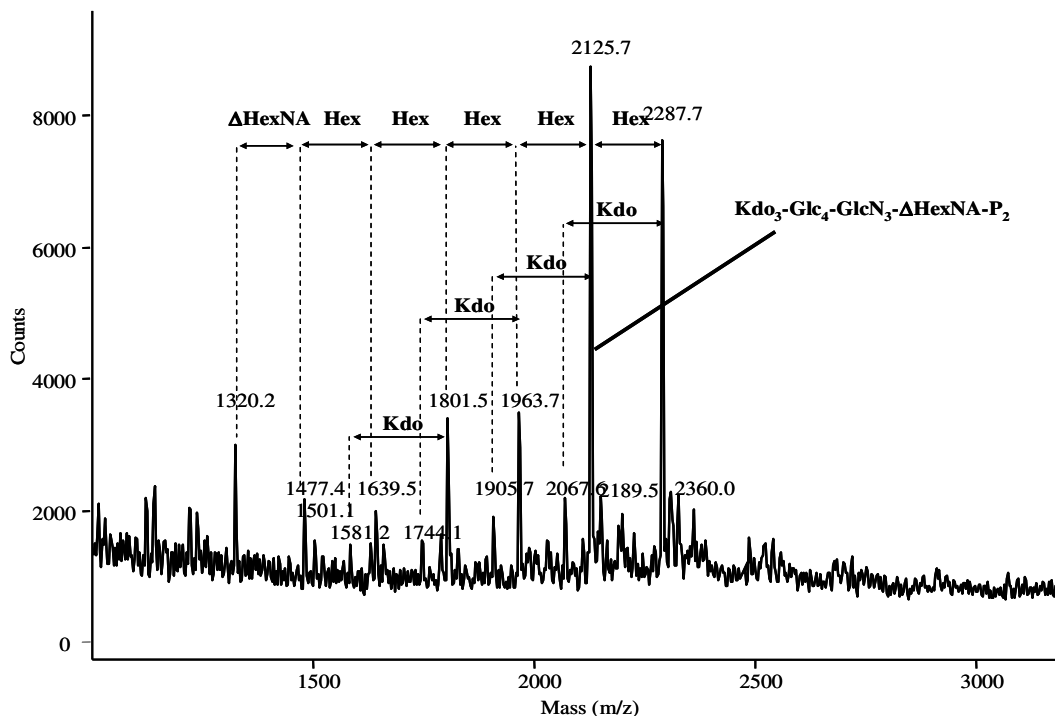
Figure 5.4 - Negative ion MALDI-TOF spectrum on **OS1**. Molecular ions are visible at *m/z* 2125.7 and 2287.7. Molecular ions for partially assembled structures are also visible.

Furthermore, the *inter*-residual NOE of H-1**O** with H-4**B**, indicated the attachment of residue **O** to *O*-4 of the GlcNA. Moreover, at high fields of proton NMR spectrum, an acetyl signal was present. Acetylation shifts downfield the NMR signal of the geminal proton, and the only ^{1}H NMR signal which showed down-field displacement due to acetylation was observed for H-2**B**, whereas all other proton resonances of the oligosaccharide did not show any significant shift attributable to acetylation.

Thus, the structure of **OS2** can be depicted as it follows:

D	**C**	**H**	**G**	**B**	**M**

α-Glc-(1-6)-α-Glc-(1-6)-β-Glc-(1-4)-β-Glc-(1-3)-α-GlcNAcA-(1-4)-α-Kdo
$\quad\quad\quad\quad\quad\quad\quad\quad\quad$ 4 $\quad\quad\quad\quad\quad\quad$ 4 $\quad\quad\quad$ 7
$\quad\quad\quad\quad\quad\quad\quad\quad$ R ⌐ $\quad\quad\quad$ α-GalN-(1⌐ $\quad$ β-GlcN ⌐

$\quad\quad\quad\quad\quad\quad\quad\quad\quad\quad\quad\quad\quad\quad\quad\quad$ **O** $\quad\quad\quad\quad$ **E**
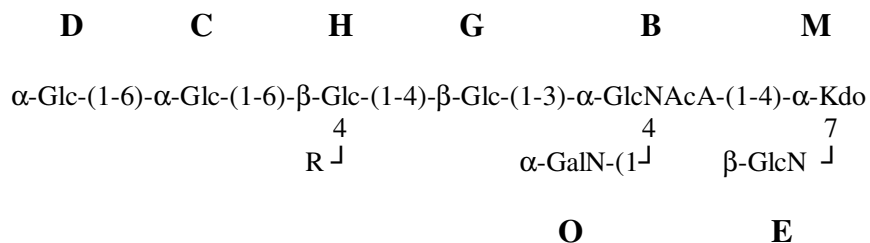
Where R = H or β-Glc (**N**)
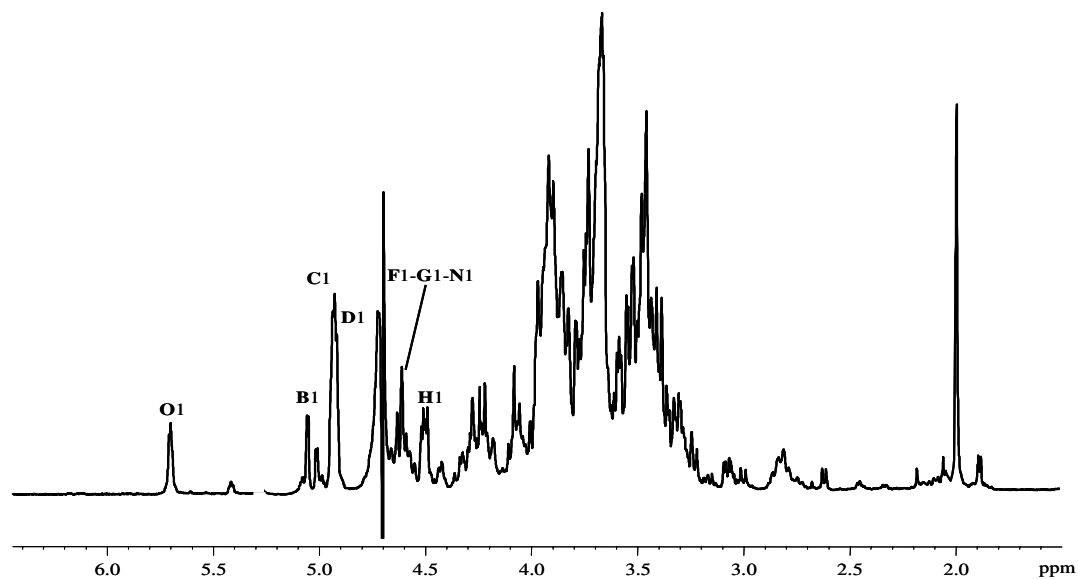
Figure 5.5 - ^{1}H-NMR of **OS2** obtained after mild acid hydrolysis of the LOS. Anomeric signals are designed with capitol letters referring to **Table 5.2**. Additional minor signals occur because of the heterogeneity due to the presence of Kdo as the reducing end of the oligosaccharide.

Table 5.2 - ^{1}H and ^{13}C chemical shifts (ppm) of **OS2**. Additional signals for N-Acetyl group at 1.997/22.46 ppm and 175.02 ppm.

	1	2	3	4	5	6
3,4-α-GlcNAcA	5.012	4.229	4.301	3.949	4.063	
B	95.2	53.6	77.6	74.4	73.7	n.d.
6-α-Glc	4.944	3.525	3.743	3.458	3.838	3.768/3.741
C	98.3	72.0	73.4	71.9	70.9	66.4
t-α-Glc	4.921	3.508	3.667	3.385	3.842	3.799
D	98.0	72.0	73.7	70.3	70.5	61.0
t-β-GlcN	4.662	2.814	3.461	3.453	3.472	3.800/3.630
E	100.0	56.5	74.1	70.0	77.2	61.3
4-β-Glc	4.624	3.317	3.578	3.686	3.512	3.896
G	103.3	73.3	74.8	79.4	72.0	61.2
6-β-Glc	4.511	3.305	3.471	3.476	3.465	3.931/3.717
H	103.2	73.7	76.2	74.1	77.6	66.4
t-β-Glc	4.604	3.339	3.519	3.671	3.521	3.874
N	103.2	73.1	75.5	73.1	75.0	60.8
t-α-GalN	5.702	3.452	3.938	3.782	3.999	3.645/3.758
O	95.7	51.2	71.1	68.3	69.1	61.1

All the above information taken together allowed to identify the complete structure of the fully de-acylated core oligosaccharide from *A. radioresistens* S13, that can be represented as follows:

| D | C | H | G | B | M | L | F | A |

α-Glc-(1→6)-α-Glc-(1→6)-β-Glc-(1→4)-β-Glc-(1→3)-α-GlcNAcA-(1→4)-α-Kdo-(2 →5)-α-Kdo-(2→1)-β-GlcN4P-(1→6)-α-GlcN1P

   4   4   7   4
R ⌋   α-GalN-(1⌋   β-GlcN-(1⌋   α-Kdo-(2⌋

                                 O   E   I
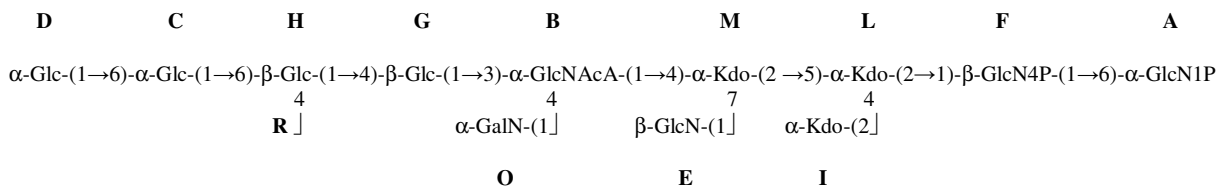
R = H o β-Glc (**N**)

5.2.2 Characterization of the Lipid A

The Lipid A fraction from *Acinetobacter radioresistens* S13 was obtained as precipitate after the mild acid hydrolysis of the LOS leading to the obtaining of **OS2**. The glycolipid fraction was then analysed by MALDI mass spectrometry. The negative-ion spectrum showed a complex appearance, due to the presence of several distinct ion clusters, representative of the micro-heterogeneity of the sample. Four main groups of signals (**A**-**D**) were detectable, indicating molecular species ranging from tetra- to hepta-acyl substitution (**Figure 5.6**), on the bis-phosphorylated disaccharide backbone, with a considerable predominance for the hepta- (**A**) and hexa-acylated (**B**) bis-phosphorylated species.
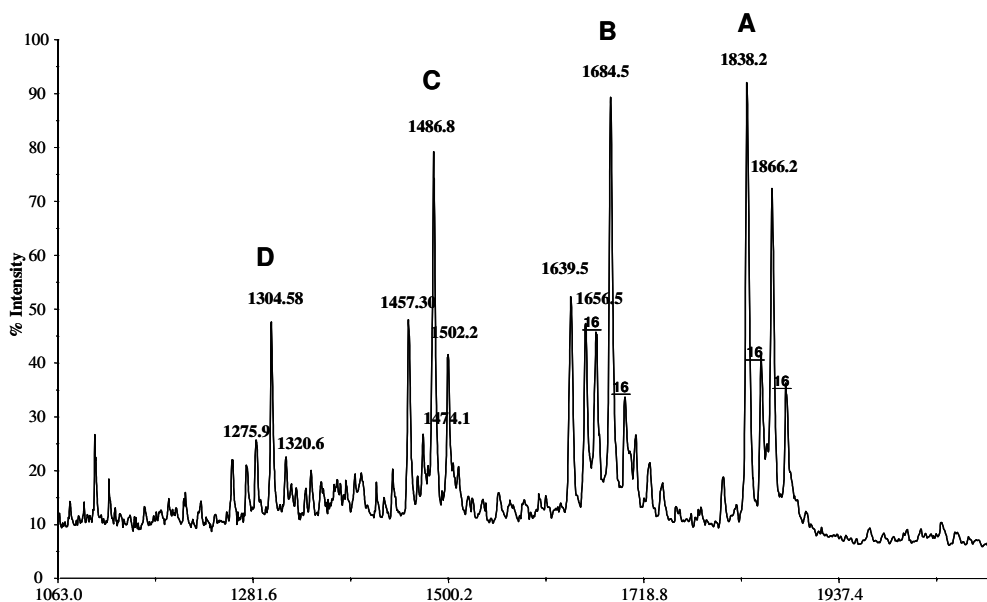
Figure 5.6 - Negative-ion MALDI mass spectrum of the intact Lipid A fraction from *Acinetobacter radioresistens* S13. Capital letters refer to the relevant ion peak clusters described in **Table 5.3** and in the text. Mass differences of 16 m/z indicate non-stoichiometric substitution of dodecanoic acid with (*S*)-2-hydroxy-dodecanoic acid.

Acyl substitution for the main peak of species **A**, in accordance with the ion peak at *m/z* 1838.2, was realised by four 12:0(3-OH) and three 12:0. A less intense peak at *m/z* 1866.2 ($\Delta m/z = 28$) was originated by the molecular species possessing three 12:0(3-OH), one 14:0(3-OH) and three 12:0 residues. Both peaks showed minor related signals with $\Delta m/z = 16$, indicating non-stoichiometric substitution of one 12:0 residue with one 12:0(2-OH). The same diversity in fatty acids substitution was observable for molecular species **B** (hexa-acyl), at *m/z* 1656.4 and 1684.5, differing from species **A** ion peaks for a secondary 12:0 less. Species **C** was in account for penta-acyl differing from **B** for one 12:0 (*m/z* 1474.1 and 1502.2, respectively) or one 12:0(3-OH) (*m/z* 1457.3 and 1486.8). Minor peaks were also observed for tetra-acyl Lipid A (species **D**), where acylation was performed by one 14:0(3-OH), two 12:0(3-OH) and two12:0. The molecular compositions for these species are explained in **Table 5.3**.

Table 5.3 - Proposed acyl content of the molecular species composing the intact Lipid A fraction from *Acinetobacter radioresistens* S13.

Observed ion (*m/z*)	Species	Acyl substitution	Fatty acids and phosphate substitution
1838.2	**A**	Hepta-acyl	$GlcN_2$-P_2-[12:0(3-OH)]$_4$-(12:0)$_3$
1866.2	**A**	Hepta-acyl	$GlcN_2$-P_2-[12:0(3-OH)]$_3$-(12:0)$_3$-14:0(3-OH)
1684.5	**B**	Hexa-acyl	$GlcN_2$-P_2-[12:0(3-OH)]$_3$-(12:0)$_2$-14:0(3-OH)
1656.4	**B**	Hexa-acyl	$GlcN_2$-P_2-[12:0(3-OH)]$_4$-(12:0)$_2$
1502.7	**C**	Penta-acyl	$GlcN_2$-P_2-[12:0(3-OH)]$_3$-14:0(3-OH)-12:0
1474.8	**C**	Penta-acyl	$GlcN_2$-P_2-[12:0(3-OH)]$_4$-12:0
1486.8	**C**	Penta-acyl	$GlcN_2$-P_2-[12:0(3-OH)]$_2$-14:0(3-OH)-12:0$_2$
1457.3	**C**	Penta-acyl	$GlcN_2$-P_2-[12:0(3-OH)]$_3$-12:0$_2$
1304.3	**D**	Tetra-acyl	$GlcN_2$-P_2-[12:0(3-OH)]$_2$-14:0(3-OH)-12:0
1276.4	**D**	Tetra-acyl	$GlcN_2$-P_2-[12:0(3-OH)]$_3$-12:0

In order to locate fatty acids residues, Lipid A underwent two parallel and complementary treatments: mild hydrolysis with NH_4OH and total dephosphorylation with 48% HF. Negative-ion MALDI mass spectrum (**Figure 5.7A**) on the ammonium treated sample, showed three main ion clusters (**E-G**). The most abundant species (**E**), at *m/z* 1106.4, was generated by a tri-acyl species carrying two phosphate groups, one 14:0(3-OH), one 12:0(3-OH) and one 12:0. Also in this case a $\Delta m/z = -28$ was observable with the peak at *m/z* 1078.4, indicating non-stoichiometric substitution by 12:0(3-OH) instead of 14:0(3-OH) on one of the two amide-linked primary fatty acids. The peak at *m/z* 1122.3 ($\Delta m/z = 16$)

evidenced, also in this case, the occurrence of non-stoichiometric substitution of a 12:0(2-OH) instead of a 12:0 residue. A less intense couple of peaks (**F**), at *m/z* 1260.8 and 1288.8, was generated by the species possessing one additional secondary 12:0 residue, whereas the peaks at *m/z* 896.8 and 925.8 (**G**) were generated by the GlcN disaccharide carrying two 12:0(3-OH) or one 12:0(3-OH) and one 14:0(3-OH) respectively. In correspondence of the tetra-acyl species (**F**), minor peaks were observable, at *m/z* 1276.8 and 1304.0, representative of non stoichiometric secondary substitution by one or two 12:0(2-OH) secondary fatty acids replacing 12:0. For all the clusters, $\Delta m/z = 80$ were observed, namely lacking a phosphate groups, an event previously undetected in the intact Lipid A or LOS (see section 5.2.1) MALDI spectra. Partial phosphate loss might originate as a consequence of the ammonium treatment performed. Interestingly, the relative intensity ratio between the peaks differing by *m/z* 28 in correspondence of the species **E** (tri-acyl) and **F** (tetra-acyl) resembles the intensity ratio of the correspondent peaks for **B** (hexa-acyl) and **A** (hepta-acyl) in the intact Lipid A spectrum, proving that in the fully acylated species substitution by two 12:0(3-OH) on the amide position is a more frequent event than substitution by one 12:0(3-OH) and one 14:0(3-OH), as conversely observed in the other molecular species within the natural blend. Positive-ion MALDI mass spectrum on the ammonium treated sample (**Figure 5.7B**) allowed the observation, besides the molecular ion peaks for the already described species, of the oxonium ion peak, generated by the in source cleavage of the glycosidic linkage of the non-reducing GlcN, at *m/z* 622.1. This value was in account for the protonated molecular ion of a species composed by one GlcN residue carrying one phosphate group, one 12:0(3-OH) and one 12:0. A minor amount of non-phosphorylated species could also be observed at *m/z* 542.1 ($\Delta m/z$ = -80). The absence of signals for the species with one 14:0(3-OH) suggested that the heterogeneity in amide substitution was localized on the GlcN I.

To define the final fatty acid substitution, the HF treated sample was analysed by MALDI MS in positive ion mode. The positive-ion spectrum (**Figure 5.8**) showed the occurrence of two main signals, at *m/z* 739.5 and 922.1 respectively. These peaks were assignable to oxonium ions for GlcN II with two different degrees of acylation, namely tri-acyl, substituted by two 12:0(3-OH) and one 12:0, and tetra-acyl, with an additional 12:0, likely linked as acyloxyacyl to the ester-linked 12:0(3-OH). Also in this case, there was no evidence for substitution by 14:0(3-OH) on GlcN II, pointing out that this fatty acid must selectively link GlcN I. The ion peak at *m/z* 721.5 ($\Delta m/z$ = 18 from 739.5) was originated by de-hydration of the tri-acyl species, likely due to the high laser energy used.
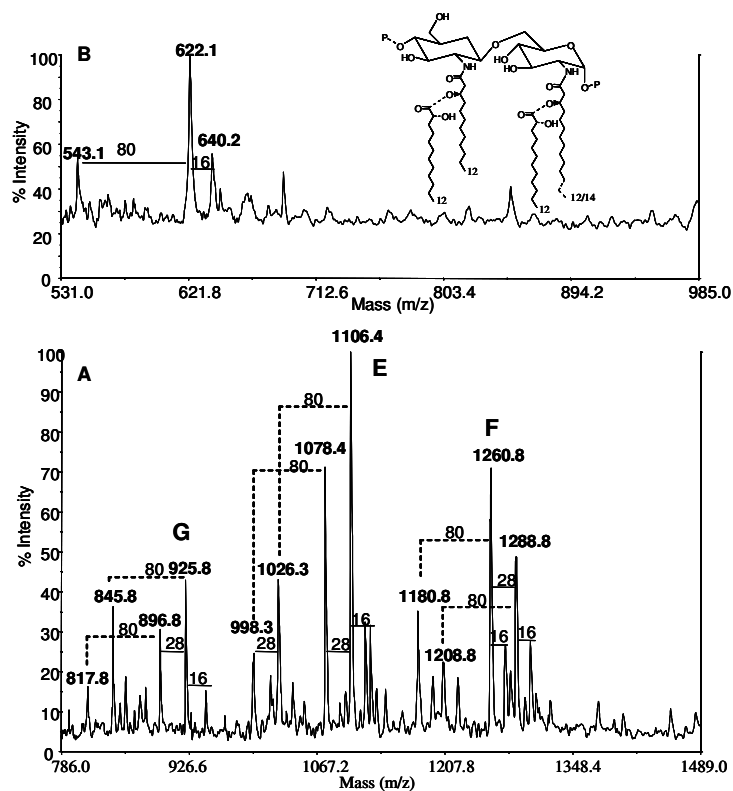
Figure 5.7 - Negative- (**A**) and section of the positive- (**B**) ion MALDI mass spectra of the ammonium treated Lipid A fraction from *A. radioresistens* S13. Capital letters refer to the identified molecular species. Mass differences of 80 *m/z* indicate non-stoichiometric phosphate substitution. The structure sketches fatty acids substitution. Dotted linkages indicate non-stoichiometric substitution.
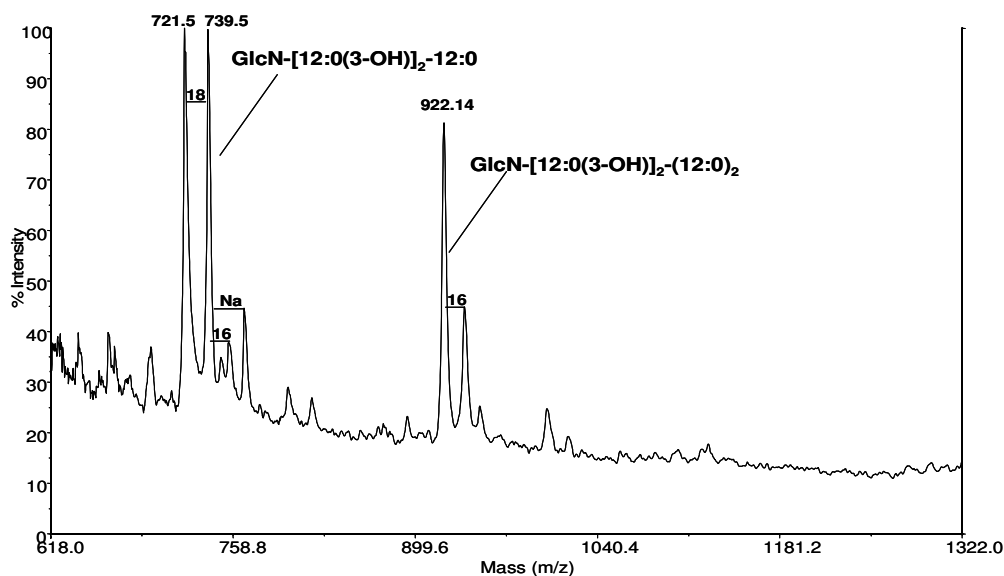
Figure 5.8 - Section of the positive-ion MALDI mass spectrum of the dephosphorilated Lipid A fraction from *A. radioresistens* S13. Mass differences of 16 *m/z* indicate non-stoichiometric replacement of dodecanoic acid with (*S*)-2-hydroxy-dodecanoic acid. Mass difference of 18 *m/z* indicates de-hydration of the molecular species at 739.5 *m/z*. Peaks are visible originated by sodium adducts.

The definition of the complete acylation pattern for GlcN I was made possible by comparison of the data concerning the partially degraded Lipid A with the peaks in the intact species spectrum, finally allowing the delineation of the Lipid A from *A. radioresistens* S13. In the highest fatty acid containing species, namely the hepta-acyl Lipid A, three residues are present on GlcN I, namely one 14:0(3-OH) or 12:0(3-OH) in amide linkage with a secondary 12:0, replaced, in a very minor amount, by a 12:0(2-OH), as observed in the ammonium treated sample, and one 12:0(3-OH) in ester linkage, while GlcN II must be present in the tetra-acyl form. Hexa- and penta-acyl Lipid A differ from this molecular species by one or two 12:0, namely the acyloxyacylester on GlcN II, as proven by the ion peak in the positive spectrum of dephosphorylated sample, and/or the one of the acyloxyacylamide on GlcN II. Finally, the less abundant tetra-acyl species, differs from the penta-acyl Lipid A for one 12:0(3-OH) residue, namely the ester at *O*-3 of GlcN I. These structures, can be summarized in **Figure 5.9**.
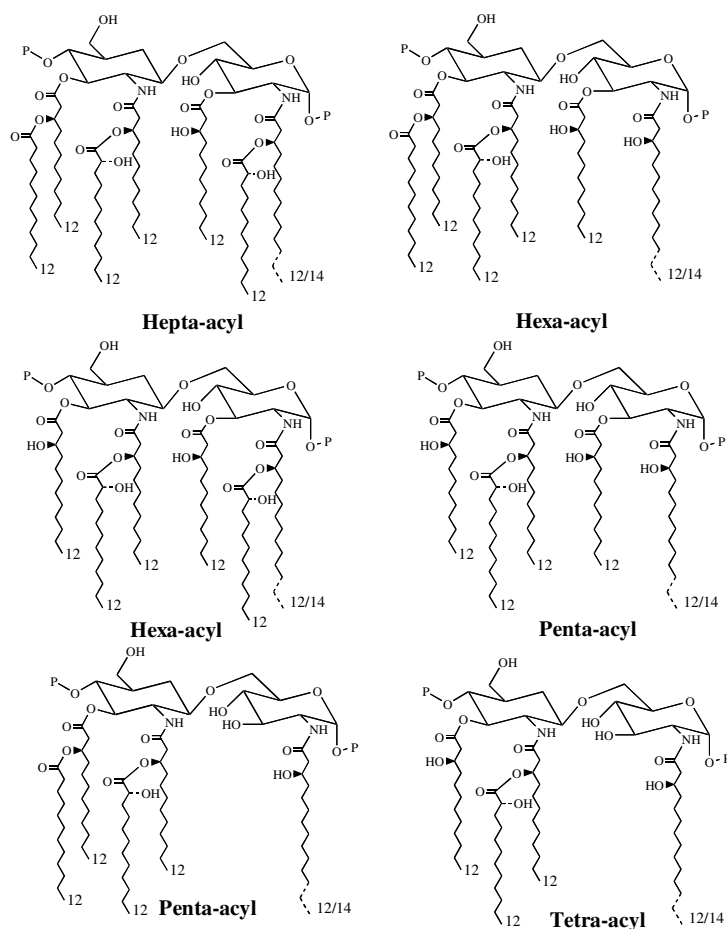
Figure 5.9 - Complete structure of the different Lipid A species from *Acinetobacter radioresistens* S13. Dotted linkages indicate non-stoichiometric substitution.

5.3 *Pseudomonas* **sp. OX1 (***P. stutzeri* **OX1)**

Pseudomonas sp. OX1 (formerly known as *Pseudomonas stutzeri* OX1) is a Gram-negative bacterium isolated from the activated sludge of a wastewater treatment plant, endowed with peculiar metabolic capabilities for the degradation of aromatic hydrocarbons (Baggi *et al.,* 1987), being able to grow on a large spectrum of aromatic compounds including phenol, cresol and dimethylphenol, and on non-hydroxylated molecules such as toluene and *o*-xylene, the most recalcitrant isomer of xylene. This microrganisms is also able to metabolize perhalogenated compounds as tetrachloroethylene (PCE), one of the groundwater pollutants commonly resistant to degradation (Ryoo *et al.,* 2000). For these metabolic peculiarities, *Pseudomonas* sp. OX1 is central in a study aiming to employ the microrganism, or its enzymatic systems, in bioremediation strategies. Attempts of immobilizing *Pseudomonas* sp. OX1 in bioreactors are under preparation, exploiting its natural tendency to biofilm formation.

The degradation of the aromatic hydrocarbons in *Pseudomonas* sp. OX1, as in other aerobic bacteria, is realized through an upper pathway, which produces dihydroxylated aromatic intermediates by the action of monooxygenases, and a lower pathway, which processes these intermediates down to molecules that enter the citric acid cycle (Powlowski and Shingler, 1990) and some of the enzymes operating in *Pseudomonas* sp. OX1 metabolism have already been cloned, expressed and characterized, namely the toluene-*o*-xylene monooxygenase (ToMO) (Cafaro *et al.,* 2002), endowed with a broad substrate specificity (Bertoni *et al.,* 1998), and the phenol hydroxylase (PH) (Arenghi *et al.,* 2001), both belonging to the upper pathway, and the catechol-2,3-dioxygenase (C2,3O), the "gateway" enzyme to the lower pathway.

The growth of *Pseudomonas* sp. OX1 on different media have been performed, and every time the structure characterization of the lipopolysaccharide fraction has been realized. In opposition to what observed in the case of *Acinetobacter radioresistens* (see section 5.2), the LPS produced by *Pseudomonas* sp. OX1 undergoes severe changes depending on the cultural conditions. In fact, cells grown on aromatic substrates produced only a LOS fraction, composed by species differing in the Core region structure, that were isolated and characterised. Conversely, after growth in the absence of hydrocarbons, beside minor amounts of LOS, bacterial cells expressed a Smooth type LPS, provided with an O-chain polysaccharide whose structure was also characterised.

In order to define the reasons for the extraordinary resistance shown by *Pseudomonas* sp. OX1, we also started the analysis of the biofilm produced, and the main exopolysaccharide fraction composing its matrix was purified and characterised.

5.3.1 Characterization of the Core Oligosaccharide

The LOS fraction was extracted and purified from dried cells of *Pseudomonas* OX1 grown on different media (see 7.1.3) as described in the previous sections (see 2.1). Compositional monosaccharide analysis led to the identification, of L,D-Hep, D-GalN, D-GlcN, D-Glc and Kdo in the relative ratios 2 : 1.0 : 3.2 : 1.1 : 1.8 and, in traces, L-Rha. 7-*O*-carbamoyl-L,D-Hep was present in stoichiometric ratio with L,D-Hep. Methylation analysis showed the presence of t-Kdo, 6-GlcN, 3-Hep, 4,5-Kdo, 3,4-GalN, 4,6-Glc, 4,6-GlcN and, in small amounts, of t-Rha and 6-Glc. In addition, the disaccharide 7-*O*-carbamoyl-Hep-(1→3)-Hep was found. Fatty acids analysis revealed the presence of typical fatty acids of pseudomonads LPS (Zähringer *et al.,* 1999), namely C12:0(3-OH), present exclusively in amide linkage and C10:0(3-OH), C12:0(2-OH) and C12:0 in ester linkage.

Complete structure determination of the Core oligosaccharide was achieved after NMR and MS analyses of the product of both alkaline and mild acid degradation of the LOS.

After *O,N*-deacylation with hydrazine and KOH, the oligosaccharide fraction was purified by High Performance Anion Exchange Chromatography (Dionex), leading to the isolation of two fractions. The more abundant was composed by the Core-Lipid A saccharidic backbone composing the main LOS from *Pseudomonas* sp. OX1 (**OS1**), whereas two minor oligosaccharides (**OS2** and **OS3**) were collected together in one fraction. ^{1}H-NMR analysis on **OS1** (**Figure 5.10**) showed the occurrence of seven signals within the anomeric region of the spectrum, indicating seven different spin systems (**A-G**, in order of decreasing chemical shift) whose complete proton and carbon chemical shifts assignment was achieved with the help of a full series of homo- and eteronuclear experiments, as described in section 2.3.2. Moreover, at high field, the characteristic signals for two chemically and magnetically distinct Kdo residues (**I-L**) were visible. Anomeric and relative configurations for all residues, as well as the definition of cyclization sizes and glycosylation sites were deduced as previously described and are collected in **Table 5.4.** In particular, residues **A** and **D** were identified as α-Hep, residue **B** was identified as the α-glucosamine belonging to the Lipid A disaccharide backbone on the basis of chemical shifts, of $^3J_{H,H}$ values and of the observed $^3J_{1,\,2}$ = 2.9 Hz and $^3J_{H1,P}$ = 8.3 Hz diagnostic of the occurrence of the anpomeric phosphate group. Spin
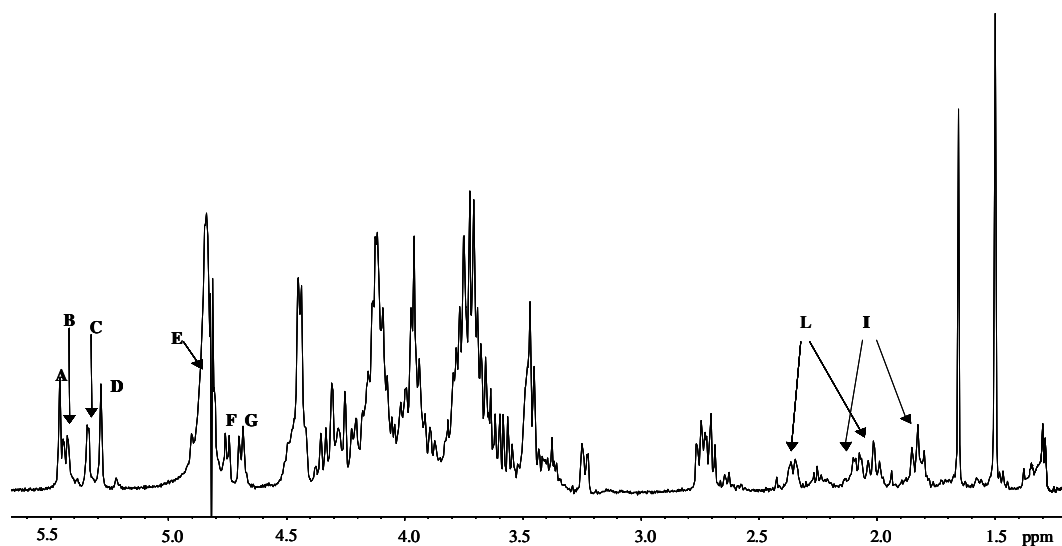
Figure 5.10 - ^{1}H-NMR spectrum of **OS1** obtained by alcaline treatment on the LOS from *Pseudomonas sp.* OX1

Table 5. 4 – [1]H, [13]C (*italic*) and [31]P (**bold**) chemical shifts (ppm) of **OS1** obtained after alkaline treatment of the LOS from *Pseudomonas* sp. OX1

Residue	1	2	3ax/eq	4	5	6	7	8
A	5.46	4.39	4.09	4.46	4.39	4.20	3.86/4.08	
Hep	*97.8*	*73.8*	***76.7***	*72.0*	*73.7*	*69.8*	*63.9*	
		1.9		**4.0**				
B	5.42	2.73	3.64	3.45	4.09	4.30/3.74		
GlcN	*95.1*	*55.9*	*73.7*	*70.8*	*72.0*	*70.1*		
	3.0							
C	5.32	3.22	4.06	4.27	4.02	3.71		
GalN	*101.3*	*51.5*	*78.3*	*77.5*	*71.5*	*61.7*		
D	5.27	4.43	4.14	4.05	4.16	4.45	3.75/4.09	
Hep	*102.7*	*69.9*	*78.2*	*67.4*	*71.7*	*74.2*	*63.7*	
						4.3		
E	4.73	3.44	3.71	3.43	3.66	3.93/3.65		
Glc	*105.8*	*75.3*	*72.9*	*75.8*	*67.7*	*64.6*		
F	4.67	2.70	3.54	3.71	3.36	4.04/3.93		
GlcN	*104.7*	*58.2*	*76.6*	*77.7*	*67.2*	*64.7*		
G	4.47	2.67	3.66	3.82	3.47	3.71/3.45		
GlcN	*103.5*	*56.9*	*73.5*	*73.4*	*76.9*	*63.7*		
				3.9				
I			1.81/2.07	4.27	4.08	3.69	4.03	3.86/3.70
Kdo	*175.0*	*101.7*	*36.1*	*65.9*	*67.7*	*73.0*	*70.1*	*63.7*
L			2.00/2.34	4.12	4.24	3.67	3.93	3.86/3.69
Kdo	*175.0*	*100.9*	*35.0*	*71.8*	*69.5*	*73.6*	*70.6*	*63.9*
S-Pyr			1.48					
	175.5	*101.9*	*25.2*					
R-Pyr			1.62					
	175.8	*99.5*	*17.2*					

system **C** was identified as α-GalN on the basis of its $J_{H,H}$ values for H-3/H-4 and H-4/H-5, diagnostic of a *galacto* configuration (3.4 Hz and less than 1 Hz, respectively). Residue **E** was identified as β-Glc, while residues **F** and **G** as β-GlcN.

The α-configuration of the two Kdo residues **I** and **L** was established on the basis of the chemical shift of their H-3*eq* protons and by measurement of the $^3J_{7,\,8a}$ and $^3J_{7,.8b}$ coupling constants (Birnbaum *et al.,* 1987; Holst *et al.,* 1994). Two methyl singlet signals were present at higher fields, at 1.48 and 1.62 ppm, respectively. Each methyl signal was in a stoichiometric 3:1 ratio with anomeric signals. These signals corresponded, in the ^{1}H,^{13}C-HSQC, to carbons at 25.2 and 17.2 ppm, respectively.

On the basis of the observed glycosylation sites detected in the ^{13}C, substitution was individuated at *O*-3**A,** *O*-6**B**, *O*-3 and *O*-4 **C**, *O*-3**D**, *O*-4 and *O*-6**E** and **F**, *O*-6 **G**, *O*-5 and *O*-4 **L**, whereas **I** was a terminal residue.

Phosphate substitution was established on the basis of ^{31}P NMR spectroscopy. The ^{31}P-NMR spectrum showed the presence of 5 monophosphate monoester signals (**Table 5.4**). The site of substitution was inferred by ^{1}H,^{31}P-HSQC spectrum that showed correlations of ^{31}P signals with H-1**B** (GlcN), H-4**A** and H-2**A** (Hep I), H-4**G** (GlcN) and H-6**D** (Hep II).

The sequence of the monosaccharide residues was determined using NOE effects of the ROESY (**Figure 5.11**) spectrum, and by ^{1}H,^{13}C-HMBC correlations. The typical Lipid A carbohydrate backbone was eventually assigned on the basis of the NOE signal between H-1 **G** and H-6$_{a,b}$ **B**.
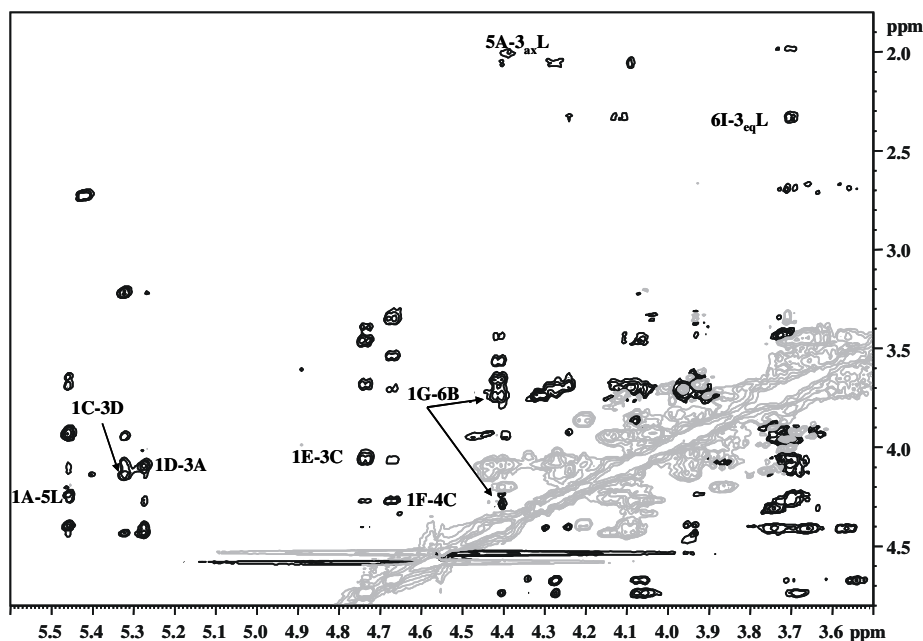

Figure 5.11 - Section of the ROESY spectrum of **OS1**. Labels refer to monosaccharides in **Table 5.4**. NOE cross peaks are in black, in antiphase with diagonal (grey lines).

In the case of Kdo units, which lack anomeric proton, the sequence was inferred by NOE contacts between the methylene-proton H-3$_{eq}$ **L** and H-6 **I**, whereas Kdo **L** was substituted by heptose **A** as indicated by the NOE effect found between H-1 **A** and H-5 **L**, and, in addition, between H-5 **A** and H-3$_{ax}$ **L**.

Heptose **A** was, in turn, substituted at *O*-3 position by heptose **D** as demonstrated by the NOE cross peak between H-1**D** and H-3**A**. A disaccharide 7-*O*-carbamoyl-Hep-(1→3)-Hep was also identified by methylation analysis of the intact LOS, thus, the carbamoyl group should be attached to *O*-7 of the heptose moiety **D**. The GalN **C** was attached to the *O*-3 position of this last heptose as shown by the NOE effect between the anomeric proton of GalN and H-3**D**.

GalN was substituted at *O*-3 by residue **E** (β-Glc) and at *O*-4 by residue **F** (β-GlcN), as suggested by the NOE contacts between the anomeric protons of these residues and the proton signals geminal to the glycosylation sites of residue **D**.

The linkage of Kdo **L** to β-GlcN **G** was deduced by exclusion. In particular, the linkage to *O*-6 of **G** was inferred by taking into account the downfield shift of the carbon signal C-6 (63.7 ppm, **Table 5.4**) indicating its involvement in a glycosidic linkage. All these data were confirmed by the analysis of the ^{1}H,^{13}C-HMBC spectrum, where, apart from the *intra*-residual correlations, the following *inter*-residual cross peaks were observed: H-5/ C-5**L** and C-1/ H-1**A**, H3/C-3**A** and C-1/H-1**D**, H3/C-3**D** and C-1/H-1**C**, H-1/C-1**E** and C-3/H-3**C**, H-1/C-1**F** and C-4/H-4**C**, H-1/C-1**G** and C-6/H-6**B**.

The HMBC experiment was also crucial for the identification and localization of the two methyl groups belonging to non-carbohydrate constituents. Plain long range correlations (**Figure 5.12A**) were found in the spectrum for each methyl signal. The signal at 1.48 ppm correlated to two different carbon signals at 101.9 and 175.5 ppm, whereas the signal at 1.62 ppm correlated to other two signals at 99.5 and 175.8 ppm. None of these four carbon signals was present in the HSQC spectrum. These data pointed to two cyclic ketals of pyruvic acid present on two distinct residues, namely **E** and **F**, whose C-4 and C-6 signals experienced a downfield displacement. This was confirmed by the HMBC spectrum where each ketal carbon signal of pyruvate residues correlated to H-4 and H-6 of **E** and **F** residues (β-D-Glc and β-D-GlcN respectively). It should be noted that the signal discrepancy in the ^{1}H and ^{13}C chemical shifts of the two pyruvate moieties is due to the different absolute configuration at C-2. In fact, methyl signal occurring at 1.48 and 25.2 ppm is assigned to the *S*-pyruvate group, whereas the one occurring at 1.62 and 17.2 ppm to a *R*-pyruvate group, as already described

(Garegg *et al.,* 1980). Moreover, the ROESY spectrum (**Fig. 5.12B**) was in complete agreement with the assignment above. In fact, the methyl signal of *R*-pyruvate residue at 1.62 ppm gave a strong NOE effect with H-4 and H-6$_a$ of **F** residue. This is in agreement with an axial orientation of the methyl group on a 1,3-dioxane ring in a chair-like conformation in which H-4 and H-6$_a$ are *syn* di-axial with respect to it. The methyl signal of *S*-pyruvate, being in equatorial orientation, only gave NOE effect with adjacent H-6 of **E** residue.

As for the presence of a minor spin systems (10%) belonging to rhamnose (anomeric signal at 4.89 ppm) and 6-substituted glucose (overlapped with terminal glucose), it might be explained by the presence of a second outer core glycoform in which rhamnose is attached at *O*-6 of the glucose residue, which obviously lacks the pyruvate group.
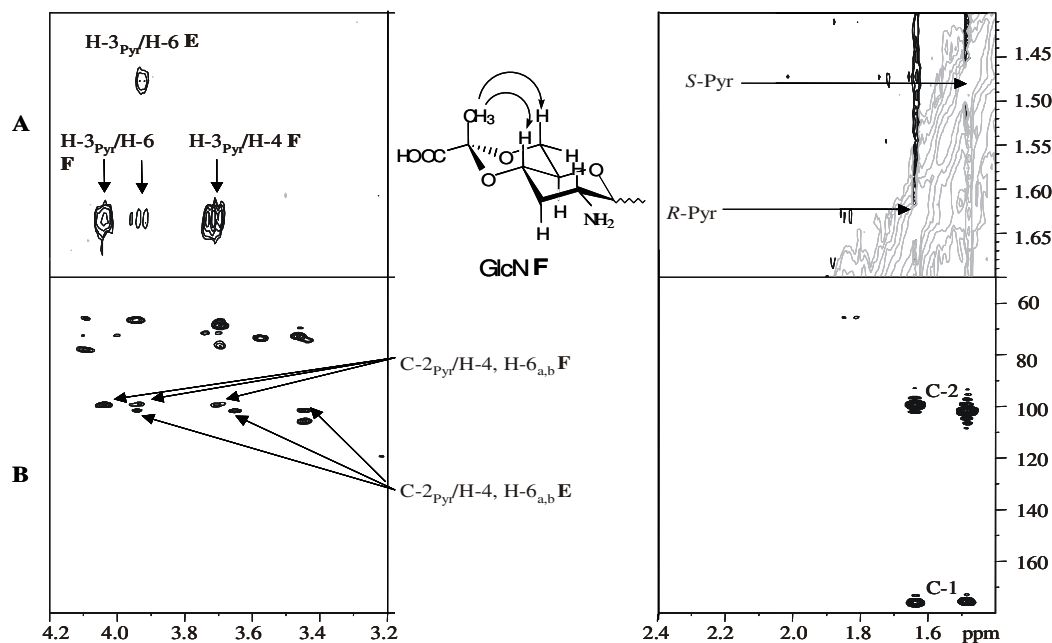
Figure 5.12 - Sections of the high field region of the (**A**) ROESY and (**B**) HMBC spectra. Correlations of pyruvate methyl groups are shown. The 4,6-(*R*)-Pyr-GlcN residue is drawn in the middle of the figure with arrows indicating the relevant NOE contacts between methyl protons of the *R*-pyruvate group and H-4 and H-6 of GlcN residue.

The MALDI mass spectrum confirmed the proposed structure. In fact, an ion peak at *m/z* 2188.4 (**Figure 5.13A**) was present, corresponding to the complete carbohydrate backbone bearing five phosphate goups and two pyruvic acid acetal residues. Moreover, at higher laser intensity, (**Figure 5.13B**) various ion peaks related to fragments were found, all fitting with
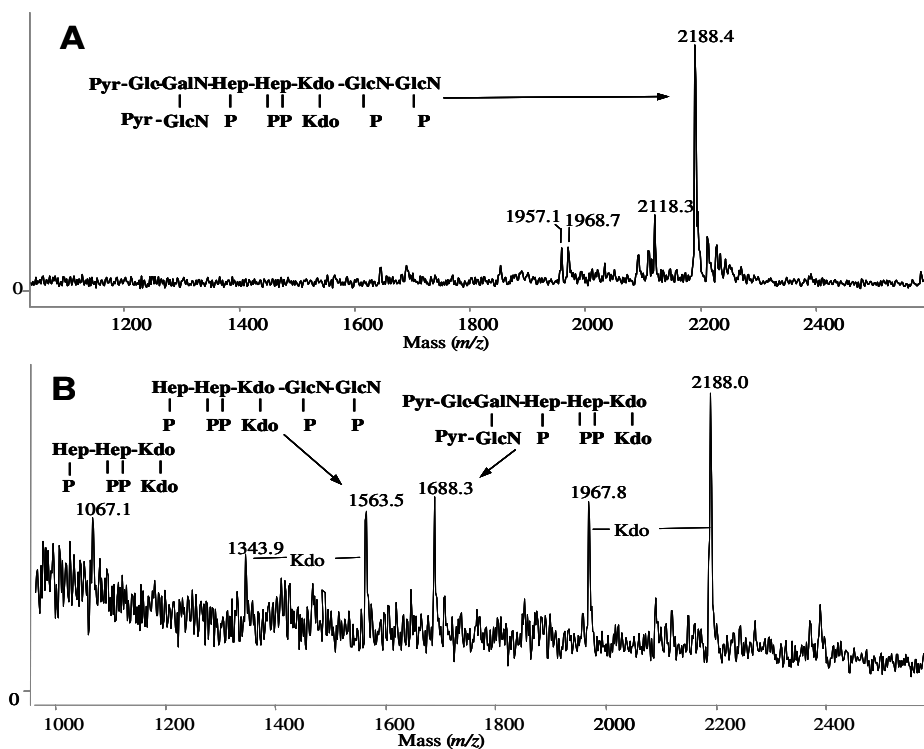
Figure 5.13 - Negative ion MALDI-TOF- mass spectra of oligosaccharide 1 obtained in linear mode at normal (**A**) and higher laser intensity (**B**). Assignments of main ion peaks are shown. P is phosphate, Pyr is pyruvic acid.
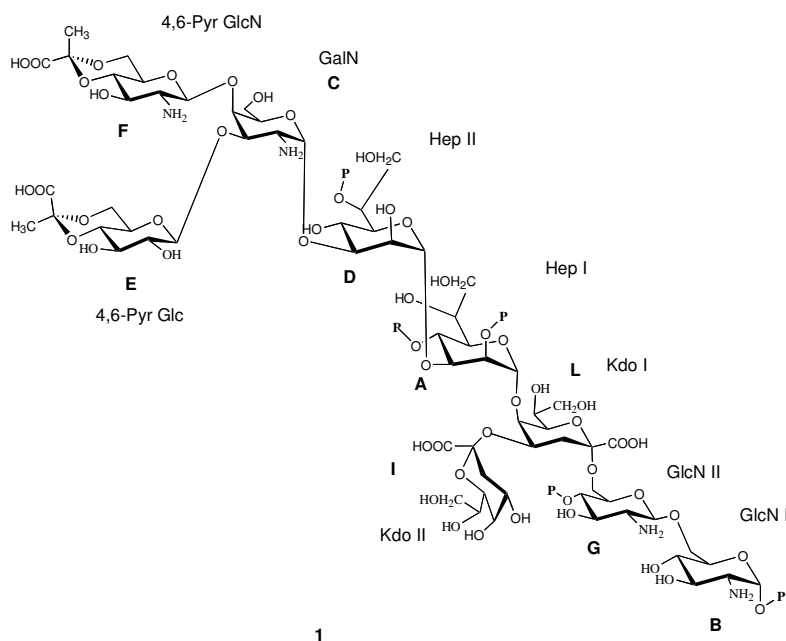
Figure 5.14 - The structure of the main oligosaccharide (**OS1**) obtained after alkaline degradation of the core region of the LPS of *Pseudomonas* sp. OX1.

the structure shown in **Figure 5.14**, depicting the main oligosaccharide from the LOS of *Pseudomonas* sp. OX1 after alkaline treatment.

The structures of the minor oligosaccharides **OS2** and **OS3** were again obtained by NMR and MALDI MS. Within ^{1}H-NMR spectrum of the blend, eight major anomeric signals (**A'-H'**) were present (**Figure 5.15**). The residues, their linkages and their sequence were identified after a full 2D-NMR analysis, in the same way as in **OS1**. [1]H chemical shifts were deduced from DQF-COSY, TOCSY and ROESY spectra, while ^{13}C and ^{31}P chemical shifts were deduced by the subsequent analysis of the ^{1}H,^{13}C-HSQC and ^{1}H,^{31}P-HSQC spectra respectively (**Figures 5.16** and **5.17**). All of these data are collected in **Table 5.5**. In particular, residues **A'** and **D'** were identified as 3-α-Hep, residue **B'** as the α-GlcN of the Lipid A backbone, residue **C'** was identified as 3,4-α-GalN, residue **H'** was identified as the β-GlcN II of Lipid A backbone, residues **F'** and **G'** were identified as β-Glc and β-GlcN, respectively. Residue **E',** present in non-stoichiometric ratio, was identified as an α-*manno*-configured monosaccharide. All of these signals described the spin systems composing the structure of **OS2**. In addition, its anomeric signal correlated to a methyl signal at 1.28 ppm in the TOCSY spectrum, thus, it was identified as an α-Rha residue. Secondary series of signals were visible for residues **C'**, **F'** and **G'** (**C"**, **F"** and **C"**, respectively), belonging to **OS3**.
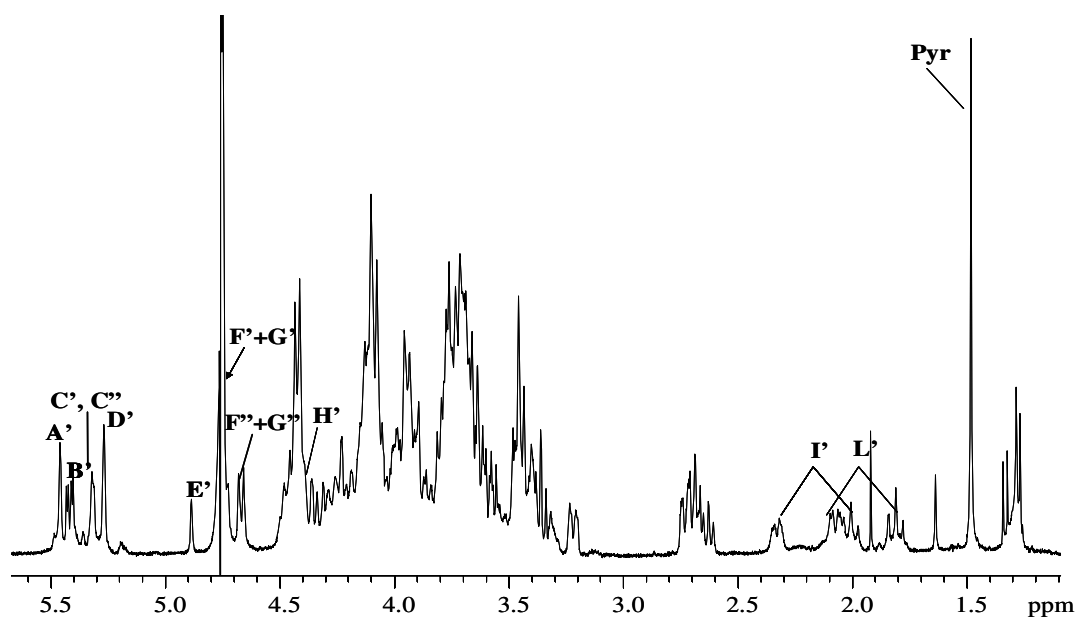
Figure 5.15 - ^{1}H-NMR spectrum and of minor oligosaccharides (**OS2** and **OS3**) obtained by alkaline degradation of the LOS from *Pseudomonas* sp. OX1.
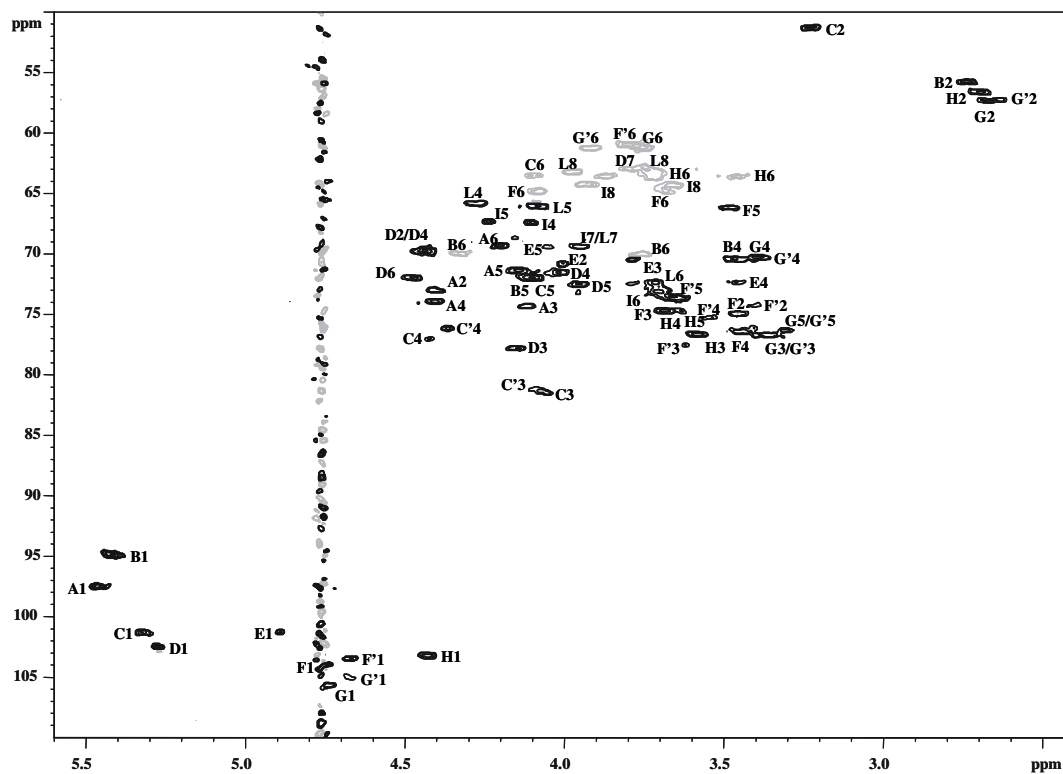
Figure 5.16 - The ^{1}H,^{13}C-HSQC spectrum of oligosaccharides **OS2** and **OS3** obtained by alkaline degradation of the LOS from *Pseudomonas* sp. OX1. All the heteronuclear correlations are assigned. Experiment was carried out with carbon multiplicity editing, and grey cross peaks refer to CH$_2$ groups.
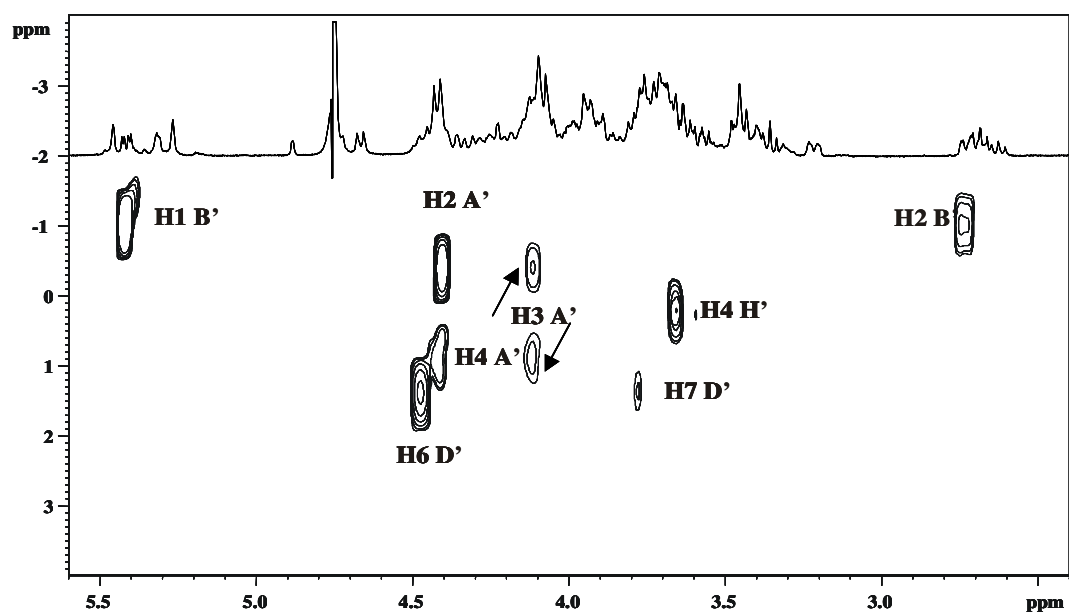
Figure 5.17 - ^{1}H,^{31}P-HSQC spectrum of **OS2** and **OS3** obtained by alkaline degradation of the LOS from *Pseudomonas* sp. OX1. All the relevant heteronuclear $^3J_{P, H}$ and $^4J_{P,H}$ correlations are visible. ^{1}H-NMR spectrum is overlapped.

Table 5.5 – [1]H, [13]C (*italic*) and [31]P (**bold**) chemical shifts for **OS2** and **OS3**. Numbers in brackets refer to Kdo residues.

|		1(H3$_{ax}$)	2(H3$_{eq}$)	3(4)	4(5)	5(6)	6(7)	7(8)
OS2	**A'**	5.46	4.40	4.10	4.41	4.14	4.20	3.87
	3-α-Hep I	*97.6*	*74.0*	*74.2*	*72.7*	*71.3*	*69.2*	*63.7*
			-0.39		**0.94**			
	B'	5.42	2.72	3.63	3.44	4.09	4.32/3.74	
	6-α-GlcN	*94.9*	*55.7*	*73.6*	*70.4*	*72.1*	*70.0*	
		-1.0						
	C'	5.31	3.21	4.07	4.36	4.11	4.09	
	3,4-α-GalN	*101.4*	*51.2*	*81.4*	*76.2*	*71.6*	*63.0*	
	D'	5.26	4.42	4.15	4.05	3.95	4.47	3.73/3.78
	3-α-HepII	*102.5*	*69.7*	*77.9*	*71.4*	*72.7*	*72.2*	*62.8*
							1.36	
	F'	4.73	3.45	3.96	3.44	3.48	3.68/4.09	
	t-β-Glc	*105.5*	*75.0*	*74.7*	*76.3*	*66.5*	*64.8*	
	G'	4.74	2.68	3.39	3.45	3.33	3.76	
	t-β-GlcN	*104.4*	*57.3*	*76.7*	*70.4*	*76.5*	*61.2*	
	H'	4.42	2.68	3.58	3.64	3.68	3.78/3.45	
	6-β-GlcN	*103.2*	*57.5*	*76.5*	*74.4*	*74.5*	*63.4*	
					0.26			
	I'	2.00	2.32	4.10	4.23	3.69	3.96	3.92/3.65
	4,5-α-Kdo	*34.8*		*67.6*	*67.3*	*73.3*	*69.3*	*64.1*
	L	1.81	2.07	4.27	4.10	3.71	3.94	3.94/3.75
	t-α-Kdo	*35.8*		*65.9*	*66.1*	*73.1*	*69.4*	*63.0*
OS3	**C''**	5.31	3.21	4.09	4.42	4.11	4.09	
	3,4-α-GalN	*101.4*	*51.2*	*80.9*	*77.1*	*71.6*	*63.0*	
	E'	4.88	4.00	3.78	3.46	4.06	1.28	
	t-α-Rha	*101.3*	*70.7*	*70.6*	*72.7*	*69.4*	*16.8*	
	F''	4.66	3.39	3.62	3.53	3.71	3.80	
	3-β-Glc	*105.0*	*74.3*	*77.6*	*75.2*	*73.1*	*60.9*	
	G''	4.67	2.62	3.35	3.38	3.31	3.74/3.91	
	t-β-GlcN	*103.4*	*57.2*	*76.6*	*70.3*	*76.3*	*61.2*	

The complete structure of both oligosaccharides was inferred by the analysis of the NOE connectivities detected in the ROESY spectrum (**Figure 5.18**). Within **OS1** structure, residues **F'** and **G'**, were linked at *O*-3 and *O*-4 of residue **C**, respectively, as shown by NOE correlations H-1**F'**-H-3**C'** and H-1**G'**-H-4**C'**, generating the same structure subunit of the Outer Core from **OS1**. According to chemical shift values for proton and carbon, residue **G'** (GlcN) was unsubstituted, whereas residue **F'** (Glc), showed a weak downfield shift of carbon resonances for C-4 and C-6. In agreement, a considerable downfield displacement of resonances for H-6$_a$ and H-6$_b$, of residue **F'** was detectable, as well. This was caused by substitution at *O*-4 and *O*-6 of residue **F'** of pyruvic acid as a cyclic ketal, as concluded by a scalar long range correlation found in the HMBC spectrum between C-2 of pyruvic acid and

H-4 and H-6 of **F'**. The lack of any strong NOE effect between the methyl group of the pyruvate residue and the **F'** ring proton signals, indicated an equatorial orientation for methyl group in a chair-like conformation of the ketal, hence the *S*-configuration at C-2 of pyruvate. This hypothesis was confirmed by the ^{1}H and ^{13}C chemical shifts of pyruvate residue that are highly diagnostic of its absolute configuration (Garegg *et al.,* 1980), as already observed in NMR analysis of **OS1**.
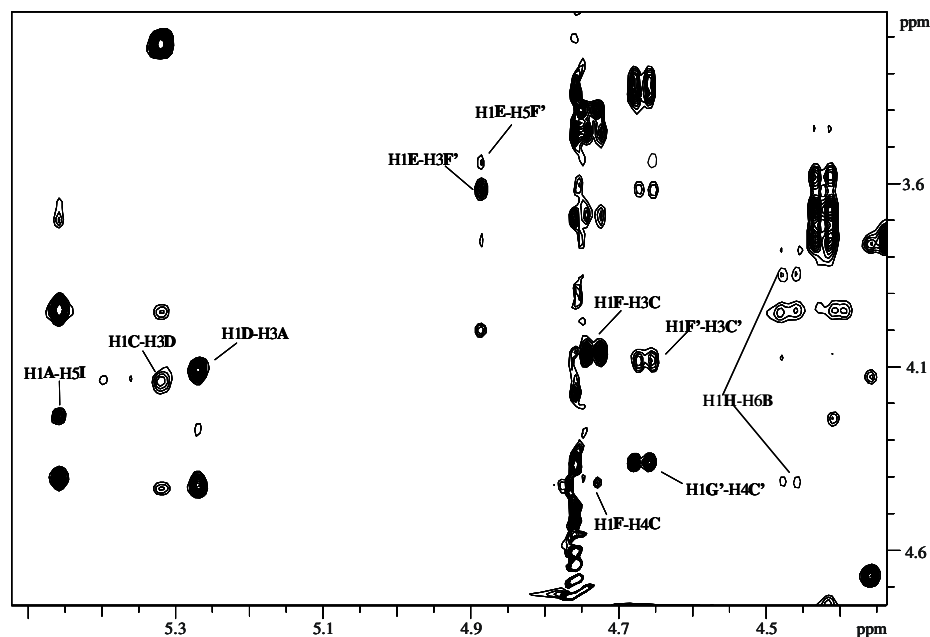
Figure 5.18- Section of the antiphase ROESY and ^{1}H-NMR spectra of oligosaccharides **OS2** and **OS3**. Annotations refer to interresidual cross-peaks. The capital letters refer to residues as denoted in **Table 5.5.**
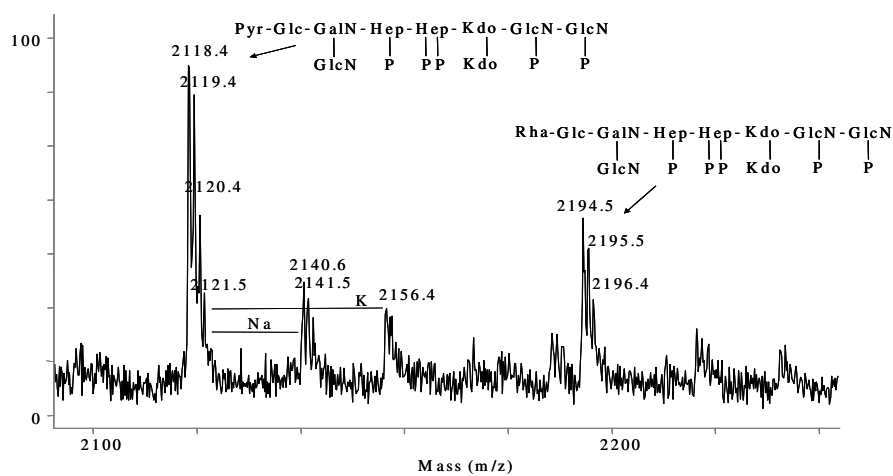
Figure 5.19 - Negative ion MALDI-TOF mass spectrum of oligosaccharides **OS2** and **OS3** obtained in reflector mode. Assignments of ion peaks are shown. Abbreviations: P is phosphate, Pyr is pyruvic acid.

The MALDI-TOF spectrum (**Figure 5.19**) of the de-acylated oligosaccharide confirmed the structural assignments. The main ion peak, at *m/z* 2118.4, was identified as **OS2** oligosaccharide, with the following chemical composition: Kdo_2-Hep_2-Hex-$HexN_4$-P_5-Pyr. The minor ion peak at *m/z* 2194.5 was in account for **OS3**, where the pyruvic acid ketal was missing and an extra rhamnose residue appeared. Thus, both structures are closely related to that of **OS1**, and they can be depicted as it follows:

OS2

F'

4,6(*S*)Pyr-β-Glc-(1⌐ **C'**　　　**D'**　　　**A'**　　　**I'**　　　**H'**　　　**B'**

3

α-GalN-(1→3)-α-Hep6*P*-(1→3)-α-Hep2*P*4*P*-(1→5)-α-Kdo-(2→6)-β-GlcN4*P*-(1→6)-α-GlcN1*P*

4　　　　　　　　　　　　　　　　　　4

β-GlcN-(1⌐　　　　　　　　　　　α-Kdo-(2⌐

G'　　　　　　　　　　　**L'**

OS3

E'　　　F''

α-Rha-(1→3)-β-Glc-(1⌐ **C''**　　　**D'**　　　**A'**　　　**I'**　　　**H'**　　　**B'**

3

α-GalN-(1→3)-α-Hep6*P*-(1→3)-α-Hep2*P*4*P*-(1→5)-α-Kdo-(2→6)-β-GlcN4*P*-(1→6)-α-GlcN1*P*

4　　　　　　　　　　　　　　　　　　4

β-GlcN-(1⌐　　　　　　　　　　　α-Kdo-(2⌐

G''　　　　　　　　　　　**L'**
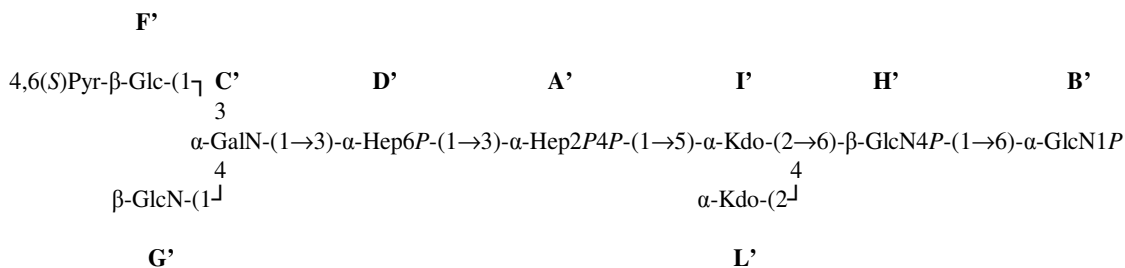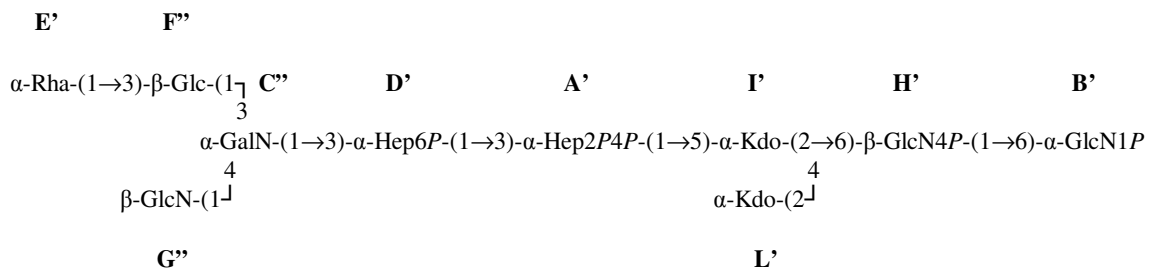
It should be underlined that both **OS2** and **OS3** structures differ from **OS1** for the absence of a pyruvic acid residue on the terminal GlcN residue (**G'** and **G''** within the structures). In the case of **OS2** structure, the only difference from the major oligosaccharide is the lacking of the pyruvic acid ketal on **G** residue.

In order to better clarify the structure of the main oligosaccharide, a second aliquot of the intact LOS underwent mild acid hydrolysis to recover information concerning the alkaline labile groups which could be present in the core region (i.e., acyl groups). As previously said, this procedure splits the labile linkage between the Kdo and the GlcN backbone, and, as a

consequence of this treatment, an oligosaccharide mixture was isolated after gel permeation chromatography which was further purified. The resulting oligosaccharide (**OS4**) was analyzed by compositional/methylation analyses, 2D NMR and MALDI MS.

The ^{1}H-NMR spectrum revealed the absence of anomeric signals from GlcN I and GlcN II of Lipid A, the lack of pyruvate methyl groups, as a consequence of the cleavage of the ketal group under acid treatment, and the presence of singlet signals at 2.00 ppm. Methylene signals of Kdo were spread because of its presence as reducing end unit, i.e., pyranose, furanose, anhydro and lactone forms present at same time. The anomeric region of the spectrum consisted of six main signals (**Figure 5.20**), five of which belonging to the main oligosaccharide backbone, named **U**-**Z**. All resonances of the monosaccharides (**Table 5.6**) were obtained from 2D-NMR spectroscopy (DQF-COSY, TOCSY, NOESY, ROESY, ^{1}H,^{13}C-DEPT-HSQC ^{1}H,^{31}P-HSQC, ^{1}H,^{13}C-HMBC and ^{1}H,^{13}C-HSQC-TOCSY). Evaluation of chemical shifts and of $^3J_{H,H}$ coupling constants led to identification of residues Hep (**U**), 7-*O*-carbamoyl-Hep (**V**), GalN (**X**), GlcN (**W**), Glc (**Z**).

Low-field shifted signals were present in the HSQC spectrum indicating substitutions at *O*-3 for residues **U**, **V** and **X** and at *O*-4 for residue **X**, whereas residues **W** and **Z** were not substituted. Given the downfield H-2 chemical shifts of **X** (GalN) and **W** (GlcN) residues, the amino groups should have been present as acylamido. The nature of the acyl groups was clarified by the analysis of the ^{1}H,^{13}C-HMBC spectrum, where all signals within the region of 2.00 ppm showed long range correlations with a carbonyl signal around 174.0 ppm which, in turn, correlated to protons at 3.67 ppm (H-2 **W**) and 4.26 ppm (H-2 **X**), indicating the presence of two acetamido groups at the C-2 of GlcN **W** and GalN **X**. Smaller methyl signals were observed for the acetyl group on residue **X**, as a consequence of oligosaccharide heterogeneity, possibly due either to adjacent heptose **V** bearing heterogeneous phosphate substitution (see below) and to reducing Kdo residue. Dipolar *inter*-residual correlations were obtained by the analysis of the 2D ROESY spectrum, pointing out the identical oligosaccharide structure identified for **OS1**.
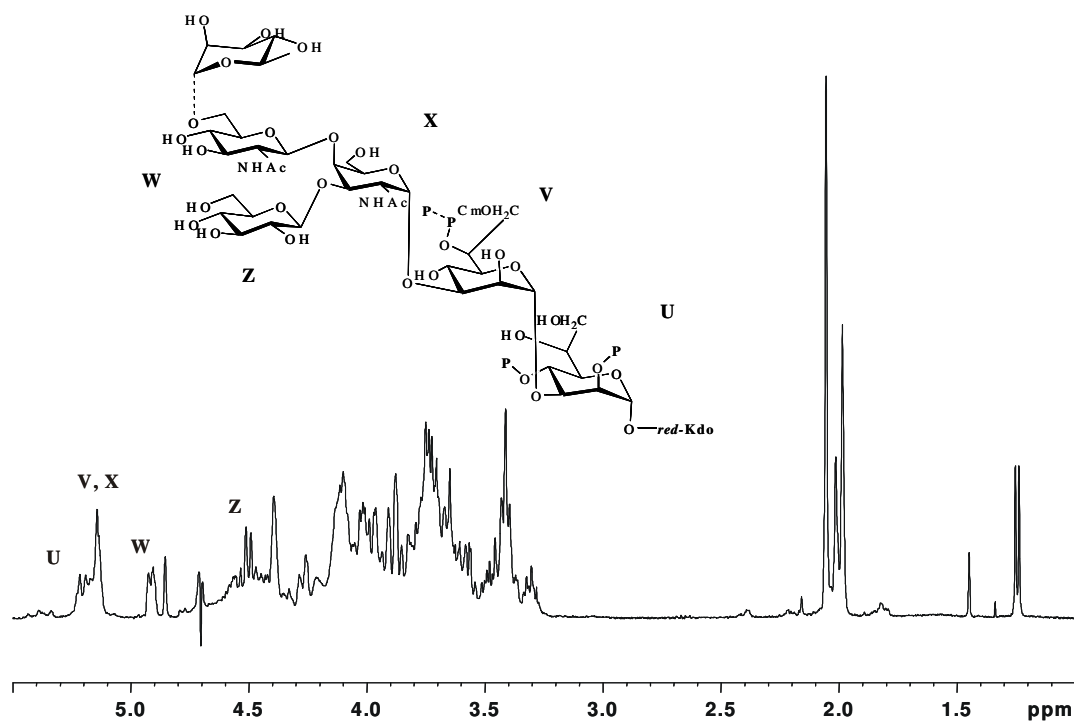
Figure 5.20 - ^{1}H-NMR spectrum of **OS4** obtained by acetic acid hydrolysis of the LOS from *Pseudomonas* OX1. The figure sketches the oligosaccharide structure. Capital letters refer to **Table 5.6**. Dotted linkages indicate non-stoichiometric substitution.

Table 5. 6- [1]H, [13]C (*italic*) and [31]P (**bold**) chemical shifts (ppm) for **OS4** obtained after acid hydrolysis of LOS from *Pseudomonas* sp. OX1. *O*-6 **V** resonances are given in parentheses when this position is monophosphorylated. P/P is referred to both resonances of pyrophosphate. Kdo signals are spread because of its multiple forms and its resonances are not given.

Residue	1	2	3	4	5	6	7
α-Hep	5.23	4.56	4.21	4.68	4.23	4.07	3.77
U	*99.2*	*73.8*	*76.8*	*73.7*	*74.5*	*70.9*	*64.1*
		1.4		**1.8**			
α-Hep	5.14	4.39	4.02	4.11	4.15	4.63 (4.46)	4.59/3.96
V	*102.7*	*69.17*	*78.1*	*67.9*	*71.6*	*71.2 (70.2)*	*62.4*
						-9.7/-5.5 (3.2)	
α-GalN	5.14	4.26	4.12	4.39	4.12	3.72	
X	*99.8*	*49.8*	*77.3*	*75.0*	*73.5*	*60.1*	
β-GlcN	4.91	3.67	3.67	3.61	3.41	3.612/3.88	
W	*101.2*	*56.1*	*72.6*	*73.6*	*70.0*	*61.2*	
β-Glc	4.53	3.29	3.49	3.48	3.40	3.74/3.89	
X	*104.4*	*73.5*	*75.6*	*70.1*	*76.9*	*60.7*	
Ac		2.0-2.1					
	174.6-175.0	*22.3*					
Cm	*160.0*						
Glc	4.53	3.30	3.52	3.79	3.80	3.93	
W	*104.4*	*73.5*	*76.5*	*70.9*	*75.1*	*69.7*	
Rha	4.86	3.96	3.73	3.42	4.01	1.26	
	101.7	*70.5*	*70.2*	*72.9*	*69.2*	*17.0*	

Other information on non-carbohydrate substituents (phosphate and carbamoyl groups) was gained by the observation of the downfield displaced heptose signals, namely, H-2/C-2 and H-4/C-4 of heptose **U** and H-6/C-6 and H-7$_{a,b}$ of heptose **V**.

The H-7$_{a,b}$ downfield shift was due to the presence of a carbamoyl group that did not undergo hydrolysis in mild acid conditions, and that has already been located at *O*-7 position of the second heptose residue on the basis of methylation analysis. In agreement with this assignment, a signal at 160.0 ppm in the HMBC spectrum correlated to both protons H-7 of monosaccharide **V**.

The degree of phosphorylation and localization of phosphate substituents was inferred by one- and two-dimensional ^{31}P NMR spectroscopy (**Fig. 5.21, Table 5.6**). Several signals were found in the ^{31}P-NMR spectrum, whose chemical shift clearly indicated that they derived from phosphate groups present in different magnetic/chemical environments.
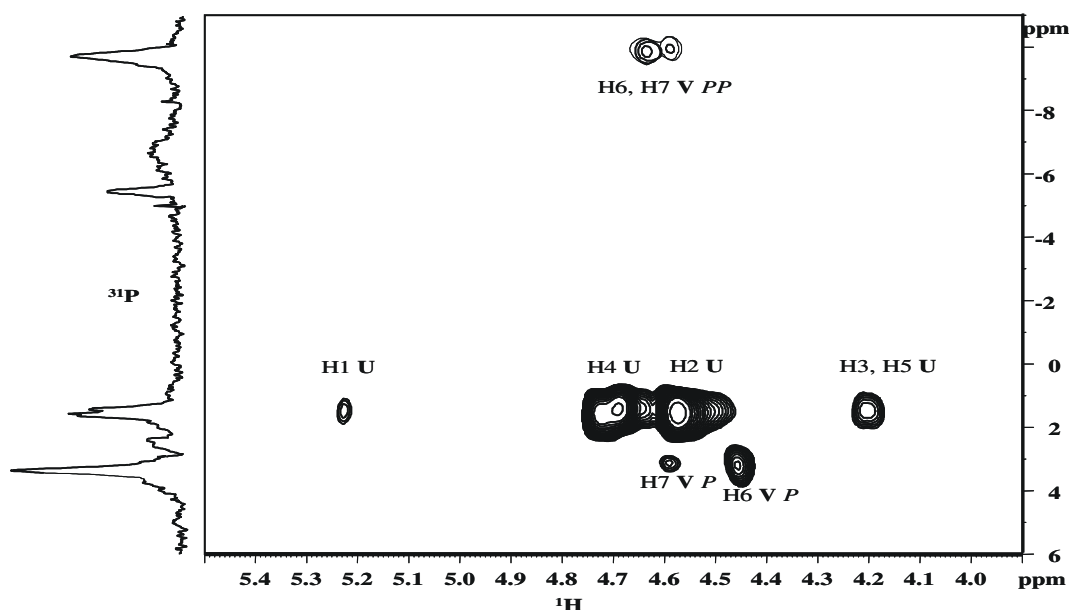
Figure 5.21 - Section of the ^{1}H,^{31}P-HSQC spectrum of **OS4**. The spectrum shows cross peaks relevant for the localization of the phosphate groups.

In addition to a number of phosphate monoester signals in the region of 1.4-3.2 ppm, two peaks of lower intensity were present at -5.5 and -9.7 ppm. These last two signals derived from a diphosphate monoester bond, i.e., a pyrophosphate group. In particular, the signal at -5.5 ppm could be identified as the distal phosphate group, whereas the phosphate at -9.7 ppm was identified as the proximal phosphate group. This pyrophosphate group was located, on the basis of the cross peak at 4.63/-9.7 ppm in the ^{1}H,^{31}P-HSQC, at *O*-6 of heptose **V**. An

alternative resonance was also observed, at 4.46/3.2 ppm, showed the occurrence of alternative substitution by a phosphate monoester group. In the same spectrum, correlations between H-2 and H-4 of heptose **U** were observed with typical signals of phosphate monoester groups.

The MALDI-TOF mass spectrum (**Figure 5.22**) of **OS4** confirmed all the assignments, as all ion peaks corresponding to the structures above were present. In fact, ion peaks were found, characteristic of the oligosaccharide HexNAc$_2$-Kdo-Hep$_2$-Hex-*Cm* bearing from two to five phosphate groups. Moreover, additional peaks at $\Delta m/z$ 146 accounted for the presence of the second core glycoform which differing from the most abundant one by the additional rhamnose residue. Ion peaks derived from loss of water from molecular ions, likely Kdo lactone or *anhydro*-Kdo forms, were also present. The presence of a very small amount of penta-phosphorylated species, which was not detected by NMR, was inferred by MALDI TOF analysis. Since in one- and two-dimensional ^{31}P NMR no other different phosphate substitution was visible, we can suppose that the fifth phosphate group is present as pyrophosphate on heptose **U**.
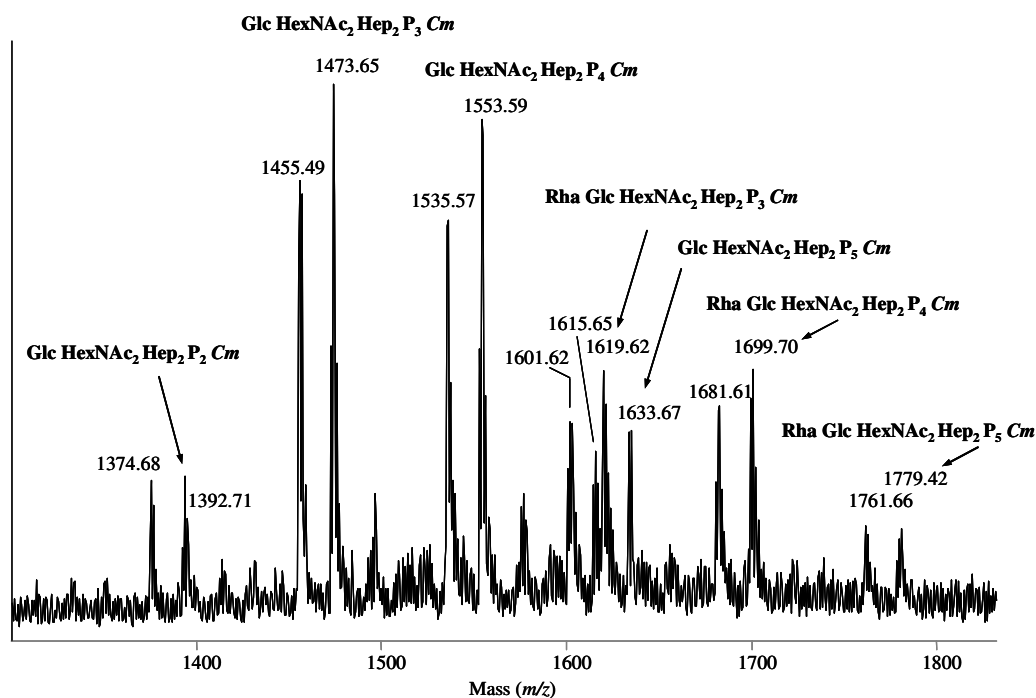
Figure 5.22 - Negative ion MALDI-TOF-MS spectrum of **OS4** recorded in reflector mode. Assignments of main ion peaks are shown. $\Delta m/z$ 18 is due to Kdo present in reducing or lactone form. P is phosphate, *Cm* is 7-O-carbamoyl, Ac is acetyl.

In conclusion, the structure of the main Core oligosaccharide from *Pseudomonas* sp. OX1 can be depicted as it follows:

```
4,6(S)Pyr-β-Glc
       1
       ↓
       3
α-GalNAc-(1→3)-α-Hep7Cm6PP-(1→3)-α-Hep2P4P-(1→5)-α-Kdo-(2→6)-β-GlcN4P-(1→6)-α-GlcN1P
       4                                                              4
       ↑                                                              ↑
       1                                                              2
4,6(R)Pyr-β-GlcNAc                                                   α-Kdo
```
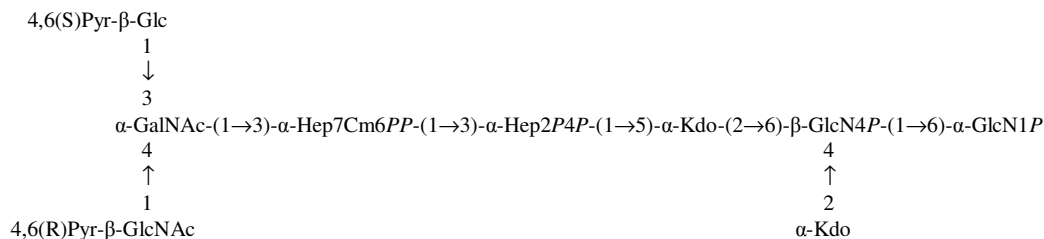
5.3.2 Characterization of the O-chain polysaccharide

Smooth form LPS was isolated by means of hot phenol/water extraction (see section 2.1) from dried cells of *Pseudomonas* sp. OX1 after growth in rich medium (LB, see section 7.1.3). The LPS, detected in the phenol extraction after purification by means of enzymatic digestion, underwent mild acid hydrolysis with 1% Acetic Acid. The polysaccharide moiety was collected after centrifugation and lyophilization of the supernatant and purified by Gel Permeation Chromatography. Compositional analyses were performed by GC-MS analyses as previously described (section 2.2) and pointed out the occurrence of two different 4-amino-4,6-dideoxy-hexoses (dHex4N), namely D-perosamine, 4-amino-4,6-dideoxy-D-mannose (D-Rha4N), and D-tomosamine, 4-amino-4,6-dideoxy-D-galactose (D-Fuc4N), identified by comparison with original standards. Methylation analysis showed the presence of the derivatives of 2-dHex4N, 2,3dHex4N and t-dHex4N, all in pyranose form (ratio 3.7 : 1 : 0.9, uncorrected detector response).

^{1}H-NMR spectrum (**Figure 5.23**) of the polysaccharide fraction presented, within the anomeric region, five signals, all appearing as broad singlets, relative to five different spin systems, **A-E**, at 5.16, 5.13, 5.07, 5.03, and 4.98 ppm, respectively, in a relative ratio 0.5:0.5:1:1:1. At lower field, two sharp singlets were observable, at 8.16 and 7.86 ppm, deriving from the two possible isomers (*Z* and *E*, respectively) of a *N*-formyl group. The different amount of the two species (relative ratio 8:1) can be explained on the basis of the higher stability of the *Z* isomer. Beside the ring proton region at 4.3 and 3.3 ppm, other significant signals were present, at 1.92-1.98 ppm belonging to *N*-acetyl groups, and between 1.13 and 1.03 ppm, belonging to methyl groups of position 6 of the deoxy-sugars.
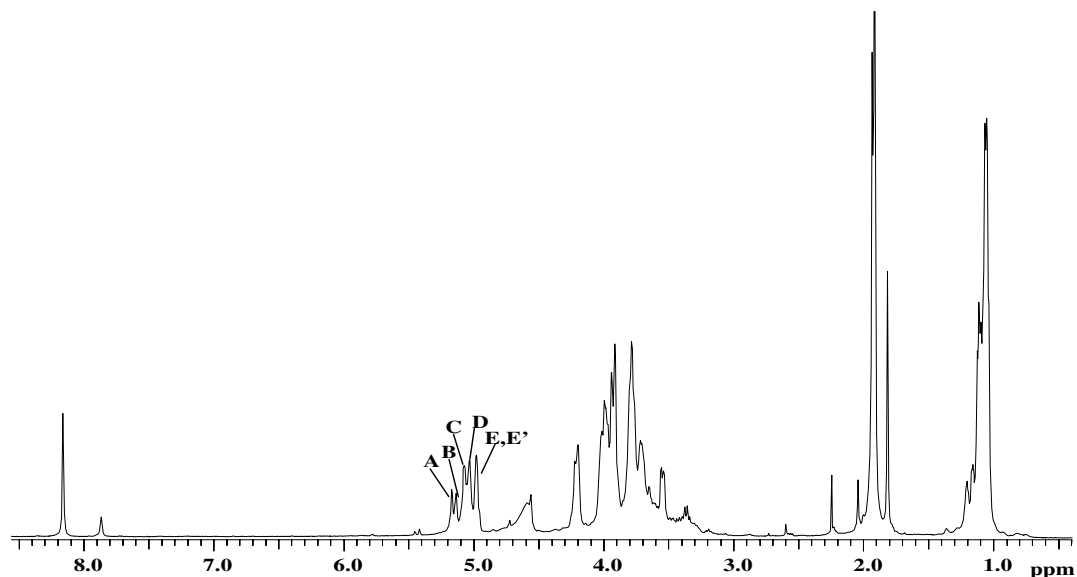
Figure 5.23 - ^{1}H-NMR of the O-polysaccharide from *Pseudomonas* sp. OX1. Anomeric signals are designated by capital letters referring to **Table 5.7**.

Despite the quite simple appearance of the spectrum, 2D-NMR spectra analysis pointed to the presence of a heterogeneous product. On the basis of DQF-COSY, TOCSY and NOESY spectra, the full proton resonances of the spin systems **A-E** could be assigned (**Table 5.7**), whereas the interpretation of the ^{1}H,^{13}C-HSQC spectrum allowed for the assignment of all ^{13}C resonances. Residues **A** and **B** were identified, on the basis of the small $^3J_{1,2}$ coupling constant value (about 1.8 Hz) inferred from the DQF-COSY spectrum, and the diagnostic H-5/C-5 chemical shift values (Lipkind *et al.,* 1988), suggested α-*manno* configuration. These residues were identified as two units of perosamine. A comparison of carbon resonances of **A** and **B** with unsubstituted residues (Ovchinnikova *et al.,* 2004; Lipinski *et al.,* 2002), gave evidence of a downfield shift of C-2 and C-3 signals for both residues indicating substitution at *O*-2 and *O*-3. Similar considerations could be made for spin systems **C** and **D** which were both finally identified as 2-substituted α-perosamine owing to the downfield glycosylation of their C-2 signal. Residue **E** was identified as unsubstituted 4-amino-4,6-dideoxy-α-galactose (α-Fuc4N). Its *galacto*-configuration was inferred by the coupling constant values of ring protons, in particular, $^3J_{3,4}$ (3 Hz). In fact, H-5 of **E** spin system was only detectable by NOESY experiment since in the TOCSY spectrum the low $^3J_{4,5}$ impaired any magnetisation transfer over H-4. The anomeric coupling constant value (3.2 Hz) of residue **E** clearly indicated α-orientation.

In the ^{1}H,^{13}C-HMBC spectrum scalar correlations were found between H-4 of **A-D** and carboxyl group signals around 175 ppm and between these latter and methyl signals at about

2.00 ppm, thus indicating that all the Rha4N residues are *N*-acetylated. On the other hand, Fuc4N **E** showed a cross peak between H-4 and a carboxyl group signal shielded at 166.2 ppm which, in turn, is correlated to the formyl proton at 8.16 ppm, thus confirming the presence of the *Z*-isomer of formyl group at *N*-4 of **E** residue. A minor series of signals in the COSY and TOCSY spectra, relative to the same anomeric proton at 4.97 ppm, described another spin system (**E'**), which was identified as Fuc4NFo, i.e., a modified residue **E**, in which the *N*-formyl group was attached as *E*-isomer. In fact, in the HMBC spectrum, H-4 **E'** and the formyl proton at 7.86 ppm both correlated to the carboxyl signal at 169.6 ppm.

Detection of dipolar and scalar long range *inter*-residual correlations within the NOESY (**Figure 5.24**) and ^{1}H,^{13}C-HMBC spectra was used to establish the monosaccharide sequence within the repeating unit. The anomeric proton of **A** residue (H-1 **A**) gave NOE effect with H-1 **C** and H-2 **C**, whereas H-1 **C** gave NOE effect with H-1 and H-2 **A**, thus indicating that **A** and **C** residues are both 2-substituted and arranged in a disaccharide structure. Likewise, **B** and **D** spin systems could be attributed to the same disaccharide structure, although in a different magnetic environment. Furthermore, no connections between **A-C** and **B-D** fragments were visible in the NOESY spectrum.

Table 5.7 - ^{1}H and ^{13}C (*italic*) NMR chemical shifts (ppm) of the intact O-polysaccharide from *Pseudomonas* sp. OX1 and of the polysaccharide after Smith degradation.

Sugar residue	1	2	3	4	5	6	C=O	CH$_3$ (H)
A	5.16	4.22	3.91	3.93	3.91	1.11	-	1.92
α-2,3-Rha4Nac	*100.9*	*73.9*	*73.4*	*52.1*	*68.6*	*17.6*	*175.2*	*23.1*
B	5.13	4.23	3.90	3.92	3.91	1.12	-	1.98
α-2,3-Rha4NAc	*101.0*	*74.8*	*73.4*	*52.1*	*68.8*	*17.4*	*174.9*	*21.0*
C	5.07	3.98	3.94	3.76	3.69	1.06	-	1.92
α-2-Rha4NAc	*100.7*	*77.7*	*69.2*	*53.7*	*69.1*	*17.5*	*175.7*	*22.8*
D	5.03	4.02	3.91	3.77	3.70	1.06	-	1.92
α-2-Rha4NAc	*101.2*	*77.6*	*69.3*	*53.7*	*69.1*	*17.5*	*175.7*	*22.8*
E	4.97	3.54	3.80	4.20	3.98	1.03	-	8.16
α-Fuc4NFo	*96.1*	*68.9*	*69.2*	*53.0*	*66.3*	*16.3*	*166.2*	-
E'	4.97	3.48	3.74	4.18	3.94	1.04	-	7.86
α-Fuc4NFo	*95.7*	*68.6*	*69.6*	*53.2*	*66.2*	*16.4*	*169.6*	-

Smith degraded polysaccharide

α-2-Rha4NAc	5.05	4.03	3.95	3.80	3.73	1.07	-	1.94
	100.9	*77.4*	*68.3*	*53.5*	*68.9*	*17.2*	*175.6*	*22.5*

The anomeric proton of **E** residue (H-1 **E**) gave a dipolar correlation with both H-3 of **A** and **B**, thus confirming our previous conclusions that **A** and **B** are 2,3-disubstituted residues and **E** residue is attached to their *O*-3 position. All the previous assumptions were confirmed by the ^{1}H,^{13}C-HMBC spectrum that contained scalar long range correlations between H-1 **A**/C-2 **C**, H-1 **C**/C-2 **A**, H-1 **B**/C-2 **D**, H-1 **D**/C-2 **B**, H-1 **E**/C-3 **A-B**.
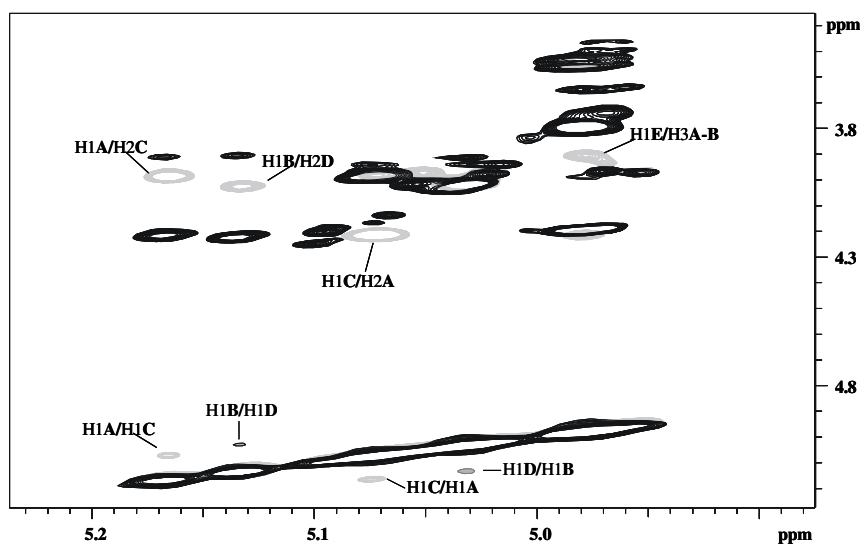
Figure 5.24 - Zoom of the TOCSY (black) and NOESY (grey) spectra of the *O*-polysaccharide from *Pseudomonas* sp. OX1. Annotations refer to *inter*-residual cross peaks of spin systems reported in **Table 5.7**.

Thus, it can be concluded that in the *O*-polysaccharide from *Pseudomonas* sp. OX1 two identical moieties were present, whose difference cannot be derived from the data above. Their structure can be drawn as it follows:

<div align="center">

A/B   **C/D**

→2)-α-Rha4NAc-(1→2)-α-Rha4NAc-(1→
3
α-Fuc4NFo(1⌐

E

</div>
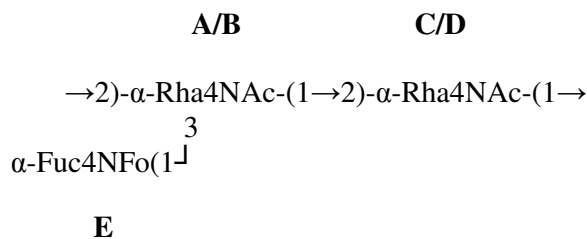
The formyl group, present as pair of isomers, was an expected source of magnetic heterogeneity, but the 1 : 9 ratio between *E* and *Z* isomers in the ^{1}H-NMR spectrum could not be the only origin for **A/B** and **C/D** duets, because most of the heterogeneity was expected and found on Fuc4N residue (**E/E'**), to which the formyl group was directly attached. The ^{1}H-NMR spectrum indicated that 2-Rha4N (**C/D** units) is present in higher amount with respect

146

to nodal Rha4N **A/B** (anomeric signal ratio, **A:B**:**C:D**, 1:1:2:2) and this would suggest that the polysaccharide heterogeneity did not only depend on *E* and *Z* isomers ratio but also on the presence of a longer and not distinguishable chain of 2-substituted Rha4N residues and that this latter, in particular, causes the splitting of each Rha4N in two signals.

In order to simplify the intricate polysaccharide structure and to further support the structural hypothesis advanced above, a Smith degradation was carried out on the polymer (see section 7.5). After purification of the products by gel permeation chromatography on a TSK HW-40 column, a product was collected, which eluted in the void volume. The compositional and 2D NMR analyses (**Figure 5.25, Table 5.7**) of this fraction indicated the presence of a highly regular polysaccharide built up of 2-α-Rha4N, in which the heterogeneity was completely removed. As expected on the basis of the data collected on the intact polysaccharide, only terminal Fuc4N residues possessed a *vic*-diol functional group, prone to oxidation by periodate reagent, and consequently it was removed from the polysaccharide by the Smith degradation. Thus, the conclusion can be drawn that most of the heterogeneity encountered in the polysaccharide is due to non stoichiometric glycosylation by the Fuc4N residue in a linear chain of 2-α-Rha4N.
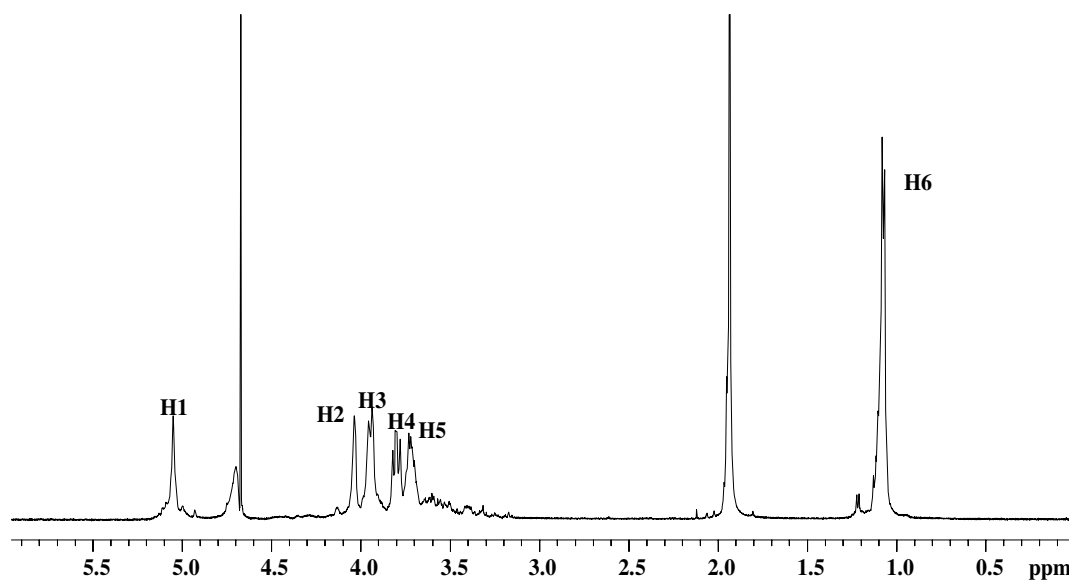
Figure 5.25 - ^{1}H-NMR of the Smith degraded *O*-polysaccharide from *Pseudomonas* sp. OX1. Capital letters indicate ring protons. Chemical shifts are reported in **Table 5.7**.

Thus, we can confidently affirm that the *O*-polysaccharide obtained from the LPS of *P. stutzeri* OX1 has the following structure:

$$\rightarrow 2)\text{-}\alpha\text{-D-Rha4NAc-}[(1\rightarrow 2)\text{-}\alpha\text{-D-Rha4NAc}]_n\text{-}(1\rightarrow$$
$$3$$
$$\alpha\text{-D-Fuc4NFo}(1^{\lrcorner}$$
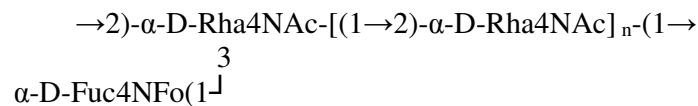
However, since both compositional analysis and anomeric signal integration in the ^{1}H NMR spectrum of the original polysaccharide were suggestive of the presence of a regular polymer, it is evident that our data do not allow to discriminate between the following structural possibilities: (i) two different repeating units are present in two regular polysaccharides, or (ii) only one polysaccharide is present, consisting of a monosaccharide backbone to which a side chain monosaccharide is attached in a non full stoichiometric fashion. Any attempt to separate by gel permeation chromatography the two putative coexisting polysaccharides failed.

5.3.3 Structure determination of the biofilm matrix polysaccharide

As already anticipated in section 5.1, cells of *Pseudomonas* sp. OX1 are able to produce a biofilm matrix when grown under stress conditions. An oligosaccharide fraction was isolated from the dialysed supernatant of *Pseudomonas* sp. OX1 cultures grown on phenol and was purified by GPC and HPLC. Chemical analysis carried out as previously described pointed out the presence of L-Guluronic Acid (L-GulA) and D-Mannuronic Acid (D-ManA). The ^{1}H-NMR spectrum showed a complex saccharide fraction (**Figure 5.26A**) with highly crowded anomeric and ring proton regions and, at high field, several methyl signals of acetyl groups. The ^{1}H,^{13}C-HSQC spectrum (**Figure 5.26A**) indicated that most of the signal in the anomeric region were correlated to carbon signals in the region 67-77 ppm, thus indicating that these were due to protons geminal to *O*-acetyl group.
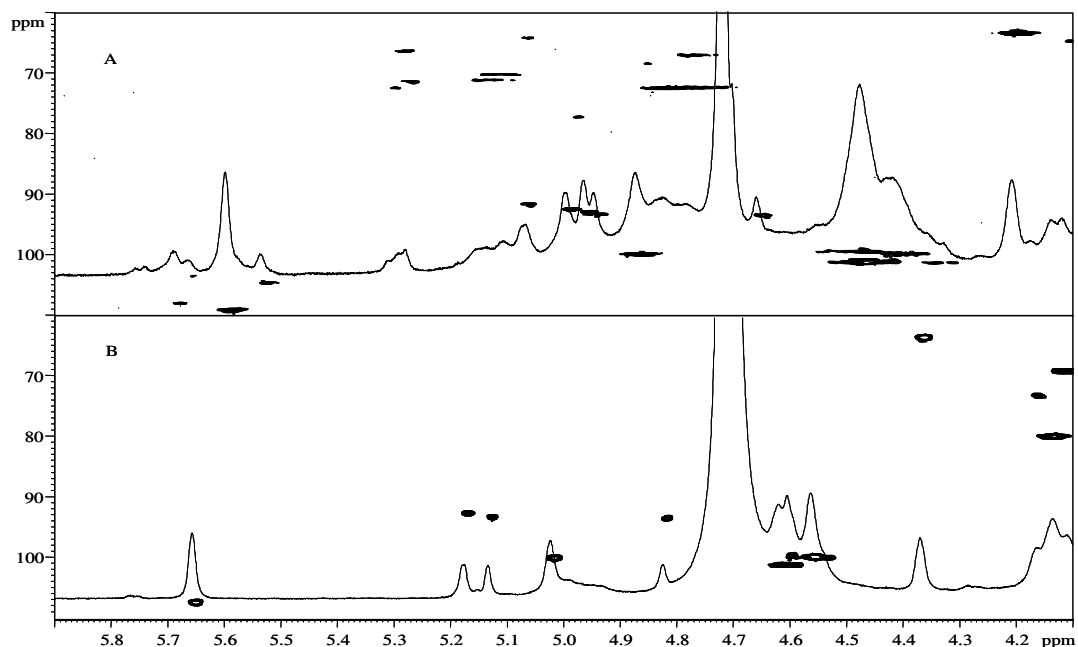
Figure 5.26 - Zoom of the anomeric region of the ^{1}H,^{13}C-HSQC and, overlapped, of ^{1}H NMR spectra of oligosaccharide fraction isolated from the supernatant of *Pseudomonas* sp. OX1 cultures before (**A**) and after (**B**) mild *O*-deacetylation.

In order to simplify the analysis, an aliquot of the sample was *O*-deacetylated with NH$_4$OH at room temperature for 16 h. The ^{1}H-NMR spectrum recorded after work-up of the reaction, showed a saccharide mixture much reduced in its heterogeneity (**Figure 5.26B** and **5.27**). A complete set of 2D NMR experiments (DQF-COSY, TOCSY, ROESY, ^{13}C-^{1}H HSQC, ^{13}C-^{1}H HMBC) was carried out. The anomeric region of the ^{1}H-NMR spectrum showed several signals, (**Figure 5.27, Table 5.8**) all belonging to ManA and GulA units in different
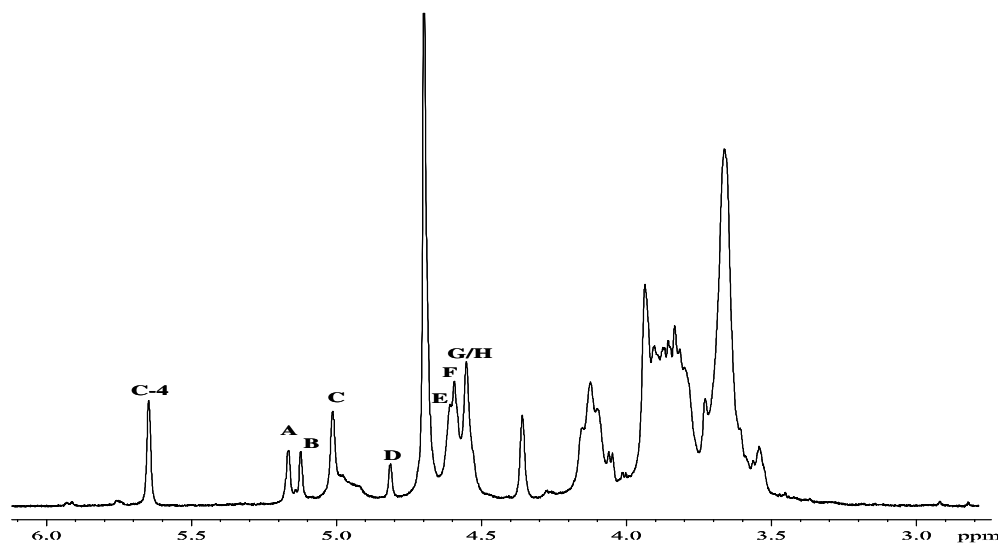
Figure 5.27 - ^{1}H-NMR spectrum of the *O*-deacetylated oligosaccharides from the biofilm matrix of *Pseudomonas* sp. OX1.

chemical/magnetic environments. In particular, numerous signals were present in the region of anomeric signals of β-ManA, and chemical shift assignment was performed for the most relevant spin systems. Identification of the residues was achieved by the complete assignment of all signals and by determination of the $^3J_{H,H}$ coupling constants. All spin systems were recognised as uronic acid units since, either in the COSY or in the TOCSY spectra, no H-6 proton signals were found, and in addition, in the HMBC spectrum the carboxy-group multitude of signals correlated to H-5 and H-4 proton signals of all spin systems. Spin systems **A/B** and **D** (**Figure 5.27, Table 5.8**) were identified as different GulA residues present as α- and β-reducing ends as confirmed by the shielded chemical shift value of their anomeric carbon signal and comparison with literature data (Zhang *et al., 2004*). Spin systems **E-H** were all attributed to β-ManA residues, given the low $^1J_{C-1,H-1}$ and $^3J_{H-1,H-2}$ values, approximately 165 Hz and 1.0 Hz. The β-anomeric orientation was further confirmed by *intra*-residual NOE effect between H-1 and H-3/H-5 signals found in the ROESY spectrum. Spin system **C** was identified as a 4-deoxy-α-L-*erythro*-hex-4-enopyranosyluronic acid (ΔHexA) residue. Actually, in the TOCSY and COSY spectra, correlations within **C** spin system ended at H-4 at low fields (5.643 ppm), that was in turn correlated, in the $^1H,^{13}C$-HSQC spectrum, to an olefin carbon signal at 107.5 ppm.

Table 5.8 - ^1H and ^{13}C (*italic*) NMR chemical shifts (ppm) for the main monosaccharides residues identified in the exopolysaccharides matrix of *Pseudomonas* sp. OX1.

Residue	1	2	3	4	5	6
→4)-α-GulA	5.164	3.728	3.902	4.128	4.104	-
A	*92.7*	*70.2*	*69.4*	*80.0*	*69.1*	*174.6*
→4)-α-GulA	5.120	3.835	3.879	3.831	4.056	-
B	*93.4*	*70.2*	*69.0*	*78.3*	*72.7*	*174.2*
α-ΔGulA-(1→	5.016	3.856	4.359	5.643	-	-
C	*100.1*	*66.2*	*63.7*	*107.5*	*145.5*	*169.5*
→4)-β-GulA	4.812	3.807	4.130	3.905	4.15	-
D	*93.5*	*70.6*	*73.3*	*78.5*	*73.3*	*175.1*
→4)-β-ManA-(1−	4.610	3.831	n.d.	n.d.	n.d.	-
E	*101.4*	*69.9*	*n.d.*	*n.d.*	*n.d.*	*n.d.*
→4)-β-ManA-(1→	4.590	3.941	3.660	3.798	3.650	-
F	*99.7*	*69.8*	*71.3*	*78.3*	*75.8*	*174.2*
→4)-β-ManA-(1→	4.551	3.929	3.657	3.828	3.671	-
G	*100.0*	*69.8*	*71.3*	*78.3*	*76.3*	*175.0*
→4)-β-ManA-(1→	4.526	3.880	3.555	3.828	3.670	-
H	*100.0*	*70.3*	*72.6*	*78.3*	*76.3*	*175.1*

This residue clearly derived from an uronic acid residue that lost the substituent at *O*-4 by a β-elimination, recognisable either as a former α-GulA residue or a β-ManA, since the loss of

chirality at C-5 for both monosaccharides leads to the same product. All the ManA residues and the reducing end guluronic residue were found to be *O*-4 substituted, as suggested by the low field displacement of their C-4 NMR signals, all around 80 ppm. This information was confirmed by the HMBC spectrum that showed *inter*-residue scalar correlations H-1/C-4 and C-1/H-4 of two vicinal residues.

The MALDI MS spectrum (**Figure 5.28**) of the *O*-deacetylated product confirmed the presence of an oligosaccharide blend. In fact, few ion peaks were visible and the most abundant ion at *m/z* 1056.2 contained six residues, the unsaturated guluronic and the uronic acid residues. The other ion peaks in the spectrum differed for the presence or the absence of single uronic acid units. The higher molecular weight ion species was visible at *m/z* 2111.9 and contained 12 residues, one of which was the unsaturated hexuronic acid residue. The acetyl groups were assigned by 2D NMR analysis of the native oligosaccharide mixture that showed that the chemical shift of guluronate residues were in agreement with those of a non substituted residue whereas H-2 and H-3 chemical shifts of ManA spin systems were alternatively shifted to lower field because of acetylation. In fact, in the COSY spectrum when H-2 was shifted downfield by acetylation it always correlated, to an upfield H-3 signal and similarly, H-3 downfield signal always correlated to an upfield H-2.

Therefore, it can be concluded that GulA residues are always non acetylated whereas ManA is always *O*-acetylated at C-2 and C-3. Thus, from the data above, it was possible to identify the oligosaccharides of the biofilm matrix of *Pseudomonas* sp. OX1 as alginate, i.e (1→4)-linked α-D-ManA and β-L-guluronic acid residues.
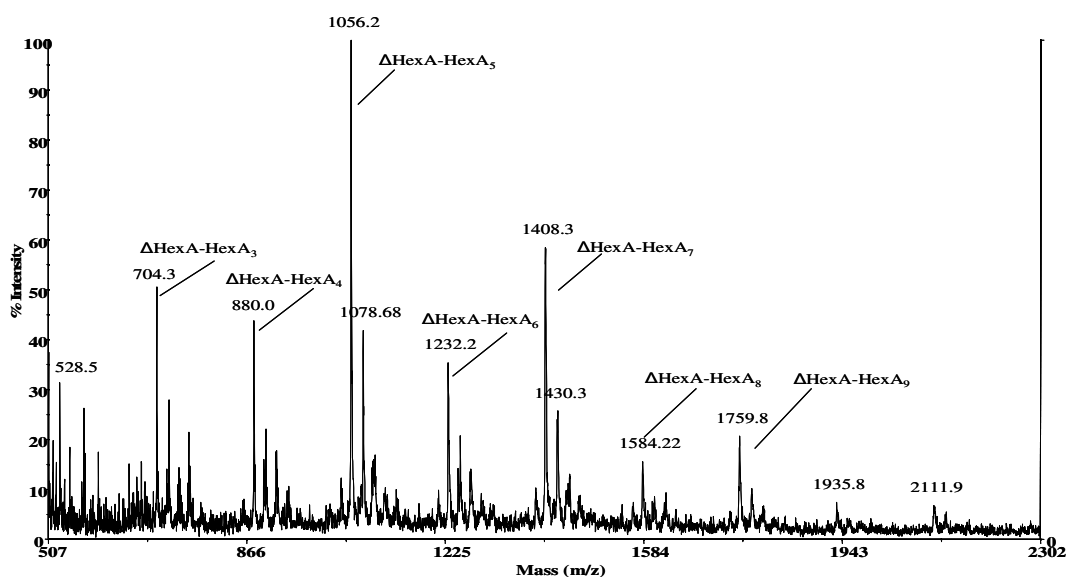
Figure 5.28 - MALDI mass spectrum of the *O*-deacetylated oligosaccharides from the biofilm matrix of *Pseudomonas* sp. OX1.

5.4 Conclusions

The results shown in the present section point out the possible involvement of LPS in the adaptation mechanism towards polluted sites. The oligosaccharide characterized from *Acinetobacter radioresistens* S-13 presents common traits with the previously described oligosaccharides from pathogen *Acinetobacter* starins, namely *A. haemolyticus* NCTC 10305 (Vinogradov *et al.,* 2002), *A. baumannii* NCTC 10303 (Vinogradov *et al.,* 2002) and *A. baumannii* ATCC 19606 (Vinogradov *et al.,* 1998): they all lack heptose residues and possess a peculiar Kdo oligosaccharide arrangement. In *A. baumannii* ATCC 19606 LPS, as well as in the present study, the Kdo residue linking the core region to lipid A is in turn linked by two Kdo residues, one of which is present in the main chain and not in the side chain, *i.e.*, in the linear oligosaccharide chain two Kdo residues are present. The novel structure of the carbohydrate backbone of the LPS from *A. radioresistens* S13 closely resembles the one from *A. baumannii* ATCC 19606 LPS, but it differs in the glucose oligosaccharide present in the outer core. Phosphate substitution is present only in the Lipid A backbone, in apparent contrast with the proposed trend of an increase of negative charge density during stressing events. Actually, in this case the majority of the negative charge is provided by the Kdo trisaccharide, and this is likely assuring an efficient protection of the bacterial cell to the uncontrolled entrance of organics in the cytoplasm. Moreover, in all the examined conditions, *A. radioresistens* produces an O-polysaccharide as well, whose repeating unit has not been completely defined yet, but whose chemical composition comprises an acidic non-ulosonic residue and a 2,4,6-trideoxy-2,4-amino-galactose residue bearing, as amide substituent at *N*-4, a succynic acid residue (Leone *et al.,* unpublished results). The occurrence of such an acidic polysaccharide can support the shielding effect of the Core an make unnecessary the introduction of structure modifications in response to the organic solvents exposure, as already observed for *Pseudoalteromonas issachenkonii* (see 3.5) and in an opposite trend respect to what observed in *Pseudomonas* sp. OX1. Another factor assuring the resistance to organics is the production of the powerful extracellular emulsifier, Alasan, strictly involved in solubilization of hydrophobic molecules and structurally related to the Outer Membrane Protein OmpA (Walzer *et al.,* 2006).

Also in the case of the Lipid A primary structure, no significant difference has been encountered subsequent to organics exposure. Nevertheless, the structure investigation can have an interesting biomedical impact, since for the first time the Lipid A of an *Acinetobacter* strain was completely clarified. Bacteria belonging to *Acinetobacter* genus have in fact earned

importance in the last years because of the role they play in triggering severe nosocomial infections. It is known that the strength of the observed immune response is closely related to three-dimensional conformation effects exerted by the Lipid A moiety (Seydel *et al.,* 2000). Studies performed on *Escherichia coli* Lipid A showed that the highest biological activity is associated either to high acylation degree, to asymmetrical distribution of the alkyl chain with respect to the two glucosamine residues and to phosphate content. These factors lead to conformational changes in the Lipid A, that are closely related to the ability of induction of citokyne host reaction. In section 1.2.2, it was demonstrated that the Lipid A from *Acinetobacter radioresistens* S13 is composed by an heterogeneous blend of molecules differing in the acylation degree, among which the more abundant is represented by the hepta-acyl species. This molecular species is associated to the highest level of activation of the human immune system (Seydel *et al.,* 2000). Nonetheless, the symmetrical hexa-acyl species is also present in a comparable amount, and this latter is associated to low toxicity levels. Given the intra-genus regularity of the Lipid A, it is possible to surmise that a similar architecture, with minor structure modifications, is conserved in other *Acinetobacter* strains of recognized toxicity. The higher pathophysiological impact associated, for example, to the *A. baumannii - A. calcoaceticus* complex (Gerner-Smidt, 1992), could be in part ascribed to structural changes on this Lipid A skeleton, for example a further acylation. The activation of the innate immune system is, in fact, performed by the natural blend of variously acylated Lipid A species produced by the bacterium; pathogen strains likely express higher percentages of hepta-acyl Lipid A, and this may be one of the reasons of the elevated response observed in the colonized organisms.

Pseudomonas sp. OX1 showed the most interesting results for what concerns the structure/function relationship of LPS in response to different culture conditions. The Core oligosaccharide elucidated showed similarities with the inner Core architecture of other *Pseudomonas* strains, primiarily from *P. aeruginosa* (Beckmann *et al.,* 1995; Masoud *et al.,* 1994; Sanchez-Carballo *et al.,* 1999; Knirel *et al.,* 2001), indicating a conservative biosynthetic control, evident in the fragment containing two Kdo residues, two L,D-Hep, one *O*-carbamoyl group (*Cm*), linked to the *O*-7 of the second Hep residue, and a GalN as the oligosaccharide branching point. This inner core region is always characterized by the presence of a large number of negative charges, usually carried by phosphate groups, linked to heptose residues, in addition to the key phosphate residues attached to the Lipid A backbone. The Rha residue often encountered in the Outer Core usually constitute the key residue for the *O*-polysaccharide transfer (Bystrova *et al.,* 2002; 2003).

The structure determined for *Pseudomonas* sp. OX1 is of special interest, both for its novelty with respect to the structures already determined, and for its biosynthetic implications. To our knowledge, a GlcNAc residue directly linked to GalN has never been found in the core region structure of *Pseudomonas*. Moreover, both of the two *gluco*-configured residues are blocked at position *O*-4 and *O*-6 by a pyruvate ketal linkage.

The presence of pyruvate residues in the core region of LPSs is a brand new element. In fact, although pyruvate residues are frequently found in bacterial exopolysaccharides (Cescutti *et al.,* 1999; 1995), and in O-polysaccharides (Vinogradov *et al.,* 1997) as a post polymerization decoration, they have never been found as Core constituents. This finding could be relevant in the understanding of adaptive chemical alterations of the outer membrane of *Pseudomonas* sp. OX1 as a consequence of its exposure to solvents, especially in relation to the O-polysaccharide found after conventional cultivation. Our hypothesis is based on the consideration that insertion of two bulky pyruvate groups at the end of the oligosaccharide chain blocks its elongation, by creating a structural hindrance to the action of glycosyl transferases. Thus, the presence of pyruvate moieties might represent a chemical camouflage of the glycosyl transferases substrate, obtained by linking a key molecule from the primary metabolism in a simple and mild chemical bond. This chemical protection is very similar to the isopropylidene group, one of the most widespread protecting groups in coupling reactions of oligosaccharide syntheses. This hypothesis is supported also by the finding of the alternative and minor glycoforms of the LOS, with the typical oligosaccharide structure of a potential substrate for chain elongation and O-polysaccharide attachment. In this latter chain a rhamnose residue is present at *O*-6 of the glucose residue substituting the pyruvate moiety. This finding would confirm that pyruvate residues are used to block chain elongation in the LOS of *Pseudomonas* sp. OX1, and analogous observation would apply to minor oligosaccharides structures.

Thus, the structure of the LOS we have found in *Pseudomonas* sp. OX1 would represent an adaptive response of the microrganism to a hydrocarbon-containing environment, since the presence of a long hydrophilic O-polysaccharide chain could have hindered its suitability to an external medium characterized by the presence of aromatic hydrocarbons.

Moreover, the peculiar presence of bulky pyruvate residues as blocking groups might offer an additional advantage to *Pseudomonas* sp. OX1, as these residues could help preventing the massive entrance of external organic compounds, which could be detrimental to its catabolism. In fact, their presence increases the total negative charges of the LOS, thus altering the physical properties of the external membrane, offering the further advantage of

allowing the polyanionic LOS molecules to electrostatically bind divalent cations, favouring a denser packing of the membrane in order to create a selective barrier to the entrance of organic molecules (Nikaido and Vaara, 1985; Raetz and Whitfield, 2002).

Further support to the hypothesis of a growth dependent inhibition of the O-polysaccharide biosynthesis can be understood taking a look to the structure of the O-chain expressed by *Pseudomonas* sp. OX1 after conventional growth. Apart from the novelty of the structure elucidated, that constitutes a further evidence for the existence of non regular polymers in the outer membrane of Gram negative bacteria [this is the case of several O-polysaccharide chains isolated from LPS of other *Pseudomonas* and *Xanthomonas* strains (Zdorovenko *et al.,* 2001; Knirel, *et al.,* 1996; Molinaro *et al.,* 2002; 2003), it is noteworthy that this polysaccharide does not own the acidic character evidenced in the case of all other stress adapted bacteria studied. Thus, organics exposed cells react to the stress condition removing this polysaccharide, in favour of the expression of highly negatively charged molecules of LOS.

The adaptation of *Pseudomonas* sp. OX1 to the organics contaminated habitats is also favoured by the production of the exocellular alginate matrix described in section 5.3.3. It has been revealed in recent studies that alginate hydrolysates and their derivatives exhibit many important bioactivities. All the alginate oligosaccharides isolated were constituted by a mannuronan chain starting with a guluronate residue, whereas the monosaccharide at the non-reducing end was transformed in a hex-en-uronic residue, most likely by the action of an alginate lyase. A number of alginate lyases from brown algae, molluscs and bacteria have been described (Wong *et al.,* 2000) and they usually cut alginate molecules by β-elimination, a mechanism similar to that of alkaline degradation to glycuronans. From the structure determined in the present study for *Pseudomonas* sp. OX1 it can be suggested that the lyase selectively hydrolyses the glycoside linkage of GulA, since the oligosaccharides found always bear this monosaccharide at the reducing end. In general, the content and distribution of GulA residues strongly affects the physicochemical properties of alginate molecules. Therefore, the epimerization process of ManA to GulA is of great importance from an applied point of view. In all *Pseudomonas*, the epimerization process and consequently the content of GulA resides is biologically controlled by acetylation. In fact, the acetylated ManA residues cannot be converted to GulA since they are not recognised by the mannuronate epimerase. The distribution of monosaccharide residues and the high degree of acetylation is associated in alginates from *Pseudomonas* to an enhanced water-binding capacity that is important in particular dehydrating conditions, e.g., for *P. aeruginosa* during infection and colonization of

the lungs (Pier *et al.,* 2001). The hypothesis can be advanced that the high degree of acetylation we have found in alginates from *Pseudomonas* is associated to an enhanced water-binding capacity that might be relevant under dehydrating conditions like those occurring during the growth of *Pseudomonas* sp. OX1 in the presence of aromatic hydrocarbons. This is in line with the very recent finding that *Rhodococcus* sp. 33, a benzene tolerant microorganism, produces a pyruvylated EPS and that the pyruvic acid moiety plays a crucial role in the tolerance and in the growth of the bacterium on benzene. In fact, *Rhodococcus* benzene sensitive mutants that did not produce EPS were able to grow on benzene, only after addition of wild type EPS, and were not able to grow after addition of depyruvylated EPS (Urai *et al.,* 2006)**.**

6

Concluding Remarks

The adaptation process of bacterial cells to environmental stressors involves several physiological and metabolic responses, and the mechanisms allowing survival in extreme habitats have not yet been completely elucidated. Several processes occurring in cells during stressing events have been described, and they involve all the biomolecules composing the cell, namely nucleic acids, proteins and membrane lipids. The responses effected by these stressing events in mesophilic prokaryotes can be compared to the evolutionary processes occurred in extremophiles in order to adapt to their native inhospitable environments. In the present thesis, the attempt has been made to understand the role of membrane constituents other than common phospholipids in the adaptation process. In particular, the glycolipid portion composing the Outer Membrane of Gram-negative bacteria has been studied, both in the case of obliged extremophiles and in mesophilic microrganisms suitable for life in extreme conditions. The results described point out interesting features to which the capability of thriving in harsh habitats can be related. In our opinion, in particular, it has been demonstrated that the response charging the Outer Membrane constituents is strictly dependent on the nature of the stressing events, and the molecular features characterizing glycolipids from extremophiles are highly specific on the basis of the isolation environment. As discussed in section 3, for instance, Marine Bacteria must develop contemporaneous resistance to several parameters typifying the marine environment. Marine bacteria described in the present work are all barophilic and psychrofilic, with a variable halophilic character. Due to the similar nature of their isolation environment, we can suppose that they have reacted in a comparable way to environmental conditions, in order to retain the correct cell physiology. The LPSs from *Alteromonas addita* KMM 3600[T], *Shewanella pacifica* KMM 3601[T] and *Pseudoalteromonas issachenkonii* KMM 3549 have been described. A comparison between the structures reported suggests the idea that bacteria accustomized to marine environments provide the outer membrane with molecules with uncommon negative charge density, adapted during evolution in order to provide optimal protection of the cell. In particular, in case of rough strains, producing only Lipooligosaccharides, the enhancement of the cation binding capacity of the membrane may have been achieved through the constitutive shortening of the oligosaccharide chains and the addition of anionic decorations of both

glycidic and non-glycidic nature. When the bacterium constitutively produces S-LPS molecules, a similar trend is observed in the O-chain structure, as in case of *Pseudoalteromonas issachenkonii*, where charged groups are integrated in the repeating unit structure as acidic monosaccharides, conferring to the molecule an anionic character. Such structural features increase the capability of binding environmental cations (Ca^{+2} and Mg^{+2}), by which the molecules overcome the electrostatic repulsion that would otherwise arise among them. In the same way, charged glycolipids can organize themselves in a rigid net of cross-linkages through the metallic ions, providing higher resistance to physical stressors. This effect is in our opinion closely related to barophily, thus to mechanical pressures acting on the cell. Halophily may reflect in the enhancement of water retention in the immediate surrounding of the cell, as a reaction to the osmotic pressure generating between the cytoplasm and the external sea environment. The salt content in the different cell compartments may be modulated by the creation of a microenvironment around the cell with an increased water attraction capability due to charged groups, confirming the trend already outlined for glycolipids within the cytoplasmic membrane.

A further consideration deals with fatty acids composition of the Lipid A moieties characterized so far. Comparing them to the Lipid A from enterobacteriaceae, a preference is evident for shorter acyl chains [10:0(3-OH); 12:0(3-OH); 13:0(3-OH)]. It has been observed (section 1.2.2) that shortening of the fatty acids occurs in cold stressed mesophilic bacteria.

Evolutionary adaptation in obliged psycrophiles may have led to similar stratagems in membrane glycolipids, bringing to the preference for structures more suitable to counterbalance the freezing effects of cold on long chain fatty acids. Shorter lipids realizes less Van der Waals interaction between the chains, preserving the physiological fluidity of the Outer Membrane.

The response of thermophiles bacteria to the specific requisite imposed by their isolation environment results in modifications that appear quite far from the ones observed in marine bacteria. The need of a reinforcement of the chemical structure of the glycolipids composing the membrane seems to be the most striking requirement imposed by elevated temperatures. In this direction, bacteria evolutionary adapted to heat may have developed peculiar structure for their glycolipids, characterized by the replacement of the typical ester linkages occurring between fatty acids and glycerol in glycerophospholipids and glucosamines in Lipid A with more stable alkyl chains, as in the case of the octadecane-1,2-diol present in the main glycolipid from *Thermus thermophilus*. This consideration is also in agreement with previous findings of ether linked glycolipids in thermophiles bacteria (see section 4), where the general

tendency to the strengthening of the primary structure of membrane constituents is respected. Such modifications are unique also respect to the other structures presented reported for marine and organic tolerant bacteria.

In this latter case, the lethal consequences of organic solvents exposure are counterbalanced by structural features resembling the ones encountered in marine bacteria. The two microrganisms analysed, belonging to this category, offer the further opportunity of comparing the molecular features developed in correspondence of the stress events and in normal growth conditions. The effect of organic molecules on membranes assembly has been discussed in section 1.2.5. A tighter packing of the membrane can be a device for blocking their disrupting action and, as already observed for marine bacteria, this can be achieved by introducing a higher negative charge density in the outer layer of the membrane itself. This condition can be satisfied by the LPS molecules spontaneously synthesized by *Acinetobacter radioresistens*, given the anionic character of the O-polysaccharide produced and the occurrence of the Kdo trisaccharide in the Core region. Such a situation does not occur for routinely growth cells of *Pseudomonas* sp. OX1, since the O-chain produced by the bacterium in such conditions is composed only by neutral monosaccharides. Thus, in our opinion, mechanisms may act by blocking the biosynthesis of this moiety in correspondence of the exposure to the aromatics, favouring the expression of molecules more suitable to confer a rigid packing to the membrane. Thus, the introduction of the pyruvic acid ketals would act either by blocking the elongation of the polysaccharide and by increasing the total number of negative charges to better protect the cell.

Acinetobacter radioresistens and *Pseudomonas* sp. OX1 are both skilled with metabolic capacity towards the aromatics. The hypothesis may be advanced that the entrance of these substrates within the cell can be regulated by creating a less hydrophilic environment in the membrane itself.

7

Materials and Methods

7.1 Cell culture

7.1.1 Marine bacteria

Cells of *Shewanella pacifica* KMM 3601, KMM 3605, KMM 3772, *Alteromonas addita* KMM 3600[T] and *Pseudoalteromonas issachenkonii* KMM 3549[T] were cultivated on a liquid medium containing glucose (1g/L), pepton (5g/L), yeast extract (2.5g/L), K_2HPO_4 (0.2g/L), $MgSO_4$ (0.05g/L), sea water (750 ml), and distilled water (250 ml). Cells were collected by centrifugation, washed with water and next dried with acetone (three times) obtaining among 5 and 12 g of dried cells from 20 L of the cultural fluid.

7.1.2 Thermophile bacteria

Thermus thermophilus Samu-SA1 (DSM 15284, ATTC BAA-951) and *Geobacillus thermoleovorans* strain Fango (ATCC BAA-872) were grown at 75°C and 70°C, respectively, in a 50 l fermenter (Biostat-D, Braun) with a mechanical agitation of 100 rpm and an aeration flux of 56%. Growth was followed turbidimetrically at 540 nm. For *T. thermophilus,* The standard culture medium (TH medium) contained: (gr/L) peptone (Oxoid) 8.0, yeast extract (Oxoid) 4.0, NaCl 2.0 at pH 7.0. For *G.thermoleovorans,* the standard culture medium (YN medium) contained: (gr/L) yeast extract (Oxoid) 6.0, NaCl 2.0; pH 6.8.

Cells were harvested in the stationary phase of growth by continuous-flow centrifugation.

7.1.3 Organic Solvent Tolerant Bacteria

In the case of *Pseudomonas* sp. OX1, culture with phenol were performed as it follows: cells were routinely grown on M9-agar plates supplemented with 10 mM malic acid as the sole carbon source, at 27°C. For growth in liquid medium a single colony from a fresh plate was inoculated in 1 mL of the medium and grown 18 h at 27°C under constant shaking. This saturated culture was used to inoculate 100 mL of the same medium and grown at 27°C up to about 1 OD_{600}. Final growth was started by inoculating the appropriate volume of the latter

culture into 1 L of fresh medium to 0.02 OD_{600}. Cells were grown at 27°C, until $OD_{600} = 1$ was reached and recovered by centrifugation at 3,000 x g, for 15 min, at 4°C, washed with an isotonic buffer and lyophilized. Growth was carried out in M9 salt medium supplemented with 4 mM phenol, as the sole carbon and energy source.

Cells cultured in rich medium were routinely grown in liquid Luria-Bertani medium, at 27°C for 10 h up to about 1 OD_{600} /mL. Cells were recovered by centrifugation (6,000 rpm, 15 min, 4°C), washed with water and lyophilised.

Acinetobacter radioresistens S13 was cultured in the Sokol and Howell minimal medium (Sokol and Howell, 1981) supplemented with phenol (400 mg/L), benzoate (400 mg/L), or acetate (400 mg/L) as sole carbon source.

7.2 Glycolipids extraction and purification

For extraction of LOSs, dried cells were extracted three times with a mixture of aqueous 90% phenol/chloroform/petroleum ether (2:5:8 v/v/v, 10 mL / g dry cells) as described (Galanos *et al.,* 1969). After removal of the organic solvents under vacuum, the LOS fraction was precipitated from phenol with water, washed first with aqueous 80% phenol, and then three times with cold acetone, each time centrifuged, and lyophilized.

LPS, Teichoic acids and Glycolipids extraction was subsequently performed extracting the cells thrice with 45% aqueous phenol at 68°C (20 mL/g dry cells), according to the conventional hot phenol-water procedure (Westphal and Jann, 1965). The water and the diluted phenol phase were dialysed against water (3.500 kDa molecular weight cut-off). After dialysis, the extract was centrifuged (8000 x g) and lyophilised. The extracts were digested with DNase, RNase and Proteinase K, dialysed and freeze-dried.

Sodium dodecyl sulfate polyacrylamide gel electrophoresis (SDS-PAGE) was performed as described on all the fraction obtained. For detection of LPS and LOS, 12%-polyacrylamide gels were stained with silver nitrate according to the described procedure. (Kittelberger and Hilbink, 1993).

Silica gel purification of the glycolipid extract from *Thermus thermophilus* Samu-Sa1 was performed as described (Leone *et al.,* 2006). In general, the glycolipid blend was performed

on Silica-gel (Merk, 230-400 mesh) eluted with $CHCl_3$:MeOH (9:1 to 1:1, by vol.) and the fraction collected were monitored by TLC, developed with $CHCl_3$:MeOH:H_2O (65:25:4, by vol.) and visualized with 0.1% $Ce(SO_4)_2 \cdot 4H_2O$, 5% $(NH_4)_6Mo_7O_{24} \cdot 4H_2O$ in 5.8 % v/v H_2SO_4.

Chromatographic purification of *Geobacillus thermoleovorans* Fango Teichoic Acids was achieved as described (Leone *et al.*, 2006). Purification of **TA1** (20 mg after purification) was achieved with a column of Sephacryl S-400 (1.5 cm x 96 cm, Amersham) in 25 mM NH_4HCO_3 buffer, whereas **TA2** (5 mg) was purified by HPLC on a column of TSK G-5000 (7.8mm x 30 cm, Tosoh Bioscience) in 20 mM NH_4OAc buffer (pH 4.7), and monitored with an UV detector at 220 nm and for the phosphate content.

7.3 Monosaccharide and Fatty Acid analyses

Monosaccharide analyses were realised by means of GC-MS of acetylated *O*-methyl glycosides derivatives, obtained after methanolysis (2M HCl/MeOH, 85°C, 24 h) and acetylation with acetic anhydride in pyridine (85°C, 30 min). The absolute configuration of the monosaccharides was obtained according to the published method (Leontein and Lönngren, 1978).

Methylation analysis was performed using the modified Hakomori procedure (Hakomori, 1964) by Ciucanu and Kerek (Ciucanu and Kerek, 1984). After chloroform/water extraction, the organic phase was evaporated and hydrolysed with 4 M trifluoroacetic acid (100°C, 3h), carbonyl reduced with $NaBD_4$, acetylated with acetic anhydride: pyridine (1:1, v/v) and analysed by GC-MS.

For LOS oligosaccharides, methylation analysis of Kdo region was achieved by carboxy-methylation with methanolic HCl (0.1 M, 5 min) and then with diazomethane to improve LOS solubility in DMSO. Methylation was carried out as described above. LOS was hydrolyzed with 2 M trifluoroacetic acid (100°C, 1 h), carbonyl-reduced with $NaBD_4$, carboxy-methylated as described above, carboxyl-reduced with $NaBD_4$ (4°C, 18 h), acetylated and analyzed by GC-MS.

For identification of octadecane-1,2-diol, heptadecane-1-amine and N-glyceroyl-heptadecane-1-amine in *Thermus thermophilus* Samu-Sa1, trimethylsililation was achieved treating the sample with bis(trimethylsilyl)trifluoroacetamide, 60°C, 30 min, followed by vacuum centrifugation.

Fatty Acids were revealed as their Methyl Esters derivatives. Total fatty acids content was determined after strong hydrolysis of Lipid A, first with 4 M HCl (100°C, 4 h) and subsequently with 5 M NaOH (100°C, 30 min). Fatty acids were then extracted with chloroform, methylated with diazomethane and analysed by GC-MS. Ester bound fatty acids were analysed after selective alkaline hydrolysis with 0.5 M NaOH/ MeOH (1:1 v/v, 85°C, 2 h). After acidification and extraction with chloroform, fatty acids were methylated with diazomethane and analysed by GC-MS. Absolute configurations of fatty acids were determined as described (Rietschel, 1976).

7.4 Isolation of Lipid A, Oligosaccharides and Polysaccharides

In order to obtain phosphorylated oligosaccharides, aliquots of LOSs were dissolved in anhydrous hydrazine (1 ml/ 20 mg sample), stirred at 37°C for 90 min, cooled, poured into ice-cold acetone (10 ml/ml Hydrazine), and allowed to precipitate. The precipitate was then centrifuged (3000 × g, 30 min), washed twice with ice-cold acetone, dried, dissolved in water and lyophilized.

This material was eventually *N*-deacylated with 4 M KOH as described (Holst, 2000). Salts were removed using a Sephadex G-10 (Pharmacia) column (50 × 1.5 cm). The resulting oligosaccharides constitute the complete carbohydrate backbone of the Lipid A-core region.

Other aliquots of LOSs were hydrolyzed in 1% acetic acid (100°C, 2h). LPSs underwent the same treatment to yield Polysaccharides. After this procedure, the precipitates (Lipid A) were removed by centrifugation (8000 × g, 30 min). The supernatant were separated by gel-permeation chromatography on a P-2 column (85 × 1.5 cm) for oligosaccharides and on a Sephacryl S-400 for polysaccharides.

7.5 Smith degradation

In order to perform the degradation of the O-chain from *Pseudomonas* sp. OX1 growth in rich medium, an aliquot of the polysaccharide (20 mg) was dissolved in 2 ml H_2O to which 5 ml of 0.5 M $NaIO_4$ solution were added. The oxidation was conducted for 72 h at 4°C, and subsequently quenched with 26 μl of ethylene glycol. The sample (pH 7) was then reduced with 30 mg $NaBH_4$, 2 h, room temperature. The excess of hydride was neutralized with drops of concentrated HCl and the sample was desalted on a Sephadex G-10 column. The fraction eluted in the void volume was then recollected and hydrolyzed with 6% AcOH (2 ml), 2 h,

164

100°C. Subsequently, the sample was separated by gel-permeation chromatography on a TSK HW-40 column.

7.6 Preparation of the Mosher ester derivatives from Kdo8N

In order to determine the absolute configuration of Kdo8N, an aliquot of LOS (10 mg) was de-phosphorylated with 300 μl 48% aq. HF, 3 h, room temperature. The sample was then dried and washed three times with water. Methanolysis was performed with 1 M MeOH/HCl, 3 h, 85°C. After washing with methanol, the sample underwent *N*-acetylation with 50 μl Acetic anhydride in 100 μl pyridine and 500 μl methanol, 2 h, 40°C. After lyofilization, the sample was *O*-deacetylated with aqueous 33% NH$_4$OH, 16 h, room temperature. The sample obtained was separated by reverse phase HPLC on a Supelco C-18 column eluted with water.

7.7 MS analyses of glycolipids

MALDI-TOF mass spectra were recorded in the negative and positive polarity in linear mode on a Perseptive (Framingham, MA, USA) Voyager STR equipped with delayed extraction technology. Ions formed by a pulsed UV laser beam (nitrogen laser, λ = 337 nm) were accelerated by 24 kV. The mass spectra reported are the result of 256 laser shots. Resolution was about 1500.

The Lipid A samples were dissolved in CHCl$_3$/CH$_3$OH (50:50, v/v) at a concentration of about 25 pmol/μL. The matrix solution was prepared by dissolving 2,4,6-trihydroxyacetophenone (THAP) in CH$_3$OH/0.1% trifluoroacetic acid/CH$_3$CN (7:2:1, v/v) at a concentration of 75 mg/mL. A sample/matrix solution mixture (1:1, v/v) was deposited (1 μL) onto a stainless-steel gold-plated 100-sample MALDI probe tip, and left to dry at room temperature.

The LOSs and the *O*-deacylated LOSs were prepared as recently reported (Sturiale *et al.,* 2005). Briefly, a small amount of LOS was first suspended in a mixture of methanol/water (1:1) containing 5mM ethylenediaminetetraacetic acid (EDTA) and allowed to dissolve by a brief ultrasonication. A few microliters of the obtained mixture were then desalted on a small piece of Parafilm^{TM} with some grains of cation-exchange beads (Dowex 50WX8-200, Sigma–Aldrich), previously converted into the ammonium form; 0.3 μL of this sample solution was finally deposited, together with the same volume of 20 mM dibasic ammonium citrate, in a thin layer of homogeneous matrix film obtained from a solution whose components were

2,4,6-trihydroxyacetophenone (THAP), 200 mg/mL in methanol, and nitrocellulose (Trans-blot membrane, BioRad), 15mg/mL in acetone/propan-2-ol (1:1 v/v), mixed in a 4:1 v/v ratio.

For the MS analysis of the glycolipid extract from *Thermus thermophilus* Samu-Sa1, Fourier-transform mass spectrometry was performed in the negative and positive ion modes using an APEX II – Instrument (Bruker Daltonics, Billerica, MA, USA) equipped with an actively shielded 7 Tesla magnet and an (nano) ESI source. Mass spectra were acquired using standard experimental sequences as provided by the manufacturer. For the negative ion spectra samples (~ 10 ng·µl^{-1}) were dissolved in a 50:50:0.001 (v/v/v) mixture of 2-propanol, water, and triethylamine. For the positive ion mode 50:50:0.03 (v/v/v) mixture of 2-propanol, water, 30mM ammonium acetate adjusted with acetic acid to pH 4.5 was used. The samples were sprayed at a flow rate of 2 µL·min^{-1}. Capillary entrance voltage was set to 3.8 kV, and drying gas temperature to 150°C. The spectra shown are charge-deconvoluted, using the xmass-6.1 software, and mass numbers given refer to the monoisotopic molecular masses.

7.6 NMR analyses on Glycolipids

1D and 2D ^{1}H-NMR spectra on oligo-/polysaccharides were recorded on solutions of 6 mg in 0.6 mL D$_2$O. Spectra on the O-polysaccharide from *Pseudoalteromonas issachenkonii* KMM 3549^T were recorded dissolving the sample in 600µL H$_2$O/D$_2$O 9:1, by vol. All the spectra were calibrated with internal acetone [δ_H 2.225, δ_C 31.45]. Aqueous 85% phosphoric acid was used as external reference (0.00 ppm) for ^{31}P NMR spectroscopy.

Spectroscopic analyses on *Thermus thermophilus* Samu-Sa1 glycolipids were carried out in a solution of MeOD:CDCl$_3$ (2:1, by vol.) at 25°C. Spectra were calibrated with internal methanol (δ_H 3.300, δ_C 49.5). ^{1}H- and ^{13}C-NMR experiments were carried out using a Varian Inova 500 or a Bruker DRX-600 equipped with a cryogenic probe. For ^{31}P NMR spectra a Bruker DRX-400 spectrometer was used. Rotating frame Overhauser enhancement spectroscopy (ROESY) was measured using data sets (t1 · t2) of 4096 · 1024 points, and 16 scans were acquired. A mixing time of 200 ms was used. Double quantum-filtered phase-sensitive COSY experiments were performed with 0.258 s acquisition time, using data sets of 4096 · 1024 points, and 64 scans were acquired. Total correlation spectroscopy experiments (TOCSY) were performed with a spinlock time of 100 ms, using data sets (t1 · t2) of 4096 · 1024 points, and 16 scans were acquired. In all homonuclear experiments the data matrix was zero-filled in the F1 dimension to give a matrix of 4096 · 2048 points and was resolution

enhanced in both dimensions by a shifted sine-bell function before Fourier transformation. Coupling constants were determined on a first-order basis from 2D phase sensitive double quantum filtered correlation spectroscopy (DQF-COSY) (Piantini, *et al.*, 1982; Rance *et al.*, 1983). Heteronuclear single quantum coherence (HSQC) and heteronuclear multiple bond correlation (HMBC) experiments were measured in the ^{1}H-detected mode via single quantum coherence with proton decoupling in the ^{13}C domain, using data sets of $2048 \cdot 512$ points, and 64 scans were acquired for each t1 value. Experiments were carried out in the phase-sensitive mode according to the described method (States *et al.*, 1982). A 60 ms delay was used for the evolution of long-range connectivity in the HMBC experiment. In all heteronuclear experiments the data matrix was extended to $2048 \cdot 1024$ points using forward linear prediction extrapolation (de Beer and van Ormondt, 1992; Hoch and Stern, 1996).

References

Adams, M.W.W. 1993. Enzymes and proteins from organisms that grow near and above 100°C. *Annu. Rev. Microbiol.* **47**. 627-358.

Adinolfi, M.; De Castro, C.; Iadonisi, A.; Lanzetta, R. and Molinaro, A. 1998. Applicability of the Mosher MPTA-ester methodology to monosaccharides. *J. Carbohydr. Chem.* **17**. 987-992.

Akira, S.; Uematsu, S. and Takeuchi, O. 2006. Pathogen recognition and innate immunity. *Cell.***124**. 783-801.

Alexander, C. and Rietschel, E.Th. 2001. Bacterial lipopolysaccharides and innate immunity. *J. Endotoxin Res*. **7.** 167-202.

Allen, E.E.; Facciotti, D. and Bartlett, H.H. 1999. Monounsaturated but not polyunsaturated fatty acids are required for growth at high pressure and low temperature in the deep-sea bacterium *Photobacterium profundum* strain SS9. *Appl. Environ. Microbiol.* **65**. 1710-1720.

Antranikian, G., Vorgias C.E. and Bertoldo, C. 2005. Extreme environments as a resource for microorganisms and novel biocatalysts. *Adv Biochem Eng Biotechnol.* **96**. 219-62.

Araki, I. and Ito, E. 1989. linkage units in cell walls of Gram-positive bacteria. *CRC Crit. Rev. Microbiol.* **17**. 121-135.

Archibald, A.R.; Baddiley, J. and Blumson, N.L. 1968. The teichoic acids. *Adv. Enzymol. Relat. Areas Mol. Biol.* **30**. 223-253.

Arenghi, F.L.; Berlanda, D.; Galli, E.; Sello G. and Barbieri, P. 2001. Organization and regulation of meta cleavage pathway genes for toluene and o-xylene derivative degradation in *Pseudomonas stutzeri* OX1. *Appl Environ Microbiol.* **67.** 3304-3308.

Auzanneau, F.I.; Charon, D. and Szabò, L. 1988. Synthesis of 1,5 lactones of 3-deoxy-D-manno-2-octulopyranosonic acid. *Carbohydr. Res*. **179**. 125-136.

Baggi, G.; Barbieri, P.; Galli, E. and Tollari, S. 1987. Isolation of a *Pseudomonas stutzeri* strain that degrades o-xylene. *Appl Environ Microbiol.* **53**. 2129-2132.

Bartlett, D.H. 2002. Pressure effects on in vivo microbial processes. *Biochem. Biophys. Acta.* **1595**. 367-381.

Bartlett, D.H.; Kato, C. and Horikoshi, K. 1995. High pressure influences on gene and protein expression. *Res. Microbiol.* **146**. 697-706.

Baumann, L.; Baumann, P.; Mandel, M. And Allen, R. D. 1972. *Taxonomy* of aerobic marine eubacteria. *J. Bacteriol*. **110**. 402-429.

Baxter, R.M. and Gibbons, N.E. 1956. Effects of sodium and potassium chloride on certain enzymes of *Micrococcus halodenitrificans* and *Pseudomonas salinaria. Can. J. Microbiol.* **2**. 599-606.

References

Beckmann, F.; Moll, H.; Jager, K.E. and Zähringer, U. 1995. Preliminary communication 7-*O*-carbamoyl-L-*glycero*-D-*manno*-heptose: a new core constituent in the lipopolysaccharide of *Pseudomonas aeruginosa. Carbohydr. Res.* **267.** C3-C7.

Bertoni, G.; Martino, M.; Galli, E. and Barbieri, P. 1998. Analysis of the gene cluster encoding toluene/o-xylene monooxygenase from *Pseudomonas stutzeri* OX1. *Appl Environ Microbiol.* **64.** 3626-3632.

Birnbaum, G.I.; Roy, R.; Brisson, J.R. and Jennings, H.J. 1987. Conformations of ammonium 3-deoxy-D-manno-2-octulosonate (Kdo) and α- and β-ketopyranosides of Kdo: X-ray structure and ^{1}H NMR analyses. *J. Carbohydr. Chem.* **6**. 17–39.

Bock, K.; Vinogradov, E.; Holst, O. and Brade, H. 1994. Isolation and structural analysis of oligosaccharide phosphates containing the complete carbohydrate chain of the lipopolysaccharide from Vibrio cholerae strain H11 (non-O1). *Eur. J. Biochem.* **225**. 1029-1039.

Brock, T.D. 1967. Micro-organisms adapted to high temperatures. *Science*. **214**. 282-285.

Brock, T.D. ed .1978. Thermophilic microorganisms and life at high temperatures, 72-91. Springer-Verlag, New York, N.Y.

Bubb, W.A. 2003. NMR spectroscopy in the study of carbohydrates: characterizing the structural complexity, *Concepts Magn. Reson.* Part A. **19**. 1-19.

Bystrova, O.V. ; Shashkov, A.S. ; Kocharova, N.A. ; Knirel, Y.A. ; Lindner, B. ; Zähringer, U. and Pier, G. 2002. Structural studies on the core and the O-polysaccharide repeating unit of *Pseudomonas aeruginosa* immunotype 1 lipopolysaccharide. *Eur. J.Biochem.* **269**. 2194-2203.

Bystrova, O.V.; Shashkov, A.S.; Kocharova, N.A.; Knirel, Y.A.; Zähringer, U. and Pier, G. 2003. Elucidation of the structure of the lipopolysaccharide core and the linkage between the core and the O-antigen in *Pseudomonas aeruginosa* immunotype 5 using strong alkaline degradation of the lipopolysaccharide. *Biochemistry(Moscow)* **68**. 918-925.

Cafaro, V.; Scognamiglio, R.; Viggiani, A.; Izzo, V.; Passaro, I.; Notomista, E.; Piaz, F.D.; Amoresano, A.; Casbarra, A.; Pucci, P. and Di Donato, A. 2002. Expression and purification of the recombinant subunits of toluene/*o*-xylene monooxygenase and reconstitution of the active complex. *Eur. J. Biochem.* **69**. 5689-99.

Carty, S.M.; Sreekumar, K.R. and Raetz, C.R. 1999. Effect of cold shock on lipid A biosynthesis in *Escherichia coli*. Induction At 12 degrees C of an acyltransferase specific for palmitoleoyl-acyl carrier protein. *J. Biol. Chem.* **274**. 9677-9685.

Cescutti, P.; Osman, S.F.; Fett, W.P. and Weisleder, D. 1995. The structure of the acidic exopolysaccharide produced by *Pseudomonas "gingeri"* strain Pf9. *Carbohydr. Res*. **275**. 371–379.

Cescutti, P.; Toffanin, R.; Polesello, P and Sutherland, I.W. 1999. Structural determination of the acidic exopolysaccharide produced by a *Pseudomonas* sp. strain 1.15. *Carbohydr. Res*. **315**. 159–168.

Chang, E.L. 1994. Unusual thermal stability of liposomes made from bipolar tetraether lipids. *Biochem. Biophys. Res. Commun*. **202**. 673-679.

Chintalapati, S.; Kiran, M.D. and Shivaji, S. 2004. Role of membrane lipid fatty acids in cold adaptation. *Cell. Mol. Biol.* **50**. 631-642.

Choquet, C.G.; Patel, G.B.; Beveridge, T.J. and Sprott, G. 1994. Stability of pressure-extruded liposomes made from archaeobacterial ether lipids. *Appl. Microbiol. Biotechnol*. **42**. 375-384.

Ciucanu, I. and Kerek, F. 1984. A simple and rapid method for the permethylation of carbohydrates. *Carbohyd. Res*. **131**. 209-217.

Coleman Jr, W.G. 1983. The *rfaD* gene codes for L-*glycero*-D-*manno*-heptose-6-epimerase: an enzyme for lipoplysaccharide core biosynthesis. *J. Biol. Chem.* **258**. 1985-1990.

da Costa, M. S. and Rainey, F. A. 2001. Family I. *Thermaceae* fam. nov. In Boone, D.R., Castenholz, R.W. and Garrity, G.M. (eds.) *Bergey's Manual of Systematic Bacteriology*, 2nd edn, vol. 1, *The Archaea and the Deeply Branching and Phototrophic Bacteria*. Springer, New York. 403–404.

Dale, J.A. and Mosher, H.S. 1973. Nuclear magnetic resonance enantiomer regents. Configurational correlations via nuclear magnetic resonance chemical shifts of diastereomeric mandelate, O-methylmandelate, and .alpha.-methoxy-.alpha.-trifluoromethylphenylacetate (MTPA) esters. *J. Am. Chem. Soc*. **95**. 512

D'Amico, S.; Collins, T.; Marx, J.C.; Feller, G. and Gerday, C. 2006. Psychrophilic microorganisms: challenges for life. *EMBO Rep.* **7**. 385-389.

Danson, M.J.; Hough, D.W. and Lunt, G.G. 1992. The archaeabacteria: biochemistry and biotecnology. Portland press. London.

de Beer, R. and van Ormondt, D. 1992. Analysis of NMR data using time domain fitting procedures. *NMR Basic Princ. Prog*. **26**. 201.

De Rosa, M.; Gambacorta, A.; Huber, R.; Lanzotti, V.; Nicolaus, B.; Stetter, K.O. and Trincone, A. 1989. In da Costa, M.S., Duarte, J.C. and Williams, R.A.D. (Eds), *Microbiology of estreme environments and its potential for biotechnology*. Elsevier, London, England, 167-173.

De Rosa, M.; Trincone, A.; Nicolaus, B. and Gambacorta, A. 1991. Archaeabacteria: lipids, membrane structures, and adaptations to environmental stresses. In: di Prisco, G. (ed.) Life under extreme conditions. Springer. Berlin Heidelberg New York. 61-87.

de Vos, W.M. 2005. Lipotechoic acid in lactobacilli: D-alanine makes the difference *Proc. Natl. Acad. Sci. USA,* **102**. 10763-10764.

De Vrij, W.; Bulthuis, R.A. and Konings, W.N. 1988 Comparative study of energy-transducing properties of cytoplasmic membranes from mesophilic and thermophilic *Bacillus* species. *J. Bacteriol*. **170**. 2359-2366.

Ding, L.; Seto, B.L., Ahmed, S.A. and Coleman, W.G. 1994. Purification and properties of the *Escherichia coli* K12 NAD-dependant nucleotide diphosphosugar epimerase, ADP-L-*glycero*-L-*manno*-6-epimerase. *J. Biol. Chem.* **269.** 24384-24390.

References

Domon, B. and Costello, C.E. 1988. Structure elucidation of glycosphingolipids and gangliosides using high-performance tandem mass spectrometry. *Glycoconjugate J.,* **5.** 397-409.

Driscoll, D.A.; Jonas, J. and Jonas, A. 1991. High pressure ^{2}H nuclear magnetic resonance study of the gel phases of dipalmitoyl-phosphatidylcholine. *Chem. Phys. Lipids.* **58**. 97-104.

Fisher**,** W. In *Handbook of Lipid Research*; Plenum Press: New York, 1990; Series Donald J. Hanahan; Vol. 6, pp.123-234.

Galanos, C.; Lüderitz, O. and Westphal, O. 1969. A new method for the extraction of R lipopolysaccharides. *Eur. J. Biochem.* **9**. 245-249.

Garegg, P.J.; Jansson, P. E.; Lindberg, B.; Lindh, F. and Lonngren, J. 1980. Configuration of the acetal carbon atom of pyruvic acid acetals in some bacterial polysaccharides. *Carbohydr. Res.* **78**. 127–132.

Gauthier, G.; Gauthier, M. and Christen, R. 1995. Phylogenetic analysis of the genera Alteromonas, Shewanella, and Moritella using genes coding for small-subunit rRNA sequences and division of the genus Alteromonas into two genera, Alteromonas (emended) and Pseudoalteromonas gen. nov., and proposal of twelve new species combinations. *Int. J. Syst. Bacteriol.* **45**. 755-761.

Gerner-Smidt, P. 1992. Ribotyping of the *Acinetobacter calcoaceticus-Acinetobacter baumannii* complex. *J. Clin. Microbiol.* **30**. 2680-2685.

Gibson, B.W.; Engstrom, J.J.; Hines, C.M.W. and Falick, A.M. 1997. Characterization of bacterial lipooligosaccharides by delayed extraction matrix-assisted laser desorption ionization time-of-flight mass spectrometry. *J. Am. Soc. Mass Spectrom.* **8.** 645-658.

Gilbert, J.A.; Hill, P.J.; Dodd, C.E. and Laybourn-Parry, J. 2004. Demonstration of antifreeze protein activity in Antarctic lake bacteria. *Microbiology.* **150**. 171-180.

Goel, V.K. and Kapil, A. 2001. Monoclonal antibodies against the iron regulated outer membrane proteins of *Acinetobacter baumannii* are bactericidal. *BMC Microbiol.* **1**. 16-24.

Gorshkova, R.P.; Nazarenko, E.L.; Zubkov, V.A.; Ivanova, E.P.; Ovdov, Y.S.; Shashkov, A.S. and Knirel, Y.A. 1993. Structure of the repeating link of the acid polysaccharide of Alteromonas haloplanktis KMM 156. *Bioorg. Khim.* **19**. 327-336.

Gulik, A.; Luzzati, V.; De Rosa, M. and Gambacorta, A. 1985. Structure and polymorphism of bipolar isopranyl ether lipids from archaebacteria. *J. Mol. Biol.* **182**. 131-149.

Haeffner-Cavaillon, N.; Cavaillon, J.M.; Moreau, M. and Szabo L. 1984. Interleukin 1 secretion by human monocytes stimulated by the isolated polysaccharide region of the Bordetella pertussis endotoxin. *Mol. Immunol.* **21**. 389-395.

Hakomori, S. 1964. A rapid permethylation of glycolipid, and polysaccharide catalyzed by methylsulfinyl carbanion in dimethylsulfoxide. *J. Biochem. (Tokio).* **55**. 205-208.

Hancock, I.C. and Baddiley, J. 1985- Biosynthesis of the bacterial envelope polymers teichoic acid and teichuronic acid. In: Martonosi, A.N. (ed.) The enzymes of biological membranes, vol. 2. Plenum. New York. 279-307

Hanniffy, O.M.; Shashkov, A.S.; Senchenkova, S.Y.N.; Tomshich, S.V.; Komandrova, R.A.; Romanenko, L.A.; Knirel, Y.A. and Savage, A.V. 1998. Structure of a highly acidic *O*-specific polysaccharide of lipopolysaccharide of *Pseudoalteromonas haloplanktis* KMM 223 (44-1) containing L-iduronic acid and D-QuiNHb4NHb. *Carbohydr. Res.* **307**. 291-298.

Hanniffy, O.M.; Shashkov, A.S.; Senchenkova, S.Y.N.; Tomshich, S.V.; Komandrova, R.A.; Romanenko, L.A.; Knirel, Y.A. and Savage, A.V. 1999. Chemical structure of a polysaccharide from Campylobacter jejuni 176.83 (serotype O:41) containing only furanose sugars. *Carbohydr. Res.* **321**. 132-138.

Head, I.M.; Jones, D.M.; Roling, W.F. 2006. Marine microrganisms make a meal of oil. *Nat. Rev. Microbiol.* **4**. 173-182.

Hart, D.J. and Vreeland, R.H. 1988.Changes in the Hydrophilic-hydrophobic cell surface character of *Halomonas elongate* in response to NaCl. *J. Bacteriol.* **37**. 345-350.

Hoch, J.C. and Stern, A.S. 1996. In Hoch, J.C. and Stern, A.S. (Eds.) *NMR data processing.* Wiley Inc. New York. 77-101.

Holst, O. 1999. Chemical structure of the Core Region of Lipopolysaccharides. In: Brade, H.; Morrsion, D.C.; Opal, S. and Vogel, S. (eds.) Endotoxin in Health and Disease. Marcel Dekker Inc., New York, NY. 115-154.

Holst, O. 2000. In *Methods in Molecular Biology, Bacterial Toxins: Methods and Protocols* (Holst, O., ed). Humana Press Inc., Totowa, NJ. 345-353.

Holst, O.; Bock, K.; Brade, L. and Brade, H. 1995. The structures of oligosaccharide bisphosphates isolated from the lipopolysaccharide of a recombinant Escherichia coli strain expressing the gene gseA [3-deoxy-D-manno-octulopyranosonic acid (Kdo) transferase] of Chlamydia psittaci 6BC. *Eur. J. Biochem.* **229**. 194-200.

Holst, O.; Thomas-Oates, J.E. and Brade, H. 1994. Preparation and structural analysis of oligosaccharide monophosphates obtained from the lipopolysaccharide of recombinant strains of *Salmonella minnesota* and *Escherichia coli* expressing the genus-specific epitope of Chlamydia lipopolysaccharide. *Eur. J. Biochem.* **222.** 183–194.

Horikoshi, K. 1998. Barophiles: deep-sea microrganisms adapted to an extreme environment. *Curr. Op. Microbiol.* **1**. 291-295.

Huang, Y. and Anderson, R. 1989. Structure of a novel glucosamine-containing phosphoglycolipid from *Deinococcus radiodurans*. *J. Biol. Chem.* **264**. 18667-18672.

Huang, Y. and Anderson, R. 1992. Fatty acids are precursor of alkylamines in *Deinococcus radiodurans*. *J. Bacteriol*. **174**. 7168-7173.

Huber, R.; Wilharm, T.; Huber, D.; Trincone, A.; Burggraf, S.; Konig, H.; Rachel, R.; Rockinger, I.; Fricke, H. and Stetter, K. O. 1992. *Aquifex pyrophilus* gen nov., sp. nov., represents a novel group of marine hyperthermophilic hydrogen-oxidizing bacteria. *Syst. Appl. Microbiol*. **15**. 340-351.

Ingram, L.O. 1976. Adaptation of membrane lipids to alcohols. *J. Bacteriol.* **125**. 670-678.

References

Ingram, L.O. 1977. Changes in lipid composition of *Escherichia coli* resulting from growth with organic solvents and with food additives. *Appl. Environ. Microbiol.* **33**. 1233-1236.

Isken, S. and de Bont, J.A.M. 1998. Bacteria tolerant to organic solvents. *Extremophiles*. **2**. 229-238.

Ivanova E.P.; Bowman, J.P.; Lysenko, A.M.; Zhukova, N.V.; Gorshkova, N.M.; Sergeev, A.F. and Mikhailov, V.V. 2005. Alteromonas addita sp. nov. *Int. J. Syst. Evol. Microbiol.* **55**. 1065-1068.

Ivanova, E. P.; Sawabe, T.; Alexeeva, Y. A.; Lysenko, A.M.; Gorshkova, N. M.; Hayashi, K.; Zhukova, N. V.; Christen, R. and Mikhailov, V. V. 2002. Pseudoalteromonas issachenkonii sp. nov., a bacterium that degrades the thallus of the brown alga Fucus evanescens. *Int. J. Syst. Evol. Microbiol.* **52**. 229-234.

Ivanova, E.P.; Gorshkova, N.M.; Bowman, J.P.; Lysenko, A.M.; Zhukova, N.V.; Sergeev, A.F.; Mikhailov, V.V. and Nicolau, D.V. 2004. Shewanella pacifica sp. nov., a polyunsaturated fatty acid-producing bacterium isolated from sea water. *Int. J. Syst. Evol. Microbiol.* **54**. 1083-1087.

Ivanova, E.P.; Sawabe, T.; Gorshkova, N.M.; Svetashev, V.I.; Mikhailov, V.V.; Nicolau, D.V. and Christen, R. 2001. Shewanella japonica sp. nov. *Int. J. Syst. Evol. Microbiol.* **51.** 1027-1033.

Ivanova, E.P.; Sawabe, T.; Zhukova, N.V.; Gorshkova, N.M.; Nedashkovskaya, O.I.; Hayashi, K.; Frolova, G.M.; Sergeev, A.F.; Pavel, K.G.; Mikhailov, V.V. and Nicolau, D.V. 2003. Occurrence and diversity of mesophilic Shewanella strains isolated from the North-West Pacific Ocean. *Syst. Appl. Microbiol.* **26**. 293-301.

Jackson, T.J.; Ramalaey, R.F. and Meinschein, W.G. 1973. *Thermomicrobium*, a new genus of extremely thermophilic bactera. *Int. J. Syst. Bacteriol*. **23**. 28-36.

Jawad, A.; Seifert, H.; Snelling, A.M.; Heritage, J. and Hawkey, P.M. 1998. Survival of *Acinetobacter baumannii* on dry surfaces: comparison of outbreaks and sporadic isolates. *J. Clin. Microbiol.* **36**. 1938-1941.

Johns, G.C. and Somero, G.N. 2004. Evolutionary convergence in adaptation of proteins to temperature: A4-lactate dehydrogenases of Pacific damselfish (*Chromis* spp.). *Mol. Biol. Evol.* **21**. 314-320.

Joly-Guillou, M. L. 2005. Clinical impact and pathogenity of *Acinetobacter. Clin. Microbiol. Infect*. **11**. 868-873.

Kandler, O. and König, H. 1985. Cell envelopes of Archaeabacteria. In: Woese, C.R. and Wolfe, R. (eds.) The bacteria, vol.8. Academic Press. Orlando, FL. 413-458.

Kates, M. 1996. Structural analysis of phospholipids and glycolipids in extremely halophilic bacteria. *J. Microbiol. Methods.* **25**. 113-128.

Kawahara, K.; Brade, H.; Rietschel, E.T. and Zähringer, U. 1987. Studies on the chemical structure of the core-lipid A region of the lipopolysaccharide of Acinetobacter calcoaceticus NCTC 10305. Detection of a new 2-octulosonic acid interlinking the core oligosaccharide and lipid A component. *Eur. J. Biochem*. **163.** 489-95.

Kawahara, K.; Isshiki, Y.; Ezaki, T.; Moll, H.; Kosma, P. and Zähringer, U. 1994. Chemical characterization of the inner core Lipid A region of the lipopolysaccharide isolated from *Pseudomonas (Burkholderia) cepacia. J. Endotoxin Research.* **1**. 52.

Kieboom, J.; Dennis, J.J.; de Bont, J.A.M. and Zylstra, G.J. 1998. Identification and molecular characterization of an efflux pump involved in *Pseudomonas putida* S12 solvent tolerance. *J. Biol. Chem.* **273**. 85-91.

Kim, K.; Lee, S.; Lee, K. and Lim, D. 1998. Isolation and characterization of toluene sensitive mutants from the toluene-resistant bacterium *Pseudomonas putida* GM73. *J. Bacteriol.* **180**. 3692-3696.

Kittelberger, R. and Hilbink, F. 1993. Sensitive silver-staining detection of bacterial lipopolysaccharides in polyacrylamide gels. *J. Biochem. Biophys. Meth.* **26**. 81-86.

Klein, W.; Weber, M.H. and Marahiel, M.A. 1999. Cold shock response of *Bacillus subtilis*: isoleucine-dependent switch in the fatty acid branching pattern for membrane adaptation to low temperatures. *J. Bacteriol.* **181**. 5341-5349.

Knirel, Y. A.; Bystrova, O.V.; Shashkov, A.S.; Lindner,B.; Kocharova, N.A.; Senchenkova, S.N., Moll, H.; Zähringer, U.; Hatano, H. and Pier, G. 2001. Structural analysis of the lipopolysaccharide core of a rough, cystic fibrosis isolate of *Pseudomonas aeruginosa*. *Eur. J.Biochem.* **268**. 4708-4719.

Knirel, Y.A.; Moll, H.; Helbig, J.H. and Zahringer, U. 1997. Chemical characterization of a new 5,7-diamino-3,5,7,9-tetradeoxynonulosonic acid released by mild acid hydrolysis of the *Legionella pneumophila* serogroup 1 lipopolysaccharide. *Carbohydr. Res.* **304**. 307-309.

Knirel, Y.A.; Zdorovenko, G.M.; Paramonov, N.A.; Veremeychenko, S.P.; Toukach, F.V. and Shashkov, A.S. 1996. Somatic antigens of pseudomonads: structure of the O-specific polysaccharide of the reference strain for Pseudomonas fluorescens (IMV 4125, ATCC 13525, biovar A). *Carbohydr. Res.*, **291**. 217-224.

Kobayashi, H.; Uematsu, K.; Hirayama, H. and Horikoshi, K. 2000. Novel toluene elimination systems in a toluene tolerant microrganism. *J. Bacteriol.* **182**. 6451-6455.

Kocsis, B. and Kontrohr, T. 1984. Isolation of adenosine 5'-diphosphate-L-*glycero*-D-*manno*-heptose, the assumed substrate for Heptose transferase(s) from *Salmonella Minnesota* R595 and *Shigella sonnei* Re mutants. *J. Biol. Chem.* **259**. 11858-11860.

Koga, Y.; Nishitara, M.; Morii, H. and Agawa-Matsushita, M. 1993. Ether polar lipids of methanogenic bacteria: structures, comparative aspects and biosynthesis. *Microbiol. Rev.* **57**. 164-182.

Koronakis, V.; Sharff, A.; Koronakis, E.; Luisi, B. and Hughes, C. 2000. Crystail structure of the bacterial membrane protein TolC central to multidrug efflux and protein export. *Nature.* **405**. 914-919.

References

Sturiale, L.; Garozzo, D.; Silipo, A.; Lanzetta, R.; Parrilli, M. and Molinaro, A. 2005. New conditions for matrix-assisted laser desorption/ionization mass spectrometry of native bacterial R-type lipopolysaccharides. *Rapid Comun. in Mass Spectrom.* **19**. 1829-1834.

Lai, M.C. and Gunsalus, R.P. 1992. Glycine betaine and potassium ion are the major compatible solutes in the halophilic methanogenic archaeabacteria. *J. Bacteriol.* **173**. 5352-5358.

Lanyi, J.K.; Renthal, R. and MacDonald, R.E. 1976. Light induced glutamate transport in *Halobacterium halobium* envelope vescicles. II. Evidence that the driving force is a light dependent sodium gradient. *Biochemistry.* **15**. 1603-1610.

Leeson, D.T.; Gai, F.; Rodriguez, H.M.; Gregoret, L.M. and Dyer, R.B. 2000. Protein folding and unfolding on a complex energy landscape. *Proc. Natl. Acad. Sci. U S A*. **97**. 2527-2532.

Leone, S.; Molinaro, A.; Lindner, B.; Romano, I.; Nicolaus, B.; Parrilli, M.; Lanzetta, R. and Holst, O. 2006. The structures of glycolipids isolated from the highly thermophilic bacterium *Thermus thermophilus* Samu-SA1. *Glycobiology.* **16**. 766-775.

Leone, S.; Molinaro, A.; Pessione, E.; Mazzoli, R.; Giunta, C.; Sturiale, L.; Garozzo, D.; Lanzetta R. and Parrilli, M. 2006. Structural elucidation of the core-lipid A backbone from the lipopolysaccharide of *Acinetobacter radioresistens* S13, an organic solvent tolerant Gram-negative bacterium. *Carbohydr. Res*. **341.** 582-90.

Leontein, K. and Lönngren, J. 1978. Determination of the absolute configuration of sugars by gas-liquid chromatography of their acetylated 2-octyl glycosides. *Meth. Carbohydr. Chem*. **62**. 359-362.

Linzer, R. and Neuhaus, F.C. 1973. Biosynthesis of membrane teichoic acid. A role of the D-alanine-activating enzyme. *J. Biol. Chem.* **248**. 3196-3201.

Liparoti, V.; Molinaro, A.; Sturiale, L.; Garozzo, D.; Nazarenko, E.L.; Gorshkova, R.P. ;Ivanova, E.P.; Shevcenko, L.S.; Lanzetta, R. and Parrilli, M. 2006. Structural Analysis of the Deep Rough Lipopolysaccharide from Gram Negative Bacterium *Alteromonas macleodii* ATCC 27126T: The First Finding of β-Kdo in the Inner Core of Lipopolysaccharides. *Eur. J. Org. Chem.* **20**. 4710-4716.

Lipinski, T.; Zatonsky, G.V; Kocharova, N.A.; Jaquinod, M. ; Forest, E. ; Shashkov, A.S.; Gamian, A. and Knirel, Y.A. 2002. Structures of two O-chain polysaccharides of Citrobacter gillenii O9a,9b lipopolysaccharide. A new homopolymer of 4-amino-4,6-dideoxy-D-mannose (perosamine). *Eur. J. Biochem.,* **269**. 93-99.

Lipkind, G.M.; Shashkov, A.S.; Knirel, Y.A.; Vinogradov, E.V. and Kochetkov, N.K. 1988. A computer-assisted structural analysis of regular polysaccharides on the basis of 13C-n.m.r. data. *Carbohydr. Res*. **175**. 59–75.

Loffeld, B. and Keweloh, H. 1996. *Cis-trans* isomerizationof unsaturated fatty acids as a possible control mechanism of membrane fluidity in *Pseudomonas putida* L8. *Lipids.* **31.** 811-815.

Lomovskaya, O.; Lee, A.; Hoshino, K.; Ishida, K. and Mistry, A. 1999. Use of a genetic approach to evaluate the consequences of inhibition of efflux pumps in *Pseudomonas aeruginosa. Antimicrob. Agents Chemother.* **43**. 1340-1346.

Lomovskaya, O.; Warren, M.S.; Lee, A.; Galazzo, J. and Fronko, R. 2001. identification and characterization of inhibitors of multidrug resistanceefflux pumps in *Pseudomonas aeruginosa*: novel agents for combination therapy. *Antimicrob. AgentsChemother.* **45**. 105-116.

Lu, T.L.; Chen, C.S.; Yang, F.L.; Fung, J.M.; Chen, M.Y.; Tsay, S.S.; Li, J.; Zou, W. and Wu, S.H. 2004. Structure of major glycolipid from *Thermus oshimai* NTU-063. *Carbohyd. Res*. **339**. 2593-2598.

Macdonald, A.G. and Cossins, A.R. 1985. The theory of homeoviscous adaptation of membranes applied to deep-sea animals. *Soc. Exp. Biol. Symp.* **39**. 301-332.

Mancuso-Nichols, C.A.; Guezennec, J. and Bowman, J.P. 2004. Bacterial exopolysaccharides from extreme marine environments with special consideration of the southern ocean, sea ice, and deep-sea hydrothermal vents. *Mar. Biotechnol.* **7**. 253-271.

Marquis, R.E. 1994. High pressure microbiology. In: Bennet, P.B. and Marquis, R.E, (eds.) Basic and applied high pressure biology. University of Rochester Press, Rochester, NY. 1-14.

Masoud, H.; Altman, E.; Richards, J.C. and Lam, J.S. 1994. General strategy for structural analysis of the oligosaccharide region of lipooligosaccharides. Structure of the oligosaccharide component of *Pseudomonas aeruginosa* IATS serotype 06 mutant R5 rough-type lipopolysaccharide. *Biochemistry.* **33**. 10568-10578.

Medzhitov, R. 2001. Toll-like receptors and innate immunity. *Nature Rev. Immunol.* **1**. 135-145.

Melchior, D.L. 1982. Lipid phase transitions and regulation of membranes fluidity in prokaryotes. *Curr. Top. Membr. Transp.* **17**. 263-316.

Mojica, F.J.M.; Cisneros, E.; Ferrer, C.; Rodriguez-Valera, F. and Juez, G. 1997. Osmotically induced response in representatives of the halophilic prokaryotes: the bacterium *Halomonas elongata* and the archaeon *Haloferax volcanii. J. Bacteriol.* **179**. 5471-5481.

Molinaro, A.; De Castro, C.; Lanzetta, R.; Parrilli, M.; Petersen, B.O.; Broberg, A. and Duus, J.Ø. 2002. NMR and MS evidences for a random assembled O-specific chain structure in the LPS of the bacterium Xanthomonas campestris pv. Vitians. A case of unsystematic biosynthetic polymerization. *Eur. J. Biochem.,* **269**. 4185-4193.

Molinaro, A.; Evidente, A.; Lo Cantore, P.; Iacobellis, N.S.; Bedini, E.; Lanzetta, R. and Parrilli, M. 2003. Structural Determination of a Novel O-Chain Polysaccharide of the Lipopolysaccharide from the Bacterium Xanthomonas campestris pv. Pruni. *Eur. J. Org. Chem*, 2254-2259.

Monteoliva-Sanchez, M.; Ramos-Comenzana, A. and Russel, J. 1993. The effect of salinity and compatible solutes on the biosynthesis of cyclopropane fatty acids in *Pseudomonas halosaccharolytica. J. Gen. Microbiol.* **139**. 1877-1884.

Morell, V. 1997. Microbiology's scarred revolutionary. *Science*. **276**. 699.

References

Muldoon, J.; Shashkov, A.S.; Senchenkova, S.Y.N.; Tomshich, S.V.; Komandrova, R.A.; Romanenko, L.A.; Knirel, Y.A. and Savage, A.V. 2001. Structure of an acidic polysaccharide from the marine bacterium *Pseudoalteromonas flavipulchra* NCIMB 2033(T). *Carbohydr. Res.* **330**. 231-239.

Mullakhanbhai, M.F. and Larsen, H. 1975. *Halobacterium volcanii* spec. nov., a Dead Sea halobacterium with a moderate salt requirement. *Arch. Microbiol.* **104**. 207-204.

Murray, R.G.E. 1986. Genus *Deinococcus* Brock and Murray 1981, 354[vp]. In Krieg, N.R. and Holt, J.G. (Eds.), *Bergey's manual of systematic bacteriology, vol.2*. The Williams and Wilkins Co., Baltimore, Md. 1035-1043.

Myers, C.R. and Nealson, K.H. 1990. Respiration-linked proton translocation coupled to anaerobic reduction of manganese(IV) and iron(III) in Shewanella putrefaciens MR-1. *J. Bacteriol.* **172**. 6232-6238.

Nazarenko, E.L.; Komandrova, N.A.; Gorshkova, R.P.; Tomshich, S.V.; Zubrov, V.A.; Kilcoyne, M.; Savage, A.V. 2003. Structures of polysaccharides and oligosaccharides of some Gram-negative marine *Proteobacteria. Carbohyd. Res.* **338**. 2449-2457.

Nazina, T.N.; Tourova, T.P.; Poltaraus, A.B.; Novikova, E.V.; Grigoryan, A.A.; Ivanova, A.E.; Lysenko, A.M.; Petrunyaka, V.V.; Osipov, G.A.; Belyaev, S.S. and Ivanov, M.V. 2001. Taxonomic study of aerobic thermophilic bacilli: descriptions of *Geobacillus subterraneus* gen. nov., sp. nov. and Geobacillus uzenensis sp. nov. from petroleum reservoirs and transfer of *Bacillus stearothermophilus, Bacillus thermocatenulatus, Bacillus thermoleovorans, Bacillus kaustophilus, Bacillus thermodenitrificans* to *Geobacillus* as the new *combinations G. stearothermophilus, G. th. Int. J. Syst. Evol. Microbiol.*, **5.** 433-446.

Neuhaus, F.C. and Baddiley, J. 2003. A continuum of anionic charge: structures and functions of D-alanyl-teichoic acids in gram-positive bacteria. *Microbiol. Mol. Biol. Rev.* **67**. 686-723.

Nicolaus, B., Lama, L., Manca, M.C. and Gambacorta, A. 1999. Extremophiles: Polysaccharides and enzymes degrading polysaccharides. *Recent Res. Devel. Biotech. & Bioeng.* **2**. 37-64.

Nikaido, H. and Vaara, M. 1985. Molecular basis of bacterial outer membrane permeability. *Microbiol Rev.* **21**. 243-277.

Ovchinnikova, O.; Kocharova, N.A.; Katzenellenbogen, E.; Zatonsky, G.V; Shashkov, A.S.; Knirel, Y.A.; Lipinski, T.; and Gamian, A. 2004. Structures of two O-polysaccharides of the lipopolysaccharide of Citrobacter youngae PCM 1538 (serogroup O9). *Carbohydr. Res.* **339**. 881-884.

Pask-Hughes, R.A. and Shaw, N. 1982. Glycolipids from some extreme thermophilic bacteria belonging to the genus *Thermus*. *J. Bacteriol.* **149**. 54-58.

Perego, M.; Glaser, P.; Minutello, A.; Strauch, M.A.; Leopold, K. and Fischer, W. 1995. Incorporation of D-alanine into lipoteichoic acid and wall teichoic acid in Bacillus subtilis. Identification of genes and regulation. *J. Biol. Chem.* **270**. 15598-15606.

Perry, J.J. 1992. The genus *Thermomicrobium*. In Balows, A., Trüper, H.G, Dworkin, M. Harder, W. and Schleifer, K.H. (Eds.), *The prokaryotes*, 2nd ed. Springer-Verlag, New York. N.Y. 3775-3779.

Pessione, E. and Giunta, C. 1997. Acinetobacter radioresistens metabolizing aromatic compounds. 2. Biochemical and microbiological characterization of the strain. *Microbios*. **89**. 105-117.

Phadtare, S. 2004. Recent developments in bacterial cold shock response. *Curr. Issues Mol. Biol.* **6**. 125-136.

Piantini, U.; Sørensen, O.W. and Ernst, R.R. 1982. Multiple quantum filters for elucidating NMR coupling networks. *J. Am. Chem. Soc*. **104**. 6800-6801.

Pier, G.B.; Coleman, F.; Grout, M.; Franklin M. and Ohman, D.E. 2001. Role of alginate O acetylation in resistance of mucoid Pseudomonas aeruginosa to opsonic phagocytosis. *Infect. Immun*. **69**. 1895-1901.

Pinkhart, H.C. and White, D.C. 1997. Phospholipids biosynthesis and solvent tolerance in *Pseudomonas putida* strains. *J. Bacteriology*. **179**. 4219-4226.

Powlowski, J. and Shingler, V. 1990. In vitro analysis of polypeptide requirements of multicomponent phenol hydroxylase from *Pseudomonas* sp. strain CF600. *J. Bacteriol* **172**. 6834-6840.

Prado, A.; da Costa, M.S.; Laynez, J. And Madeira, V.M. 1988. Physical properties of membrane lipids isolated from a thermophilic eubacterium (*Thermus* sp.). *Adv. Exp. Med. Biol*. **238.** 47-58.

Quintela, J.C.; Pittenauer, E.; Allmaier, G.; Arán, V. and de Pedro, M.A. 1995. Structure of peptidoglycan from *Thermus thermophilus* HB8. *J. Bacteriol*. **177.** 4947-4962.

Raetz, C.R.H. and Whitfield, C. 2002. Lipopolysaccharide endotoxins. *Annu. Rev. Biochem*. **71.** 635-700.

Ramos, J.L.; Duque, E.; Gallegos, M.T.; Godoy, P.; Ramos-Gonzalez, M.I.; Rojas, A.; Teran, W. and Segua, A. 2002. Mechanisms of solvent tolerance in Gram-negative bacteria. *Annu. Rev. Microbiol.* **56**. 743-768.

Ramos, J.L.; Duque, E.; Gallegos, M.T.; Godoy, P.; Ramos-Gonzàlez, M.I.; Rojas, A.; Teràn, W. and Segura, A. 2002. Mechanisms of solvent tolerance in Gram-negative bacteria. *Annu. Rev. Microbiol.* **56**. 743-768.

Ramos, J.L.; Duque, E.; Rodriguez-Herva, J.J. and Godoy, P. 1997. Mechanisms for solvent tolerance in bacteria. *J. Biol. Chem.* **272**. 3887-3890.

Ramos, J.L.; Gallegos, M.T.; Marques, S.; Ramos-Gonzalez, M.I.; Espinosa-Urgel, M. and Segua, A. 2001. Responses of Gram-negative bacteria to certain environmental stressors. *Curr. Opin. Microbiol.* **4**. 166-171.

Rance, M.; Sørensen, O.W.; Bodenhausen, G.; Wagner, G.; Ernst, R.R. and Wüthrich, K. 1983. Improved spectral resolution in COSY ^{1}H NMR spectra of proteins via double quantum filtering. *Biochem. Biophys. Res. Commun.* **117**. 479-485.

Rathinavelu, S.; Y. Zavros, and J. L. Merchant. 2003. *Acinetobacter lwoffii* infection and gastritis. *Microbes Infect.* **5**. 651-657.

References

Reizer J, Grossowicz N, Barenholz Y. 1985. The effect of growth temperature on the thermotropic behavior of the membranes of a thermophilic Bacillus. Composition-structure-function relationships. *Biochim. Biophys. Acta*. **815**. 268-80.

Rietschel, E.T. 1976. Absolute configuration of 3-hydroxy fatty acids present in lipopolysaccharides from various bacterial groups. *Eur. J. Biochem.* **64**. 423-428.

Romano, I.; Lama, L.; Schiano Moriello, V.; Poli, A.; Gambacorta, A. and Nicolaus, B. 2004. Isolation of a new thermohalophilic *Thermus thermophilus* strain from hot spring, able to grow on a renewable source of polysaccharide. *Biotechnol. Lett*. **26.** 45-49.

Rugeaux, H.; Guezennec, J.; Carlson, R.W; Kervarec, N.; Pichon, R. and Talaga, P. 1999. Structural determination of the exopolysaccharide of *Pseudoalteromonas* strain HYD 721 isolated from a deep-sea hydrothermal vent. *Carbohydr. Res.* **315**. 273-285.

Russel, N.J. and Kogut, M. 1985. Haloadaptation: salt sensing and cell-envelope changes. *Microbiol. Sci.* **2**. 345-350.

Ryoo, D.; Shim, H.; Canada, K.; Barbieri, P. and Wood, TK. 2000. Aerobic degradation of tetrachloroethylene by toluene-o-xylene monooxygenase of *Pseudomonas stutzeri* OX1. *Nat. Biotechnol.* **18**. 775-778.

Sadovskaya, I.; Vinogradov, E.; Li, J. and Jabbouri, S. 2004. Structural elucidation of the extracellular and cell-wall teichoic acids of Staphylococcus epidermidis RP62A, a reference biofilm-positive strain. *Carbohyd. Res.* **339**. 1467-1473.

Sanchez Carballo, P. M.; Rietschel, E.Th.; Kosma, P. and Zähringer, U. 1999. Elucidation of the structure of an alanine-lacking core tetrasaccharide trisphosphate from the lipopolysaccharide of *Pseudomonas aeruginosa* mutant H4. *Eur. J.Biochem*. **261**. 500-508.

Sardessai, Y. And Bhosle, S. 2002. Tolerance of bacteria to organic solvents. *Res. in Microbiol.* **153**. 263-268.

Schäffer, C. and Messner, P. 2005. The structure of secondary cell wall polymers: how Gram-positive bacteria stick their wall together. *Microbiology.* **151**. 643-651.

Semple, K.M. and Westlake, D.W. 1987. *Can. J. Microbiol.* **33**. 366-371.

Seydel, U.; Oikava, M.; Fukase, K.; Kusumoto, S. and Brandeburg, K. 2000. Intrinsic conformation of Lipid A is responsible for agonistic and antagonistic activity. *Eur. J. Biochem.* **267**. 3032-3039.

Seydel, U.; Oikava, M.; Fukase, K.; Kusumoto, S. and Brandeburg, K. 2000. Intrinsic conformation of Lipid A is responsible for agonistic and antagonistic activity. *Eur. J. Biochem.* **267**. 3032-3039.

Shashkov, A.S.; Torgov, V.I.; Nazarenko, E.L.; Zubkov, V.A.; Gorshkova, N.M.; Gorshkova, R.P. and Widmalm, G. 2002. Structure of the phenol-soluble polysaccharide from Shewanella putrefaciens strain A6. *Carbohydr. Res.* **337**. 1119-1127.

Silipo, A.; Lanzetta, R.; Amoresano, A.; Parrilli, M. and Molinaro, A. 2002. Ammonium hydroxyde hydrolysis: a valuable support in the MALDI-TOF mass spectrometry analysis of Lipid A fatty acids distribution. *J. Lipid Res.* **43**. 2188-2195.

Silipo, A.; Leone, S.; Molinaro, A. Sturiale, L.; Garozzo, D.; Nazarenko, E.L.; Gorshkova, R.P.; Ivanova, E.P.; Lanzetta, R. and Parrilli, M. 2005. Complete structural elucidation of a novel lipooligosaccharide from the Outer Membrane of the marine bacterium *Shewanella pacifica. Eur. J. Org. Chem.* 2281-2291.

Silipo, A.; Molinaro, A.; De Castro, C.; Ferrara, R.; Romano, I.; Nicolaus, B.; Lanzetta, R. and Parrilli, M. 2004. Structural analysis of a novel polysaccharide of the lipopolysaccharide-deficient extremophile Gram-negative bacterium *Thermus thermophilus* HB8. *Eur. J. Org. Chem.* **2004**. 5047-54.

Silipo, A.; Molinaro, A.; Nazarenko, E.L.; Sturiale, L.; Garozzo, D.; Gorshkova, R.P.; Nedashkovskaya, O. I.; Lanzetta, R. and Parrilli, M. 2005. Structural characterization of the carbohydrate backbone of the lipooligosaccharide of the marine bacterium *Arenibacter certesii* strain KMM 3941(T). *Carbohyd. Res.* **340**. 2540-2549.

Silipo, A.; Molinaro, A.; Comegna, D.; Sturiale, L.; Cescutti, P.; Garozzo, D.; Lanzetta, V. Parrilli**, M.** 2006. Full Structural Characterisation of the Lipooligosaccharide of a Burkholderia pyrrocinia Clinical Isolate**.** *Eur. J. Org. Chem.* **2006**. 4874-4883.

Singer, S.J. and Nicolson, G.L. 1972. The fluid mosaic model of the structure of cell membranes. *Science.* **75.** 720-731.

Smith, F. and Montgomery, R. 1956. End group analysis of polysaccharides. *Methods Biochem. Anal.* **3***, 153.

Sokol, W. and Howell, J.A. 1981. *Biotechnol. Bioeng.,* **23**. 2039-2049.

Staaf, M.; Weinstraub, A. and Widmalm, G, 1999. Structure determination of the *O*-antigenic polysaccharide from the enteroinvasive *Escherichia coli* O136. *Eur. J. Biochem.* **263**. 656-661.

States, D.J.; Haberkorn, R.A. and Ruben, D.J. 1982. A two dimensional nuclear overhauser experiment with pure absorption phase in four quadrants. *J. Magn. Res.* **48**. 286-292.

Steen, A.; Palumbo, E.; Deghorian, M.; Cocconcelli, P.S.; Delcour, J.; Kuipers, O.P.; Kok, J.; Buist, G. and Hols, P. 2005. Autolysis of Lactococcus lactis is increased upon D-alanine depletion of peptidoglycan and lipoteichoic acids. *J. Bacteriol.* **187**. 114-124.

Susskind, M.; Brade, L.; Brade, H. and Holst, O. 1998. Identification of a novel heptoglycan of alpha1-2-linked D-*glycero*-D-*manno*-heptopyranose. Chemical and antigenic structure of lipopolysaccharides from Klebsiella pneumoniae sp. pneumoniae rough strain R20 (O1:K20). *J. Biol. Chem.* **273**. 7006-7017.

Towner, K.J., Bergogne-Bérézin, E. and Fewson, C.A. 1991. *Acinetobacter*: portrait of a genus. In: The biology of Acinetobacter: Taxonomy, Clinical Importance, Molecular Biology, Physiology, Industrial Relevance. K. J. Towner, E. Bergogne-Bérézin, C. A. Fewson, editors. Plenum Press, New York, NY. 1-24.

References

Urai, M.; Anzai, H.; Ogihara, J; Iwabuchi, N.; Harayama, S.; Sunairi, M. and Nakajima, M. 2006. Structural analysis of an extracellular polysaccharide produced by Rhodococcus rhodochrous strain S-2. *Carbohydr. Res.* **341**. 766-775.

Van de vossenberg, J.C.L.M.; Ubbink-Kok, T.; Elferink, M.G.L.; Driessen, A.J.M. and Konings, W.N. 1995. Ion permeability of the cytoplasmic membrane limits the maximal growth temperature of bacteria and Archaea. *Mol. Microbiol.* **18**. 925-932.

Van de Vossenberg, J.L.; Driessen, A.J. and Konings, W.N. 1998. The essence of being extremophilic: the role of the unique archaeal membrane lipids. *Extremophiles*. **2**. 163-70

Van den Burg, B. 2003. Extremophiles as a source of novel enzymes. *Curr. Op. Microbiol.* **6**. 213-218.

Ventosa, A.; Nieto, J.J. and Oren, A. 1998. Biology of moderately halophilic aerobic bacteria. *Microbiol. Mol. Biol. Rev.* **62**. 504-544.

Vieille, C.; Burdette, D.S. and Zeikus, J.G. 1996. In: Gewely M.R.E. (ed.), Biotechnology Annual Review, vol.2. 1. Elsevier Science, New York.

Vinogradov, E.; Bock, K.; Petersen, B.O.; Holst, O. and Brade, H. 1997. The structure of the carbohydrate backbone of the lipopolysaccharide from Acinetobacter strain ATCC 17905. *Eur. J. Biochem.* **243**. 122-127.

Vinogradov, E.; Korenevsky, A. and Beveridge, T.J. 2003. The structure of the rough-type lipopolysaccharide from Shewanella oneidensis MR-1, containing 8-amino-8-deoxy-Kdo and an open-chain form of 2-acetamido-2-deoxy-D-galactose. *Carbohyd. Res.* **338**. 1991-1997.

Vinogradov, E.; Korenevsky, A. and Beveridge, T.J. 2004. The structure of the core region of the lipopolysaccharide from Shewanella algae BrY, containing 8-amino-3,8-dideoxy-D-manno-oct-2-ulosonic acid. *Carbohydr. Res.* **339**. 737-740.

Vinogradov, E.; Korenevsky, A. and Beveridge, T.J. 2003. The structure of the O-specific polysaccharide chain of the Shewanella algae BrY lipopolysaccharide. *Carbohydr. Res.* **338**. 385-388.

Vinogradov, E.; Sadovskaya, I.; Li, J. and Jabbouri, S. 2006. Structural elucidation of the extracellular and cell-wall teichoic acids of Staphylococcus aureus MN8m, a biofilm forming strain. *Carbohyd. Res.* **341**. 738-743.

Vinogradov, E.V.; Duus, J.Ø.; Brade, H. and Holst, O.2002. The structure of the carbohydrate backbone of the lipopolysaccharide from *Acinetobacter baumannii* strain ATCC 19606. *Eur. J. Biochem.* **269**. 422-430.

Vinogradov, E.V.; Müller-Loennies, S.; Petersen, B.O.; Meshkov, S.; Thomas-Oates, J.E.; Holst, O. and Brade, H. 2002 Structural investigation of the lipopolysaccharide from Acinetobacter haemolyticus strain NCTC 10305 (ATCC 17906, DNA group 4). *Eur. J. Biochem.* **247**. 82-90.

Vinogradov, E.V.; Pantophlet, R.; Haseley, S.R.; Brade, L.; Holst, O. and Brade, H. 1997. Structural and serological characterisation of the O-specific polysaccharide from lipopolysaccharide of *Acinetobacter calcoaceticus* strain 7 (DNA group 1). *Eur.J.Biochem.* **243**. 167-173.

Vinogradov, E.V.; Petersen, B.O.; Thomas-Oates, J.E.; Duus, J.Ø.; Brade, H. and Holst, O. 1998. Characterization of a novel branched tetrasaccharide of 3-deoxy-D-manno-oct-2-ulopyranosonic acid. The structure of the carbohydrate backbone of the lipopolysaccharide from Acinetobacter baumannii strain nctc 10303 (atcc 17904). *J. Biol. Chem*, **273**. 28122-28131.

Vreeland, R.H. 1987. Mechanisms of halotolerance in microorganisms. *CRC Crit. Rev. Microbiol.* **14**. 311-356.

Wait, R.; Carreto, L.; Nobre, M.F.; Ferreira, A.M. and Da Costa, M.S. 1997. Characterization of novel long-chain 1,2-diols in *Thermus* species and demonstration that *Thermus* strains contain both glycerol-linked and diol-linked glycolipids. *J. Bacteriol*. **179**. 6154-6162.

Walzer, G., Rosenberg, E. and Ron, E.Z. 2006. The Acinetobacter outer membrane protein A (OmpA) is a secreted emulsifier. *Environ. Microbiol*. **8**. 1026-1032.

Ward, J.B. Teichoic and teichuronic acids: biosynthesis, assembly, and location. *Microbiol. Rev.*, **1981**, *45*, 211-243.

Weber F.J. and de Bont, J.A.M. 1996. Adaptation mechanisms of microrganisms to the toxic effects of organic solvents on membranes. *Biochem. Biophys. Acta.* **1286**. 225-245.

Welsh, D.T. and Herbert, R.A. 1999. Osmotically-induced intracellular threalose, but not glycine betaine accumulation promotes desiccation tolerance in *Escherichia coli. FEMS Microbiol. Lett.* **174**. 57-63.

Westphal, O. and Jann, K. 1965. Bacterial lipopolysaccharides. Extraction with phenol ∕ water and further application of the procedure. *Meth. Carbohydr. Chem.* **5**. 83–91.

Wong, T.Y.; Preston, L.A. and Schiller, N.L. 2000. ALGINATE LYASE: review of major sources and enzyme characteristics, structure-function analysis, biological roles, and applications. *Annu. Rev. Microbiol.* **54**. 289-340.

Yamada, T.; Shiio, I. and Egami, F. 1954. On the halophilic alkaline phosphomonoesterase. *Proc. Jpn. Acad. Sci*. **30**. 113-115.

Yamauchi, K.; Doi, K.; Kinoshita, M.; Kii, F. and Fukuda, H. 1992. Archaebacterial lipid models: highly salt-tolerant membranes from 1,2-diphytanylglycero-3-phosphocholine. *Biochem. Biophys. Acta.* **1110**. 171-177.

Yamauchi, K.; Doi, K.; Yoshida, Y. and Kinoshita, M. 1993. Archaebacterial lipids: highly proton-impermeable membranes from 1,2-diphytanyl-sn-glycero-3-phosphocholine. *Biochim. Biophys. Acta*. **1146**. 178-182.

Yang, F.L.; Lu, C.P.; Chen, C.S.; Hsiao, H.L.; Su, Y.; Tsay, S.S.; Zou, W. and W., S.H. 2004. Structural determination of the polar glycoglycerolipids from thermophilic bacteria *Meiothermus taiwanensis. Eur. J. Biochem*. **271**. 4545-51.

Zähringer, U.; Lindner, B. and Rietschel, E.T. 1994. Molecular structure of Lipid A, the endotoxic center of bacterial lipopolysaccharides. *Adv. Carbohydr. Chem. Biochem.* **50**. 211-276.

Zähringer, U.; Lindner, B. and Rietschel, E.T. 1999. Chemical structure of Lipid A: recent advances in structural analysis of biologically active molecules. In: Brade, H.; Morrsion, D.C.; Opal, S. and Vogel, S. (eds.) Endotoxin in Health and Disease. Marcel Dekker Inc., New York, NY. 93-114.

Zdorovenko, E.L.; Zatonsky, G.V; Zdorovenko, G.M.; Pasichnyk, L.A.; Shashkov, A.S. and Knirel, Y.A. 2001. Structural heterogeneity in the lipopolysaccharides of Pseudomonas syringae with O-polysaccharide chains having different repeating units. *Carbohydr. Res.*, **336**. 329-336.

Zhang, Z.; Yu, G.; Guan, H.; Zhao, X.; Du, Y. and Jiang, X. 2004. Preparation and structure elucidation of alginate oligosaccharides degraded by alginate lyase from Vibro sp. 510. *Carbohydr. Res.* **339.** 1475-1481.

ZoBell, C.E. and Morita, R.Y. 1957. Barophilic bacteria in some deep-sea environments. *J. Bacteriol.* **73**. 563-568.